Investigating ecosystem-scale responses to changes in lake food webs

By
Tyler J. Butts

A dissertation submitted in partial fulfillment of
the requirements for the degree of

Doctor of Philosophy

(Freshwater and Marine Sciences)

at the

UNIVERSITY OF WISCONSIN-MADISON
2023

Date of final oral examination: 05/03/2023

The dissertation is approved by the following members of the Final Oral Committee:

Grace M. Wilkinson, Assistant Professor, Integrative Biology
Claudio Gratton, Professor, Entomology
M. Jake Vander Zanden, Professor, Integrative Biology
Gretchen Gerrish, Director of Trout Lake Station, Integrative Biology

TABLE OF CONTENTS

ACKNOWLEGEMENTS

They say it takes a village to raise a child, well, for this dissertation it took two academic institutions and help from a horde of mentors, collaborators, and friends. While I may be writing this dissertation it only exists because of the hours graciously given, help generously offered, and endless support from all of the people who I've had the pleasure to work with for the past five years.

To my advisor, Grace, thank you for your superhuman patience and brilliant guidance always pushing me to not only ask if I can, but if I should. I truly struck gold when you agreed to let me join you out in Iowa. I've grown so much as a scientist and as a person over the last five years in large part to the caring and supportive culture you've built for your lab group. I am incredibly proud to say that I'm a member of the Wilkinson Lab, and I promise I'll never ask you to help me stock fish into experimental ponds at 2am ever again!

To my advisory committee, Claudio Gratton, Jake Vander Zanden, Gretchen Gerrish, thank you for being willing to take on a student already halfway through their program, and to Mike Weber, thanks for sticking with me! I truly appreciated the support and kind words from you all as I transitioned to a new institution and thank you for your guidance to help improve this dissertation. To my advisory committee that helped start my journey in grad school, Haldre Rogers, Brian Wilsey, and Clay Pierce, thank you for your insightful ideas and early feedback that vastly improved this work.

To my coauthors, thank you for your brilliance that I have tried my very best to absorb. To Eric Moody, thank you for showing me the wonderful world of stoichiometry. To Marty, thank you for always being generous with your time and letting me claim, in part, to be a fisheries scientist, and to Robert Johnson, thank you for guiding me through the world of

ecosystem metabolism. To Ben Martin, Joe Mrnak, Greg Sass, and Carol Warden, thank you for letting me build upon the incredible food web work you've been doing for years and being incredibly supportive and generous collaborators, I hope this is only the start.

Thank you to the grad student community from ISU, especially Ben, Jerilyn, Elizabeth, Caleb, Josh, and Alex, your friendship made my time in Ames a period I'll always cherish. To the CFL community, thank you for welcoming me with open arms and countless orders from Paul's. To my fellow, past and current, members of the Wilkinson Lab, Rachel Fleck King, Helen Schlimm, Elena Sandry, Haley Grigel, Quin Shingai, David Ortiz, and Danny Szydlowski I was, and continue to be, honored to work with you all. The long days in the field and long nights in the office never felt so long working with friends. To Ellen, thank you for the constant mentorship and guidance. This dissertation would not be possible without all the help and support you've generously offered to me over the past five years, I'll always try to follow in your footsteps.

This work only exists because of the unending love and support of the folks I've been truly blessed to call my friends. To Dan, Adam, and Sean thanks for always reminding me to take things less seriously, to Sophia, Jamie, Hannah, Jack, Sam, Holly, Maya, and Colleen it has been a privilege to be even a small part of your lives. To my brother AJ, I've only ever tried to emulate the paths and choices you've taken in life, and they've never led me astray so far, thank you for being my guide. To my mom and dad, words cannot state the debt I owe you for all the sacrifices and encouragement you've given me my entire life. Everything I do, I do to make you proud, and to show you that your son loves you dearly. This work, and all the things I'll ever do, are for you both. To my Auntie Robbie and Grandpa Roy, you were the first to show me the power of being curious and asking questions, though you're not here to read this, I hope I've done you justice.

ABSTRACT

Aquatic ecosystems are increasingly facing ecosystem-scale disturbances that affect water quality and ecosystem services. Food webs have substantial influences on how disturbances are propagated through ecosystems and the structure of trophic interactions shapes nutrient cycling and energy flow. In my dissertation, I used food webs to improve the understanding of dynamics in disturbed ecosystems, and develop our understanding of how food webs mediate, and respond to, increasingly frequent and intense disturbances. **Chapter 1** used lower food web dynamics to assess consumer nutrient cycling within a hypereutrophic reservoir, demonstrating that the lower food web has a substantial influence on early summer phosphorus availability and phytoplankton size structure. **Chapter 2** quantified zooplankton and macroinvertebrate size structure as a tool to assess food web response to an incentivized harvest of common carp (*Cyprinus carpio*) and bigmouth buffalo (*Ictiobus cyprinellus)*. This analysis showed that the biomanipulation did not significantly affect food web structure potentially explaining the lack of water quality response. Expanding to the whole food web, **chapter 3** tested whether food web structure mediates ecosystem responses to discrete disturbance—storm-driven nutrient loading—finding greater benthic-pelagic coupling increased the resistance and resilience of algal biomass response to pulsed nutrient loading events. **Chapter 4** used a bioenergetics approach to explore changes in energy flux and food web stability over 19 years in the Trout Lake pelagic food web, including an invasion by a mid-trophic level invader, *Bythotrephes longimanus*. This analysis highlighted how a mid-trophic level invader alters the trajectory of an ecosystem by decreasing energy flux and temporarily altering food web stability. In summary, this research has advanced our understanding of how food webs drive ecosystem function and mediate ecosystem-scale responses within aquatic ecosystems.

INTRODUCTION

As the pace of climate change accelerates, the disturbances ecosystems face are increasing in frequency and intensity resulting in a greater likelihood of changes to ecosystem function (Turner et al. 2020; Seneviratne et al. 2021). For aquatic ecosystems, extreme precipitation events in agricultural watersheds are accelerating eutrophication that may lead to toxin-producing algal blooms (Ho and Michalak 2020), while expansions in the distribution and ranges of species and globalization have generated more pathways for biological invasions (Rahel and Olden 2008; Hulme 2017). Understanding ecosystem responses to such disturbances, and the internal mechanisms that shape that response, are of interest to managers as changing and interacting drivers of ecosystem function may generate novel dynamics (Zscheischler et al. 2018). Thus, there is a pressing need to better understand the drivers and dynamics of aquatic ecosystems subjected to presses and pulses of disturbance.

Food webs have long been recognized as a mediating mechanism of ecosystem function, shaping ecosystem response to disturbances (Lindeman 1942; Odum 1968; McMeans et al. 2016; Pelletier et al. 2020). Changes in food web structure can be strongly related to changes in ecosystem dynamics through time (Pimm et al. 1991; Kortsch et al. 2021). Lower food web interactions (i.e., zooplankton, phytoplankton, macroinvertebrates) can substantially alter nutrient cycling dynamics (Elser et al. 2000; Vanni 2021) and changes in lower food web size structure have been suggested as a metric responsive to ecosystem-scale disturbance (Sprules and Barth 2016; Evans et al. 2022). However, it is unclear whether lower food web dynamics can affect ecosystem function within extremely nutrient rich ecosystems, and whether size structure can be used to effectively assess food-web changes. It is theorized that food web structures that couple benthic and pelagic food chains can better mediate ecosystem disturbances

(Vadeboncoeur et al. 2005; Rooney and McCann 2012; Marklund et al. 2019). Yet, there is limited empirical evidence demonstrating mechanistically, and to what degree, benthic-pelagic coupling may mediate ecosystem responses. Food web structure is also highly dynamic which can drive changes in energy flux and food web stability through time (De Ruiter et al. 1995; Kortsch et al. 2021), especially following species invasion (Flood et al. 2020). It is unclear how strongly, and how long, an invasion would affect the magnitude and distribution of energy flux, and food web stability dynamics, over time. These knowledge gaps guided my dissertation research toward the goal of expanding our understanding of ecosystem-scale response to disturbances in aquatic ecosystems, mediated by food web structure.

In **chapter 1**, I used lower food web dynamics to assess the significance of consumer nutrient cycling on phosphorus (P) and nitrogen (N) availability in a hypereutrophic reservoir. Both phytoplankton and zooplankton composition can influence the stoichiometry of nutrients recycled through consumers (Balseiro et al. 1997; Hessen et al. 2013), though much of our understanding comes from oligotrophic and eutrophic ecosystems (Moegenburg and Vanni 1991; Elser et al. 2000). A previous analysis of mesozooplankton community and seston stoichiometry demonstrated that zooplankton N:P ratios in hypereutrophic ecosystems shifted towards N-rich species, suggesting zooplankton may contribute to higher phosphorus availability in hypereutrophic lakes (Moody and Wilkinson 2019). However, this analysis did not consider seasonal variability in zooplankton biomass, phytoplankton biomass, and nutrient concentrations (Sommer et al. 2012). I quantified zooplankton and phytoplankton community composition and biomass dynamics over the course of a growing season in a hypereutrophic reservoir (total P = 239 ± 154 μg L^{-1}, mean ± standard deviation), using allometric equations to estimate zooplankton excretion (Hébert et al. 2016), and individual measurements of zooplankton and

phytoplankton size to assess size structure dynamics. Through this analysis I estimated the contribution of zooplankton excretion to phosphorus availability and the influence of grazing on phytoplankton size structure.

For **Chapter 2,** I used interannual changes in lower food web size structure as a tool to assess whether incentivized harvest of common carp (*Cyprinus carpio*) and bigmouth buffalo (*Ictiobus cyprinellus*) significantly altered food web structure in a set of shallow, eutrophic lakes. Biomanipulation is a common management tool designed to shift pathways of energy and nutrient flow to improve ecosystem services (Shapiro et al. 1975; Jeppesen et al. 2012). However, when biomanipulations fail to improve water quality, it is difficult to disentangle whether the management intervention failed to alter food web structure or other drivers of water quality were more influential (Meijer et al. 1990, 1999). Assessing food web changes can be expensive and time intensive. The relationship between abundance and body size, or size spectrum, has been found to be a fundamental ecosystem property (Sprules and Barth 2016; Mehner et al. 2018), and changes in easily measured zooplankton and benthic macroinvertebrate size spectra may be an indicator of changes in food web structure (Barth et al. 2019; Evans et al. 2022). Thus, size spectra analysis may be a relatively simple yet useful tool to assess whether food web structure changes occurred following biomanipulation or not. I used size spectra analysis of zooplankton and benthic macroinvertebrates to quantify changes in food web structure in harvested (n=4) and non-harvested (n=3) shallow lakes and evaluate if this was a sensitive tool for monitoring restoration outcomes. This analysis indicated that the lack of water quality improvements following incentivized harvest were due to insufficient shifts in food web structure.

In **Chapter 3**, I quantified the resistance and resilience of primary production in ponds with varying food web structure to discrete disturbances (i.e., pulse additions of nutrients). High connectivity between benthic and pelagic food chains is theorized to generate greater top-down control and increase ecosystem resistance and resilience of primary production to nutrient loading (Vadeboncoeur et al. 2005; Blanchard et al. 2011; Rooney and McCann 2012), though there is limited empirical evidence. I designed an ecosystem experiment to quantify the response to two simulated storm-induced pulse disturbances in six paired (i.e., disturbed and reference) experimental ponds. The three food web structures varied between low, intermediate, and high degrees of benthic-pelagic coupling. This experiment provided empirical evidence that a greater degree of benthic-pelagic coupling conferred greater resistance and resilience to repeated perturbations.

In **Chapter 4,** I quantified the dynamics and distribution of energy fluxes and food web stability over 19 years in the pelagic food web of a north-temperate lake. Changes in food web structure through time can result in substantial changes to the magnitude and pathways of energy flow as trophic interactions shift (Barnes et al. 2018; Bartley et al. 2019). I leveraged a long-term dataset of biomass dynamics in Trout Lake, WI which underwent distinct changes in food web structure, including an invasion by the mid-trophic level macroinvertebrate, *Bythotrephes longimanus* (Martin et al. 2022). Using a bioenergetic approach (Gauzens et al. 2019; Jochum et al. 2021), I showed the influence of food web structure changes to ecosystem function and provide an ecological context to long-term changes in food web stability. This chapter demonstrated the ecosystem-level impacts of a mid-trophic level invader and the ability of a food web to absorb the shock of a species invasion, evidenced by long-term food web stability dynamics.

References

Balseiro, E. G., B. E. Modenutti, and C. P. Queimaliños. 1997. Nutrient recycling and shifts in N:P ratio by different zooplankton structures in a South Andes Lake. J Plankton Res **19**: 805–817. doi:10.1093/plankt/19.7.805

Barnes, A. D., M. Jochum, J. S. Lefcheck, N. Eisenhauer, C. Scherber, M. I. O'Connor, P. de Ruiter, and U. Brose. 2018. Energy Flux: The Link between Multitrophic Biodiversity and Ecosystem Functioning. Trends Ecol Evol **33**: 186–197. doi:10.1016/j.tree.2017.12.007

Barth, L. E., B. J. Shuter, W. G. Sprules, C. K. Minns, and J. A. Rusak. 2019. Calibration of the zooplankton community size spectrum as an indicator of change in canadian shield lakes. Canadian Journal of Fisheries and Aquatic Sciences **76**: 2268–2287. doi:10.1139/cjfas-2018-0371

Bartley, T. J., K. S. McCann, C. Bieg, and others. 2019. Food web rewiring in a changing world. Nat Ecol Evol **3**: 345–354. doi:10.1038/s41559-018-0772-3

Blanchard, J. L., R. Law, M. D. Castle, and S. Jennings. 2011. Coupled energy pathways and the resilience of size-structured food webs. Theor Ecol **4**: 289–300. doi:10.1007/s12080-010-0078-9

Elser, J. J., R. W. Sterner, A. E. Galford, and others. 2000. Pelagic C:N:P Stoichiometry in a Eutrophied Lake: Responses to a Whole-Lake Food-Web Manipulation. Ecosystems **3**: 293–307. doi:10.1007/s100210000027

Evans, T. M., Z. S. Feiner, L. G. Rudstam, and others. 2022. Size spectra analysis of a decade of Laurentian Great Lakes data. Canadian Journal of Fisheries and Aquatic Sciences **79**: 183–194. doi:10.1139/cjfas-2020-0144

Flood, P. J., A. Duran, M. Barton, A. E. Mercado-Molina, and J. C. Trexler. 2020. Invasion impacts on functions and services of aquatic ecosystems. Hydrobiologia **847**: 1571–1586. doi:10.1007/s10750-020-04211-3

Gauzens, B., A. Barnes, D. P. Giling, and others. 2019. fluxweb: An R package to easily estimate energy fluxes in food webs. Methods Ecol Evol **10**: 270–279. doi:10.1111/2041-210X.13109

Hébert, M. P., B. E. Beisner, and R. Maranger. 2016. A meta-analysis of zooplankton functional traits influencing ecosystem function. Ecology **97**: 1069–1080. doi:10.1890/15-1084.1

Hessen, D. O., J. J. Elser, R. W. Sterner, and J. Urabe. 2013. Ecological stoichiometry: An elementary approach using basic principles. Limnol Oceanogr **58**: 2219–2236. doi:10.4319/lo.2013.58.6.2219

Ho, J. C., and A. M. Michalak. 2020. Exploring temperature and precipitation impacts on harmful algal blooms across continental U.S. lakes. Limnol Oceanogr **65**: 992–1009. doi:10.1002/lno.11365

Hulme, P. E. 2017. Climate change and biological invasions: evidence, expectations, and response options. Biological Reviews **92**: 1297–1313. doi:10.1111/brv.12282

Jeppesen, E., M. Søndergaard, T. L. Lauridsen, and others. 2012. Biomanipulation as a Restoration Tool to Combat Eutrophication. Recent Advances and Future Challenges.

Jochum, M., A. D. Barnes, U. Brose, B. Gauzens, M. Sünnemann, A. Amyntas, and N. Eisenhauer. 2021. For flux's sake: General considerations for energy-flux calculations in ecological communities. Ecol Evol **11**: 12948–12969. doi:10.1002/ece3.8060

Kortsch, S., R. Frelat, L. Pecuchet, and others. 2021. Disentangling temporal food web dynamics facilitates understanding of ecosystem functioning. Journal of Animal Ecology 633. doi:10.1111/1365-2656.13447

Lindeman, R. L. 1942. The Trophic-Dynamic Aspect of Ecology. Ecology **23**: 399–417.

Marklund, M. H. K., R. Svanbäck, and P. Eklöv. 2019. Habitat coupling mediates trophic cascades in an aquatic community. Ecosphere **10**. doi:10.1002/ecs2.2863

Martin, B. E., J. R. Walsh, and M. J. Vander Zanden. 2022. Rise of a native apex predator and an invasive zooplankton cause successive ecological regime shifts in a North Temperate Lake. Limnol Oceanogr **67**: S163–S172. doi:10.1002/lno.12049

McMeans, B. C., K. S. McCann, T. D. Tunney, A. T. Fisk, A. M. Muir, N. Lester, B. Shuter, and N. Rooney. 2016. The adaptive capacity of lake food webs: From individuals to ecosystems. Ecol Monogr **86**: 4–19. doi:10.1890/15-0288.1

Mehner, T., B. Lischke, K. Scharnweber, K. Attermeyer, S. Brothers, U. Gaedke, S. Hilt, and S. Brucet. 2018. Empirical correspondence between trophic transfer efficiency in freshwater food webs and the slope of their size spectra. Ecology **99**: 1463–1472. doi:10.1002/ecy.2347

Meijer, M. L., I. De Boois, M. Scheffer, R. Portielje, and H. Hosper. 1999. Biomanipulation in shallow lakes in The Netherlands: An evaluation of 18 case studies. Hydrobiologia **408–409**: 13–30. doi:10.1007/978-94-017-2986-4_2

Meijer, M. L., M. W. de Haan, A. W. Breukelaar, and H. Buiteveld. 1990. Is reduction of the benthivorous fish an important cause of high transparency following biomanipulation in shallow lakes? Hydrobiologia **200–201**: 303–315. doi:10.1007/BF02530348

Moegenburg, S. M., and M. J. Vanni. 1991. Nutrient regeneration by zooplankton: Effects on nutrient limitation of phytoplankton in a eutrophic lake. J Plankton Res **13**: 573–588. doi:10.1093/plankt/13.3.573

Moody, E. K., and G. M. Wilkinson. 2019. Functional shifts in lake zooplankton communities with hypereutrophication. Freshw Biol **64**: 608–616. doi:10.1111/fwb.13246

Odum, E. P. 1968. Energy Flow in Ecosystems: A Historical Review. Am Zool **8**: 11–18.

Pelletier, M. C., J. Ebersole, K. Mulvaney, and others. 2020. Resilience of aquatic systems: Review and management implications. Aquat Sci **82**. doi:10.1007/s00027-020-00717-z

Pimm, S., J. Lawton, and J. Cohen. 1991. Food web patterns and their consequences. Nature **350**: 669–674.

Rahel, F. J., and J. D. Olden. 2008. Assessing the effects of climate change on aquatic invasive species. Conservation Biology **22**: 521–533. doi:10.1111/j.1523-1739.2008.00950.x

Rooney, N., and K. S. McCann. 2012. Integrating food web diversity, structure and stability. Trends Ecol Evol **27**: 40–46. doi:10.1016/j.tree.2011.09.001

De Ruiter, P. C., A.-M. Neutel, and J. C. Moore. 1995. Energetics, Patterns of Interaction Strengths, and Stability in Real Ecosystems. Science **269.** https://www.jstor.org/stable/2888010.

Seneviratne, S., X. Zhang, M. Adnan, and others. 2021. Weather and Climate Extreme Events in a Changing Climate, p. 1513–1766. *In* V. Masson-Delmotte, P. Zhai, A. Pirani, et al. [eds.], Climate Change 2021: The Physical Science Basis. Contribution of Working Group I to the Sixth Assessment Report of the Intergovernmental Panel on Climate Change. Cambridge University Press.

Shapiro, J., V. Lamarra, and M. Lynch. 1975. Biomanipulation: an ecosystem approach to lake restoration. Water Quality Management through Biological Control 85–96.

Sommer, U., R. Adrian, L. De Senerpont Domis, and others. 2012. Beyond the Plankton Ecology Group (PEG) Model: Mechanisms Driving Plankton Succession. Annu Rev Ecol Evol Syst **43**: 429–448. doi:10.1146/annurev-ecolsys-110411-160251

Sprules, W. G., and L. E. Barth. 2016. Surfing the biomass size spectrum: Some remarks on history, theory, and application. Canadian Journal of Fisheries and Aquatic Sciences **73**: 477–495. doi:10.1139/cjfas-2015-0115

Turner, M. G., W. J. Calder, G. S. Cumming, and others. 2020. Climate change, ecosystems and abrupt change: Science priorities. Philosophical Transactions of the Royal Society B: Biological Sciences **375**. doi:10.1098/rstb.2019.0105

Vadeboncoeur, Y., K. S. McCann, M. J. Vander Zanden, and J. B. Rasmussen. 2005. Effects of multi-chain omnivory on the strength of trophic control in lakes. Ecosystems **8**: 682–693. doi:10.1007/s10021-003-0149-5

Vanni, M. J. 2021. Invasive mussels regulate nutrient cycling in the largest freshwater ecosystem on earth. Proc Natl Acad Sci U S A **118**: 10–12. doi:10.1073/pnas.2100275118

Zscheischler, J., S. Westra, B. J. J. M. Van Den Hurk, and others. 2018. Future climate risk from compound events. Nat Clim Chang **8**: 469–477. doi:10.1038/s41558-018-0156-3

CHAPTER 1

CONTRIBUTION OF ZOOPLANKTON NUTRIENT RECYCLING AND EFFECTS ON PHYTOPLANKTON SIZE STRUCTURE IN A HYPEREUTROPHIC RESERVOIR

Published in the *Journal of Plankton Research:*

Butts, T.J., E.K. Moody, G.M. Wilkinson. 2022. Contribution of zooplankton nutrient recycling and effects on phytoplankton size structure in a hypereutrophic reservoir. *Journal of Plankton Research* 44(6) 861-865. https://doi.org/10.1093/plankt/fbac045.

Author contributions: Butts designed the study; performed all field and laboratory work cleaned, analyzed, and visualized the data; and wrote the manuscript. Moody and Wilkinson contributed to study design and data analysis in addition to providing feedback on writing.

ABSTRACT

Consumer nutrient recycling influences aquatic ecosystem functioning by altering the movement and transformation of nutrients. In hypereutrophic reservoirs, zooplankton nutrient recycling has been considered negligible due to high concentrations of available nutrients. A comparative analysis (Moody and Wilkinson, 2019) found that zooplankton communities in hypereutrophic lakes are dominated by nitrogen (N)-rich species, which the authors hypothesized would increase phosphorus (P) availability through excretion. However, zooplankton nutrient recycling likely varies over the course of a growing season due to changes in biomass, community composition, and grazing pressure on phytoplankton. We quantified zooplankton, phytoplankton, and nutrient concentration dynamics during the summer of 2019 in a temperate, hypereutrophic reservoir. We found that the estimated contribution of zooplankton excretion to the dissolved nutrient pool on a given day was equivalent to a substantial proportion (21-39%) of

the dissolved inorganic P standing stock in early summer when P concentrations were low and limiting phytoplankton growth. Further, we found evidence that zooplankton affected phytoplankton size distributions through selective grazing of smaller phytoplankton cells likely affecting nutrient uptake and storage by phytoplankton. Overall, our results demonstrate zooplankton excretion in hypereutrophic reservoirs likely helped drive springtime phytoplankton dynamics through nutrient recycling while grazing influenced phytoplankton size distributions.

INTRODUCTION

Animal consumers contribute to nutrient cycling in aquatic ecosystems by controlling the movement and transformation of nutrients over time and across space (Atkinson *et al.*, 2017). Aquatic consumers, like zooplankton, ingest phytoplankton then excrete and egest metabolized and unassimilated materials as waste, recycling nutrients back into the ecosystem (Vanni, 2002). Bioavailable nutrients are then taken up by phytoplankton to produce new biomass controlled by rates of nutrient uptake, cell size, and elemental stoichiometry (Finkel *et al.*, 2010; Sarnelle and Knapp, 2005). Imbalances between consumer demand for and assimilation efficiency of nutrients, as well as the elemental composition of phytoplankton, drives the stoichiometry of nutrients recycled back into the ecosystem (Elser and Hassett, 1994; Sterner, 1990). Consumer-resource imbalances lead to greater nutrient recycling of a particular element that may result in changes to ecosystem nutrient limitation and alter trophic interactions between consumers and their resource (Elser *et al.*, 2000; Dobberfuhl and Elser, 2000).

The community composition of both phytoplankton and zooplankton can influence the stoichiometry of recycled nutrients and generate strong differences in nitrogen (N) and phosphorus (P) recycling (Balseiro *et al.*, 1997). For example, copepods and small cladocerans

generally retain more N whereas *Daphnia* generally retain more P (Elser and Urabe, 1999). Differences in N and P retention between zooplankton taxa can result in copepod and small cladoceran-dominated communities retaining more N and recycling more P, potentially driving phytoplankton to N-limitation (Elser *et al.*, 2000, 1988). Further, differences in zooplankton preferred food size influence the species and morphology of phytoplankton subjected to grazing. For example, *Bosmina spp.* are moderately selective filter feeders, many copepods are highly selective raptorial feeders, and *Daphnia* are highly general filter feeders (Barnett *et al.*, 2007; *but see*, Hood and Sterner, 2010). Selection for phytoplankton based on zooplankton community grazing preferences and selectivity may then alter the phytoplankton community cell sizes and elemental composition ultimately influencing nutrient recycling (Finkel *et al.*, 2010). Phytoplankton community composition varies with trophic state, grazing pressure, and nutrient availability as different genera preferentially assimilate different forms of nitrogen (Andersen *et al.*, 2020). Cyanobacteria-dominated phytoplankton communities, which often arise in nutrient enriched ecosystems, are particularly resistant to zooplankton grazing due to the ability of many genera to form colonies or filaments, their poor nutritional quality, and toxin production (Moustaka-gouni and Sommer, 2020). During periods of cyanobacterial dominance, the majority of the zooplankton community can shift to grazing on smaller, unicellular phytoplankton that have different elemental stoichiometry and nutrient uptake rates (Beardall *et al.*, 2009). In combination, zooplankton-phytoplankton interactions affect nutrient recycling in aquatic ecosystems; however, the effects may vary depending on the severity of nutrient enrichment.

Much of our understanding regarding zooplankton nutrient recycling comes from oligotrophic and eutrophic ecosystems (Elser *et al.*, 2000; Moegenburg and Vanni, 1991), though many temperate lakes and reservoirs are increasingly becoming hypereutrophic due to continued

land use conversion and climate change (Stoddard *et al.*, 2016). The extremely high nutrient concentrations in hypereutrophic reservoirs can produce unique conditions compared to less enriched waterbodies such as large seasonal variability in nutrient limitation of phytoplankton growth (Andersen *et al.*, 2020), substantial internal P loading under oxic and anoxic conditions (Albright and Wilkinson, 2022; Song and Burgin, 2017), and a more complex mix of top-down and bottom-up forces affecting phytoplankton communities (Matsuzaki *et al.*, 2018). However, the contribution of zooplankton nutrient recycling in hypereutrophic ecosystems is often considered less important than other consumers like fish which can reach higher biomass in nutrient-rich ecosystems (Spooner *et al.*, 2013; Wilson and Xenopoulos, 2011; Vanni *et al.*, 2006). Despite this, zooplankton may still influence nutrient availability in hypereutrophic reservoirs as nutrient limitation and zooplankton biomass shift throughout the growing season. Additionally, selective feeding on small phytoplankton by small-bodied zooplankton can increase the dominance of large phytoplankton species, including filamentous and colonial cyanobacteria (Erdoğan *et al.*, 2021). This shift may influence nutrient availability as cyanobacteria have the capacity for luxury nutrient uptake, subsequent storage of excess nutrients, and the ability of some to fix atmospheric N (Cottingham *et al.*, 2015). As hypereutrophic lakes and reservoirs are often dominated by smaller-bodied zooplankton including microzooplankton and ciliates, selective grazing pressure on the phytoplankton community may indirectly influence nutrient availability.

A recent analysis of mesozooplankton (i.e., copepods, cladocerans, and rotifers; hereafter zooplankton) stoichiometric traits found that community N:P ratios shifted towards N-rich species with increasing eutrophication (Moody and Wilkinson, 2019). As such, in hypereutrophic ecosystems, zooplankton may contribute to P availability through recycling. This hypothesis was

supported by the fact that the seston N:P ratio was lower in hypereutrophic lakes and reservoirs compared to less-enriched ecosystems. This analysis suggested that the unique functioning of hypereutrophic lakes and reservoirs, even compared to eutrophic ecosystems, was due in part to the consumers inhabiting them. However, this was a comparative study among many lakes and reservoirs based on a single sampling point in the late summer. It is well established that zooplankton and phytoplankton communities are dynamic and undergo a seasonal succession during the summer driven by both top-down and bottom-up processes, which can vary depending on trophic state and other variables (Sommer *et al.*, 2012). Furthermore, the balance of top-down and bottom-up forces in lakes and reservoirs varies with nutrient ratios and concentrations across a season (Rogers *et al.*, 2020). In the scope of this comparative study (Moody and Wilkinson, 2019), the seasonal variability within zooplankton, phytoplankton, and nutrient dynamics was not captured. As such, it remains unclear how nutrient availability and phytoplankton communities are influenced by nutrient recycling and top-down grazing throughout the summer in hypereutrophic ecosystems.

We investigated the role of zooplankton nutrient recycling and top-down grazing on nutrient availability, phytoplankton biomass, and community composition in a hypereutrophic reservoir across a summer growing season. Specifically, our objectives were to (1) evaluate the temporal dynamics and magnitude of the contribution of zooplankton body nutrient storage and excretion to nutrient availability and (2) assess the effect of zooplankton grazing on phytoplankton biomass, community composition, and size structure over the growing season. To estimate the storage and flux of nutrients driven by zooplankton consumers we used effect traits that link individual body size and elemental composition to ecosystem processes (Hébert *et al.*, 2017; Hébert *et al.*, 2016b). We hypothesized that zooplankton excretion would contribute most

substantially to P availability early in the growing season due to higher zooplankton biomass in the spring (Sommer et al. 2012), low zooplankton community P storage, and lower rates of internal loading during this period. Conversely, we expected the contribution of zooplankton to N availability would be low at this time with high external loading of N from the watershed in the spring. We also hypothesized that zooplankton grazing, varying with community composition over the summer, would affect phytoplankton size structure due to selective grazing on smaller phytoplankton as well as drive changes in phytoplankton community composition. As such, smaller zooplankton body size would be associated with larger individual phytoplankton cell, colony, or filament sizes.

METHODS

Study Lake

Green Valley Lake (41°05’54” N, 94°23’02” W) is a hypereutrophic reservoir built in 1952 as an impoundment of the Platte River in southwestern Iowa (USA). The maximum depth is 7.3 m, with an average depth of 3.2 m and a surface area of 156 ha. Crappie (*Pomoxis spp.),* bluegill (*Lepomis macrochirus*), and largemouth bass (*Micropterus salmoides*) dominate the fish community. Additionally, there is a small population of common carp (*Cyprinus carpio*) and channel catfish (*Ictalurus punctatus*) (IDNR, 2022). The watershed is dominated by row crop agriculture (68.4% corn/soybean rotation). Consequently, Green Valley Lake is enriched with nutrients and beset by annual phytoplankton blooms dominated by cyanobacteria (Supplementary Figure S1). To characterize zooplankton nutrient recycling in Green Valley Lake, we sampled zooplankton, phytoplankton, and nutrient concentrations weekly at the deepest point in the reservoir from early May (day of year; DOY 143) to early September (DOY 251) of

2019. We sampled again on DOY 273, but only collected zooplankton and nutrient samples at that time. Additionally, we deployed a YSI EXO3 sonde (Yellow Springs Instruments, Yellow Springs, Ohio, USA) at 0.5 m at the deepest point in the reservoir and collected temperature and pH measurements every 15 minutes. We used daily averages for the dates sampled of each variable in our analyses.

Nutrient Measurements

The concentration and form of nutrients in Green Valley Lake were measured throughout the growing season to compare to the magnitude and temporal dynamics of zooplankton excretion (objective 1) and to assess the drivers of phytoplankton biomass and community composition (objective 2). We collected surface water samples at a depth of 0.25 m at the deep point. We filtered a subset of the water sample through Whatman glass fiber filters (pore size = 0.45 μm) in the field, preserved with concentrated sulfuric acid to a pH of 2, and stored at 4 ºC until later analysis for soluble reactive phosphorus (SRP) and nitrate + nitrite (NOx). Ammonium is rarely detectable in Green Valley Lake during the summer (see Supplementary Material) and was therefore not measured for our study. We preserved unfiltered sample water with concentrated sulfuric acid to a pH of 2 and stored at 4 ºC until later analysis for total phosphorus (TP) and total nitrogen (TN). We used the ascorbic acid method to quantify P concentrations with filtered water for SRP and unfiltered water that had undergone persulfate digestion for TP. We used second-derivative ultraviolet spectroscopy to quantify NOx concentrations in filtered samples and TN concentrations following persulfate digestion. The N species were analyzed using an Agilent Cary 8454 UV-VIS spectrophotometer (Agilent Technologies Inc, Santa Clara, CA, USA) and analyzed P species using a Seal Analytical AQ2 Discrete Analyzer (Seal

Analytical Inc. Mequon, WI, USA). For data analysis, nutrient concentrations below the limit of detection were replaced with the instrument-specific long-term method detection limit.

The nutrient concentrations were used to calculate total and dissolved inorganic molar N:P ratios. Nutrient limitation of phytoplankton growth was estimated based on the molar TN:TP ratio with N:P > 20 indicating P limitation (Guildford and Hecky, 2000).

Plankton Measurements

For each sampling event, zooplankton biomass and community composition were quantified to estimate the magnitude of nutrient excretion as well as the stoichiometry of nutrient storage (objective 1). In addition, phytoplankton biomass and community composition were quantified to compare with zooplankton dynamics across the summer growing season. Phytoplankton size structure and community composition were quantified to assess the temporal dynamics of zooplankton grazing (objective 2). Zooplankton were sampled via a vertical tow of a Wisconsin net (63 μm mesh) from 6 m depth. The samples were preserved with a formaldehyde solution (5% concentration after sample addition) in the field and later transferred to 70% ethanol. Phytoplankton samples were a composite sample over depth. We collected water in a 4 L Van Dorn sampler from 0.25, 1, 2, 3, and 4 m depths (the top of the thermocline), then mixed it in a 20 L carboy in the field. We then took a 1 L sample from the carboy following thorough mixing and preserved with Lugol's solution in the field.

We identified and enumerated zooplankton samples with a Leica MZ8 stereomicroscope connected to Motic Images software. For each sample, a 1 mL subsample was taken and a minimum of 60 individual zooplankton were identified to genus for cladocerans and rotifers, order for copepods, and class for ostracods. Copepod nauplii could not be identified to order and

were simply identified as nauplii. If less than 60 organisms were in the subsample, we counted a second 1 mL subsample. We measured zooplankton lengths for up to 25 individuals per taxon per sample to calculate dry mass per liter using length-mass regressions (McCauley, 1984; Dumont *et al.*, 1975). For visual display of the zooplankton data, they were separated into ten taxonomic groups: *Daphnia, Simocephalus, Ceriodaphnia*, *Bosmina, Chydorus*, rotifers, calanoids, cyclopoids, nauplii, and ostracods (Supplementary Table S1). *Simocephalus* contributed only 7% of total community biomass at its peak and so were grouped with *Daphnia* for further statistical analyses.

We transferred the 1 L phytoplankton samples to a graduated cylinder and allowed phytoplankton to settle in a dark environment for 8 days before removing the supernatant with a vacuum pump, leaving 50 mL of concentrated sample. We then removed a subsample from the concentrated sample and identified and enumerated individuals using a modified Palmer-Maloney chamber. We identified phytoplankton to genus and measured them using a calibrated ocular reticle on a Leitz DM IL inverted microscope at 400x magnification. For each sample, we measured a minimum of 300 natural units across 8 fields. We calculated biovolume per liter based on phytoplankton shape and then converted to wet biomass per liter assuming a 1:1 ratio between wet mass and biovolume (Hillebrand *et al.*, 1999; Sournia, 1978). We also measured the greatest axial linear dimension (GALD) of phytoplankton as the greatest distance across an individual cell, colony, or filament (i.e., natural unit), such as would be encountered by a zooplankton grazer. Like zooplankton, we separated phytoplankton genera into six groups for visual display: bacillariophytes, chlorophytes, chryso- and cryptophytes, *Aphanothece*, *Microcystis,* and other cyanophytes (Supplementary Table S2). Both *Aphanothece* and

Microcystis were the dominant genera of cyanobacteria, contributing the majority of phytoplankton biomass (88 ± 18%; s.d.) and therefore were visualized separately.

Zooplankton Stoichiometry and Excretion Analysis

To assess the contribution of zooplankton excretion to nutrient availability (objective 1) we calculated zooplankton community elemental composition, nutrient storage, and excretion rate. We estimated elemental composition and total nutrient storage by zooplankton (L^{-1} d^{-1}) following methods described previously (Moody and Wilkinson, 2019). Briefly, we used taxa-specific %N and %P information collected from the literature (Hamre, 2016; Hébert *et al.*, 2016a; Hessen *et al.*, 2007) to estimate total nutrient storage by multiplying %N and %P by the biomass of each taxa and summing across the community on each sampling date. Although we are using trait data from largely oligotrophic lakes, zooplankton have fairly strong stoichiometric homeostasis (Persson *et al.*, 2010) as well as low intraspecific stoichiometric variation between aquatic ecosystems (Prater *et al.*, 2017) and variable food quality (Teurlincx *et al.*, 2017). Thus, it is unlikely that intraspecific variation in %N and %P have a large influence on our calculations.

We estimated excretion rates of N and P by zooplankton using published allometric equations (Supplementary Material). The equations relate zooplankton body size to N (ammonia) and P (phosphate) derived from a compiled dataset of marine and freshwater zooplankton species (Hébert *et al.*, 2016b, 2016a). Temperature is an important control on an organism's metabolism, however, the excretion rates used to calculate the allometric equations accounted for differences in temperature by applying a standardized temperature correction (Hébert *et al.*, 2016a; Hernández-León and Ikeda, 2005). Therefore, the temperature dependence of metabolism and

excretion is not being incorporated into the seasonal aspect of our study. Additionally, the allometric equations were not derived using data from rotifers, but rather for copepods and cladocerans. As such, we removed rotifers from our excretion analyses. For each sampling event, we used the average dry mass of each zooplankton taxon present to calculate individual N and P excretion rates (μM N or P individual^{-1} hour^{-1}) using the allometric equations. We then converted the hourly excretion rate to a daily rate (day^{-1}) and multiplied the daily rate by the density of each taxon (individuals L^{-1}) to calculate the taxon-specific daily excretion rates. Finally, we summed the daily excretion rates across all taxa on a sampling date to calculate the total zooplankton community excretion rate (μM N or P day^{-1}). Uncertainty in the excretion estimates was calculated by propagating the variation in the slope and intercept from the allometric equations presented in Hébert *et al.*, (2016b) through our calculations of the community excretion rates. Given that these calculations are an estimate, we also calculated zooplankton excretion using other published allometric equations from Wen and Peters (1994) derived from different underlying datasets. The overall pattern of zooplankton excretion did not differ between the two methods; however, excretion estimates derived from the Wen and Peters (1994) allometric equations were slightly higher (Supplementary Table S3). We chose to use the more conservative estimate of zooplankton excretion rates based on Hébert et al. (2016) in our analysis as the available information also allowed us to estimate uncertainty.

To assess the magnitude of zooplankton N and P excretion in Green Valley Lake we compared the estimated concentration of excreted N and P over the course of a day to the measured surface water concentrations of dissolved inorganic N and P for each sampling event, assuming diel nutrient concentrations remain relatively stable over 24 hours (Shirokova *et al.*,

2020; Nimick *et al.*, 2011). We expressed this value as a percent of the dissolved inorganic nutrient pool:

$$\left(\frac{\mu M\ N\ or\ P\ excreted\ by\ zooplankton\ community\ in\ a\ day}{\mu M\ of\ inorganic\ N\ or\ P\ present\ in\ the\ surface\ waters}\right) * 100 \qquad (1)$$

To assess how zooplankton excretion would affect nutrient cycling over the course of the growing season we calculated the zooplankton nutrient turnover time of the dissolved inorganic P pool (Conroy *et al.*, 2005). Zooplankton nutrient turnover time relates to nutrient cycling by estimating the number of days it would take for zooplankton excretion to replenish the mass of P (the standing stock) measured in the reservoir on a given day independent of nutrient uptake. The turnover time varies depending on the rate of zooplankton excretion and concentration of inorganic dissolved P in the surface waters. Short turnover times indicate zooplankton are contributing substantially to the dissolved inorganic P pool in Green Valley Lake. Long turnover times indicate factors other than zooplankton excretion are driving nutrient availability.

Zooplankton Grazing and Phytoplankton Size Structure Analysis

To assess the effect of zooplankton grazing on phytoplankton size structure and community composition (objective 2) we estimated the relative strength of top-down v. bottom up-control, compared zooplankton and phytoplankton size distributions, estimated zooplankton feeding range, and assessed the drivers of phytoplankton community composition across the growing season in Green Valley Lake. We determined the relative importance of top-down v. bottom-up control in lakes by calculating the ratio (expressed as a percentage of zooplankton biomass relative to phytoplankton biomass (Filstrup *et al.*, 2014; Heathcote *et al.*, 2016). A high zooplankton to phytoplankton biomass percentage (~40-50%) indicates strong top-down control,

whereas a low percentage (~10%) indicates weak top-down control (Leroux and Loreau, 2015; Havens and Beaver, 2013). Additionally, we compared the size distributions of zooplankton and phytoplankton communities over time using our measurements of zooplankton length and phytoplankton GALD. Phytoplankton sizes span orders of magnitudes and are selected for by diverse pressures, thus the distribution of phytoplankton GALD can be used to infer nutrient uptake and grazing pressure (Litchman *et al.*, 2010). We compared distributions of zooplankton length and body mass to the distribution of phytoplankton GALD for each sampling date to investigate the size distribution dynamics over time. Additionally, we performed a Pearson correlation of mean phytoplankton GALD versus mean zooplankton size to assess whether phytoplankton GALD was dictated by zooplankton body size.

In addition to zooplankton body size, functional feeding groups can affect how zooplankton interact with phytoplankton, either through selective raptorial feeding or non-discriminate grazing (Barnett *et al.*, 2007). We collected data from the literature on food size range, the smallest and largest reported particles consumed by a taxa, based on constituents of the zooplankton community on each sample date. We then incorporated the zooplankton community food size range into our comparison of zooplankton and phytoplankton size distributions (Supplementary Material). Briefly, we compiled the minimum and maximum reported food size range for groups of taxa we observed within our study (Supplementary Table S4). We then calculated a daily mean minimum and maximum food size range for the zooplankton community weighted by taxon biomass. The effective food size range was then compared to the distributions of zooplankton length and phytoplankton GALD. To assess the drivers of phytoplankton community composition across the growing season we performed a distance based-redundancy analysis (db-RDA). We included potentially important environmental

variables such as dissolved inorganic nutrient concentrations (Filstrup and Downing, 2017), temperature (Striebel *et al.*, 2016)**,** and pH (Rönicke *et al.*, 2010), as well as zooplankton biomass, excretion N:P, and body stoichiometry (Table 1**).** We used a Hellinger transformation for the phytoplankton genera biomass data and removed genera that only occurred once in the full dataset and contributed <1% of total biomass to decrease the weight of rare species. Environmental variables were z-transformed in order to correct for differences in scale and magnitude (Legendre and Legendre, 1998). We performed the db-RDA using a Bray-Curtis distance matrix taking the square root of dissimilarities to avoid negative eigenvalues (Legendre and Anderson, 1999). We removed missing or lost samples from the final analysis. Forward and backward stepwise regression was used to select the best model. We determined model significance using a Monte Carlo permutation test (999 permutations, p-value < 0.05). We then confirmed the variables used in the final model did not contain any multicollinearity by ensuring the square root of each variable's variance inflation factor was less than two.

All analyses were performed using the statistical software R version 4.0.4 (R Core Team, 2021) with the*, magrittr,* and *vegan* packages (Bach and Wickham, 2020; Oksanen *et al.*, 2020).

RESULTS

Seasonal Dynamics

Nutrient concentrations and inferred limitation of phytoplankton growth were dynamic throughout the summer (Figure 1). Dissolved inorganic N concentrations were highest in the spring and decreased by 80% from the peak after DOY 178 (Figure 1A). At the same time, there was a rapid increase in dissolved inorganic P by 394% from DOY 172 to 178 and a 937% increase from DOY 178 to DOY 206 (Figure 1B). Molar TN:TP declined rapidly in mid-July

(DOY 192), transitioning the ecosystem from P- to intermittent N-limitation. There was also a shift in dissolved inorganic N:P to N-limitation in mid-July that was persistent for the remainder of the summer (Figure 1C). Zooplankton elemental body composition was dominated by N storage in both the early and late summer. Zooplankton P storage remained relatively low, but nearly equaled dissolved inorganic P concentrations in the water column early in the summer (Figure 1B). Zooplankton community body N:P was quite variable with the highest N:P ratios in early to mid-summer and relatively low values near the end of summer (Figure 1D). However, the increases in dissolved inorganic P observed in the water column were not concurrent with increases in zooplankton community body N:P and instead were likely driven by other processes in the lake.

Zooplankton and phytoplankton biomass and community composition varied substantially over the summer growing season. Zooplankton biomass peaked at 249 $\mu g\ L^{-1}$ in late May and early June (DOY 150-164), rapidly decreased (~2 $\mu g\ L^{-1}$) in mid-July to late August (DOY 192 – DOY 234), before increasing in early autumn (Figure 2A). The early summer zooplankton community was dominated by *Daphnia* and calanoid copepods which transitioned in early July (DOY 199) to *Chydorus* and cyclopoid copepods, before transitioning back to *Daphnia* in late August (Figure 2A). Similarly, phytoplankton biomass was initially high in the spring, mainly composed of bacillariophytes, before rapidly decreasing during the clear-water period between DOY 150 – 164 (Figure 2B). Following DOY 172, the phytoplankton community was overwhelmingly composed of cyanophytes, mainly *Microcystis*, with phytoplankton reaching peak biomass on DOY 213 (~329 $mg\ L^{-1}$). *Daphnia* biomass decreased rapidly following increasing *Microcystis* biomass coinciding with an overall decrease in

zooplankton biomass (Figure 2). The other abundant cyanophyte was the diazotroph *Aphanothece,* which was present from DOY 192 – 228.

Zooplankton Excretion

The daily estimated concentration of P excreted by zooplankton was equivalent to a substantial portion of the dissolved inorganic P pool. However, this contribution was only particularly large from late May to late June (DOY 143-172). The concentration of daily excretion during this early summer period was between 21-39% of the dissolved inorganic P standing stock (Figure 3A). This proportionally high contribution from zooplankton P excretion coincided with a period of higher zooplankton body N:P (Figure 1D) and higher zooplankton body N storage. Following DOY 172, the concentration of P excreted by zooplankton dropped below 1% of the dissolved inorganic P pool for the remainder of the sampling period. Zooplankton excretion contributed to a rapid turnover of the dissolved inorganic P pool in early summer with turnover times ranging between 3 – 5 days but increased beyond 200 days as dissolved inorganic P concentrations increased in late June (Supplementary Table S5). Estimated zooplankton N excretion was never equivalent to more than 3.3% of the dissolved inorganic N pool (Figure 3B). The N:P ratio of zooplankton excretion was relatively stable over the course of the growing season (Supplementary Figure S2).

Plankton Size Structure

The ratio of zooplankton: phytoplankton biomass was less than 7% throughout the summer, indicating minimal top-down control on phytoplankton biomass (Supplementary Figure S3). However, based on the plankton size distributions, zooplankton likely influenced

phytoplankton GALD in mid- to late summer. Small zooplankton dominated from late June to early August (DOY 178 – 213) concurrent with a period in which larger phytoplankton dominated the GALD distribution (Figure 4A). Phytoplankton average GALD was greatest in July (mean = 32.5 ± 19.6 µm; s.d.) when zooplankton average length was at its lowest (mean = 171 ± 102 µm; s.d.). During this period (DOY 192 – 199) the zooplankton community food size range included 0 - 3% of individual phytoplankton GALD measurements, which were the lowest percentages of the entire growing season (Supplementary Figure S4). We also found evidence that smaller zooplankton body size was associated with larger phytoplankton GALD supporting our prediction**.** In late July through August, the difference in zooplankton length and phytoplankton GALD steadily increased, surpassing the mean differences observed in early summer (Figure 4B). A similar pattern was observed between phytoplankton GALD and zooplankton dry mass (Supplementary Figure S5). Additionally, there was a weak negative correlation between GALD and zooplankton length (p=0.0119, r(12)=-0.65; Supplementary Figure S6A), and zooplankton body mass (p=0.0306, r(12)=-0.58; Supplementary Figure S6B).

Contrary to our hypothesis, the db-RDA analysis showed that variation in phytoplankton community composition was not significantly influenced by zooplankton (Figure 5, Table 2). Following variable selection and removal of multicollinear variables only dissolved inorganic N (p=0.043) and temperature (p=0.003) were significantly correlated with variation in phytoplankton community composition explaining 21.9% of total variation. Additionally, only the first axis was significant which separated the phytoplankton community between pre- and post-dominance of cyanobacteria (F=3.62, p=0.004). Phytoplankton community composition was correlated with dissolved inorganic N in early summer prior to the cyanobacteria bloom.

Beginning on DOY 172 phytoplankton community composition became more correlated with temperature.

DISCUSSION

We sought to better understand zooplankton nutrient cycling in hypereutrophic ecosystems by observing zooplankton-phytoplankton dynamics and nutrient concentrations across a summer growing season. We used size and stoichiometric traits to infer excretion and body stoichiometry to assess the degree to which zooplankton influenced the transformation and flux of nutrients within the water column despite the high variability observed in these pools over time. We found that zooplankton excretion contributed substantially to P availability during the early summer, potentially having a bottom-up effect on phytoplankton biomass (objective 1). In late summer, we found zooplankton size structure likely influenced phytoplankton community size structure with smaller-bodied zooplankton having a top-down effect, resulting in increased phytoplankton GALD (objective 2). However, contrary to our hypothesis, we found that zooplankton did not influence phytoplankton community composition.

Nutrient and Plankton Seasonal Dynamics

The seasonal transition between P and N-limitation or co-limitation we observed in Green Valley Lake has also been reported in other eutrophic and hypereutrophic ecosystems (Andersen *et al.*, 2020; Wang *et al.*, 2019). In Green Valley, the large increase in dissolved inorganic P beginning on DOY 178 resulted in the transition from strong P-limitation to co-limitation or N-limitation. This increase in dissolved P in the surface waters was driven by both oxic and anoxic internal P loading (Albright and Wilkinson, 2022). Zooplankton and phytoplankton biomass and

community composition were quite variable, though they both roughly followed expected patterns of seasonal succession (Sommer *et al.* 2012).

Effect of zooplankton excretion on nutrient availability

Supporting our first hypothesis, we found that zooplankton excretion of P was equivalent to a large portion (21 – 39%) of the dissolved inorganic P pool in Green Valley Lake, but only during early summer (objective 1). It was during this period that dissolved inorganic P was at relatively low concentrations in the water column (0.13 – 0.19 μM) and phytoplankton growth was likely P-limited, indicating that zooplankton-mediated recycling contributed to meeting nutrient demand by phytoplankton during this time. This early-season P availability, facilitated by zooplankton recycling, may have helped initialize the cyanotoxin-producing cyanobacteria bloom that flourished later in the season and persisted until late summer (Isles and Pomati, 2021). The contribution of zooplankton excretion to dissolved inorganic P availability is consistent with the hypothesis from Moody and Wilkinson (2019) that N-rich zooplankton communities can contribute to increased P availability within nutrient-rich ecosystems. However, we found that zooplankton community N:P and zooplankton excretion dynamics were context- and time-dependent over the course of the growing season. As such, zooplankton-mediated flux of P was mainly confined to the early part of the growing season when zooplankton biomass was high, zooplankton community N-storage was relatively high, and dissolved inorganic P concentrations were relatively low. Furthermore, our estimates of P turnover by zooplankton indicated rapid turnover of dissolved inorganic P during early summer, but turnover drastically slowed once P concentrations rose. These results support our conclusions that zooplankton

nutrient recycling was an important P flux during the early summer growing season, but not an important flux once internal loading increased P availability.

Overall, the contribution of zooplankton nutrient-recycling to the dissolved inorganic N pool in Green Valley Lake was negligible. However, the uptake of ammonium from zooplankton excretion by phytoplankton may have been too fast to result in a measurable concentration, masking the contribution of zooplankton excretion to N availability. Alternatively, we may be underestimating N excretion given that our estimates of zooplankton excretion were not taxon-specific, but instead based on a consolidated dataset of both cladocerans and copepods. This is particularly true when daphniids dominate in the early and late-summer periods, which could increase community N excretion as *Daphnia* retain more P than N due largely to their body stoichiometry (Elser *et al.*, 1988). Overall, our estimates of zooplankton excretion were low relative to the concentrations of dissolved inorganic nutrients in the ecosystem across the summer; however, they were comparable with other studies using similar allometric equations (Conroy *et al.*, 2005) or direct measurement (den Oude and Gulati, 1988) in eutrophic ecosystems. The low variability in zooplankton excretion N:P was likely an artifact of the allometric equations we used to estimate excretion. The excretion estimates used to build the allometric equations were derived from a combination of copepod and cladoceran species in both freshwater and marine environments. This collation of multiple species likely masked any variation in excretion N:P we would expect to observe from differences in food quality and species elemental composition.

In addition to zooplankton, other consumers can play a key role in nutrient recycling in eutrophic lakes and reservoirs, particularly detritivores and planktivores such as gizzard shad (Sharitt *et al.*, 2021; Vanni *et al.*, 2006) and mussels (Arnott and Vanni, 1996). However, neither

gizzard shad nor zebra mussels have been reported in Green Valley Lake. While we did not quantify the contribution of nutrient recycling by other consumers to availability in Green Valley Lake, these organisms certainly contributed. There is a common carp (*Cyprinus carpio*) population in Green Valley Lake which can influence nutrient cycling through bioturbation and excretion (Weber and Brown, 2009); however, the population is small. We hypothesize that the contributions of fish and other organisms would have a similar seasonality given the large contribution of internal P in the latter half of the season.

Role of zooplankton excretion and grazing on phytoplankton community structure

In support of our second hypothesis, we found evidence that zooplankton community size structure may have influenced the size structure of the phytoplankton community (objective 2). This is despite the fact that we observed weak top-down control on phytoplankton biomass, consistent with other studies in hypereutrophic lakes (Rogers *et al.*, 2020; Matsuzaki *et al.*, 2018). The negative correlation between zooplankton length and phytoplankton GALD is consistent with other studies in hypereutrophic ecosystems indicating that small-bodied zooplankton preferentially graze on smaller phytoplankton, increasing the dominance of large filamentous and colonial phytoplankton (Bairagi *et al.*, 2019; Onandia *et al.*, 2015). By grazing on smaller sized phytoplankton cells or colonies, zooplankton can reduce the abundance of smaller phytoplankton leaving a greater proportion of individuals with large GALD to dominate the overall size distribution. This was evidenced by the phytoplankton community size structure shifting towards higher GALD, likely driven by an increase in *Microcystis* colonies observed in July through early August. It is likely that smaller-bodied zooplankton were contributing, in part, to the dominance of *Microcystis* colonies and higher phytoplankton GALD by removing smaller

phytoplankton cells. The low percentage of phytoplankton GALD measurements that fell within the zooplankton community food size range midsummer suggests that zooplankton were grazing on smaller phytoplankton cells, increasing the average GALD of the phytoplankton community. Effectively, the phytoplankton left behind following zooplankton grazing were mostly large colonial *Microcystis.*

However, it is unlikely zooplankton were the sole cause of increased phytoplankton GALD. The drawdown of dissolved inorganic N we observed midsummer coincided with the bloom of *Microcystis* beginning on DOY 172, suggesting efficient N uptake by *Microcystis*. Availability of dissolved inorganic N promotes *Microcystis* growth and was likely influencing the proliferation of *Microcystis* colonies (Chen *et al.*, 2019). However, nutrients and grazing can interact to affect phytoplankton GALD, where grazing by zooplankton, along with increased nutrients, promotes greater phytoplankton community GALD (Cottingham, 1999). While *Microcystis* toxicity can dampen zooplankton grazing, zooplankton community grazing on toxic *Microcystis* has been documented previously (Davis et al. 2012). Furthermore, over the summer growing season, the increased incidence of toxin-producing Cyanobacteria can even induce shifts towards toxin-resistant phenotypes in zooplankton populations (Schaffner *et al.*, 2019). Thus, it is likely that zooplankton grazing on toxic cyanobacteria occurred in Green Valley Lake, influencing phytoplankton size structure. The size structure of communities is closely tied to food web structure and energy flow (Brose *et al.*, 2017), thus the influence of the zooplankton community on phytoplankton size structure we observed was likely influential on the transfer, uptake, and recycling of nutrients by phytoplankton.

It is also likely that microzooplankton and ciliates played an important role grazing on small phytoplankton species; however, we did not quantify these communities in this study.

Furthermore, our phytoplankton counting methods were unable to facilitate the identification of nano- or picophytoplankton species in the water column. Microzooplankton, nano- and picophytoplankton are increasingly recognized as key components of the plankton food web and contribute a significant percentage of grazing pressure on phytoplankton in highly productive ecosystems (Agasild *et al.*, 2007; Zingel *et al.*, 2007). Future studies should examine their seasonal dynamics and potential contribution to ecosystem processes more thoroughly as they can be key components of zooplankton-phytoplankton interactions in nutrient-rich reservoirs.

The redundancy analysis (db-RDA) suggested that neither zooplankton top-down control nor nutrient recycling significantly affected variation in phytoplankton community composition. The db-RDA was able to discriminate the phytoplankton community between pre- and post-cyanobacterial dominance likely driven by the overwhelming dominance of *Microcystis* beginning on DOY 172. The early summer phytoplankton community was significantly related to the concentration of dissolved inorganic N which corresponds with the seasonal dynamic of nutrient limitation we observed as both chlorophytes and bacillariophytes perform well under P-limitation (Berg *et al.*, 2003). Furthermore, the dissolved inorganic N pool was highest in early summer and predominantly composed of nitrate which can be taken up and used by bacillariophytes (Andersen *et al.*, 2020). The mid- to late-summer phytoplankton community was significantly related to temperature, consistent with other studies describing increasing temperature as a key driver of cyanobacteria dominance (Hayes *et al.*, 2020). Other unobserved environmental factors were likely influencing the phytoplankton community as the db-RDA described only 21.88% of variation in the phytoplankton community composition. Phytoplankton community turnover is a complex phenomenon driven by a multitude of environmental factors (Wentzky *et al.*, 2020; Sommer *et al.*, 2012), including nutrient and light availability, the latter of

which we did not measure. Given the high biomass of phytoplankton, light limitation through self-shading likely played a significant role in phytoplankton dynamics.

CONCLUSIONS

While the importance of consumer-driven nutrient recycling has been demonstrated in less eutrophic waterbodies, the role that zooplankton consumers have on nutrient availability and phytoplankton dynamics in hypereutrophic reservoirs is understudied. Our results support a previous comparative study indicating that zooplankton community composition may influence nutrient availability in hypereutrophic ecosystems, as well as extend our understanding of the temporal dynamics of zooplankton and phytoplankton interactions. We found evidence of the importance of zooplankton nutrient cycling in a hypereutrophic reservoir with zooplankton excretion providing a large portion of the available P early in the summer, prior to the onset of the cyanobacteria-dominated bloom later in the season. If we had only assessed the late summer period or only a few time points across the summer, we would have likely missed the important dynamics in nutrient availability and zooplankton nutrient cycling we observed. In addition to the bottom-up influences of zooplankton, we found that zooplankton affected phytoplankton size structure contributing to increased phytoplankton community GALD. While we did not observe total top-down control of the phytoplankton community, the influence of zooplankton on phytoplankton size structure has important implications to nutrient recycling as size is a key trait regulating biogeochemical cycling in phytoplankton. As demonstrated here, the role of zooplankton nutrient recycling in hypereutrophic reservoirs is an important component of phytoplankton dynamics and ecosystem function that should be considered in greater detail. Unlike previous assumptions that zooplankton do not contribute substantially to nutrient cycling and phytoplankton dynamics in hypereutrophic ecosystems, our results suggest that zooplankton

do in fact contribute to those dynamics, predominantly for a short period early in the summer. Future work should investigate the dynamics of zooplankton nutrient recycling across different climate contexts and over longer time periods, including dynamics through winter and autumn.

ACKNOWLEDGEMENTS

We would like to thank Shania Walker, Halle Rosenboom, Quin Shingai, Rachel Fleck, Elena Sandry, Psalm Amos, Julia Schneller, Adriana Le-Compte, and Ellen Albright for assistance with sample collection and analysis. Additionally, we thank Riley Barbour for assistance with phytoplankton identification and enumeration. We thank Dr. Marie-Pier Hébert and one anonymous reviewer for providing insightful comments that improved the manuscript.

FUNDING

This project was funded by the Iowa Department of Natural Resources (Grant # 19CRDLWBMBALM-0010) and the U.S. Department of Agriculture National Institute of Food and Agriculture (Grant # 2018-09746)**.** This material is based upon work supported by the National Science Foundation (NSF) Graduate Research Fellowship Program (Grant # DGE-1747503) and NSF Grant # 2200391 to Wilkinson. Any opinions, findings, and conclusions or recommendations expressed in this material are those of the authors and do not necessarily reflect the views of the National Science Foundation.

DATA ARCHIVING

The data (Butts *et al.* 2022) and analysis code (Butts, 2022) are available from Zenodo (https://doi.org/10.5281/zenodo.6991082).

REFERENCES

Agasild, H. *et al.* (2007) Contribution of different zooplankton groups in grazing on phytoplankton in shallow eutrophic Lake Võrtsjärv (Estonia). *Hydrobiologia*, **584**, 167–177.

Albright, E. and Wilkinson, G. (2022) Sediment phosphorus composition controls hot spots and hot moments of internal loading in a temperate reservoir. *Ecosphere,* **13,** e4201.

Andersen, I. M. *et al.* (2020) Nitrate, ammonium, and phosphorus drive seasonal nutrient limitation of chlorophytes, cyanobacteria, and diatoms in a hyper-eutrophic reservoir. *Limnol. Oceanogr.*, **65**, 962–978.

Arnott, D. L. and Vanni, M. J. (1996) Nitrogen and phosphorus recycling by the zebra mussel (*Dreissena polymorpha*) in the western basin of Lake Erie. *Can. J. Fish. Aquat. Sci.*, **53**, 646–659.

Atkinson, C. L. *et al.* (2017) Consumer-driven nutrient dynamics in freshwater ecosystems: from individuals to ecosystems. *Biol. Rev.*, **92**, 2003–2023.

Bach, S. and Wickham, H. (2020) magrittr: A forward-Pipe Operator for R. R package version 2.0.1. https://CRAN.R-project.org/package=magrittr.

Bairagi, N. *et al.* (2019) Zooplankton selectivity and nutritional value of phytoplankton influences a rich variety of dynamics in a plankton population model. *Phys. Rev. E*, **99**, 012406.

Balseiro, E. G. *et al.* (1997) Nutrient recycling and shifts in N:P ratio by different zooplankton structures in a South Andes Lake. *J. Plankton Res.*, **19**, 805–817.

Barnett, A. J. *et al.* (2007) Functional diversity of crustacean zooplankton communities : towards a trait-based classification. *Freshw. Biol.* **52,** 796–813.

Beardall, J. *et al.* (2009) Allometry and stoichiometry of unicellular, colonial and multicellular phytoplankton. *New Phytol.*, **181**, 295–309.

Berg, G. M. *et al.* (2003) Plankton community composition in relation to availability and uptake of oxidized and reduced nitrogen. *Aquat. Microb. Ecol.*, **30**, 263–274.

Brose, U. *et al.* (2017) Predicting the consequences of species loss using size-structured biodiversity approaches. *Biol. Rev.*, **92**, 684–697.

Butts, T.J. (2022). tjbutts/hyper-plankton: Contribution of zooplankton nutrient recycling and effects on phytoplankton size structure in a hypereutrophic reservoir. *Zenodo*. https://doi.org/10.5281/zenodo.6991082

Butts, T.J., Moody, E.K., Wilkinson, G.M., and Barbour, R.J. (2022). Summer water chemistry, phytoplankton and zooplankton community composition, size structure, and biomass in a shallow, hypereutrophic reservoir in southwestern Iowa, USA (2019). ver 1. *Environmental Data Initiative*. https://doi.org/10.6073/pasta/46c2de115b4a4b16699f5ebc9976ca01.

Chen, Q. *et al.* (2019) Physiological effects of nitrate, ammonium, and urea on the growth and microcystins contamination of Microcystis aeruginosa: Implication for nitrogen mitigation. *Water Res.*, **163**, 114890.

Conroy, J. D. *et al.* (2005) Soluble nitrogen and phosphorus excretion of exotic freshwater mussels (Dreissena spp.): Potential impacts for nutrient remineralisation in western Lake Erie. *Freshw. Biol.*, **50**, 1146–1162.

Cottingham, K. L. *et al.* (2015) Cyanobacteria as biological drivers of lake nitrogen and phosphorus cycling. *Ecosphere*, **6**, 1–19.

Cottingham, K. L. (1999) Nutrients and zooplankton as multiple stressors of phytoplankton communities: Evidence from size structure. *Limnol. Oceanogr.*, **44**, 810–827.

Davis, T. W., Koch, F., Marcoval, M. A., Wilhelm, S. W., and Gobler, C. J. (2012) Mesozooplankton and microzooplankton grazing during cyanobacterial blooms in the western basin of Lake Erie. *Harmful Algae*, **15**, 26–35.

Dobberfuhl, D. R. and Elser, J. J. (2000) Elemental stoichiometry of lower food web components in arctic and temperate lakes. *J. Plankton Res.*, **22**, 1341–1354.

Dumont, H. J. *et al.* (1975) The dry weight estimate of biomass in a selection of Cladocera, Copepoda and Rotifera from the plankton, periphyton and benthos of continental waters. *Oecologia*, **19**, 75–97.

Elser, J. and Hassett, R. (1994) A stoichiometric analysis of the zooplankton-phytoplankton interaction in marine and freshwater ecosystems. *Nature*, **370**, 211–213.

Elser, J. J. *et al.* (2000) Pelagic C:N:P Stoichiometry in a Eutrophied Lake: Responses to a Whole-Lake Food-Web Manipulation. *Ecosystems*, **3**, 293–307.

Elser, J. J. *et al.* (1988) Zooplankton-mediated transitions between N- and P-limited growth. *Limnol. Oceanogr.*, **33**, 1–14.

Elser, J. and Urabe, J. (1999) The Stoichiometry of Consumer-Driven Nutrient Recycling: Theory, Observations, and Consequences. *Ecology*, **80**, 735–751.

Erdoğan, Ş. *et al.* (2021) Determinants of phytoplankton size structure in warm, shallow lakes. *J.*

Plankton Res., **43**, 353–366.

Filstrup, C. T. *et al.* (2014) Cyanobacteria dominance influences resource use efficiency and community turnover in phytoplankton and zooplankton communities. *Ecol. Lett.*, **17**, 464–474.

Filstrup, C. T. and Downing, J. A. (2017) Relationship of chlorophyll to phosphorus and nitrogen in nutrient-rich lakes. *Inl. Waters*, **7**, 385–400.

Finkel, Z. V. *et al.* (2010) Phytoplankton in a changing world: Cell size and elemental stoichiometry. *J. Plankton Res.*, **32**, 119–137.

Guildford, S. J. and Hecky, R. E. (2000) Total nitrogen, total phosphorus, and nutrient limitation in lakes and oceans: Is there a common relationship? *Limnol. Oceanogr.*, **45**, 1213–1223.

Hamre, K. (2016) Nutrient profiles of rotifers (Brachionus sp.) and rotifer diets from four different marine fish hatcheries. *Aquaculture*, **450**, 136–142.

Havens, K. E. and Beaver, J. R. (2013) Zooplankton to phytoplankton biomass ratios in shallow Florida lakes: An evaluation of seasonality and hypotheses about factors controlling variability. *Hydrobiologia*, **703**, 177–187.

Hayes, N. M. *et al.* (2020) Effects of lake warming on the seasonal risk of toxic cyanobacteria exposure. *Limnol. Oceanogr. Lett.*, **5**, 393–402.

Heathcote, A. J. *et al.* (2016) Biomass pyramids in lake plankton: influence of Cyanobacteria size and abundance. *Inl. Waters*, **6**, 250–257.

Hébert, M. P. *et al.* (2016a) A compilation of quantitative functional traits for marine and freshwater crustacean zooplankton. *Ecology*, **97**, 1081.

Hébert, M. P. *et al.* (2016b) A meta-analysis of zooplankton functional traits influencing ecosystem function. *Ecology*, **97**, 1069–1080.

Hébert, M. P. *et al.* (2017) Linking zooplankton communities to ecosystem functioning: Toward an effect-Trait framework. *J. Plankton Res.*, **39**, 3–12.

Hernández-León, S. and Ikeda, T. (2005) Zooplankton respiration. In del Giorgio, P. A. and le B. Williams, P. (eds), *Respiration in aquatic ecosystems*. Oxford University Press, Oxford (UK), p. 582.

Hessen, D. O. *et al.* (2007) RNA responses to N- and P-limitation; reciprocal regulation of stoichiometry and growth rate in Brachionus. *Funct. Ecol.*, **21**, 956–962.

Hillebrand, H. *et al.* (1999) Biovolume calculation for pelagic and benthic microalgae. *J.*

Phycol., **35**, 403–424.

Hood, J. M. and Sterner, R. W. (2010) Diet mixing: Do animals integrate growth or resources across temporal heterogeneity? *Am. Nat.*, **176**, 651–663.

Iowa Department of Natural Resources (IDNR) (2022) Fish Survey Data. Iowa Department of Natural Resources, Des Moines, IA. https://www.iowadnr.gov/Fishing/Fish-Survey-Data

Isles, P. D. F. and Pomati, F. (2021) An operational framework for defining and forecasting phytoplankton blooms. *Front. Ecol. Environ.*, in press.

Legendre, P. and Anderson, M. (1999) Distance-based redundancy analysis: Testing multispecies responses in multifactorial ecological experiments. *Ecol. Monogr.*, **69**, 1–24.

Legendre, P. and Legendre, L. (1998) *Numerical Ecology*. 2nd ed. Elsevier, Amsterdam.

Leroux, S. and Loreau, M. (2015) Theoretical perspectives on bottom-up and top-down interactions across ecosystems. In Hanley, T. and La Pierre, K. (eds), *Trophic Ecology: Bottom-up and top-down interactions across aquatic and terrestrial systems*. Cambridge University Press, pp. 3–27.

Litchman, E. *et al.* (2010) Linking traits to species diversity and community structure in phytoplankton. *Hydrobiologia*, **653**, 15–28.

Matsuzaki, S. Ichiro, S., Suzuki, K., Kadoya, T., Nakagawa, M., and Takamura, N. (2018) Bottom-up linkages between primary production, zooplankton, and fish in a shallow, hypereutrophic lake. *Ecology*, **99**, 2025–2036.

McCauley, E. (1984) The estimation of the abundance and biomass of zooplankton in samples. In Downing, J. and Rigler, F. (eds), *A manual on methods for the assessment of secondary productivity in fresh waters*. Blackwell Publishing Ltd, Oxford (UK), pp. 228–265.

Moegenburg, S. M. and Vanni, M. J. (1991) Nutrient regeneration by zooplankton: Effects on nutrient limitation of phytoplankton in a eutrophic lake. *J. Plankton Res.*, **13**, 573–588.

Moody, E. K. and Wilkinson, G. M. (2019) Functional shifts in lake zooplankton communities with hypereutrophication. *Freshw. Biol.*, **64**, 608–616.

Moustaka-gouni, M. and Sommer, U. (2020) Effects of Harmful Blooms of Large-Sized and Colonial Cyanobacteria on Aquatic Food Webs. *Water*, **12**, 1–19.

Nimick, D. A. *et al.* (2011) Diel biogeochemical processes and their effect on the aqueous chemistry of streams: A review. *Chem. Geol.*, **283**, 3–17.

Oksanen, J. *et al.* (2020) vegan: Community Ecology Package. R package version 2.5-7.

https://CRAN.R-project.org/package=vegan.

Onandia, G. *et al.* (2015) Zooplankton grazing on natural algae and bacteria under hypertrophic conditions. *Limnetica*, **34**, 541–560.

den Oude, P. J. and Gulati, R. D. (1988) Phosphorus and nitrogen excretion rates of zooplankton from the eutrophic Loosdrecht lakes, with notes on other P sources for phytoplankton requirements. *Hydrobiologia*, **169**, 379–390.

Persson, J. *et al.* (2010) To be or not to be what you eat: Regulation of stoichiometric homeostasis among autotrophs and heterotrophs. *Oikos*, **119**, 741–751.

Prater, C. *et al.* (2017) Interactive effects of genotype and food quality on consumer growth rate and elemental content. *Ecology*, **98**, 1399–1408.

R Core Team (2021) R: A language and environment for statistical computing. R foundation for Statistical Computing, Vienna, Austria. https://www.R-project.org.

Rogers, T. *et al.* (2020) Trophic control changes with season and nutrient loading in lakes. *Ecol. Lett.*, **23**, 1287–1297.

Rönicke, H. *et al.* (2010) Changes of the plankton community composition during chemical neutralisation of the Bockwitz pit lake. *Limnologica*, **40**, 191–198.

Sarnelle, O. and Knapp, R. A. (2005) Nutrient recycling by fish versus zooplankton grazing as drivers of the trophic cascade in alpine lakes. *Limnol. Oceanogr.*, **50**, 2032–2042.

Schaffner, L. R. *et al.* (2019) Consumer-resource dynamics is an eco-evolutionary process in a natural plankton community. *Nat. Ecol. Evol.*, **3**, 1351–1358.

Sharitt, C. A. *et al.* (2021) Nutrient excretion by fish supports a variable but significant proportion of lake primary productivity over 15 years. *Ecology*, **0**, 1–8.

Shirokova, L. S. *et al.* (2020) Diel cycles of carbon, nutrient and metal in humic lakes of permafrost peatlands. *Sci. Total Environ.*, **737**, 139671.

Sommer, U. *et al.* (2012) Beyond the Plankton Ecology Group (PEG) Model: Mechanisms Driving Plankton Succession. *Annu. Rev. Ecol. Evol. Syst.*, **43**, 429–448.

Song, K. and Burgin, A. J. (2017) Perpetual Phosphorus Cycling: Eutrophication Amplifies Biological Control on Internal Phosphorus Loading in Agricultural Reservoirs. *Ecosystems*, **20**, 1483–1493.

Sournia, A. (1978) Phytoplankton Manual. *Monographs on Oceanographic Methodology*. UNESCO, Paris.

Spooner, D. E. *et al.* (2013) Nutrient loading associated with agriculture land use dampens the importance of consumer-mediated niche construction. *Ecol. Lett.*, **16**, 1115–1125.

Sterner, R. W. (1990) The Ratio of Nitrogen to Phosphorus Resupplied by Herbivores : Zooplankton and the Algal Competitive Arena. *Am. Nat.*, **136**, 209–229.

Stoddard, J. L. *et al.* (2016) Continental-Scale Increase in Lake and Stream Phosphorus: Are Oligotrophic Systems Disappearing in the United States? *Environ. Sci. Technol.*, **50**, 3409–3415.

Striebel, M. *et al.* (2016) Phytoplankton responses to temperature increases are constrained by abiotic conditions and community composition. *Oecologia*, **182**, 815–827.

Teurlincx, S. *et al.* (2017) Species sorting and stoichiometric plasticity control community C:P ratio of first-order aquatic consumers. *Ecol. Lett.*, **20**, 751–760.

Vanni, M. J. (2002) Nutrient cycling by animals in freshwater ecosystems. *Annu. Rev. Ecol. Syst.*, **33**, 341–370.

Vanni, M. J. *et al.* (2006) Nutrient cycling by fish supports relatively more primary production as lake productivity increases. *Ecology*, **87**, 1696–1709.

Wang, M. *et al.* (2019) Seasonal Pattern of Nutrient Limitation in a Eutrophic Lake and Quantitative Analysis of the Impacts from Internal Nutrient Cycling. *Environ. Sci. Technol.*, **53**, 13675–13686.

Weber, M. J. and Brown, M. L. (2009) Effects of Common Carp on Aquatic Ecosystems 80 Years after “Carp as a Dominant”: Ecological Insights for Fisheries Management. *Rev. Fish. Sci.*, **17**, 524–537.

Wen, Y. H. and Peters, R. H. (1994) Empirical models of phosphorus and nitrogen excretion rates by zooplankton. *Limnol. Oceanogr.*, **39**, 1669–1679.

Wentzky, V. C. *et al.* (2020) Seasonal succession of functional traits in phytoplankton communities and their interaction with trophic state. *J. Ecol.*, **108**, 1649–1663.

Wilson, H. F. and Xenopoulos, M. A. (2011) Nutrient recycling by fish in streams along a gradient of agricultural land use. *Glob. Chang. Biol.*, **17**, 130–139.

Zingel, P. *et al.* (2007) Ciliates are the dominant grazers on pico- and nanoplankton in a shallow, naturally highly eutrophic lake. *Microb. Ecol.*, **53**, 134–142.

TABLES

Table 1. List of initial explanatory variables input to the distance based-Redundancy Analysis of phytoplankton community composition.

Explanatory Variable	Mean	Range
Zooplankton Biomass (μg L^{-1})	87.88	1.78 - 248.55
Zooplankton N:P Excretion	3.05	2.56 - 3.52
Zooplankton Community N:P	18.29	13.62 - 23.59
Dissolved Inorganic N (μM)	33.44	2.86 - 103.50
Temperature (°C)	87.88	1.78 - 248.55
pH	18.29	13.62 - 23.59

Table 2. Statistics for the distance based-Redundancy Analysis of phytoplankton community composition in Green Valley Lake from May to September 2019.

Permutation test variable	Sums of Squares	pseudo-*F*	*p*-value
Full model	1.27	2.68	**0.001**
First axis	0.86	3.62	**0.004**
Second axis	0.41	1.74	0.073
Inorganic N	0.47	2.00	**0.043**
Temperature (°C)	0.80	3.36	**0.003**
Residual	2.37		

FIGURES

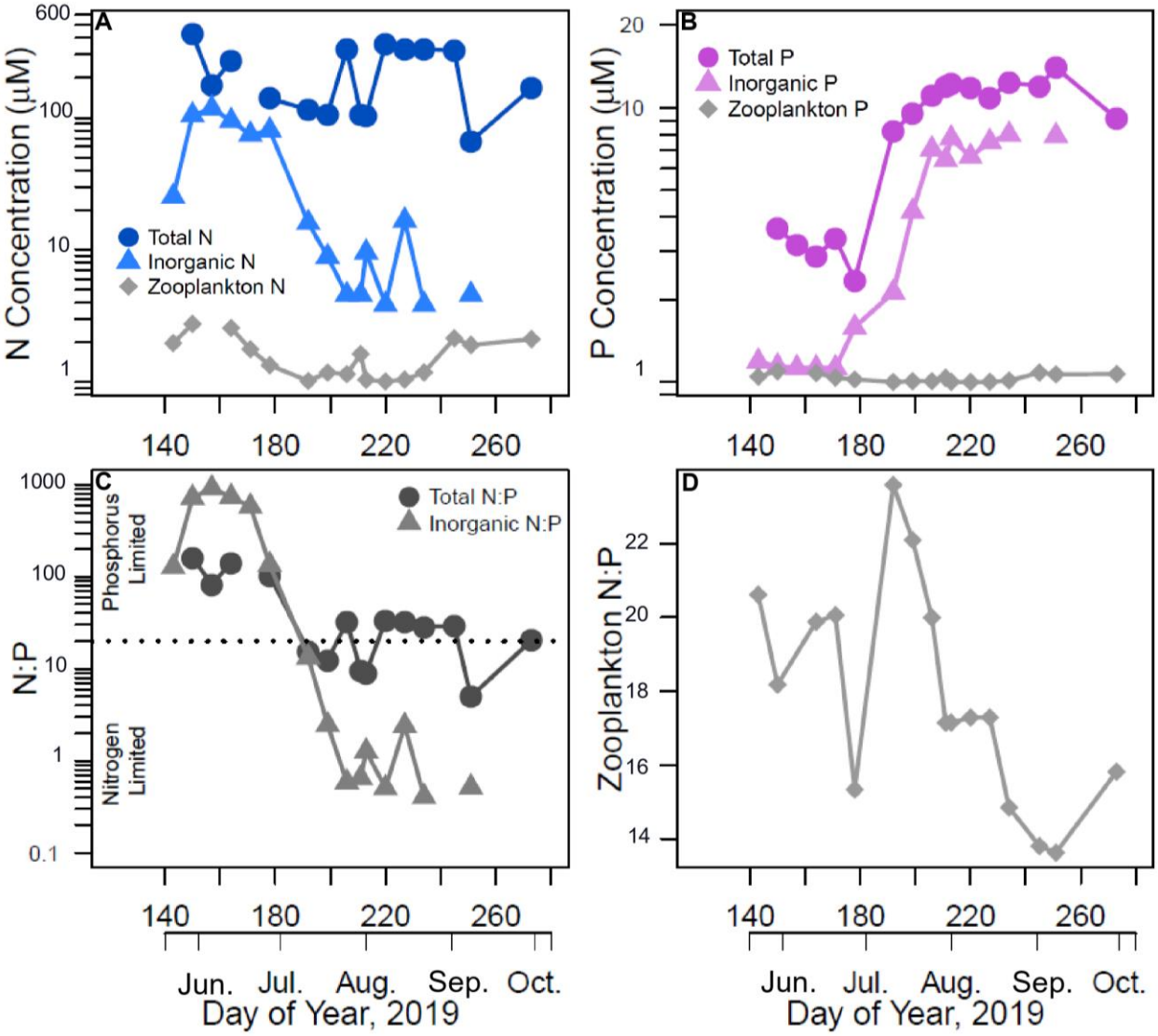

Figure 1. (A) Surface water nitrogen and (B) phosphorus concentrations split between total, dissolved inorganic, and zooplankton body storage over the course of the growing season. (C) surface water molar nitrogen: phosphorus (N:P) ratios split between total and inorganic pools with the dashed line denoting inferred nutrient limitation (Guildford and Hecky, 2000). (D) molar N:P ratios of the zooplankton community.

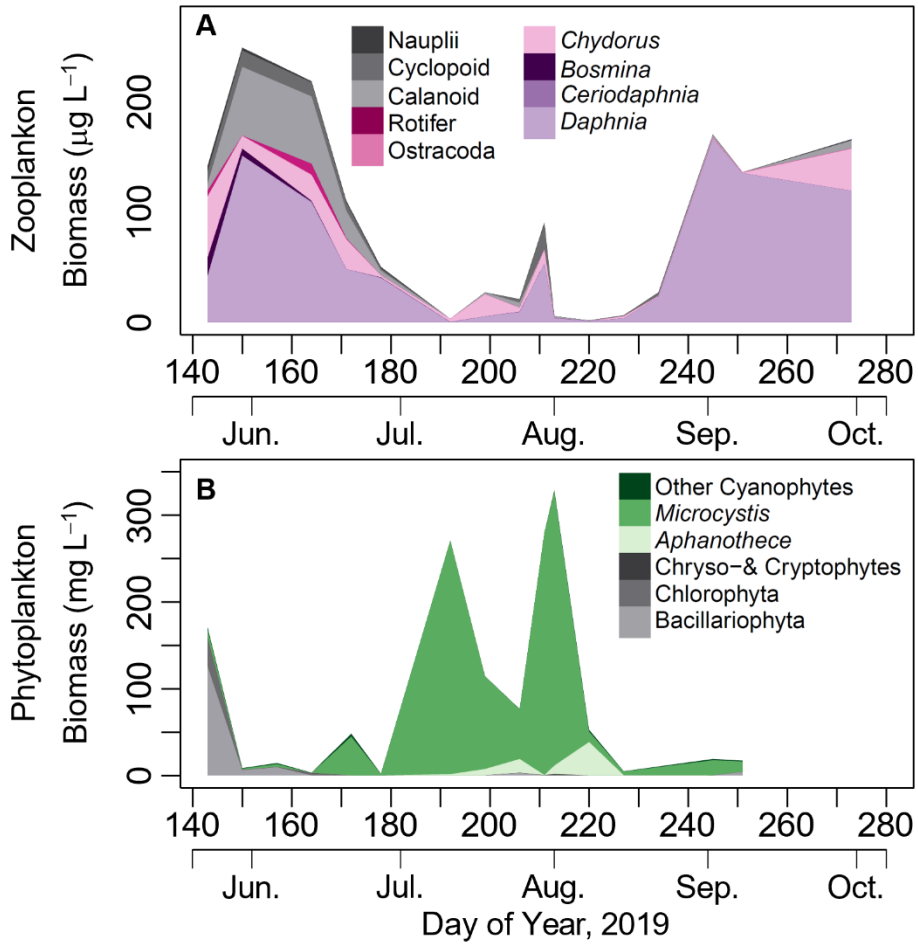

Figure 2. (A) Zooplankton biomass and community composition and (B) phytoplankton biomass and community composition over the course of the growing season in Green Valley Lake, IA.

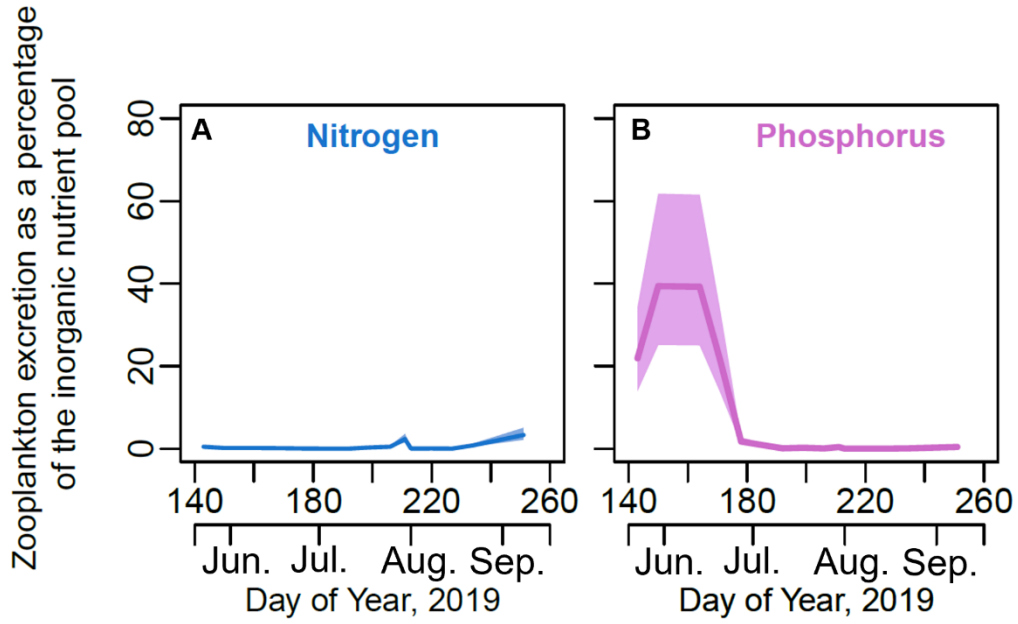

Figure 3. The estimated concentration of total zooplankton community excretion produced over a day compared with the surface water dissolved (A) nitrogen and (B) phosphorus concentrations measured the same day as a percentage. Estimates of zooplankton excretion were derived from published allometric equations of zooplankton body size and excretion rate (Hébert, *et al.*, 2016). The dark lines represent the estimated excretion of either phosphorus or nitrogen, and the shaded area represents the error associated with the estimate for each sampling day.

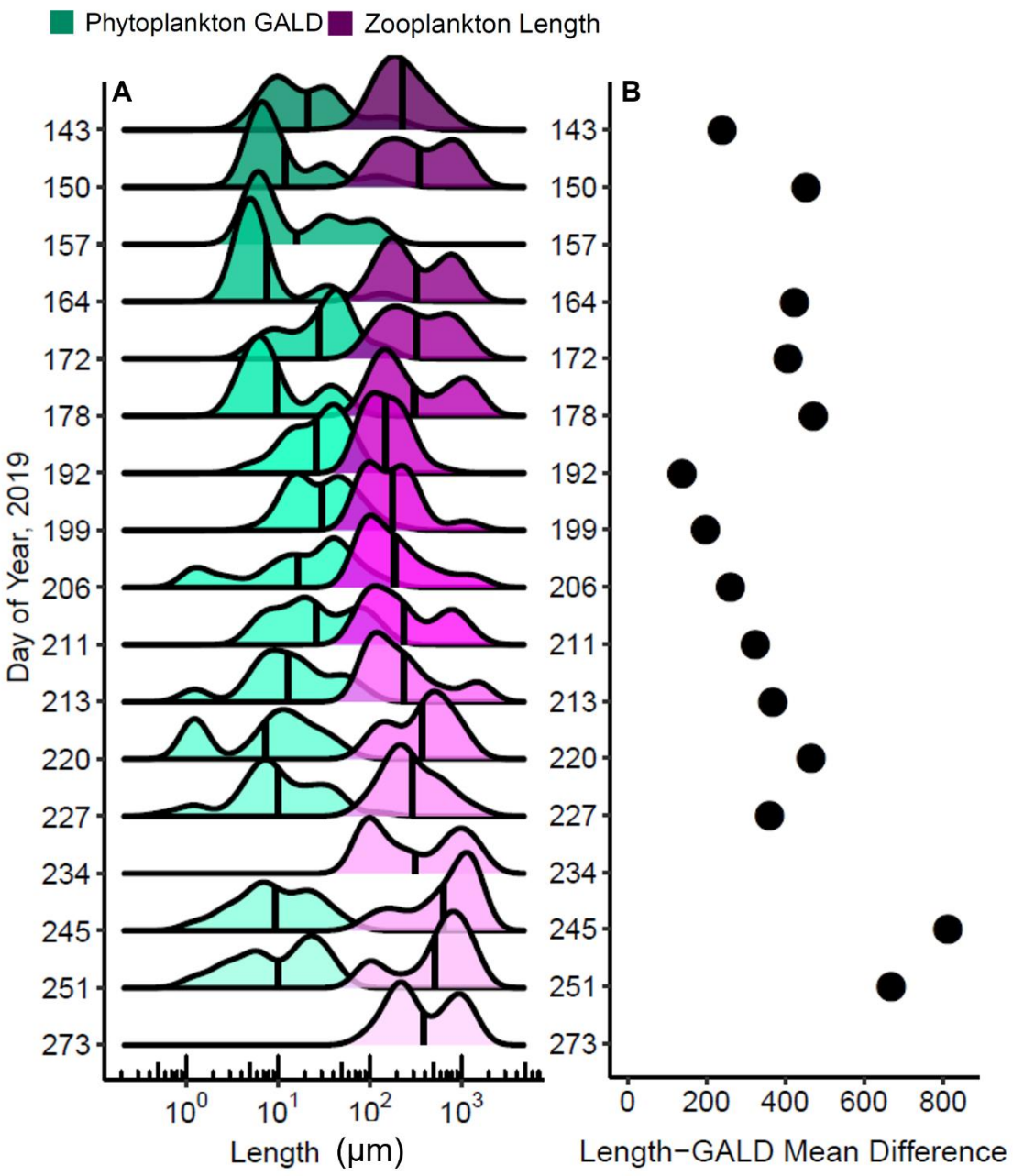

Figure 4. (A) Density ridgeline plots of phytoplankton greatest axial linear dimension (GALD, µm) and zooplankton body size (µm) over the course of the growing season in Green Valley Lake, IA. The black vertical line within each distribution represents the mean. (B) Mean difference between zooplankton length and phytoplankton GALD. DOYs that are missing either phytoplankton GALD or zooplankton length are the result of sample loss or no available data.

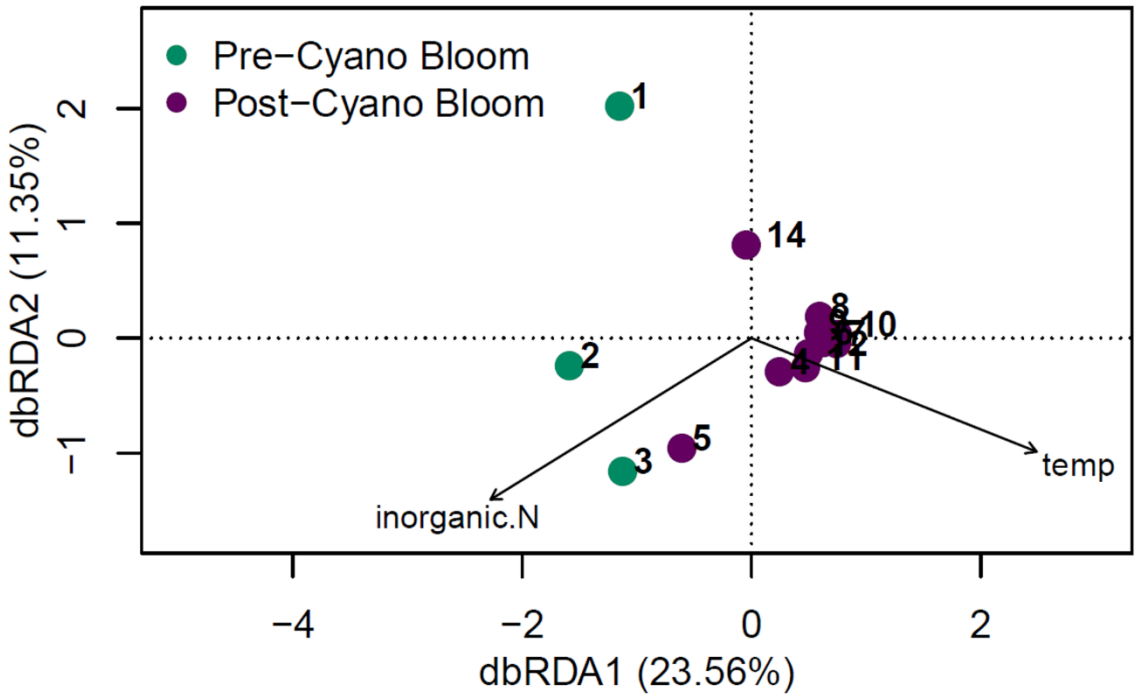

Figure 5. Distance based-Redundancy Analysis (db-RDA) of the phytoplankton community in Green Valley Lake from May to September 2019. Dots represent sampling points, and the numbers 1-14 are DOY 143, 150, 164, 172, 178, 192, 199, 206, 211, 213, 220, 227, 245, 251, respectively. DOY 245 (13) was omitted from the diagram as there were no available data for inorganic N and P thus the data were omitted from the analysis. The significant explanatory variables are represented by black arrows.

SUPPLEMENTARY INFORMATION FOR CHAPTER 1

SUPPLEMENTARY METHODS

Nutrient concentrations and speciation

The following equations describe how we defined the major fractions of nitrogen (N) and phosphorus (P) in Green Valley Lake. Total N in freshwater is composed organic and inorganic fractions:

$$TN = orgN + DIN \quad (1)$$

where *TN* is total N, *orgN* is organic N in both the particulate (organisms and detritus) and dissolved (urea) form, and *DIN* is dissolved inorganic N composed of *NOx* and *NHx* representing nitrate + nitrite and ammonium + ammonia, respectively. Previous data from the last decade in Green Valley Lake indicated *NHx* were extremely low or undetectable in the surface waters during the summer months. If we assume that *NHx* is undetectable (1) simplifies to:

$$TN = orgN + NOx \quad (2)$$

allowing calculation of *orgN* by rearranging (2):

$$orgN = TN - NOx \quad (3)$$

Thus, we could characterize N pools as total (*TN*) representing dissolved and particulate forms of N, organic (*orgN*) representing dissolved organic N (urea) and seston, and inorganic N (*NOx)* representing *DIN* in the surface waters. For our analyses we focused on the TN and DIN pools.

Similarly, P is composed of organic and inorganic fractions in reservoir surface waters:

$$TP = POP + PIP + DIP + DOP \quad (4)$$

where *TP* is total P, *POP* is particulate organic P, *PIP* is particulate inorganic P, *DIP* is dissolved inorganic P, and *DOP* is dissolved organic P. *DIP* and *PIP* were both present within the water column, but our focus for this study was on *DIP* which is far more bioavailable to phytoplankton

than *PIP* (Zhou *et al.*, 2005) and thus more influential to nutrient cycling via zooplankton-phytoplankton interactions. Previous data from the last decade in Green Valley Lake indicated *PIP* was extremely low or undetectable in the surface waters during the summer months. Thus, (4) can be simplified by combining *DOP* and *POP* to one organic pool (*orgP*) and using *SRP* as a measure of *DIP* over the course of the growing season:

$$TP = orgP + SRP \quad (5)$$

Therefore, we could characterize P pools as total (*TP*) representing dissolved and particulate forms of P, organic (*orgP*) representing dissolved organic P and seston, and inorganic (*SRP*) representing *DIP* in the surface waters. For our analyses we focused on the TP and SRP pools.

Ammonium + ammonia (NHx) (EPA method 103-A v6) and inorganic suspended solids were measured at the same location in the lake three times during the summer by the Iowa Ambient Lakes Monitoring program (IDNR 2021)**.** Ammonium was analyzed through the alkaline phenate method on a Seal Analytical AQ2 Discrete Analyzer and inorganic particulates were determined via difference between total and volatile suspended solids (USGS method I-3765-85).

Zooplankton excretion equations

Individual zooplankton excretion of P was determined using the following equation from Hébert *et al.*, (2016):

$$ln\left(P_{exc,h}\right) = 0.56 + \left(0.70ln(Z_{BS})\right) \quad (6)$$

where $P_{exc,h}$ is excreted P (nM of P individual^{-1} hour^{-1}) and Z_{BS} is the dry mass of an individual zooplankter (mg). Zooplankton excretion of N was determined in a similar manner:

$$ln\left(N_{exc,h}\right) = 2.50 + \left(0.84ln(Z_{BS})\right) \quad (7)$$

where $N_{exc,h}$ is excreted N (nM of N individual^{-1} hour^{-1}).

Data were then converted to µM of N or P per day using the following conversions:

$$\frac{nmol\ N\ or\ P}{individual\ \cdot hour} \cdot \frac{24\ hours}{1\ day} \cdot \frac{individuals}{L} \cdot \frac{1\ \mu mol}{1000\ nmol} = \frac{\mu M\ N\ or\ P}{day} \quad (8)$$

The allometric equations were derived from a combined dataset of marine and freshwater zooplankton. Using only the freshwater data did not significantly change the slope, nor was the relationship between excretion and body size significant due to the much smaller sample size. Thus, we only present the combined freshwater and marine model as presented in Hébert *et al.* (2016). Additionally, we used zooplankton excretion equations from Wen and Peters (1994). Specifically, we used their multivariate regression equations for crustacean zooplankton which corrected for temperature (K) and experimental duration (h) in their estimates of excretion. As our data did not have an experimental duration, we dropped the experimental duration correction resulting in the following equations:

$$Log_{10}(P_{exc,wp}) = -5.28 + (0.61 * log_{10}(Z_{BS})) + (0.01 * T) \quad (9)$$

Where $P_{exc,wp}$ is excreted P (µg d^{-1}), Z_{BS} is the body size of an individual zooplankter (µg), and T is water temperature (K).Similarly, for N excretion:

$$Log_{10}(N_{exc,wp}) = -3.47 + (0.74 * log_{10}(Z_{BS})) + (0.00002 * T^2) \quad (10)$$

Where $N_{exc,wp}$ is excreted N (µg d^{-1}), Z_{BS} is the body size of an individual zooplankter (µg), and T is water temperature (K). The pattern of zooplankton excretion was consistent between the two methods; however, the magnitude of excretion was different (Supplementary Table S3).

Zooplankton Food Size Range

We collected data on the reported food size range of *Bosmina, Ceriodaphnia, Chydorus, Daphnia, Diaphanosoma,* Cyclopoida, Calanoida, Rotifera, and nauplii from the literature

(Sweeney *et al.*, 2022; Helenius and Saiz, 2017; Barnett *et al.*, 2007). If a species primarily fed on zooplankton rather than phytoplankton, they were not included within our trait data. We did not find appropriate food size range data for Ostracods and thus they were removed from our analysis. If there were multiple size ranges reported for different species within a larger taxonomic group (e.g., *Daphnia*) we calculated the mean of the minimum food size range and maximum food size range (Supplementary Table S4).

SUPPLEMENTAL REFERENCES

Barnett, A. J. *et al.* (2007) Functional diversity of crustacean zooplankton communities : towards a trait-based classification. 796–813.

Havens, K. E. and Beaver, J. R. (2013) Zooplankton to phytoplankton biomass ratios in shallow Florida lakes: An evaluation of seasonality and hypotheses about factors controlling variability. *Hydrobiologia*, **703**, 177–187.

Hébert, M. P. *et al.* (2016) A meta-analysis of zooplankton functional traits influencing ecosystem function. *Ecology*, **97**, 1069–1080.

Helenius, L. K. and Saiz, E. (2017) Feeding behaviour of the nauplii of the marine calanoid copepod Paracartia grani Sars: Functional response, prey size spectrum, and effects of the presence of alternative prey. *PLoS One*, **12**, 1–20.

Iowa Department of Natural Resources (IDNR) (2021) Water Quality Monitoring and Assessment Section. AQuIA [database].

Leroux, S. and Loreau, M. (2015) Theoretical perspectives on bottom-up and top-down interactions across ecosystems. In Hanley, T. and La Pierre, K. (eds), *Trophic Ecology: Bottom-up and top-down interactions across aquatic and terrestrial systems*. Cambridge University Press, pp. 3–27.

Sweeney, K. *et al.* (2022) Grazing impacts of rotifer zooplankton on a cyanobacteria bloom in a shallow temperate lake (Vancouver Lake , WA ,. *Hydrobiologia*.

Wen, Y. H. and Peters, R. H. (1994) Empirical models of phosphorus and nitrogen excretion rates by zooplankton. *Limnol. Oceanogr.*, **39**, 1669–1679.

Zhou, A. *et al.* (2005) Phosphorus adsorption on natural sediments: Modeling and effects of pH

and sediment composition. *Water Res.*, **39**, 1245–1254.

SUPPLEMENTAL TABLES

Supplementary Table S1. Zooplankton genera, order, or class identified over the course of the growing season in Green Valley Lake.

Taxonomic Group	Taxa identified in Green Valley Lake included in grouping
Large Cladocera	*Daphnia* *Simocephalus* *Ceriodaphnia*
Small Cladocera	*Bosmina* *Chydorus*
Ostracod	Ostracoda
Calanoids	Calanoida
Cyclopoids	Cyclopoida
Nauplii	Copepod nauplii
Rotifers	*Asplanchna* *Keratella cochlearis* *Keratella quadrata* *Pompholyx* *Trichocerca* *Filinia*

Supplementary Table S2. Phytoplankton genera identified over the course of the growing season in Green Valley Lake.

Taxonomic Group	Taxa identified in Green Valley Lake included in grouping
Bacillariophyta	*Asterionella*
	Fragilaria
	Stephanodiscus
	Unknown pennate bacillariophyte
	Unknown centric bacillariophyte
Chlorophyta	*Chalmydomonas*
	Coelastrum
	Cosmarium
	Desmodesmus
	Elakatothrix
	Eudorina
	Monoraphidium
	Oocystis
	Pediastrum
	Schroederia
	Staurastrum
	Unknown chlorophyte
Chyrso - & Cryptophytes	*Mallomonas*
	Cryptomonas
	Komma
Aphanothece (Cyanophyte)	*Aphanothece*
Microcystis (Cyanophyte)	*Microcystis*
	Microcystis (Single-celled)
Other Cyanophytes	*Aphanizomenon*
	Aphanocapsa
	Merismopedia
	Planktolyngbya
	Pseudanabaena
	Snowella
	Woronichinia
	Dolichospermum

Supplementary Table S3. Estimated zooplankton excretion of N and P (μM d^{-1}) using different published allometric equations from Hébert *et al.* (2016) and Wen and Peters (1994). Uncertainty estimates derived from the allometric equation parameters in Hébert *et al.* (2016) are presented in parentheses.

	Zooplankton Excretion (μM N or P day^{-1})			
	Nitrogen Excretion		**Phosphorus Excretion**	
DOY	Hébert	Wen & Peters	Hébert	Wen & Peters
143	0.159 (0.143- 0.242)	0.073	0.062 (0.040-0.100)	0.080
150	0.177 (0.116-0.270)	0.082	0.056 (0.036-0.088)	0.072
164	0.167 (0.110-0.255)	0.083	0.058 (0.037-0.091)	0.081
171	0.087 (0.057-0.133)	0.039	0.029 (0.018-0.045)	0.036
178	0.034 (0.022-0.051)	0.014	0.010 (0.007-0.016)	0.012
192	0.003 (0.002-0.004)	0.002	0.001 (0.001-0.002)	0.002
199	0.022 (0.014-0.033)	0.012	0.008 (0.005-0.012)	0.011
206	0.015 (0.010-0.022)	0.007	0.005 (0.003-0.007)	0.006
211	0.068 (0.045-0.104)	0.035	0.023 (0.014-0.035)	0.032
213	0.004 (0.002-0.005)	0.002	0.001 (0.001-0.007)	0.001
220	0.001 (0.001-0.002)	0.001	0.000 (0.000-0.002)	0.001
227	0.005 (0.003-0.007)	0.002	0.002 (0.001-0.003)	0.002
234	0.018 (0.012-0.027)	0.008	0.005 (0.003-0.008)	0.007
245	0.109 (0.072-0.167)	0.046	0.031 (0.020-0.049)	0.037
251	0.095 (0.062-0.145)	0.042	0.029 (0.019-0.046)	0.036
273	0.120 (0.079-0.183)	0.051	0.039 (0.025-0.061)	0.046

Supplementary Table S4. Zooplankton taxa food size range data collected from the literature. Minimum food size range (Min FSR (µm)) and maximum food size range (Max FSR (µm)) represent either a single species or an average of multiple species. When an average was taken, the standard deviation is presented.

Taxa	Min FSR (µm)	Standard Deviation	Max FSR (µm)	Standard Deviation	Source
Bosmina	1.4	NA	5	NA	Barnett et al. 2007
Ceriodaphnia	0.4	NA	7	NA	Barnett et al. 2007
Chydorus	0.4	NA	2	NA	Barnett et al. 2007
Daphnia	1.1	0.5	30	10	Barnett et al. 2007
Diaphanosoma	0.25	NA	5	NA	Barnett et al. 2007
Cyclopoida	6.9	6.1	54.2	43.5	Barnett et al. 2007
Calanoida	9.4	11.6	64	23	Barnett et al. 2007
Nauplii	4.5	NA	19.8	NA	Helenius & Saiz 2017
Rotifera	0	NA	75	NA	Sweeney et al. 2022

Supplementary Table S5. Potential zooplankton nutrient turnover of soluble reactive phosphorus in Green Valley Lake. Values represent the number of days it would take zooplankton excretion alone to replenish the water column concentration of dissolved inorganic phosphorus on a given sampling day. Missing values were the result of sample loss or the lack of available data and are denoted by NA.

Nutrient Pool	***DOY 143***	***DOY 150***	***DOY 164***	***DOY 172***	***DOY 178***	***DOY 192 - 273***
Soluble Phosphorus	5 d	3 d	3 d	5 d	57 d	>200 d

SUPPLEMENTAL FIGURES

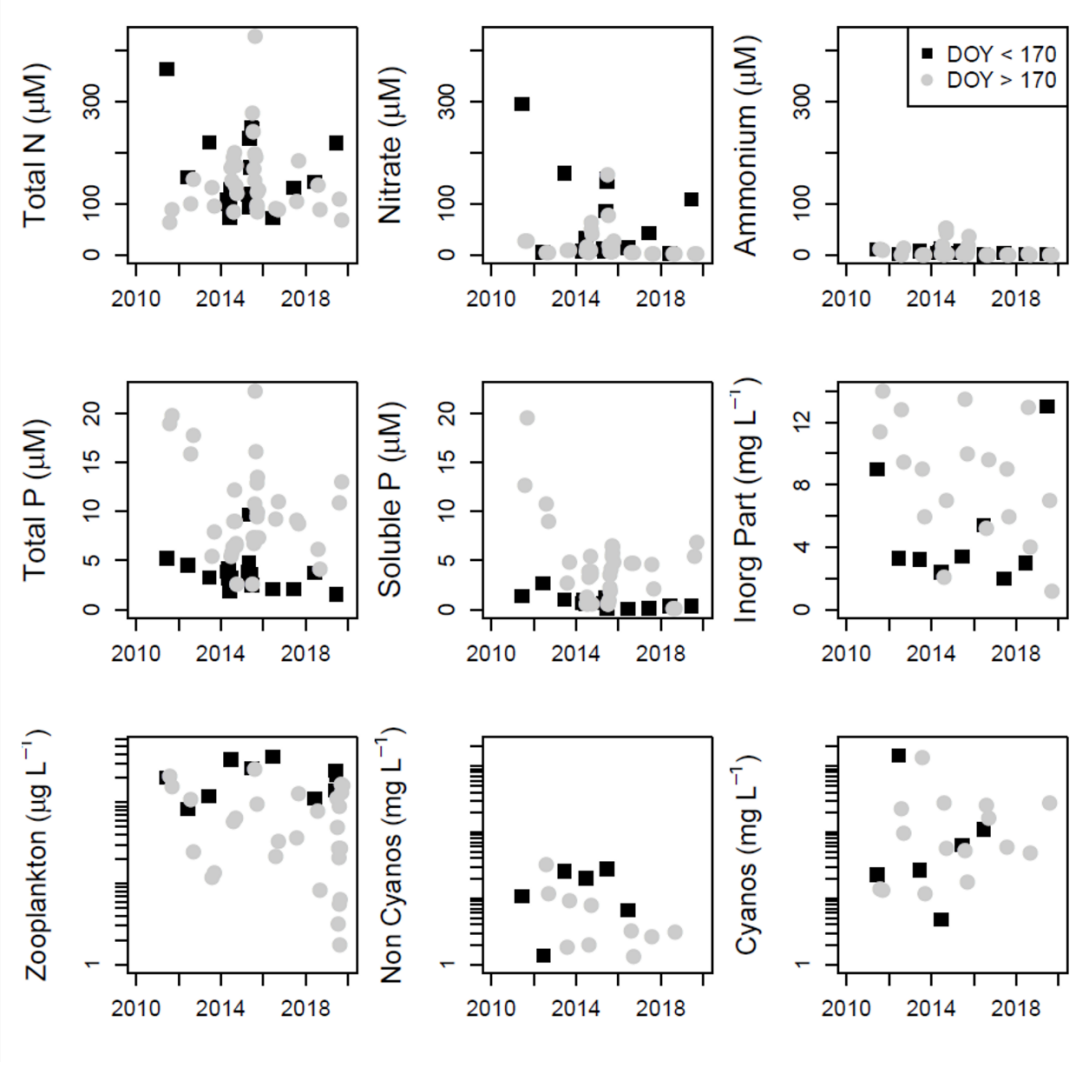

Supplementary Figure S1. Historical water quality and plankton data for Green Valley Lake. The different colors represent before or after the clear-water period which we determined was around DOY 170 using a breakpoint analysis for the period 2011 – 2019. Dark color and square shape denote data before DOY 170, and light color and circle shape denote data post DOY 170. From left to right, top to bottom the variables represented are total nitrogen, nitrate, ammonium, total phosphorus, soluble reactive phosphorus, inorganic particulates, zooplankton biomass, non-Cyanophyta biomass, and Cyanophyta biomass. Data were collated from the Ambient Lakes Monitoring program in the state of Iowa (IDNR, 2021).

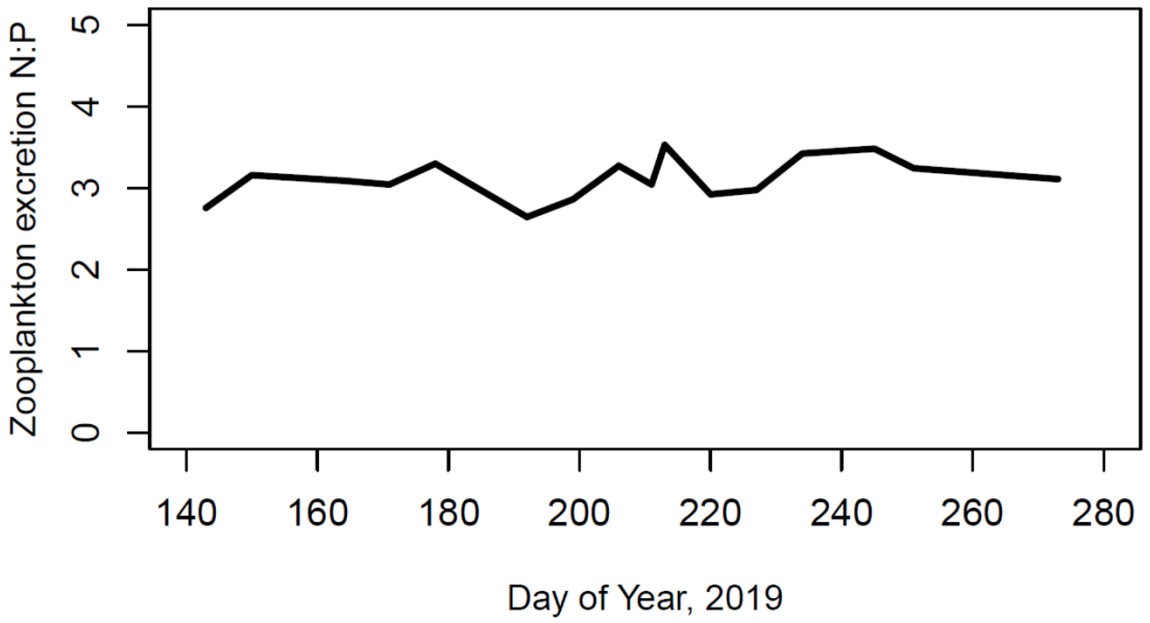

Supplementary Figure S2. The estimated zooplankton excretion nitrogen: phosphorus ratio derived from published allometric equations of zooplankton body size and excretion rate (Hébert *et al.*, 2016).

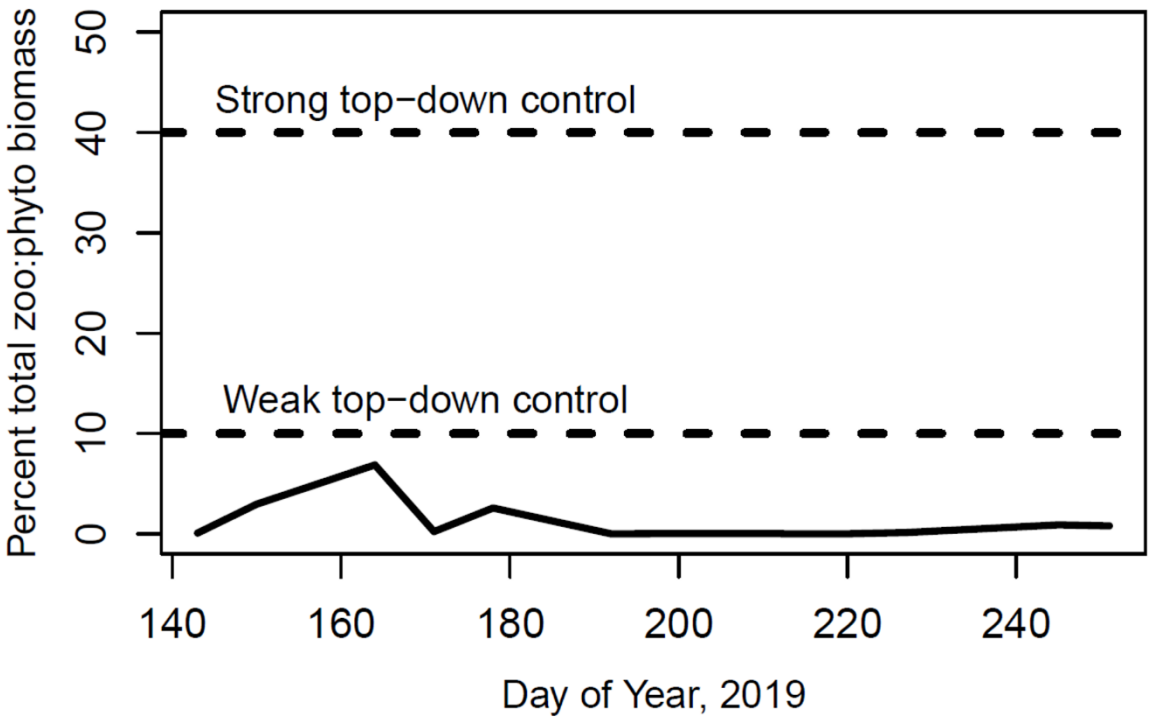

Supplementary Figure S3. The ratio of zooplankton: phytoplankton biomass across the summer growing season in Green Valley Lake. The dashed lines represent the threshold for either weak (~10%) or strong (~40-50%) top-down control on phytoplankton biomass (Leroux and Loreau, 2015; Havens and Beaver, 2013).

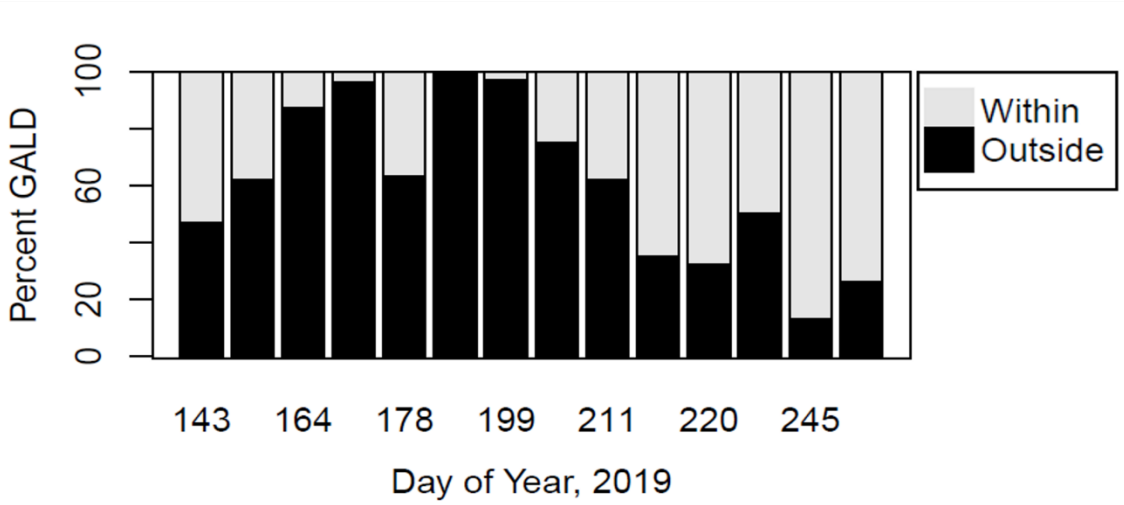

Supplementary Figure S4. The percentage of individual phytoplankton GALD measurements per sampling date that fell within the zooplankton community food size range calculated for the same sampling date. Dark bars represent the percentage of phytoplankton GALD measurements that fell within the zooplankton food size range and light bars represent the percentage that fell outside of that range.

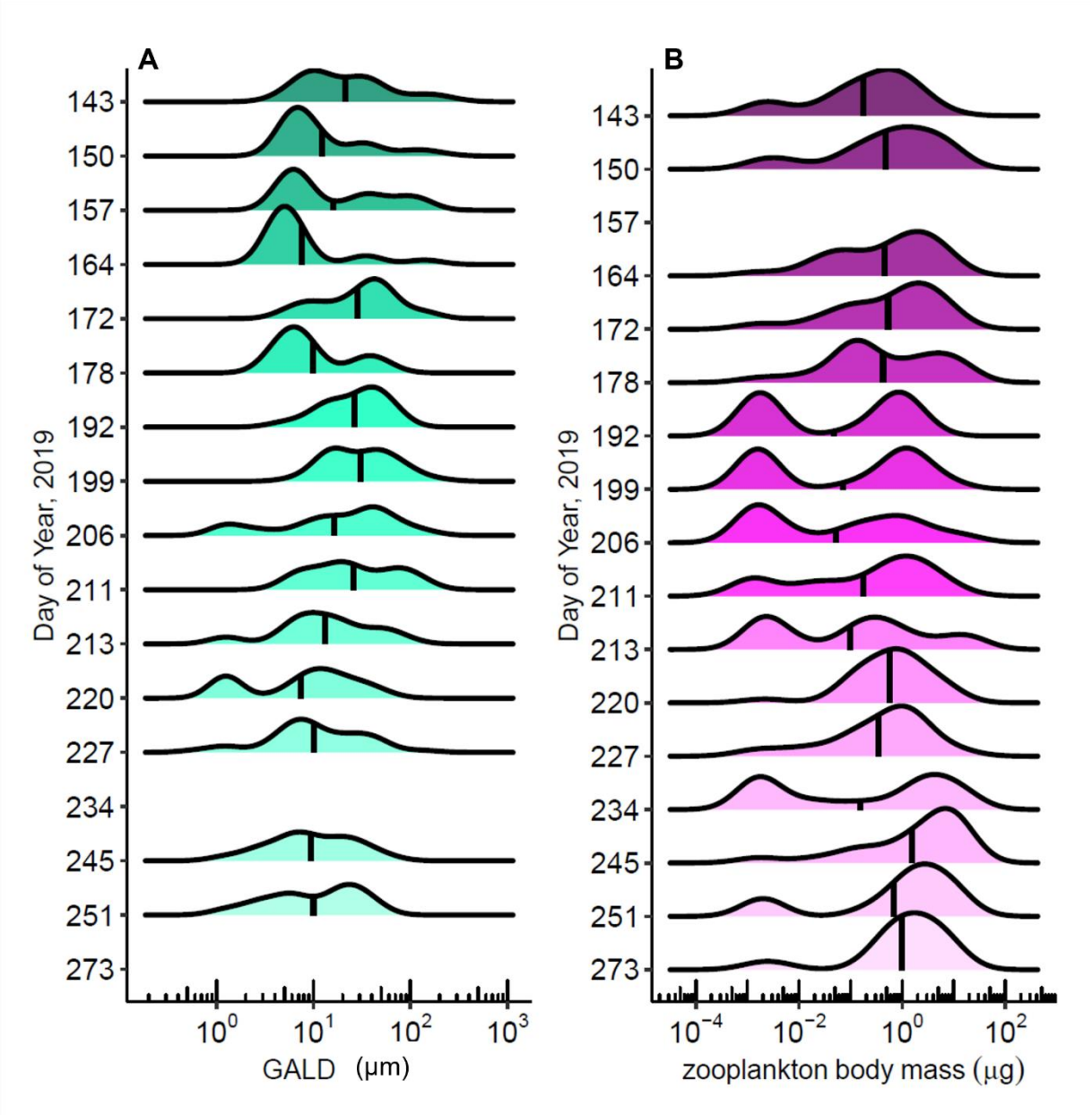

Supplementary Figure S5. Density ridgeline plots of phytoplankton greatest axial linear dimension (GALD, µm) and zooplankton body mass (µg) over the course of the growing season in Green Valley Lake, IA. The black vertical line within each distribution represents the mean. DOYs that are missing either phytoplankton GALD or zooplankton length are the result of sample loss or no available data.

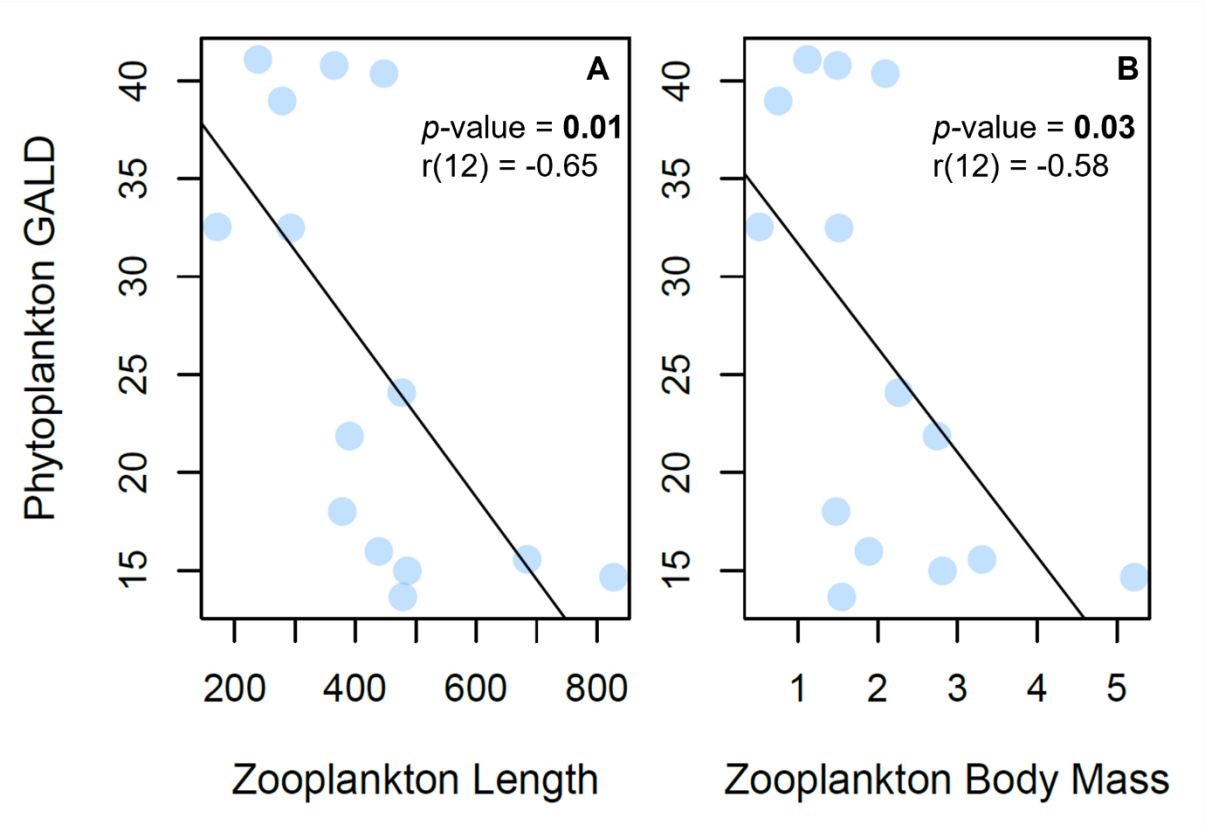

Supplementary Figure S6. Pearson correlations of (A) zooplankton body length (µm) and (B) zooplankton body mass (µg) by phytoplankton greatest axial linear dimension (GALD, µm).

CHAPTER 2

INVESTIGATING CHANGES TO FOOD WEB STRUCTURE IN SHALLOW LAKES FOLLOWING REMOVAL OF COMMON CARP (*CYPRINUS CARPIO*) AND BIGMOUTH BUFFALO (*ICTIOBUS CYPRINELLUS*)

In preparation for submission with coauthors M. Simonson, M.J. Weber, and G.M. Wilkinson to *Ecological Indicators*

Author Contributions: Butts designed the study; performed the necessary field and laboratory work, performed the data cleaning, analysis, and visualization; and drafted the manuscript. Simonson, Weber, and Wilkinson contributed to study design, data collection, and data analysis.

ABSTRACT

Biomanipulation is a common management intervention to address eutrophication. But, when there is no improvement in water quality as intended, it is difficult to disentangle whether the biomanipulation failed to substantially alter food web structure or was unable to overcome external drivers of poor water quality. Traditional food web model analyses to monitor management interventions can be prohibitively time and data intensive. Size spectra—the relationship between species abundance and body size--could be used to detect changes in food web structure following major disturbances. As such, size spectra may be a powerful tool to investigate the effects of food web interventions such as biomanipulation, particularly when coupled with complex harvest structures such as incentivized commercial harvest. We fit size spectra in seven shallow, nutrient rich lakes in northwest Iowa from 2018 – 2020, four of which underwent incentivized harvest of common carp (*Cyprinus carpio*) and bigmouth buffalo (*Ictiobus cyprinellus*) during this period, with three lakes serving as reference ecosystems. There

were no improvements in water quality in any of the lakes. Based on the size spectra slopes, there were also no significant changes in species size structure due to incentivized harvest (p = 0.072) or harvest intensity of common carp (p = 0.191) or bigmouth buffalo (p = 0.069). Ecosystem productivity, based on the size spectra height (predicted number of organisms at the midpoint) decreased across all years (p = 0.002) in all lakes, likely reflecting broadscale regional influences. We demonstrated that incentivized harvest was unable to significantly shift size spectra slopes as intended, providing evidence that the lack of improvements in water quality may be due to a failure to induce strong top-down effects despite substantial removals of bigmouth buffalo and common carp. Size spectra analyses can be a powerful tool to understand and guide food web-focused management interventions.

INTRODUCTION

Manipulating food web structure (i.e., biomanipulation) can be a powerful management tool to shift pathways of energy and nutrient flow within an ecosystem to enhance ecosystem services (Hansson et al., 1998; Fraser et al., 2015; Vander Zanden, Olden & Gratton, 2016). In eutrophic waterbodies, biomanipulation is used to reduce phytoplankton standing stocks through both top-down and bottom-up controls. Common biomanipulations in eutrophic lakes to improve water clarity include removal of planktivorous fish biomass to increase zooplankton biomass and grazing pressure and removing benthivorous fishes to reduce sediment disturbance and internal nutrient loading (Shapiro et al., 1975; Søndergaard et al., 2017; Weber and Brown, 2009). While the purpose of these manipulations is to improve water quality by altering food web structure, the effectiveness of biomanipulations is often assessed by changes in water clarity, algal biomass, nutrient concentrations, and native fish biomass, all of which are also subject to non-food web

drivers of change (Jeppesen et al., 2012; Meijer et al., 1999, 1990). Indirect, outcome-based metrics of biomanipulation success are often used because quantitatively assessing changes in food web structure can be costly and difficult (Pringle and Hutchinson, 2020; Ripple et al., 2016). Thus, methods leveraging data collection in existing monitoring programs are necessary to quantify food web responses to biomanipulation to better evaluate their success or failure (Hansson et al., 1998).

A wealth of ecological theory and analyses have demonstrated that the relationship between abundance and body size of species, or size spectrum, is fundamental property of size-structured food webs (Sheldon and Parsons, 1967; Sprules, 2008; Sprules and Barth, 2016). This simple relationship is based upon a log-log negative linear relationship between body size and abundance where large individuals have lower densities than small individuals within an ecosystem (Sprules and Barth, 2016). The slope of this relationship generally tends to be -1.0 reflecting a steady state condition where biomass is distributed between logarithmically equal size bins and reflects size-dependent metabolic and predation rates (Rossberg, 2012). Shifts away from the theoretical slope of -1.0 can be used to assess changes in food web structure away from its steady state condition. The slope reflects the relative abundance of small and large organisms (i.e., species size structure) and thus a shallower slope than the theoretical estimate of -1.0 would indicate more energy is available for higher trophic levels in addition to stronger top-down control (Mehner et al., 2018; Barth et al., 2019). Changes in the size spectra height, or the abundance of organisms at the mid-point of the size spectrum, can be used to infer ecosystem productivity and facilitate cross-ecosystem comparisons (Guiet et al., 2016). Slopes and intercepts are often correlated, and thus size spectrum height can be used as an independent metric, in addition to comparing size spectrum slope (Evans et al., 2022). Analyzing changes in

size spectrum slope and height can be a useful tool to assess changes in food web structure following a disturbance (Sprules and Barth, 2016; Barth et al., 2019). Collecting size and abundance data requires far less effort than the intensive sampling and biomass estimates needed for more rigorous food web modeling (Colvin et al., 2015; Delmas et al., 2019). As such, this tool could be useful for assessing changes in food web structure in lakes following biomanipulation using relatively easily collected size and abundance data, especially when water quality metrics fail to improve.

Zooplankton and benthic macroinvertebrates represent taxa commonly collected within sampling programs that can also reflect changes in overall food web structure and energy availability within ecosystems (Barth et al., 2019; Evans et al. 2022). Zooplankton taxa are sensitive to disturbances due to their intermediate trophic position and fast generation times, making their body size distribution a sentinel of change for ecosystem trophy and food web dynamics (Barth et al., 2019; Chiba et al., 2018; Jeppesen et al., 2011). Benthic macroinvertebrates are also a critical link to higher trophic levels, particularly within benthic food chains providing key energy and nutrient subsidies to consumers, particularly in shallow lakes (Vander Zanden and Vadeboncoeur 2020, Evans et al. 2022). Size spectra analyses of zooplankton and benthic macroinvertebrates may be useful for disentangling responses to management strategies that target food web structure like biomanipulation. This may be particularly helpful when natural resource agencies contract with commercial fishers (e.g., through incentivized harvest) to reduce fish populations (Bahls, 1992; Bouska et al., 2020; Fritz, 1987; Weber et al., 2016) and harvest is heterogeneous across lakes due to fluctuations in market forces and fisher behavior (Branch et al., 2006; Fulton et al., 2011; Smith and McKelvey, 1986). Given the complex socio-economic realities of incentivized harvest biomanipulations, and the

inconsistent responses of water quality response variables (Hansson et al., 1998), size spectra analyses may be useful for assessing whether the intended food web changes occurred but were masked by other drivers, or if the food web remained unaltered despite intervention.

In 2018, the Iowa Department of Natural Resources (IDNR) began a feasibility study to assess whether an incentivized harvest management program of common carp (*Cyprinus carpio*) and bigmouth buffalo (*Ictiobus cyprinellus*) removal could improve water quality and sport fisheries in shallow, eutrophic lakes. Incentivized harvest for biomanipulation had been successfully implemented in the past in this region in individual lakes (Colvin et al., 2012; Meerbeek and Hawkins, 2021); but it was unclear whether this management mechanism could be applied at a broader scale and replicated successfully (Simonson et al., 2022). Common carp are widespread, non-native, benthivorous feeders that negatively affect water quality, endemic fish populations, and benthic macroinvertebrates (Weber and Brown, 2011, 2009). Alternatively, bigmouth buffalo are native to the region and can reach high biomass densities in shallow lakes generating strong top-down control on zooplankton communities (Wilkinson et al., 2022). The value of bigmouth buffalo is approximately three times common carp, so selection of this species for biomanipulation was also an additional financial incentive (Simonson et al., 2022). Despite substantial removals of common carp and bigmouth buffalo over three years, no improvements in water quality were observed (Figures S1 – S2).

Our objectives for this study were to (1) assess the interannual variability in species size structure (i.e., size spectra slope) and productivity (i.e., size spectra height) in harvested (n=4) and non-harvested (n=3) reference lakes; (2) determine whether the incentivized harvest program had a measurable and directional effect on species size structure and productivity; (3) quantify whether changes in size spectra through time scaled with harvest intensity; and (4), assess

interannual changes in zooplankton and macroinvertebrate community composition across all seven study lakes. We expected size spectra slopes to become shallower than the theoretical slope of -1.0 following harvest reflecting a greater abundance of large benthic macroinvertebrates and zooplankton due to a combination of less top-down control on zooplankton from bigmouth buffalo (Wilkinson et al., 2022) and reduced direct and indirect negative effects on benthic macroinvertebrates from common carp (Weber and Brown, 2009). Including both taxa within the size spectra analysis provides a stronger signal of food web change (Evans et al, 2022), that may be masked by assessing only zooplankton or benthic macroinvertebrates. We also expected size spectra height (i.e., inference of ecosystem productivity) to decrease in lakes following harvest of common carp and bigmouth buffalo due to a shift in zooplankton and macroinvertebrate abundances (i.e., a more even distribution of small and large individuals). We also expected that the magnitude of the shift in size spectra slope, and height, would increase with harvest intensity of common carp and bigmouth buffalo. Finally, we expected that a greater change in zooplankton and macroinvertebrate size spectra would align with substantial changes in the species composition and biomass of zooplankton and macroinvertebrates.

METHODS

Study Sites

The seven lakes included in this study were six eutrophic, shallow, glacial lakes located in northwestern Iowa, USA with one eutrophic oxbow lake (Blue Lake) located in western Iowa, USA (Table 1). The glacial lakes are near the western edge of the Des Moines Lobe with Blue Lake located within the Missouri Alluvial Plain. All lakes are shallow, polymictic, and heavily

influenced by nutrient loading from row crop agriculture in the watershed (Table 1; Arbuckle & Downing, 2001). This has led to persistent water quality issues including impairments related to algal biomass (Table 1; Carlson, 1977). All the glacial lakes had large common carp and bigmouth buffalo populations. However, Blue Lake likely had a smaller bigmouth buffalo population than the glacial lakes as evidenced by only one individual bigmouth buffalo being captured within Blue Lake over the three-year study period (Simonson et al. 2022).

Incentivized Harvest

During the study period, the Iowa Department of Natural Resources (IDNR) entered short-term contracts with commercial fishing operations for the removal of common carp and bigmouth buffalo from four of the lakes (Figure 1). Each contract provided exclusive commercial fishing rights for one calendar year. Harvest was prohibited between May and early September and removals via seining were required at least twice per contract period. Common carp and bigmouth buffalo were required to be removed when caught no matter their physical condition or size with biomass removed reported to IDNR biologists. Exploitation estimates were generated by dividing the total biomass of common carp or bigmouth buffalo harvested by population biomass estimates produced from capture-mark-recapture analysis using a modified Schnabel estimator for multiple recaptures (Ricker, 1975; Simonson et al., 2022). However, population estimates had wide 95 % confidence intervals exploitation estimates were sometimes over 100% for bigmouth buffalo and common carp (Table S1). Thus, we use the biomass density (kg ha^{-1}) of fish removed in our subsequent analyses.

Food Web Quantification

We sampled zooplankton three to ten times during the ice-free period (median = 7) from May to September via a vertical tow of a Wisconsin net (63 µm mesh) from 0.5 m above the sediments to the surface at the lake's deepest point (APHA, 1998). Samples were preserved in the field with a 5% formaldehyde solution and later transferred to 70% ethanol for storage. Zooplankton taxa were identified and enumerated from a 1 mL subsample using a Leica MZ8 stereomicroscope connected to Motic Images software. Individuals were identified to genus for cladocerans and rotifers and order for copepods. Copepod nauplii could not be identified to order and were recorded simply as nauplii. If less than 60 organisms were present within a subsample, an additional 1 mL subsample was processed. Taxa were also measured to the nearest 0.1 µm for up to 25 individuals per taxon per sample, used to calculate biomass using standard length-dry mass regressions (Dumont et al., 1975; McCauley, 1984). We calculated abundance (zooplankton m^{-2}) by multiplying the volumetric density (zooplankton m^{-3}) by the depth of water column (m) sampled for each sampling event.

Benthic macroinvertebrates were collected at ten sites at a range of depths including the littoral and profundal zones of each lake (Table S2), as well as the historical deep point using an Ekman dredge (0.023 m^2) in 2018 and a Ponar dredge (0.052 m^2) in 2019 – 2020. Samples were collected once per lake and year between mid-July to early-August as densities and taxon richness are typically at their maximum (Bowman and Bailey, 1997). Sediment samples for each site were placed in a five-gallon bucket with lids and transported back to the lab where they were sieved through a 500-µm mesh (APHA, 2005; Baldwin et al., 2018) and preserved in 500 mL amber bottles with 90% ethanol and 0.1% Rose Bengal Dye solution. In the lab, invertebrates

were removed from the sediment and identified to the lowest possible order or family while annelids were identified to subclass. We calculated abundance (macroinvertebrates m^{-2}) by dividing the number of individuals identified in a sample by the surface area of sample collected by the Ekman or Ponar sampler. Individuals were also measured for length to the nearest 0.1 mm on a Leica MZ8 stereomicroscope and used in length-dry mass regressions to calculate biomass (Table S3). We used the mean areal biomass of a taxa across all ten sampling sites for our analyses such that there was one biomass value per taxon per lake for each year.

Size spectra analysis

To address our first objective of assessing variability in species size structure and productivity in each study lake we calculated the slope and height of size spectra using all available zooplankton and macroinvertebrate data combined (sensu Evans et al., 2022) for each lake and year. Zooplankton and macroinvertebrates were allocated into $\log_2$-size bins based on individual dry mass (g) where size bins were generated by logarithmically doubling (i.e., $\log_2$) the smallest recorded size until all individual sizes were represented within a given size bin (Table 2). We then calculated the average abundance (individuals m^{-2}) within each size bin. To calculate the slope of the size spectra we used ordinary least-squares regression between the average abundance within each size bin and the dry weight at the center of each size bin. To remove high leverage data points, we removed points from the regression if they had a Cook's distance greater than one (Bollen and Jackman, 1990). In our data, high leverage points were usually taxa with small body size and low abundance (e.g., a single *Keratella cochlearis* rotifer identified within a sample) or a taxon with a large body size but low abundance (i.e., a small number of mollusks) which were most likely artifacts of sampling efficiency.

Fitting size spectra using maximum likelihood methods may provide more robust estimates of confidence intervals for slopes (Edwards et al., 2020, 2017). However, our size data were collected using subsets of sampled populations and expanded to density measures rather than through individual measurement of every organism which is where maximum likelihood methods would be most appropriately applied (Edwards et al., 2020). Additionally, we wanted to compare our results to other size spectra analyses that use zooplankton and macroinvertebrates where ordinary least squares regression has been the standard (Barth et al., 2019; Evans et al., 2022).

To address our second objective of quantifying interannual and inter-lake variability in species size structure in relation to the harvest of common carp and bigmouth buffalo we tested for differences in size spectrum slope using a multivariable regression model. The full model included dummy variables to assess variation in slope with no harvest (D_{ref}), one year of harvest ($D_{harvest1}$) and two years of harvest ($D_{harvest2}$). Thus, the full model ($\log_2$[Abundance] ~ $\log_2$[middle of the dry weight bin] * lake * year * D_{ref} * $D_{harvest1}$ * $D_{harvest2}$) was used with all possible combinations of covariates. Here, abundance represents the average density of organisms within a specific size bin and the middle of the dry weight bin represents the midpoint within a particular $\log_2$-size bin. To determine the most parsimonious model we used Akaike information criterion (AIC) with forward and backward stepwise model selection (Akaike, 1973). Only models with a difference in AIC less than two were considered in our analyses following Burnham & Anderson (2004). If a covariate or interaction effect was significant, we performed pairwise comparisons using Tukey's post hoc test. To assess differences in ecosystem productivity we analyzed differences in size spectra height using a weighted regression model. Each lake and year varied in the range of dry weight bins (Table 2); thus, we weighted heights by

$1/SE^2$ where SE was the standard error of the intercept for each size spectra. The middle size bin was, on average, $2^{-18} \pm 0.91$ standard deviations (containing mostly *Chydorus*, large cladocerans, and copepods). Our calculation of height was independent of slope which was confirmed by a Pearson correlation analysis ($R^2 = 0.081$, $p = 0.73$, Figure S3). The weighted regression quantified variation in height across lakes and years (height ~ year*lake) where year was a numeric variable and lake was a factor variable.

To address our third objective, we used simple linear regression to quantify whether changes in species size structure or productivity scaled with common carp and bigmouth buffalo harvest intensity. We calculated the change in slope or height from one year to the next in relation to the cumulative harvest (kg ha^{-1}) of either common carp or bigmouth buffalo from a lake over the entire study period. Specifically, cumulative harvest was calculated by adding the cumulative biomass of a fish taxa removed in each successive year. For example, if 30 kg ha^{-1} of common carp were removed in 2018 and 50 kg ha^{-1} were removed in 2019, then the cumulative harvest of common carp would be 80 kg ha^{-1} in 2019 and 30 kg ha^{-1} in 2018. The change in slope or height was calculated by subtracting the value from the previous year so that a more negative change in slope would mean the slope was becoming steeper with harvest. In addition, we also quantified the change in slope or height in relation to the cumulative harvest of both common carp and bigmouth buffalo.

To address our fourth objective, we used permutational multivariate analysis of variance (PERMANOVA, Anderson, 2017) to assess changes in community composition between years using taxa biomass. Zooplankton were grouped by season to reflect expected changes in community composition between spring to early summer and mid-summer to early fall (Sommer et al., 1986). The spring period was set as May and June and summer was set between July and

October following Evans et al., (2022). However, most sampling dates for zooplankton fell between late-May and early September. Zooplankton data were Hellinger-transformed to reduce the weight of rare taxa and PERMANOVAs were calculated using Bray-Curtis dissimilarity matrices (999 permutations) with year acting as a fixed categorical variable (Legendre and Legendre, 1998). Pairwise comparisons across years were only computed if the full PERMANOVA model was significant ($p < 0.05$) and the *p*-value was adjusted for multiple comparisons using a Bonferroni correction (Dunn, 1961). Seasonal analysis was not possible for macroinvertebrates as community composition data was only available for one sampling point for each lake and year. For visual display of zooplankton community composition, we separated taxa into eight taxonomic groups: Rotifera, nauplii, Calanoida, Cyclopoida, Chydorids, *Bosmina*, miscellaneous Cladocera, and *Daphnia* (Table S4). Similarly, we separated macroinvertebrates into ten taxonomic groups: Gammaridae, Megaloptera, Trichoptera, Ephemeroptera, Dreissendiae, Bivalvia, Gastropoda, worms, miscellaneous Diptera, and Chironomidae (Table S5). All analyses were conducted using the statistical software R (R Core Team, 2022) using the *tidyverse* (Wickham et al., 2019)*, vegan* (Oksanen et al., 2022), *MASS* (Venables and Ripley, 2002), *EcolUtils* (Salazar, 2023), *emmeans* (Lenth, 2023) and *sizeSpectra* (Edwards, 2022) packages.

RESULTS

Size spectrum slope

The zooplankton-macroinvertebrate size spectra consisted of 27 size bins (6.985×10^{-10} to 0.094 g) although there was variation in which size bins were used depending on the lake and year (Table 2). For our statistical analysis of differences in size spectrum slope to assess interannual and inter-lake variability in species size structure, the most parsimonious model was as follows: $\log_2$[abundance] ~ $\log_2$[middle of dry weight bin] + lake + year + $D_{harvest2}$ + $\log_2$[middle of dry weight bin] * lake, where $D_{harvest2}$ was a dummy variable grouping lakes that had received 2 years of harvest or not (Table S6). The second most parsimonious model included an additional interaction term ($\log_2$[middle of dry weight bin] * year), and remaining models had a ΔAIC greater than two (Table S6). Given that two models had substantial evidence of being the most parsimonious, we chose to focus on the simplest model which also had the lowest AIC. The reduced model (Table 3) explained 63.44 % of variation in slope and indicated that there is a non-zero slope to the relationship between abundance and biomass ($p < 0.001$), significant variation in slope between lakes ($F_{6,394} = 2.50$, $p = 0.022$) along with a change in the relationships of abundance and biomass across lakes ($F_{6,394} = 4.01$, $p = 0.001$). However, there were not significant changes in slope between years ($F_{2,394} = 2.15$, $p = 0.118$) nor between lakes where harvest occurred for two years ($F_{1,394} = 3.25$, $p = 0.072$). A Tukey honest significant difference post-hoc test, holding the middle of the dry weight bin at the average across all lakes to account for the significant interaction (middle of dry weight bin = $2^{-19.7}$, mostly *Chydorus* and copepods), indicated there was only a significant difference in slope between Blue Lake and both Storm Lake (difference = -0.31 units, $p = 0.001$) and Center Lake (difference = -0.34 units, $p = 0.001$) (Figure S4, Table S7).

Size spectra varied among years in the slope and intercept across all lakes, although there was less interannual variability in lakes where no harvest occurred (Figure 2). However, slopes for all lakes were shallower (i.e., closer to zero) than the theoretical value of -1.0 (Figure 3). Reference lakes had minimal interannual variability in slope though slopes in Storm Lake and South Twin Lake became slightly shallower over time (Figure 3A – C). Lakes that were harvested in 2018 and 2019 (prior to sampling that summer) had slopes closer to the theoretical value of -1.0 after 2019 (Figure 3D – E), whereas there was not a consistent pattern for lakes that underwent harvest prior to sampling in 2019 and 2020 (Figure 3F – G). Slopes for North Twin Lake became shallower following the first harvest event then steeper, towards -1.0, following the second harvest event (Figure 3F). Slopes for Silver Lake followed the opposite pattern becoming steeper following the first harvest events, and shallower following the second harvest events (Figure 3G).

Size spectra height

Interannual and inter-lake variability in ecosystem productivity was not a significant interaction between lakes and years ($F_{6,7} = 0.437$, $p = 0.834$), thus we removed the interaction term from the full model. The reduced model (height ~ year + lake) was significant ($F_{7,13} = 10.81$, $p < 0.001$) and explained 77.44% of variation in height across all study lakes and years (Table S8). Height significantly decreased over time across all lakes (-0.52 ± 0.13, change in height ± standard error, $p = 0.002$) and heights were significantly lower in Silver Lake (-1.1 ± 0.46, difference in height ± standard error, $p = 0.038$) and significantly higher in South Twin Lake (1.3 ± 0.49, difference in height ± standard error, $p = 0.017$). There were different temporal patterns in lakes as well. Heights decreased from 2018 – 2020 in most study lakes apart from

North Twin Lake and South Twin Lake which had roughly similar height over the entire study period (Figure 4). Both lakes that underwent harvest prior to sampling in 2018 and 2019 (i.e., Center Lake, Five Island Lake) had decreased height in 2020, a year after the last harvest event occurred in these lakes (Figure 4D – E). Silver Lake, which underwent harvest prior to sampling in 2019 and 2020 followed the same pattern as Center Lake and Five Island Lake by decreasing in height in 2020 (Figure 4G).

Changes in size spectra in relation to harvest intensity

Our analysis assessing whether changes in size spectra slope or height scaled with the intensity of common carp or bigmouth buffalo harvest revealed no significant relationship (Figure 5). The cumulative harvest of common carp did not significantly explain interannual changes in slope ($F_{1,19} = 1.84$, $p = 0.191$) nor height ($F_{1,19} = 0.13$, $p = 0.723$). The models explained only 19.13% of the variation in interannual slope change and only 0.45% of the variation in interannual height change. Similarly, the cumulative harvest of bigmouth buffalo did not significantly explain interannual changes in slope ($F_{1,19} = 3.73$, $p = 0.069$) nor height ($F_{1,19} = 1.48$, $p = 0.239$). The models for bigmouth buffalo cumulative harvest explained less variation in the interannual change in slope (6.86%) and slightly more in the interannual change in height (2.33%) compared to common carp cumulative harvest. However, in both models relating interannual changes in height to cumulative harvest, the intercept was significantly different than zero. Thus, with no cumulative harvest of common carp height decreased on average by -0.55 ± 0.26 (mean ± standard error, $p = 0.047$). Similarly, with no cumulative harvest of bigmouth buffalo height decreased by -0.81 ± 0.25 (mean ± standard error, $p = 0.004$). Combining common carp and bigmouth buffalo harvest yielded similar results where the interannual change

in slope ($F_{1,19} = 4.00$, $p = 0.060$) and height ($F_{1,19} = 1.20$, $p = 0.288$) was not significantly explained by the cumulative harvest of both common carp and bigmouth buffalo together (Figure S5, Table S9). Again, the intercept of the model quantifying interannual change in height was significantly different from zero where the height decreased on average by -0.80 ± 0.25 (mean ± standard error, $p = 0.005$) with no harvest. The combined cumulative harvest model explained more of the variation in interannual change in slope (13.04%) and height (28.76%), but again, they were not significant relationships (Figure S5).

Zooplankton and macroinvertebrate community composition

The spring (May – June) zooplankton community composition was significantly different among years in Storm Lake, South Twin Lake, and North Twin Lake (Table S10). The percentage of *Daphnia* and *Ceriodaphnia* biomass increased substantially between 2018 and 2020, whereas the percentage of copepods and nauplii biomass decreased in Storm Lake (Figure S6). However, zooplankton biomass in Storm Lake was lower in 2020 in comparison to 2018 (Figure 6). The percent composition of taxa in South Twin Lake varied substantially year to year (Figure S6, South Twin Lake), which corresponded to a drop in biomass and absence of Cladocera taxa in 2019 (Figure 6, Figure S6). Furthermore, there was a substantial increase in the percent biomass of *Daphnia* and *Chydorus* in North Twin Lake driven by a large increase in Cladocera taxa (Figure 6, Figure S6). Pairwise comparisons among years only found a significant difference between 2018 and 2020 in Storm Lake ($F_{1,9} = 4.51$, $p = 0.042$, Table S11).

Summer (July – October) zooplankton community composition was significantly different between years in almost all lakes apart from Storm Lake and Center Lake (Table S10). The percent biomass of copepods and nauplii increased over time in both Blue and South Twin

Lake (Figure S7), though dynamics in biomass diverged. Zooplankton biomass in Blue Lake decreased then increased from 2018 – 2020 whereas biomass in South Twin Lake steadily decreased over time (Figure 7). The percent biomass of cyclopoids and copepods in Five Island Lake substantially increased in 2019, driven by an increase in copepod biomass, before returning to resemble the zooplankton community composition of 2018 (Figure 7, Figure S7). North Twin Lake and Silver Lake had divergent changes in zooplankton community composition where the percent biomass of *Daphnia, Bosmina,* and *Chydorus* increased in North Twin Lake over time with the opposite occurring in Silver Lake where the percent biomass of calanoids substantially increased (Figure S7). Additionally, interannual variability of zooplankton biomass was low in Silver Lake, yet zooplankton biomass in North Twin Lake quadrupled (4.4x) from 2018 to 2020 driven by an increase in cladocerans such as *Bosmina, Chydorus,* and *Daphnia* (Figure 7). However, pairwise comparisons between years only found a significant difference between 2018 and 2019 for North Twin Lake ($F_{1,7} = 7.82$, $p = 0.048$, Table S11).

The percent biomass composition for macroinvertebrate communities did not vary much across lakes with all lakes largely dominated by Oligochaeta and Hirudinea taxa followed by Chironomidae and Gastropoda (Figure S8). There are some exceptions including increased percent composition of Ephemeroptera, Trichoptera, and Megaloptera in Five Island, North Twin, and Silver Lake (Figure S8). Notably, in Storm Lake 2020, the macroinvertebrate community was overwhelmingly dominated by Dreissenidae which drove a substantial increase in biomass (Figure 8). Macroinvertebrate biomass generally decreased over the course of the study period, apart from Storm Lake. However, the magnitude of biomass varied substantially between lakes as the maximum biomass, excluding Storm Lake 2020, ranged between 260.52 – 5534.69 mg m^{-2} (Figure 8).

DISCUSSION

An incentivized harvest program of common carp (*Cyprinus carpio*) and bigmouth buffalo (*Ictiobus cyprinellus*) removal over three years (2018 – 2020) in a set of shallow, eutrophic-hypereutrophic lakes did not result in clear and substantial improvement to water quality (Simonson et al., 2022). Therefore, we sought to assess whether the incentivized harvest biomanipulation successfully changed food web structure as intended. Using size spectra analysis, we did not find strong evidence that the incentivized harvest led to significant changes in food web structure, potentially explaining the lack of water quality response to the biomanipulation. However, the interannual variability in slope was low in the reference lakes compared to the harvested lakes, indicating that the analysis method was sensitive to changes other than year-to-year variability.

Shifting size spectra slopes are associated with changes in species size structure, with shallower slopes representing a greater abundance of larger individuals and stronger top-down control (Barth et al., 2019; Mehner et al., 2018). If the incentivized harvest successfully shifted species size structure to larger zooplankton and benthic macroinvertebrates, slopes would have become ‘shallower’ over time and less negative than the theoretical slope of -1 (Mehner et al., 2018; Sprules and Barth, 2016). A shallower slope would be driven by larger size classes becoming more abundant within the lower food web reflecting less top-down control on zooplankton and macroinvertebrates and stronger top-down control on phytoplankton (Ye et al., 2013). Contrary to this expectation, size spectra slopes became steeper, not shallower (i.e., closer to zero), with increasing harvest pressure (Figure 3), but the relationship was not significant among lakes. In the reference lakes, the slopes were relatively invariant whereas the harvested lakes were substantially more dynamic among years indicating the size spectra were sensitive to

the management intervention. Additionally, all size spectra slopes were relatively shallow compared to the theoretical estimate of -1.0 which aligns with other studies that found size spectra become shallower with greater nutrient enrichment (Ahrens and Peters, 1991; Sprules and Munawar, 1986) and the inclusion of benthic taxa (Evans et al., 2022).

Influence of incentivized harvest on species size structure and productivity

In the two lakes that were harvested before summer sampling in 2018 and 2019, Center and Five Island Lakes, size spectra slopes were shallow in the two seasons immediately following harvest (i.e., 2018, 2019), but became steeper the following year (i.e., 2020). Bigmouth buffalo harvest in Center Lake was high in 2018 (222 kg ha^{-1}) and in Five Island Lake in 2019 (185 kg ha^{-1}), potentially causing flatter slopes with less predation pressure on large-bodied zooplankton (Wilkinson et al., 2022). However, both lake's size spectra slopes became steeper only a year after incentivized harvest ceased suggesting that any positive change in species size structure (e.g., shallower slopes) may have been ephemeral, as has been documented in other lakes (Barth et al. 2019). Fish compensatory responses (e.g., higher recruitment, faster growth rates) spurred by the harvest may have driven the steeper slopes observed in 2020. Common carp exploitation ranged from 7 – 26 % in Center and Five Island Lake, which is within range of other lakes where compensatory responses to harvest has been previously documented (Weber et al. 2016). Further, commercial harvest was largely targeting large, adult fish reducing the ability of harvest to control populations (Simonson et al., 2022), particularly for common carp which require intensive harvest to be controlled (Colvin et al., 2012). Compensatory responses in fish populations may result in stable, or even increased, population density despite active or recent harvest (De Roos et al., 2007; Zipkin et al., 2009). A strong recruitment class of

common carp and bigmouth buffalo, or other compensatory dynamics in 2020, may have generated steeper slopes due to increased top-down control on zooplankton from juvenile fish or higher consumption from fast-growing adults (Weber et al. 2016). Evidence of compensatory dynamics in the harvested lakes is supported by the decrease in macroinvertebrate biomass over time in Center and Five Island Lake (Figure S8), as macroinvertebrates are prey items for juvenile common carp (Rahman et al., 2009). However, changes in relative abundance of common carp and bigmouth buffalo did not show clear evidence of compensatory dynamics in our study lakes (Simonson et al., 2022).

The interannual pattern in spectra slope was not consistent between the two lakes that were harvested before sampling in 2019 and 2020, North Twin and Silver Lakes. In North Twin Lake, the size spectra became shallower in 2019 and steeper in 2020 following two years of substantial bigmouth buffalo exploitation. During this time, zooplankton biomass steadily increased (Figure S7) and the community significantly shifted to dominance by Cladocera. Macroinvertebrate abundance and size declined dramatically in 2020 while the abundance of small-bodied Cladocera increased, leading to the steeper slope. Exploitation estimates for carp were relatively high in North Twin Lake (39% in 2018, 112% in 2020), suggesting compensatory dynamics could have strongly affected macroinvertebrate biomass leading to a steeper slope. This implies incentivized harvest shifted species size structure to a greater abundance of smaller individuals despite a second year of high bigmouth buffalo harvest in 2020 (276 kg ha^{-1}). However, the 95 % confidence intervals for slope in North Twin Lake were quite wide in 2020, so it is difficult to say whether the slope became steeper, or if the change was more reflective of poorer confidence in the estimate of the size spectrum slope.

In Silver Lake, the slope became steeper following the first harvest events in 2019 and remained steep in 2020, in comparison to pre-harvest conditions in 2018. This may have been driven by a decrease in macroinvertebrate biomass, akin to North Twin Lake, and a greater proportion of gastropods, olichochaetes, and hirudinea in Silver Lake in 2019 and 2020. The largest removal of carp biomass came from Silver Lake in 2020 with exploitation estimates ranging between 8 – 108 % (Simonson et al. 2022a). Despite the uncertainty in the exploitation estimate, there may have been compensatory responses to harvest from common carp that resulted in a steady decrease in macroinvertebrate biomass from 2018 – 2020 as juvenile carp feed on benthic macroinvertebrates and affect their community composition (Miller and Crow, 2006; Miller and Provenza, 2007; Zambrano and Hinojosa, 1999). Although changes in size spectra slopes were neither significantly different across years nor between lakes, it is difficult to assess longer-term oscillatory dynamics over only three years of data (Wilkinson et al., 2020), particularly with limited pre- and post-incentivized harvest data. Still, incentivized harvest was likely having some short-term effect on species size structure as evidenced by the greater interannual changes in slope in lakes that underwent incentivized harvest in comparison to our reference ecosystems.

The multivariable regression analysis revealed a significant interaction between the middle of the dry weight size bin and lake identity, specifically between Blue Lake and both Center and Storm Lake. This was likely driven by larger zooplankton and smaller macroinvertebrate body sizes in Blue Lake relative to the other lakes. Blue Lake is an oxbow with an extremely low bigmouth buffalo population (Simonson et al. 2022) which may have contributed to a larger-bodied zooplankton community. Additionally, differences in hydrologic connectivity in oxbow lakes compared to glacial kettle lakes can affect macroinvertebrate

community structure and biomass potentially resulting in the higher macroinvertebrate body sizes observed (Gallardo et al. 2008, Obolewski et al. 2009, 2015) despite community composition being similar to the other lakes. In Storm Lake, invasive zebra mussel (*Dreissena polymorpha*) populations boomed in 2020 which could have significantly altered zooplankton community structure (Strayer, 2009). Zebra mussels were first noted in 2018, which could account for the slight decrease in both slope and height in this reference lake over the course of the study (Mellina and Rasmussen 1994).

Like the spectra slope results, we did not observe an effect of incentivized harvest on ecosystem productivity estimated from size spectra height. Ecosystem productivity (i.e., height) decreased over time in all the study lakes, including our reference ecosystems. The pattern in height likely reflected broader regional drivers in lake productivity such as interannual climate differences and not the incentivized harvest (Guiet et al., 2016; Rossberg, Gaedke & Kratina, 2019). Among lakes, the patterns in size spectra height as a proxy for productivity align with chlorophyll concentrations, a proxy for algal biomass. The greatest height values were in South Twin Lake which had consistently high chlorophyll-a concentrations, and the smallest height values in Silver Lake which had comparatively lower chlorophyll-a concentrations (Albright et al., 2022; Figure S1). Chlorophyll-*a* concentrations are correlated with phosphorus enrichment (Quinlan et al., 2021), which in turn influences zooplankton size and abundance (Hessen et al., 2006; Moody et al., 2022; Moody and Wilkinson, 2019).

Harvest intensity, defined as the cumulative biomass of fish removed from a lake among years, similarly, did not have a significant effect on species size structure or productivity based on the change in size spectra slope and height over time. Our linear regression analysis indicated that greater bigmouth buffalo harvest may result in steeper slopes, but the trend was non-

significant and explained less than 20% of the variation in interannual change in slope. There are some limitations that may have reduced our ability to detect changes in size spectra slope and height over the course of the study. Including both spring and summer zooplankton data in our size spectra analyses was done to align with our single estimate of macroinvertebrate community composition and biomass, though we may have obscured important seasonal patterns. Size spectra slopes using zooplankton data in the spring tend to be steeper than summer zooplankton data, and thus our estimates of slope may have been steeper (Barth et al., 2019). However, removing spring zooplankton data did not qualitatively change our interpretation of the size spectra (Figure S9). Further, greater temporal resolution before and after incentivized harvest likely would have allowed us to detect short-term trends in species size structure and productivity following the incentivized harvest. (Barth et al. 2019). We observed changes in size spectra only a year after incentivized harvest concluded, suggesting we were able to capture short-term interannual dynamics but did not capture changes on a shorter timescale.

Are size spectra a useful tool for assessing biomanipulations in lakes?

While there were differences in the temporal pattern of size spectra slope in harvested lakes not observed in the reference lakes, there were not significant differences between lakes nor across years. This potentially explains the lack of water quality response despite substantial removals of common carp and bigmouth buffalo biomass in some lakes and years (Simonson et al., 2022). Using size spectra analysis, we demonstrated that the incentivized harvest program likely did not substantially affect food web structure enough to overcome external drivers of water quality. Size spectra analyses have been used to assess changes in fishing pressure (Robinson et al., 2017; Shin and Cury, 2004) as well as detect changes from species invasion

(Barth et al., 2019; Evans et al., 2022); here we provide evidence it may be used as a tool to assess food web biomanipulation. Though we did not detect significant changes in size spectra slope or height in response to management interventions, the size spectra slopes appeared sensitive to incentivized harvest as they had far greater interannual variability in comparison to the relatively invariant reference size spectra slopes. Further, our study provided additional reference for the slope and height of size spectra in shallow, productive aquatic ecosystems. Size spectra slopes were shallower than those reported in temperate, oligotrophic lakes (Barth et al., 2019) as well as shallower than other lakes where benthic macroinvertebrate data were included in size spectra analyses (Evans et al., 2022). This diversity of spectra demonstrates the importance of applying size spectra analyses in a wide range of ecosystem types and trophic levels to develop baselines for monitoring food web perturbations. This is particularly important as size spectra have not been applied as often in shallow, productive ecosystems, and the inclusion of benthic data in size spectra analyses is rare for both freshwater and marine ecosystems (Boudreau and Dickie, 1992; Evans et al., 2022; Mehner et al., 2018).

In summary, the inconsistent responses of size spectra to incentivized harvest suggests that biomanipulation may require sustained and intense harvest pressure to appreciably alter food web structure. The inconsistency of harvest pressure across lakes and years in our study likely hindered significant, lasting changes to food web structure. Nonetheless, biomanipulation is a common management strategy to address eutrophication in productive ecosystems even with its varying success (Jeppesen et al., 2012; Søndergaard et al., 2017). In our study, the inclusion of bigmouth buffalo in commercial contracts was done for economic (Simonson et al., 2022) and ecological reasons (Wilkinson et al., 2022). Though often categorized with the negative label ‘rough fish’, buffalo are endemic to the region (Johnson, 1963) and have cultural and economic

ties to anglers and commercial fisheries (Lackmann et al., 2019). Despite this, bigmouth buffalo harvest is largely unregulated which has contributed to overharvest and population declines in North America potentially exacerbated by infrequent spawning (Bennett and Kozak, 2016; Lackmann et al., 2023, 2021). In our study, substantial removal of bigmouth buffalo was not enough to improve water quality nor significantly affect food web structure. Thus, including bigmouth buffalo in further harvest programs will likely be unsuccessful and potentially contribute to the decline of a native and culturally important taxa (Lackmann et al., 2019). Ultimately, we found that size spectra analyses were able to provide complementary evidence that biomanipulation in our study lakes was not successful in overcoming external drivers and significantly affecting food web structure. Thus, management interventions should focus on improving watershed practices and reducing internal drivers of high nutrient concentrations (Albright et al., 2022; Albright and Wilkinson, 2022).

ACKNOWLEDGEMENTS

We would like to thank Quin Shingai, Rachel Fleck-King, Elena Sandry, and David Ortiz for assisting field and laboratory data collection and Zach Feiner for providing feedback on study design and data analysis. All authors were supported with funds from the Iowa Department of Natural Resources (Contract No. 18CRDLWBMBALM-0013). Butts received additional support from the National Science Foundation Graduate Research Fellowship Program (DGE-1747503). Any opinions, findings, and conclusions or recommendations expressed in this material are those of the authors and do not necessarily reflect the views of the National Science Foundation.

DATA AVAILABILITY

Data for this study will be archived using the Environmental Data Initiative repository and given a unique digital object identifier. Metadata will follow the ecological metadata language and be published under a creative commons license. The data files and analysis scripts are available through GitHub (https://github.com/tjbutts/carp-foodweb-change) and will be archived on Zenodo following acceptance for publication.

REFERENCES

Ahrens, M.A., Peters, R.H., 1991. Plankton community respiration: relationships with size distribution and lake trophy, Hydrobiologia.

Akaike, H., 1973. Information theory as an extension of the maximum likelihood principle, in: Petrov, B.N., Csaki, F. (Eds.), Proceedings of the Second International Symposium on Information Theory. Computer Society Press, Budapest, Hungary, pp. 267–281.

[dataset] Albright, E.A., Wilkinson, G.M., Butts, T.J., Shingai, Q.K., 2022. Summer water chemistry; sediment phosphorus fluxes and sorption capacity; sedimentation and sediment resuspension dynamics; water column thermal structure; and zooplankton, macroinvertebrate, and macrophyte communities in eight shallow lakes in northwest Iowa, USA (2018-2020) ver 3. Environmental Data Initiative, v1. https://doi.org/10.6073/pasta/1d3797fd573208bae6f78963479445a0.

Albright, E.A., Fleck King, R., Shingai, Q.K., Wilkinson, G.M., 2022. High Inter- and Intra-Lake Variation in Sediment Phosphorus Pools in Shallow Lakes. J Geophys Res Biogeosci 127. https://doi.org/10.1029/2022JG006817

Albright, E.A., Wilkinson, G., 2022. Sediment phosphorus composition controls hot spots and hot moments of internal loading in a temperate reservoir. Ecosphere 13, e4201. https://doi.org/https://doi.org/10.1002/ecs2.4201

Anderson, M.J., 2017. Permutational Multivariate Analysis of Variance (PERMANOVA). In: Balakrishnan N., Colton, T., Everitt, B., Piegorsch, W., Ruggeri, F., Teugels, J.L., eds. Wiley StatsRef: Statistics Reference Online. Oxford: Wiley, 1–15. https://doi.org/10.1002/9781118445112.stat07841

APHA, 2005. Standard methods for the examination of water and waste-water. American Public Health Association, Washington, DC.

APHA, 1998. Standard Methods for the Examination of Water and Wastewater, 20th ed. American Public Health Association, Washington, DC.

Arbuckle, K.E., Downing, J.A., 2001. The influence of watershed land use on lake N : P in a predominantly agricultural landscape. Limnol Oceanogr 46, 970–975. https://doi.org/10.4319/lo.2001.46.4.0970

Bahls, P., 1992. The Status of Fish Populations and Management of High Mountain Lakes in the Western United States. Northwest Science 66, 183–193. https://doi.org/https://hdl.handle.net/2376/1610

Baldwin, R.C., Sundberg, M.D., Stewart, T.W., Weber, M.J., 2018. Evaluating alternative macroinvertebrate sampling methodologies in wetlands: Influence of sieve mesh size on relationships between environmental and assemblage variables. Wetlands 38, 677–687.

Barth, L.E., Shuter, B.J., Sprules, W.G., Minns, C.K., Rusak, J.A., 2019. Calibration of the zooplankton community size spectrum as an indicator of change in canadian shield lakes. Canadian Journal of Fisheries and Aquatic Sciences 76, 2268–2287. https://doi.org/10.1139/cjfas-2018-0371

Bennett, M.G., Kozak, J.P., 2016. Spatial and temporal patterns in fish community structure and abundance in the largest U.S. river swamp, the Atchafalaya River floodplain, Louisiana. Ecol Freshw Fish 25, 577–589. https://doi.org/10.1111/eff.12235

Bollen, K., Jackman, R., 1990. Regression diagnostics: An expository treatment of outliers and influential cases, in: Fox, J., Long, J.S. (Eds.), Modern Methods of Data Analysis. Newbury Park, CA, pp. 257–291.

Boudreau, P.R., Dickie, L.M., 1992. Biomass Spectra of Aquatic Ecosystems in Relation to Fisheries Yield. Canadian Journal of Fisheries and Aquatic Sciences 49, 1528–1538.

Bouska, W.W., Glover, D.C., Trushenski, J.T., Secchi, S., Garvey, J.E., Macnamara, R., Coulter, D.P., Coulter, A.A., Irons, K., Wieland, A., 2020. Geographic-scale harvest program to promote invasivorism of bigheaded carps. Fishes 5, 1–14. https://doi.org/10.3390/fishes5030029

Bowman, M.F., Bailey, R.C., 1997. Does taxonomic resolution affect the multivariate description of the structure of freshwater benthic macroinvertebrate communities? Canadian Journal of Fisheries and Aquatic Sciences 54, 1802–1807. https://doi.org/10.1139/f97-085

Branch, T.A., Hilborn, R., Haynie, A.C., Fay, G., Flynn, L., Griffiths, J., Marshall, K.N., Randall, J.K., Scheuerell, J.M., Ward, E.J., Young, M., 2006. Fleet dynamics and fishermen behavior: Lessons for fisheries managers. Canadian Journal of Fisheries and Aquatic Sciences. https://doi.org/10.1139/F06-072

Burnham, K.P., Anderson, D.R., 2004. Multimodel inference: Understanding AIC and BIC in model selection. Sociol Methods Res. https://doi.org/10.1177/0049124104268644

Carlson, R.E., 1977. A trophic state index for lakes. Limnol Oceanogr 22, 361–369. https://doi.org/10.4319/lo.1977.22.2.0361

Chiba, S., Batten, S., Martin, C.S., Ivory, S., Miloslavich, P., Weatherdon, L. v., 2018. Zooplankton monitoring to contribute towards addressing global biodiversity conservation challenges. J Plankton Res 40, 509–518. https://doi.org/10.1093/plankt/fby030

Colvin, M.E., Pierce, C.L., Stewart, T.W., 2015. A food web modeling analysis of a Midwestern, USA eutrophic lake dominated by non-native Common Carp and Zebra Mussels. Ecol Modell 312, 26–40. https://doi.org/10.1016/j.ecolmodel.2015.05.016

Colvin, M.E., Pierce, C.L., Stewart, T.W., Grummer, S.E., 2012. Strategies to control a common carp population by pulsed commercial harvest. N Am J Fish Manag 32, 1251–1264. https://doi.org/10.1080/02755947.2012.728175

De Roos, A.M., Schellekens, T., Van Kooten, T., Van De Wolfshaar, K., Claessen, D., Persson, L., 2007. Food-dependent growth leads to overcompensation in stage-specific biomass when mortality increases: The influence of maturation versus reproduction regulation. American Naturalist 170. https://doi.org/10.1086/520119

Delmas, E., Besson, M., Brice, M.H., Burkle, L.A., Dalla Riva, G. V., Fortin, M.J., Gravel, D., Guimarães, P.R., Hembry, D.H., Newman, E.A., Olesen, J.M., Pires, M.M., Yeakel, J.D., Poisot, T., 2019. Analysing ecological networks of species interactions. Biological Reviews 94, 16–36. https://doi.org/10.1111/brv.12433

Dumont, H.J., Van de Velde, I., Dumont, S., 1975. The dry weight estimate of biomass in a selection of Cladocera, Copepoda and Rotifera from the plankton, periphyton and benthos of continental waters. Oecologia 19, 75–97. https://doi.org/10.1007/BF00377592

Dunn, O.J., 1961. Multiple Comparisons among Means. J Am Stat Assoc 56, 52–64. https://doi.org/10.1080/01621459.1961.10482090

Edwards, A., 2022. sizeSpectra: Fitting Size Spectra to Ecological Data Using Maximum Likelihood. https://github.com/andrew-edwards/sizeSpectra.

Edwards, A.M., Robinson, J.P.W., Blanchard, J.L., Baum, J.K., Plank, M.J., 2020. Accounting for the bin structure of data removes bias when fitting size spectra. Mar Ecol Prog Ser 636, 19–33. https://doi.org/10.3354/meps13230

Edwards, A.M., Robinson, J.P.W., Plank, M.J., Baum, J.K., Blanchard, J.L., 2017. Testing and recommending methods for fitting size spectra to data. Methods Ecol Evol 8, 57–67. https://doi.org/10.1111/2041-210X.12641

Evans, T.M., Feiner, Z.S., Rudstam, L.G., Mason, D.M., Watkins, J.M., Reavie, E.D., Scofield, A.E., Burlakova, L.E., Karatayev, A.Y., Sprules, W.G., 2022. Size spectra analysis of a decade of Laurentian Great Lakes data. Canadian Journal of Fisheries and Aquatic Sciences 79, 183–194. https://doi.org/10.1139/cjfas-2020-0144

Fraser, L.H., Harrower, W.L., Garris, H.W., Davidson, S., Paul, D.N., Howie, R., Moody, A., Polster, D., Schmitz, O.J., Sinclair, A.R.E., Starzomski, B.M., Sullivan, T.P., Turkington, R., Wilson, D., 2015. A call for applying trophic structure in ecological restoration 23, 503–507. https://doi.org/10.1111/rec.12225

Fritz, A., 1987. Carp in North America, in: Cooper, E. (Ed.), Carp in North America. American Fisheries Society, Bethesda, Maryland, pp. 17–30.

Fulton, E.A., Smith, A.D.M., Smith, D.C., van Putten, I.E., 2011. Human behaviour: The key source of uncertainty in fisheries management. Fish and Fisheries 12, 2–17. https://doi.org/10.1111/j.1467-2979.2010.00371.x

Gallardo, B., García, M., Cabezas, Á., González, E., González, M., Ciancarelli, C., Comín, F.A., 2008. Macroinvertebrate patterns along environmental gradients and hydrological connectivity within a regulated river-floodplain. Aquat Sci 70, 248–258. https://doi.org/10.1007/s00027-008-8024-2

Guiet, J., Poggiale, J.C., Maury, O., 2016. Modelling the community size-spectrum: recent developments and new directions. Ecol Modell. https://doi.org/10.1016/j.ecolmodel.2016.05.015

Hansson, L.A., Annadotter, H., Bergman, E., Hamrin, S.F., Jeppesen, E., Kairesalo, T., Luokkanen, E., Nilsson, P.Å., Søndergaard, M., Strand, J., 1998. Biomanipulation as an

application of food-chain theory: Constraints, synthesis, and recommendations for temperate lakes. Ecosystems 1, 558–574. https://doi.org/10.1007/s100219900051

Hessen, D.O., Faafeng, B.A., Smith, V.H., Bakkestuen, V., Walseng, B., 2006. Extrinsic and intrinsic controls of zooplankton diversity in lakes. Ecology 87, 433–443. https://doi.org/10.1890/05-0352

Jeppesen, E., Nõges, P., Davidson, T.A., Haberman, J., Nõges, T., Blank, K., Lauridsen, T.L., Søndergaard, M., Sayer, C., Laugaste, R., Johansson, L.S., Bjerring, R., Amsinck, S.L., 2011. Zooplankton as indicators in lakes: A scientific-based plea for including zooplankton in the ecological quality assessment of lakes according to the European Water Framework Directive (WFD). Hydrobiologia 676, 279–297. https://doi.org/10.1007/s10750-011-0831-0

Jeppesen, E., Søndergaard, M., Lauridsen, T.L., Davidson, T.A., Liu, Z., Mazzeo, N., Trochine, C., özkan, K., Jensen, H.S., Trolle, D., Starling, F., Lazzaro, X., Johansson, L.S., Bjerring, R., Liboriussen, L., Larsen, S.E., Landkildehus, F., Egemose, S., Meerhoff, M., 2012. Biomanipulation as a Restoration Tool to Combat Eutrophication. Recent Advances and Future Challenges, Advances in Ecological Research. https://doi.org/10.1016/B978-0-12-398315-2.00006-5

Johnson, R.P., 1963. Studies on the Life History and Ecology of the Bigmouth Buffalo, Ictiobus cyprinellus (Valenciennes). Journal of the Fisheries Research Board of Canada 20, 1397–1429.

Lackmann, A.R., Andrews, A.H., Butler, M.G., Bielak-Lackmann, E.S., Clark, M.E., 2019. Bigmouth Buffalo Ictiobus cyprinellus sets freshwater teleost record as improved age analysis reveals centenarian longevity. Commun Biol 2. https://doi.org/10.1038/s42003-019-0452-0

Lackmann, A.R., Kratz, B.J., Bielak-Lackmann, E.S., Jacobson, R.I., Sauer, D.J., Andrews, A.H., Butler, M.G., Clark, M.E., 2021. Long-lived population demographics in a declining, vulnerable fishery — bigmouth buffalo (Ictiobus cyprinellus) of jamestown reservoir, north dakota. Canadian Journal of Fisheries and Aquatic Sciences 78, 1486–1496. https://doi.org/10.1139/cjfas-2020-0485

Lackmann, A.R., Sereda, J., Pollock, M., Bryshun, R., Chupik, M., McCallum, K., Villeneuve, J., Bielak-Lackmann, E.S., Clark, M.E., 2023. Bet-hedging bigmouth buffalo (Ictiobus cyprinellus) recruit episodically over a 127-year timeframe in saskatchewan. Canadian Journal of Fisheries and Aquatic Sciences 80, 313–329. https://doi.org/10.1139/cjfas-2022-0122

Legendre, P., Legendre, L., 1998. Numerical Ecology, 2nd edn. Elsevier, Amsterdam.

Lenth, R., 2023. emmeans: Estimated Marginal Means, aka Least-Squares Means.

McCauley, E., 1984. The estimation of the abundance and biomass of zooplankton, in: Downing, J., Rigler, F. (Eds.), A Manual on Methods for the Assessment of Secondary Productivity in Fresh Waters. Blackwell Scientific Publications, pp. 228–265.

Meerbeek, J., Hawkins, M., 2021. The Lost Island Lake renovation project - design, implementation, and adaptive management. Special Publication 21-02. Des Moines.

Mehner, T., Lischke, B., Scharnweber, K., Attermeyer, K., Brothers, S., Gaedke, U., Hilt, S., Brucet, S., 2018. Empirical correspondence between trophic transfer efficiency in

freshwater food webs and the slope of their size spectra. Ecology 99, 1463–1472. https://doi.org/10.1002/ecy.2347

Meijer, M.L., De Boois, I., Scheffer, M., Portielje, R., Hosper, H., 1999. Biomanipulation in shallow lakes in The Netherlands: An evaluation of 18 case studies. Hydrobiologia 408–409, 13–30. https://doi.org/10.1007/978-94-017-2986-4_2

Meijer, M.L., de Haan, M.W., Breukelaar, A.W., Buiteveld, H., 1990. Is reduction of the benthivorous fish an important cause of high transparency following biomanipulation in shallow lakes? Hydrobiologia 200–201, 303–315. https://doi.org/10.1007/BF02530348

Miller, S.A., Crow, T.A., 2006. Effects of common carp (Cyprinus carpio) on macrophytes and invertebrate communities in a shallow lake. Freshw Biol 51, 85–94. https://doi.org/10.1111/j.1365-2427.2005.01477.x

Miller, S.A., Provenza, F.D., 2007. Mechanisms of resistance of freshwater macrophytes to herbivory by invasive juvenile common carp. Freshw Biol 52, 39–49. https://doi.org/10.1111/j.1365-2427.2006.01669.x

Moody, E., Butts, T., Fleck, R., Jeyasingh, P., Wilkinson, G., 2022. Eutrophication-driven eco-evolutionary dynamics indicated by differences in stoichiometric traits among populations of Daphnia pulicaria. Freshw Biol 67, 353–364. https://doi.org/10.1111/fwb.13845

Moody, E.K., Wilkinson, G.M., 2019. Functional shifts in lake zooplankton communities with hypereutrophication. Freshw Biol 64, 608–616. https://doi.org/10.1111/fwb.13246

Obolewski, K., Glińska-Lewczuk, K., Kobus, S., 2009. Effect of hydrological connectivity on the molluscan community structure in oxbow lakes of the Łyna River. Oceanol Hydrobiol Stud 38, 75–88. https://doi.org/10.2478/v10009-009-0045-1

Obolewski, K., Glińska-Lewczuk, K., Strzelczak, A., 2015. Does hydrological connectivity determine the benthic macroinvertebrate structure in oxbow lakes? Ecohydrology 8, 1488–1502. https://doi.org/10.1002/eco.1599

Oksanen, J., Simpson, G., Blanchet, F., Kindt, R., Legendre, P., Minchin, P., O'Hara, R., Solymos, P., Stevens, M., Szoecs, E., Wagner, H., Barbour, M., Bedward, M., Bolker, B., Borcard, D., Carvalho, G., Chirico, M., De Caceres, M., Durand, S., Evangelista, H., FitzJohn, R., Friendly, M., Furneaux, B., Hannigan, G., Hill, M., Lahti, L., McGlinn, D., Ouellette, M., Ribeiro Cunha, E., Smith, T., Stier, A., Ter Braak, C., Weedon, J., 2022. vegan: Community Ecology Package.

Pringle, R.M., Hutchinson, M.C., 2020. Resolving Food-Web Structure. Annual Review of Ecology, Evolution, and Systematics and Systematics 51, 55–80.

Quinlan, R., Filazzola, A., Mahdiyan, O., Shuvo, A., Blagrave, K., Ewins, C., Moslenko, L., Gray, D.K., O'Reilly, C.M., Sharma, S., 2021. Relationships of total phosphorus and chlorophyll in lakes worldwide. Limnol Oceanogr 66, 392–404. https://doi.org/10.1002/lno.11611

R Core Team, 2022. R: A language and environment for statistical computing.

Rahman, M.M., Hossain, M.Y., Jo, Q., Kim, S.K., Ohtomi, J., Meyer, C., 2009. Ontogenetic shift in dietary preference and low dietary overlap in rohu (Labeo rohita) and common carp (Cyprinus carpio) in semi-intensive polyculture ponds. Ichthyol Res 56, 28–36. https://doi.org/10.1007/s10228-008-0062-1

Ricker, W.E., 1975. Computation and interpretation of biological statistics of fish populations. Bulletin of the Fisheries Restoration Board of Canada.

Ripple, W.J., Estes, J.A., Schmitz, O.J., Constant, V., Kaylor, M.J., Lenz, A., Motley, J.L., Self, K.E., Taylor, D.S., Wolf, C., 2016. What is a Trophic Cascade? Trends Ecol Evol 31, 842–849. https://doi.org/10.1016/j.tree.2016.08.010

Robinson, J.P.W., Williams, I.D., Edwards, A.M., McPherson, J., Yeager, L., Vigliola, L., Brainard, R.E., Baum, J.K., 2017. Fishing degrades size structure of coral reef fish communities. Glob Chang Biol 23, 1009–1022. https://doi.org/10.1111/gcb.13482

Rossberg, A.G., 2012. A Complete Analytic Theory for Structure and Dynamics of Populations and Communities Spanning Wide Ranges in Body Size, in: Advances in Ecological Research. Academic Press Inc., pp. 427–521. https://doi.org/10.1016/B978-0-12-396992-7.00008-3

Rossberg, A.G., Gaedke, U., Kratina, P., 2019. Dome patterns in pelagic size spectra reveal strong trophic cascades. Nat Commun 10. https://doi.org/10.1038/s41467-019-12289-0

Salazar, G., 2023. EcolUtils: Utilities for community ecology analysis. .

Shapiro, J., Lamarra, V., Lynch, M., 1975. Biomanipulation: an ecosystem approach to lake restoration. Water Quality Management through Biological Control.

Sheldon, R., Parsons, T., 1967. A Continuous Size Spectrum for Particulate Matter in the Sea. Journal of the Fisheries Research Board of Canada 24, 909–915.

Shin, Y.J., Cury, P., 2004. Using an individual-based model of fish assemblages to study the response of size spectra to changes in fishing. Canadian Journal of Fisheries and Aquatic Sciences 61, 414–431. https://doi.org/10.1139/f03-154

Simonson, M., Annear, A., Weber, M.J., 2022. Evaluation of Commercial Harvest of Common Carp and Bigmouth Buffalo in Shallow Natural Lakes. Final report to Iowa Department of Natural Resources (17CRDLWMBALM-0006). Des Moines, IA.

Smith, C.L., McKelvey, R., 1986. Specialist and Generalist: Roles for Coping with Variability. N Am J Fish Manag 6, 88–99. https://doi.org/10.1577/1548-8659(1986)6<88:sag>2.0.co;2

Sommer, U., Gliwicz, Z.M., Lampert, W., Duncan, A., 1986. The PEG-model of seasonal succession of planktonic events in fresh waters. Arch Hydrobiol 106, 433–471.

Søndergaard, M., Lauridsen, T.L., Johansson, L.S., Jeppesen, E., 2017. Repeated fish removal to restore lakes: Case study of lake væng, Denmark-two biomanipulations during 30 years of monitoring. Water (Switzerland) 9. https://doi.org/10.3390/w9010043

Sprules, W.G., 2008. Ecological change in Great Lakes communities - A matter of perspective. Canadian Journal of Fisheries and Aquatic Sciences 65, 1–9. https://doi.org/10.1139/F07-136

Sprules, W.G., Barth, L.E., 2016. Surfing the biomass size spectrum: Some remarks on history, theory, and application. Canadian Journal of Fisheries and Aquatic Sciences 73, 477–495. https://doi.org/10.1139/cjfas-2015-0115

Sprules, W.G., Munawar, M., 1986. Plankton size spectra in relation to ecosystem productivity, size, and perturbation. Canadian Journal of Fisheries and Aquatic Sciences 43, 1789–1794. https://doi.org/10.1139/f86-222

Strayer, D., 2009. Twenty years of zebra mussels : lessons from the mollusk that made headlines. Front Ecol Environ 7, 135–141. https://doi.org/10.1890/080020

Vander Zanden, M., Olden, J., Gratton, C., 2016. Food-Web Approaches in Restoration Ecology, in: Falk, D., Palmer, M., Zedler, J. (Eds.), Foundations of Restoration Ecology. Island Press, pp. 165–189.

Vander Zanden, M.J., Casselman, J.M., Rasmussen, J.B., 1999. Stable isotope evidence for the food web consequences of species invasions in lakes. Nature 401, 464–467.

Vander Zanden, M.J., Vadeboncoeur, Y., 2020. Putting the lake back together 20 years later: what in the benthos have we learned about habitat linkages in lakes? Inland Waters 0, 1–17. https://doi.org/10.1080/20442041.2020.1712953

Venables, W., Ripley, B., 2002. Modern Applied Statistics with S, 4th ed. Springer, New York, NY.

Weber, M.J., Brown, M.L., 2011. Relationships among invasive common carp, native fishes and physicochemical characteristics in upper Midwest (USA) lakes. Ecol Freshw Fish 20, 270–278. https://doi.org/10.1111/j.1600-0633.2011.00493.x

Weber, M.J., Brown, M.L., 2009. Effects of Common Carp on Aquatic Ecosystems 80 Years after "Carp as a Dominant": Ecological Insights for Fisheries Management. Reviews in Fisheries Science 17, 524–537. https://doi.org/10.1080/10641260903189243

Weber, M.J., Hennen, M.J., Brown, M.L., Lucchesi, D.O., St. Sauver, T.R., 2016. Compensatory response of invasive common carp Cyprinus carpio to harvest. Fish Res 179, 168–178. https://doi.org/10.1016/j.fishres.2016.02.024

Wickham, H., Averick, M., Bryan, J., Chang, W., McGowan, L., François, R., Grolemund, G., Hayes, A., Henry, L., Hester, J., Kuhn, M., Pedersen, T., Miller, E., Bache, S., Müller, K., Ooms, J., Robinson, D., Seidel, D., Spinu, V., Takahashi, K., Vaughan, D., Wilke, C., Woo, K., Yutani, H., 2019. Welcome to the Tidyverse. J Open Source Softw 4, 1686. https://doi.org/10.21105/joss.01686

Wilkinson, G., Butts, T., Sandry, E., Simonson, M., Weber, M., 2022. Experimental evaluation of the effects of bigmouth buffalo (Ictiobus cyprinellus) density on shallow lake ecosystems. Earth Arxiv.

Wilkinson, G.M., Walter, J., Fleck, R., Pace, M.L., 2020. Beyond the trends: The need to understand multiannual dynamics in aquatic ecosystems. Limnol Oceanogr Lett 5, 281–286. https://doi.org/10.1002/lol2.10153

Ye, L., Chang, C.Y., García-Comas, C., Gong, G.C., Hsieh, C. hao, 2013. Increasing zooplankton size diversity enhances the strength of top-down control on phytoplankton through diet niche partitioning. Journal of Animal Ecology 82, 1052–1061. https://doi.org/10.1111/1365-2656.12067

Zambrano, L., Hinojosa, D., 1999. Direct and indirect effects of carp (Cyprinus carpio L.) on macrophyte and benthic communities in experimental shallow ponds in central Mexico.

Zipkin, E.F., Kraft, C.E., Cooch, E.G., Sullivan, P.J., 2009. When can efforts to control nuisance and invasive species backfire? Ecological Applications 19, 1585–1595. https://doi.org/10.1890/08-1467.1

TABLES

Table 1. Lake name, coordinates, mean depth (Z_{mean}), max depth (Z_{max}), trophic state (calculated from 19-year mean of chlorophyll-a during ice-off period (2000 – 2018). Trophic state is classified as either hypereutrophic (H) or eutrophic (E) as no study lakes were classified as mesotrophic or oligotrophic.

Lake	Blue	Storm	South Twin	Center	Five Island	North Twin	Silver
Latitude	42.0334	42.6198	42.4585	43.4126	43.1545	42.4756	43.4415
Longitude	-96.1610	-95.1857	-94.6536	-95.1357	-94.648	-94.6405	-95.3353
Z_{max} (m)	3.5	6.2	1.6	5.5	8	3.7	3
Z_{mean} (m)	1.7	2.6	1.1	3.7	1.7	2.7	2
Trophic state	H	E	H	E	E	E	E

Table 2. Minimum and maximum of the $\log_2$(dry mass) size bin (g) for each lake and year.

	Minimum dry weight bin			Maximum dry weight bin		
Lake	2018	2019	2020	2018	2019	2020
Blue	2^{-29}	2^{-29}	2^{-28}	2^{-6}	2^{-7}	2^{-7}
Storm	2^{-29}	2^{-30}	2^{-29}	2^{-5}	2^{-6}	2^{-3}
South Twin	2^{-29}	2^{-29}	2^{-27}	2^{-9}	2^{-9}	2^{-9}
Center	2^{-30}	2^{-29}	2^{-29}	2^{-6}	2^{-6}	2^{-8}
Five Island	2^{-29}	2^{-29}	2^{-28}	2^{-6}	2^{-11}	2^{-6}
North Twin	2^{-30}	2^{-29}	2^{-29}	2^{-8}	2^{-7}	2^{-10}
Silver	2^{-29}	2^{-23}	2^{-28}	2^{-6}	2^{-5}	2^{-5}

Table 3. Summary statistics of the most parsimonious multivariable regression model where Log_2[MBdw] is the midpoint of a $\log_2$[dry mass] size bin in grams (g).

Variable	**df**	**SS**	**MSE**	**F value**	***p*-value**
$Log_2[MB_{dw}]$	1	4643	4643	680.81	**<0.001**
Lake	6	102	17	2.50	**0.022**
Year	2	29	15	2.15	0.118
$D_{harvest2}$	1	22	22	3.25	0.072
$Log_2[MB_{dw}]$*Lake	6	164	27	4.01	**0.001**
Residuals	394	2687	7		

Table 4. Model information slope and height v. cumulative harvest of common carp and bigmouth buffalo

Model	Coefficients	Estimate	Standard Error	T-value	*p*-value
Slope ~ Carp Harvest	Intercept	-0.019	0.044	-0.438	0.666
	Harvest	-0.002	0.001	-1.355	0.191
				$F_{1, 19}$ = 1.836, Adjusted R^2 = 19.13 %	
Slope ~ Buffalo Harvest	Intercept	-0.008	0.041	-0.185	0.855
	Harvest	-0.000	0.000	-1.930	0.069
				$F_{1, 19}$ = 3.726, Adjusted R^2 = 6.86 %	
Height ~ Carp Harvest	Intercept	-0.551	0.259	-2.128	**0.047**
	Harvest	-0.003	0.008	-0.360	0.723
				$F_{1, 19}$ = 0.130, Adjusted R^2 = 0.45%	
Height ~ Buffalo Harvest	Intercept	-0.805	0.245	-3.288	**0.004**
	Harvest	0.001	0.001	1.215	0.239
				$F_{1, 19}$ = 1.477, Adjusted R^2 = 2.33%	

FIGURES

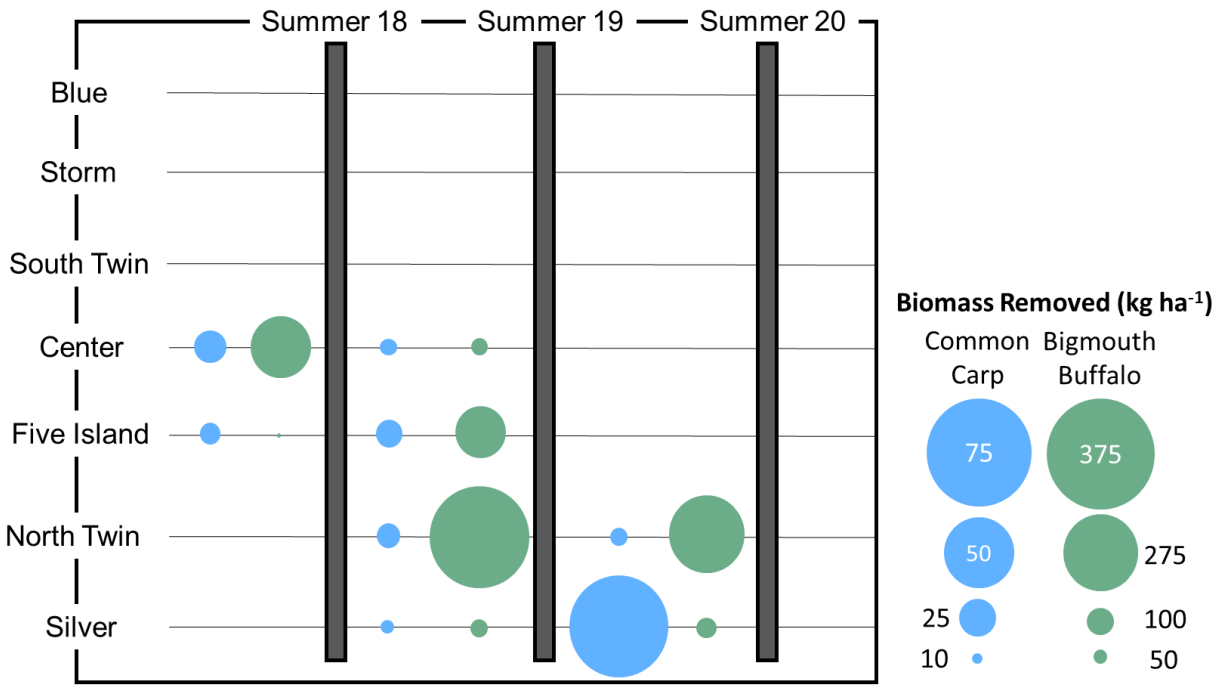

Figure 1. Removal, in kilograms per hectare (kg/ha), of common carp (*Cyprinus carpio*) and bigmouth buffalo (*Ictiobus cyprinellus*) in seven lakes in northwestern Iowa, USA. Circles represent fish biomass removed during commercial harvest, and gray bars represent when sampling took place the following summer.

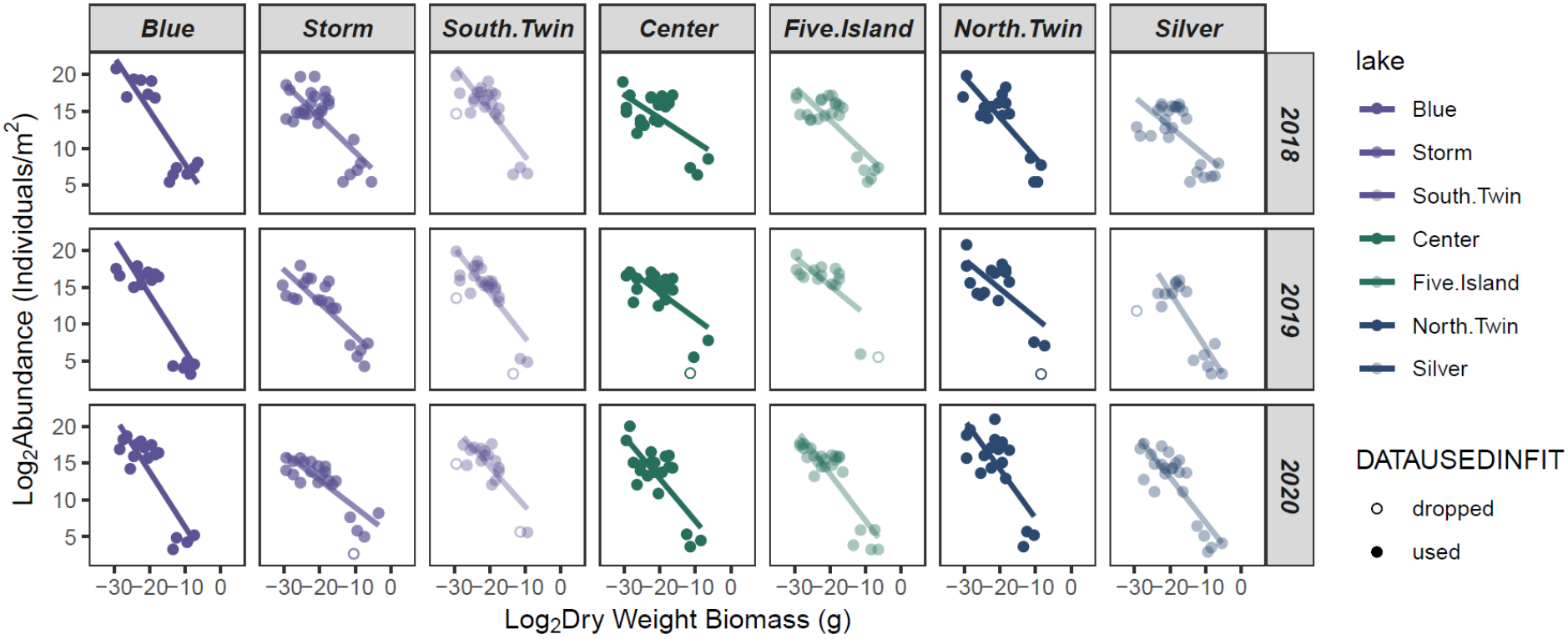

Figure 2. Zooplankton and benthic macroinvertebrate size spectra plots with slope. Color denotes the pattern of incentivized harvest with purple indicating no harvest occurred, green that harvest occurred in 2018 and 2019, and blue that harvest occurred in 2019 and 2020. Open circles denote data that was dropped due to high leverage within the ordinary least squares regression analysis.

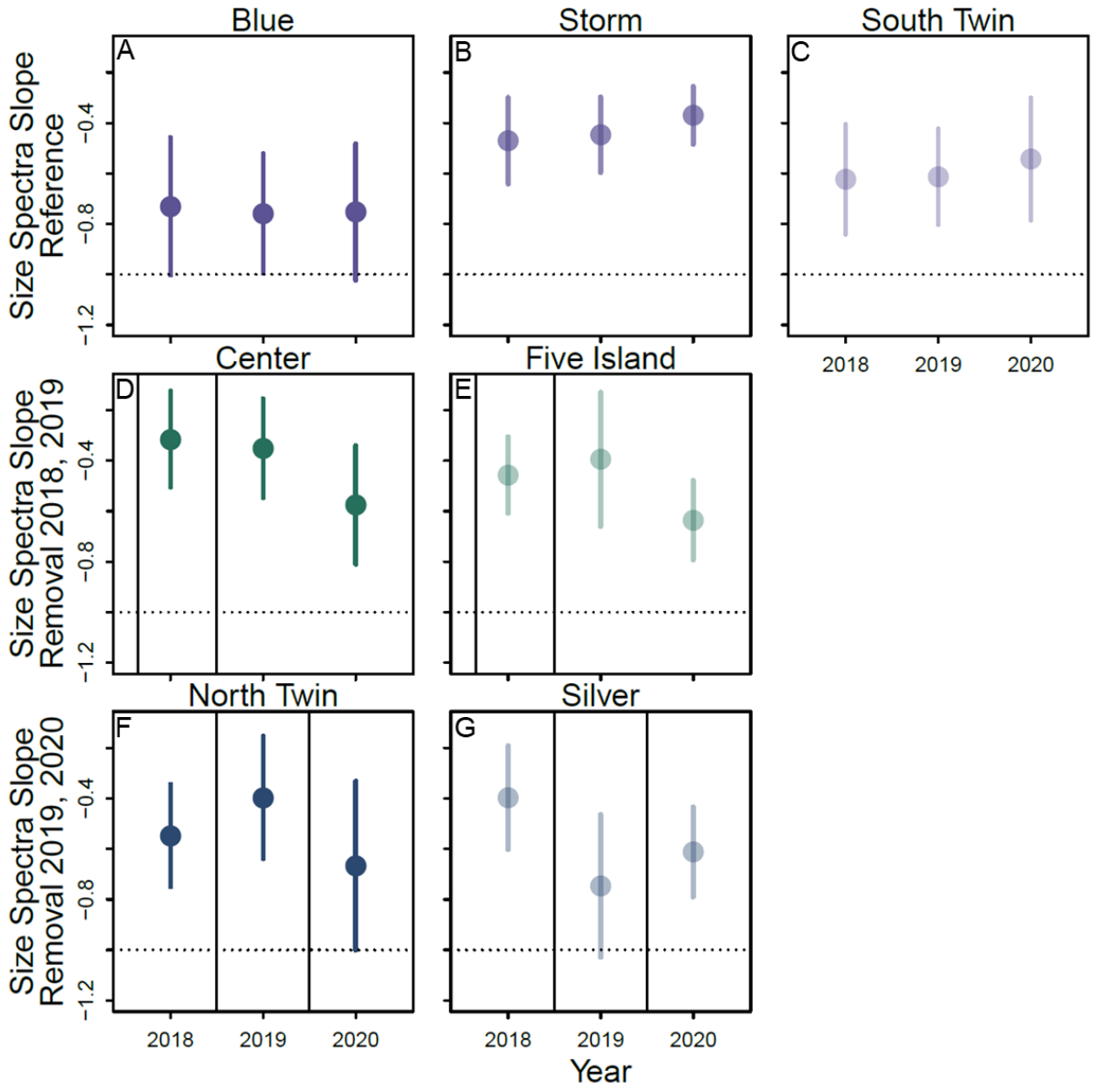

Figure 3. Slopes of each fit for the zooplankton and benthic macroinvertebrate size spectra (error bars 95% confidence intervals). Vertical lines denote when fish were harvested prior to the summer sampling season. Color denotes the pattern of incentivized harvest with purple indicating no harvest occurred (A – C), green that harvest occurred in 2018 and 2019 before sampling (D – E), and blue that harvest occurred in 2019 and 2020 before sampling (F – G).

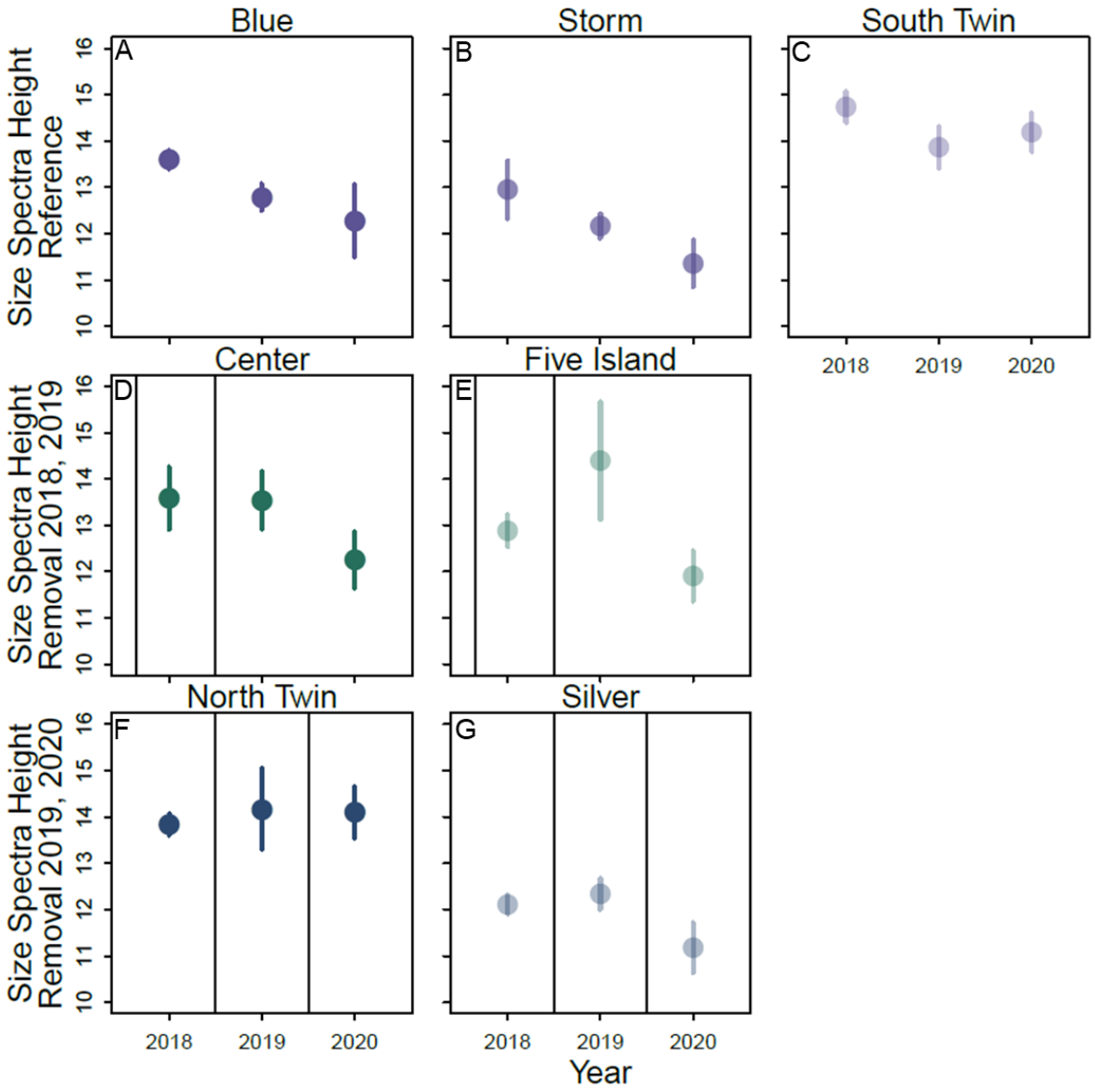

Figure 4. Height of each fit for the zooplankton and benthic macroinvertebrate size spectra (error bars 95% confidence intervals). Vertical lines denote when fish were harvested prior to the summer sampling season. Color denotes the pattern of incentivized harvest with purple indicating no harvest occurred (A – C), green that harvest occurred in 2018 and 2019 before sampling (D – E), and blue that harvest occurred in 2019 and 2020 before sampling (F – G).

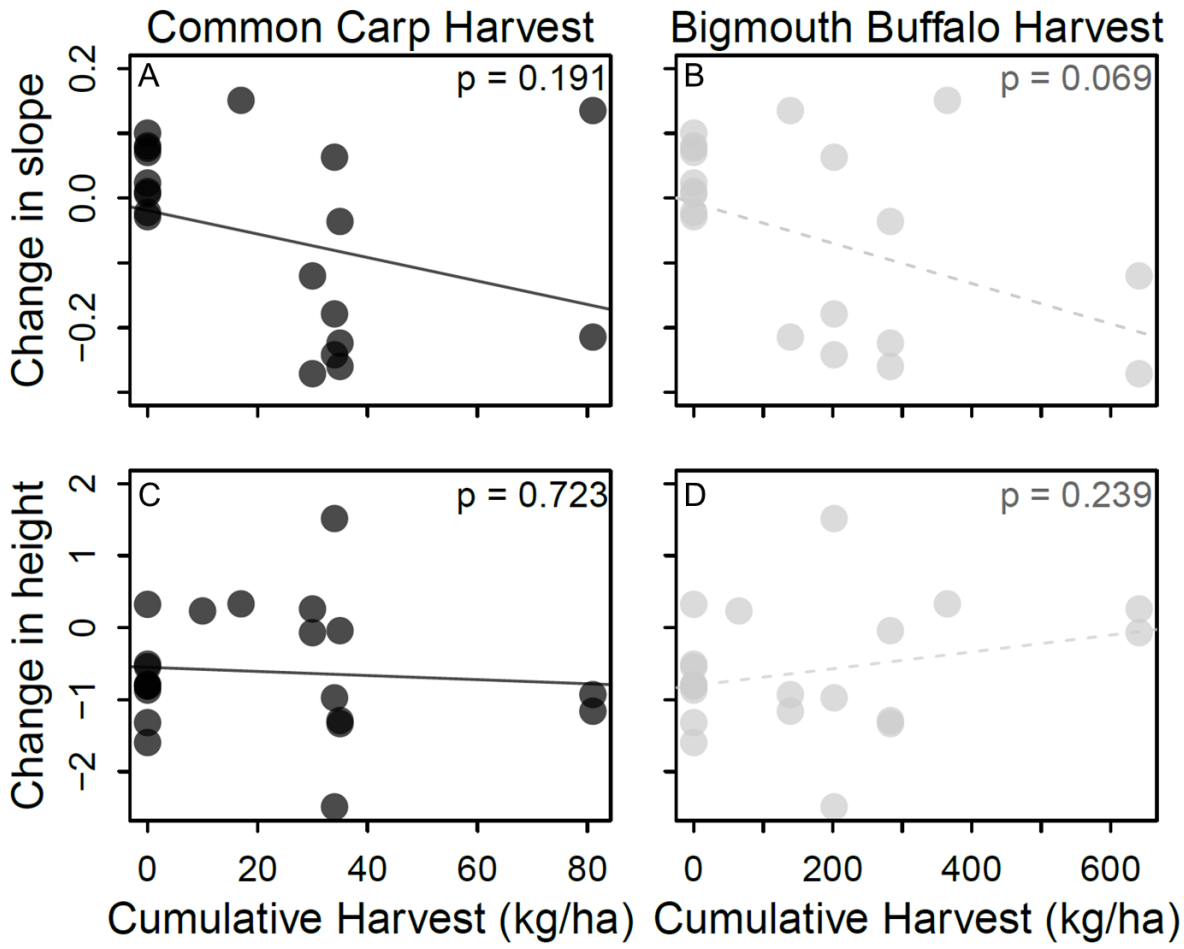

Figure 5. Simple linear regressions of the interannual change in zooplankton and benthic macroinvertebrate size spectrum slope (A – B) and height (C – D) by cumulative harvest of common carp (left column) and bigmouth buffalo (right column). Cumulative harvest represents the sum of fish harvest that occurred within a lake over the three-year study period.

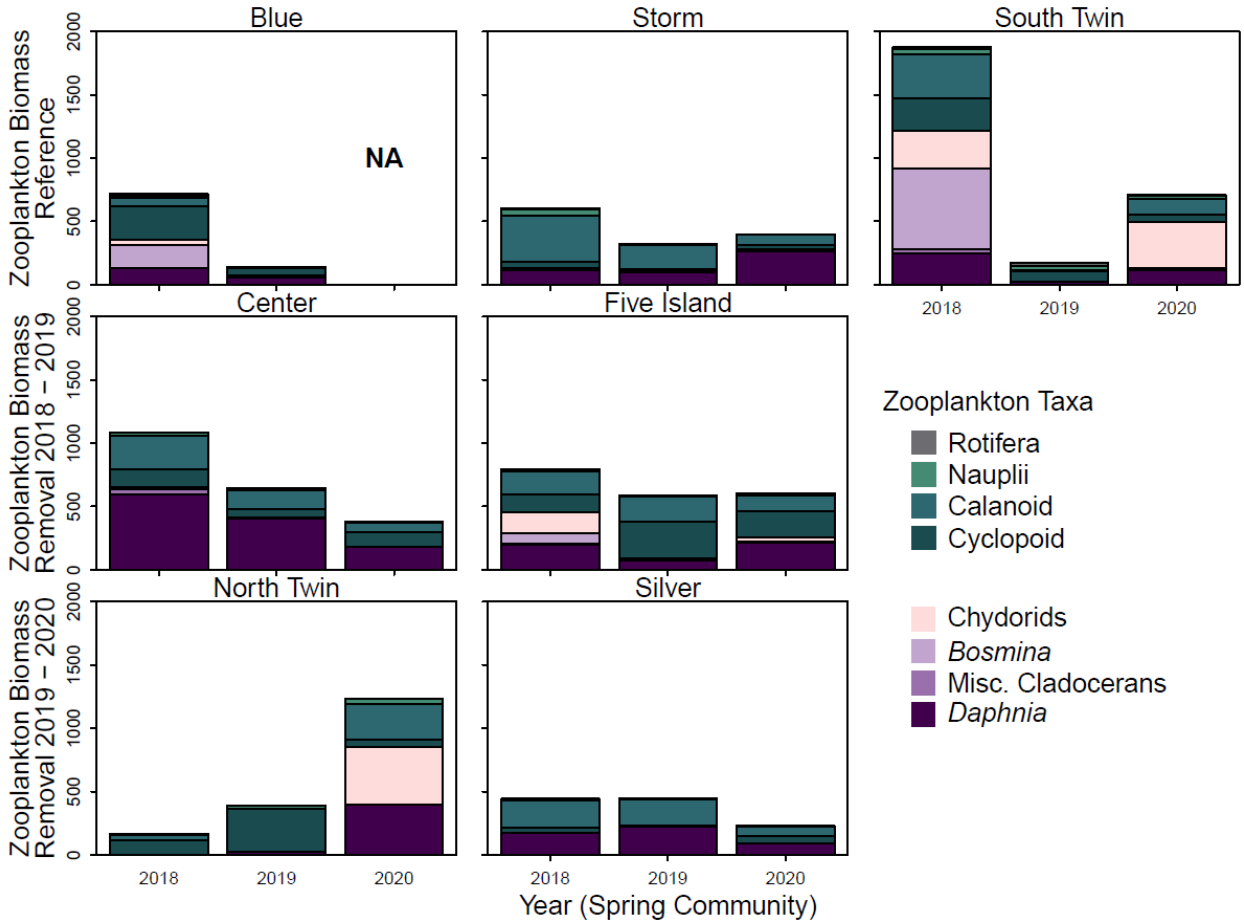

Figure 6. Spring (May – June) zooplankton community biomass (ug L^{-1})

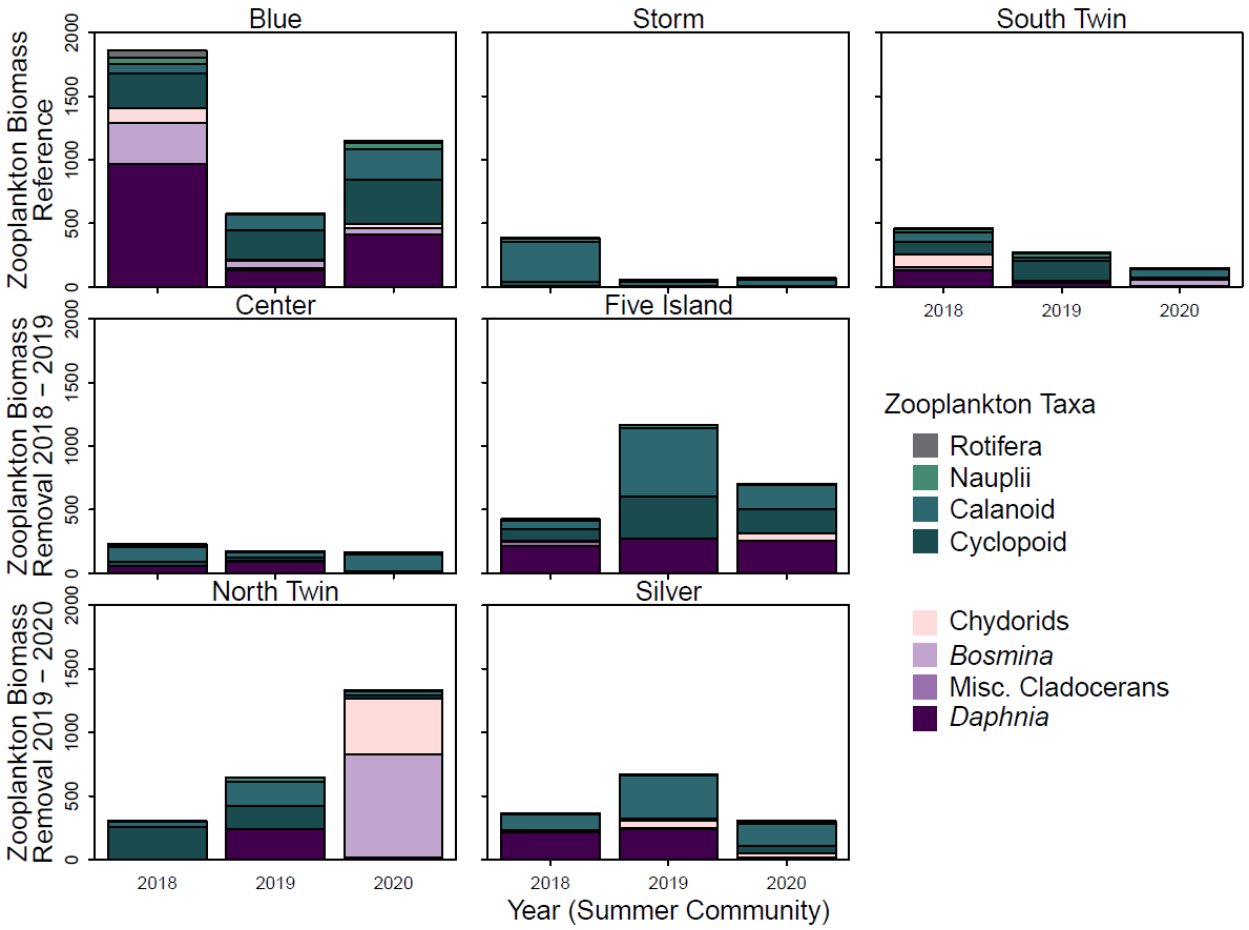

Figure 7. Summer (July – October) zooplankton community biomass (ug L^{-1})

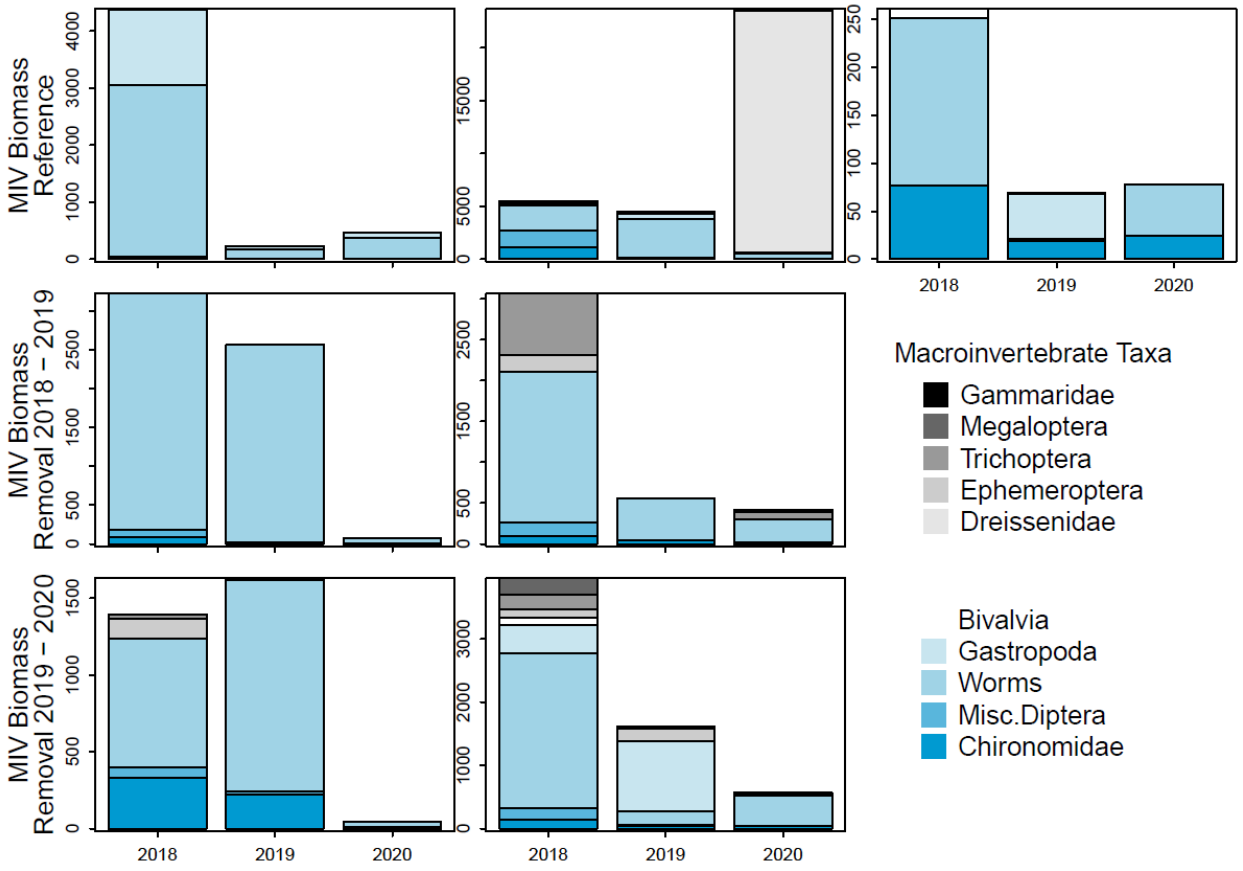

Figure 8. Macroinvertebrate (MIV) community biomass (mg m^{-2}) (note the different y-axes)

SUPPLEMENTARY INFORMATION FOR CHAPTER 2

SUPPLEMENTAL METHODS

Macroinvertebrate measurements

Oligochaeta were measured from their prostomium to their pygidium, Insecta were measured from the anterior part of their head capsule to the posterior part of their last abdominal segment, Bivalvia were measured as the longest lateral distance across their shell, and Gastropoda were measured as the lateral distance across the aperture from anterior to posterior.

SUPPLEMENTAL REFERENCES

Albright, E., Wilkinson, G., Butts, T., Shingai, Q., 2022. Summer water chemistry; sediment phosphorus fluxes and sorption capacity; sedimentation and sediment resuspension dynamics; water column thermal structure; and zooplankton, macroinvertebrate, and macrophyte communities in eight shallow lakes in northwest Iowa, USA (2018-2020) ver 3. *Environmental Data Initiative*. https://doi.org/10.6073/pasta/d3a70c1f0d534cca8bdebd7f7483ef38.

Baumgärtner, D., Rothhaupt, K.O., 2003. Predictive Length-Dry Mass Regressions for Freshwater Invertebrates in a Pre-Alpine Lake Littoral. Int Rev Hydrobiol 88, 453–463. https://doi.org/10.1002/iroh.200310632

Benke, A.C., Huryn, A.D., Smock, L.A., Wallace, J.B., 1999. Length-mass relationships for freshwater macroinvertebrates in North America with particular reference to the southeastern United States. J North Am Benthol Soc 18, 308–343. https://doi.org/10.2307/1468447

Cummins, K.W., Wilzbach, M., Kolouch, B., Merritt, R., 2022. Estimating Macroinvertebrate Biomass for Stream Ecosystem Assessments. Int J Environ Res Public Health 19. https://doi.org/10.3390/ijerph19063240

Edwards, F.K., Lauridsen, R.B., Armand, L., Vincent, H.M., Jones, J.I., 2009. The relationship between length, mass and preservation time for three species of freshwater leeches (Hirudinea). Fundamental and Applied Limnology 173, 321–327. https://doi.org/10.1127/1863-9135/2009/0173-0321

Méthot, G., Hudon, C., Gagnon, P., Pinel-Alloul, B., Armellin, A., Poirier, A.M.T., 2012. Macroinvertebrate size-mass relationships: How specific should they be? Freshwater Science 31, 750–764. https://doi.org/10.1899/11-120.1

Stoffels, R.J., Karbe, S., Paterson, R.A., 2003. Length-mass models for some common New Zealand littoral-benthic macroinvertebrates, with a note on within-taxon variability in parameter values among published models. N Z J Mar Freshwater Res 37, 449–460. https://doi.org/10.1080/00288330.2003.9517179

SUPPLEMENTAL TABLES

Table S1. Exploitation estimates for Carp and Buffalo. Percent exploitation of the Schnabel estimate of biomass (95% Confidence Interval). If a value is above 100% it means the biomass estimate was lower than the actual population present within a lake. If no harvest occurred, it is denoted as --.

	Common Carp (*Cyprinus carpio*)			Bigmouth Buffalo (*Ictiobus cyprinellus*)		
Lake	2018	2019	2020	2018	2019	2020
Center	13 % (8–190)	26 % (13–1733)	--	273 % (174–3544)	90 % (25 – 12336)	--
Five Island	7 % (5–67)	15 % (10–247)	--	84 % (43–8849)	1906 % (277–333969)	--
North Twin	--	39 % (25–713)	112 % (16–14562)	--	77 % (39–23180)	861 % (240–125057)
Silver	--	8 % (5–196)	108 % (81–2106)	--	206 % (30–66276)	549 % (315–21592)

Table S2. Range of depths for macroinvertebrate samples for each study lake. All depth values are in meters.

Site	Depth Range	Littoral Sites	Profundal Sites
Blue Lake	1.5 – 3.5	5	5
Storm Lake	2.3 – 4.6	7	3
South Twin	0.7 – 1.6	2	8
Center Lake	2.8 – 4.5	3	7
Five Island Lake	1.1 – 6.3	3	7
Silver Lake	1.7 – 2.5	4	6
North Twin	1.8 – 3.5	1	9

Table S3. Length-dry mass regressions used to calculate macroinvertebrate biomass.

Group	Taxon	Citation
Bivalvia		
	Corbiculidae	Benke et al., 1999
	Bivalvia	Benke et al., 1999
	Sphaeriidae	Benke et al., 1999
	Unionidae	Benke et al., 1999
Chironomidae		
	Chironomidae	Benke et al., 1999
Dreissenidae		
	Dreissenidae	Baumgärtner & Rothhaupt, 2003
Ephemeroptera		
	Ephemeroptera	Benke et al., 1999
	Ephemeridae	Benke et al., 1999
Gammaridae		
	Gammaridae	Benke et al., 1999
Gastropoda		
	Physidae	Cummins et al., 2022
	Planorbidae	Méthot et al., 2012
Megaloptera		
	Sialidae	Benke et al., 1999
Miscellaneous Diptera		
	Diptera	Benke et al., 1999
	Ceratopogonidae	Benke et al., 1999
	Simuliidae	Benke et al., 1999
	Ephydridae	Benke et al., 1999
Trichoptera		
	Trichoptera	Benke et al., 1999
	Molannidae	Benke et al., 1999
	Hydropsychidae	Benke et al., 1999
Worms		
	Hirudinea	Edwards et al., 2009
	Oligochaeta	Stoffels, Karbe & Paterson, 2003

Table S4. Zooplankton genera, order, or class identified within at least one of the seven study lakes from May – October (2018 - 2020).

Taxonomic Group	Taxa identified in study lakes included in group
Rotifera	*Asplanchna*
	Keratella cochlearis
	Keratella quadrata
	Polyarthra
	Anuraeopsis
	Ascomorpha
	Asplanchnopus
	Brachionus
	Conochilus
	Filinia
	Gastroopus
	Kellicottia
	Lecane
	Notholca
	Pompholyx
	Synchaeta
	Trichocerca
Nauplii	Nauplii
Calanoid	Calanoida
Cyclopoid	Cyclopoida
Chydorids	*Chydorus*
	Alona
	Alonella
Bosmina	*Bosmina*
Miscellaneous cladocerans	*Diaphanasoma*
	Leptodora
	Simocephalus
Daphnia	*Daphnia*
	Ceriodaphnia

Table S5. Macroinvertebrate family, order, or class identified within at least one of the seven study lakes (2018 – 2020).

Taxonomic Group	Taxa identified in study lakes included in group
Bivalvia	Corbiculidae Bivalvia Sphaeriidae Unionidae
Chironomidae	Chironomidae
Dreissenidae	Dreissenidae
Ephemeroptera	Ephemeroptera Ephemeridae
Gammaridae	Gammaridae
Gastropoda	Physidae Planorbidae
Megaloptera	Sialidae
Miscellaneous Diptera	Diptera Ceratopogonidae Simuliidae Ephydridae
Trichoptera	Trichoptera Molannidae Hydropsychidae
Worms	Hirudinea Oligochaeta

Table S6. AIC; forward and backward stepwise; A = abundance; MB_{dw} = Middle bin of dry weight bin (g); *BASE* = $\log_2[A]\sim\log_2[MB_{dw}]$; $D_{ref;}$ = no harvest occurred.

Model	AIC	ΔAIC
BASE + lake + year + $D_{harvest2}$ + $\log_2[MB_{dw}]$*lake	805.74	--
BASE + lake + year + $D_{harvest2}$ + $\log_2[MB_{dw}]$*lake + $\log_2[MB_{dw}]$*year	806.08	0.34
BASE + lake + year + $\log_2[MB_{dw}]$*lake + $\log_2[MB_{dw}]$*year	807.78	2.04
BASE + lake + year + $\log_2[MB_{dw}]$*lake + $\log_2[MB_{dw}]$*year + lake*year	822.62	16.88
BASE + lake + year + $\log_2[MB_{dw}]$*lake + $\log_2[MB_{dw}]$*year + lake*year + $\log_2[MB_{dw}]$*lake*year	831.17	25.43

Table S7. Tukey post-hoc comparisons of $log_2[MB_{dw}]$ x lake interaction sorted by p-value (bold if significant.

Middle of dry weight bin	$2^{-19.7}$					
$Log_2[MB_{dw}]$ trend & Lake 1	**$Log_2[MB_{dw}]$ trend & Lake 2**	**Estimate**	**SE**	**df**	**T-ratio**	**p-value**
$Log_2[MB_{dw}]$*Blue	$Log_2[MB_{dw}]$*Center	-0.34	0.08	394	-4.21	**<0.001**
$Log_2[MB_{dw}]$*Blue	$Log_2[MB_{dw}]$*Storm	-0.31	0.07	394	-4.19	**<0.001**
$Log_2[MB_{dw}]$*Blue	$Log_2[MB_{dw}]$* Five Island	-0.22	0.08	394	-2.78	0.082
$Log_2[MB_{dw}]$*Blue	$Log_2[MB_{dw}]$*Silver	-0.20	0.08	394	-2.51	0.159
$Log_2[MB_{dw}]$*Blue	$Log_2[MB_{dw}]$* North Twin	-0.21	0.08	394	-2.44	0.183
$Log_2[MB_{dw}]$*Center	$Log_2[MB_{dw}]$* South Twin	0.20	0.09	394	2.13	0.335
$Log_2[MB_{dw}]$* South Twin	$Log_2[MB_{dw}]$*Storm	-0.16	0.09	394	-1.92	0.469
$Log_2[MB_{dw}]$*Center	$Log_2[MB_{dw}]$*Silver	0.14	0.08	394	1.83	0.528
$Log_2[MB_{dw}]$*Center	$Log_2[MB_{dw}]$* Five Island	0.13	0.08	394	1.64	0.654
$Log_2[MB_{dw}]$*Center	$Log_2[MB_{dw}]$* North Twin	0.14	0.08	394	1.62	0.670
$Log_2[MB_{dw}]$*Silver	$Log_2[MB_{dw}]$*Storm	-0.11	0.07	394	-1.58	0.696
$Log_2[MB_{dw}]$*Blue	$Log_2[MB_{dw}]$* South Twin	-0.15	0.09	394	-1.57	0.703
$Log_2[MB_{dw}]$* Five Island	$Log_2[MB_{dw}]$*Storm	-0.09	0.07	394	-1.37	0.819
$Log_2[MB_{dw}]$* North Twin	$Log_2[MB_{dw}]$*Storm	-0.10	0.08	394	-1.35	0.827
$Log_2[MB_{dw}]$* Five Island	$Log_2[MB_{dw}]$* South Twin	0.07	0.09	394	0.79	0.986
$Log_2[MB_{dw}]$* North Twin	$Log_2[MB_{dw}]$* South Twin	0.06	0.09	394	0.64	0.995
$Log_2[MB_{dw}]$*Silver	$Log_2[MB_{dw}]$* South Twin	0.05	0.09	394	0.59	0.997
$Log_2[MB_{dw}]$*Center	$Log_2[MB_{dw}]$*Storm	0.03	0.07	394	0.44	0.999
$Log_2[MB_{dw}]$* Five Island	$Log_2[MB_{dw}]$*Silver	0.02	0.07	394	0.23	1.000
$Log_2[MB_{dw}]$* Five Island	$Log_2[MB_{dw}]$* North Twin	0.01	0.08	394	0.12	1.000
$Log_2[MB_{dw}]$* North Twin	$Log_2[MB_{dw}]$*Silver	0.01	0.08	394	0.10	1.000

Table S8. Model information for weighted regression of height by lake and year

Coefficients	Estimate	SE	t-value	*p*-value
Intercept	1067.74	271.07	3.94	**0.002**
Year	-0.52	0.13	-3.89	**0.002**
Center Lake	0.28	0.48	0.59	0.563
Five Island Lake	-0.23	0.45	-0.52	0.613
North Twin Lake	0.92	0.52	1.78	0.098
Silver Lake	-1.06	0.46	-2.31	**0.038**
South Twin Lake	1.32	0.49	2.72	**0.017**
Storm Lake	-0.81	0.42	-1.94	0.075

Table S9. Model information for slope and height v. total cumulative harvest

Model	Coefficients	Estimate	Standard Error	T-value	*p*-value
Slope ~ Total Harvest	Intercept	-0.002	0.042	-0.060	0.953
	Harvest	-0.000	0.000	-2.000	0.060
				$F_{1, 19} = 3.998$, Adjusted $R^2 = 13.04$ %	
Height ~ Total Harvest	Intercept	-0.799	0.254	-3.150	**0.005**
	Harvest	-0.001	0.001	-1.094	0.288
				$F_{1, 19} = 1.197$, Adjusted $R^2 = 28.76$ %	

Table S10. Summary statistics for the permutational analysis of variance of spring (May – June) and summer (July – October) zooplankton communities with 999 permutations.

Lake	**Factor**	**df**	**SS**	**R^2**	**Pseudo F**	***p*-value**
Spring Community						
Storm	Year	2	0.29	0.35	2.91	**0.013**
	Residual	11	0.54	0.65		
	Total	13	0.82	1		
South Twin	Year	2	0.53	0.66	4.76	**0.011**
	Residual	5	0.28	0.34		
	Total	7	0.81	1		
Center	Year	2	0.07	0.09	0.40	0.909
	Residual	8	0.69	0.91		
	Total	10	0.76	1		
Five Island	Year	2	0.20	0.20	0.98	0.471
	Residual	8	0.81	0.80		
	Total	10	1.00	1		
North Twin	Year	2	0.84	0.61	6.93	**0.004**
	Residual	9	0.54	0.39		
	Total	11	1.38	1		
Silver	Year	2	0.06	0.15	0.70	0.688
	Residual	8	0.35	0.85		
	Total	10	0.42	1		
Summer Community						
Blue	Year	2	0.19	0.46	2.11	**0.021**
	Residual	5	0.22	0.54		
	Total	7	0.41	1		
Storm	Year	2	0.16	0.18	0.87	0.564
	Residual	8	0.73	0.82		
	Total	10	0.89	1		
South Twin	Year	2	0.49	0.70	4.78	**0.018**
	Residual	4	0.20	0.30		
	Total	6	0.69	1		
Center	Year	2	0.18	0.24	1.42	0.229
	Residual	9	0.58	0.76		
	Total	11	0.76	1		
Five Island	Year	2	0.20	0.31	2.43	**0.027**
	Residual	11	0.45	0.69		
	Total	13	0.64	1		
North Twin	Year	2	1.01	0.65	6.50	**0.001**
	Residual	7	0.54	0.35		
	Total	9	1.55	1		
Silver	Year	2	0.30	0.35	2.98	**0.045**
	Residual	11	0.55	0.65		
	Total	13	0.84	1		

SUPPLEMENTAL FIGURES

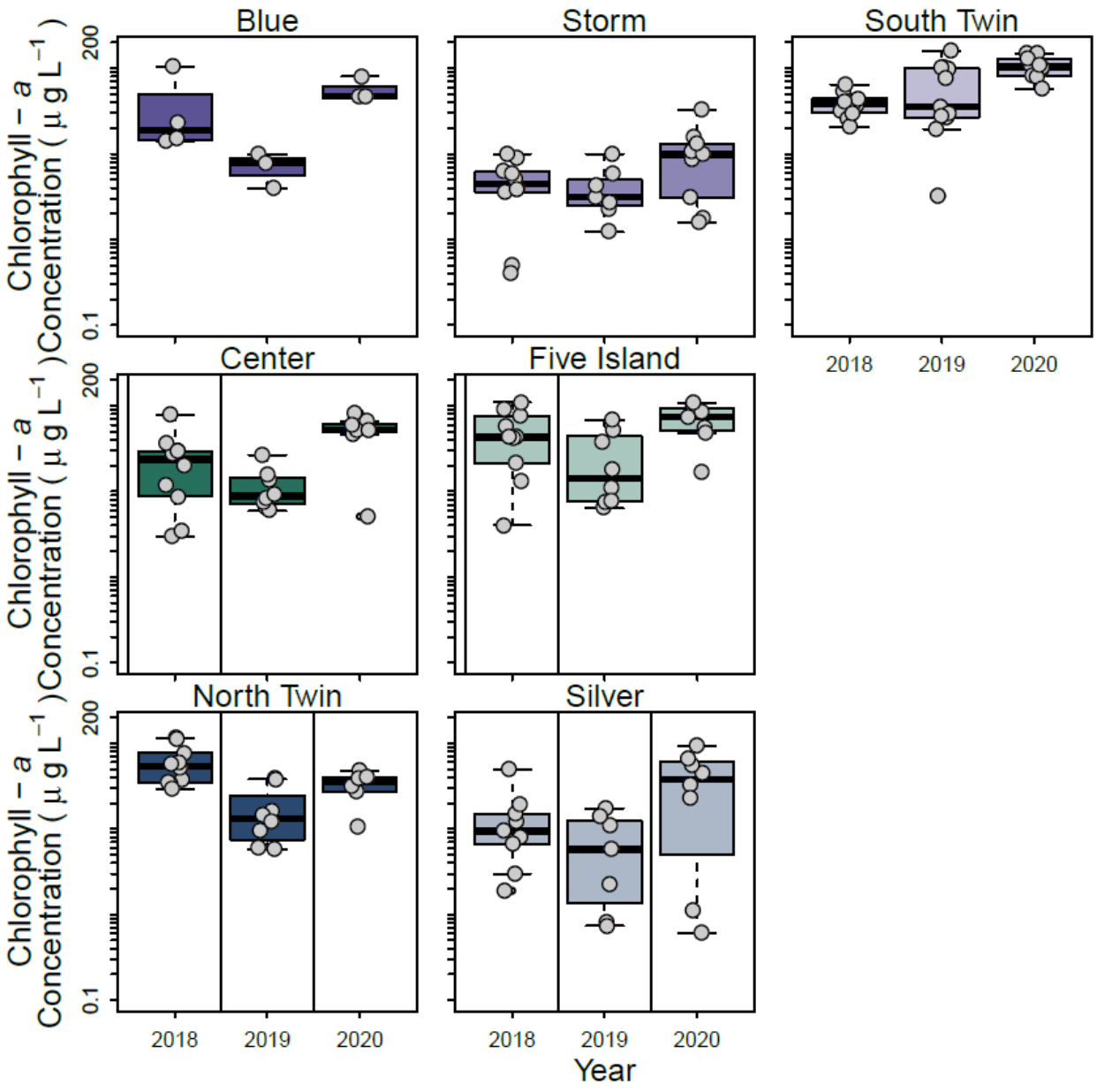

Figure S1. Chlorophyll-*a* concentration in micrograms per liter (µg L^{-1}) for each study lake from published data in Albright et al. (2022). Vertical lines denote when fish were harvested prior to the summer sampling season.

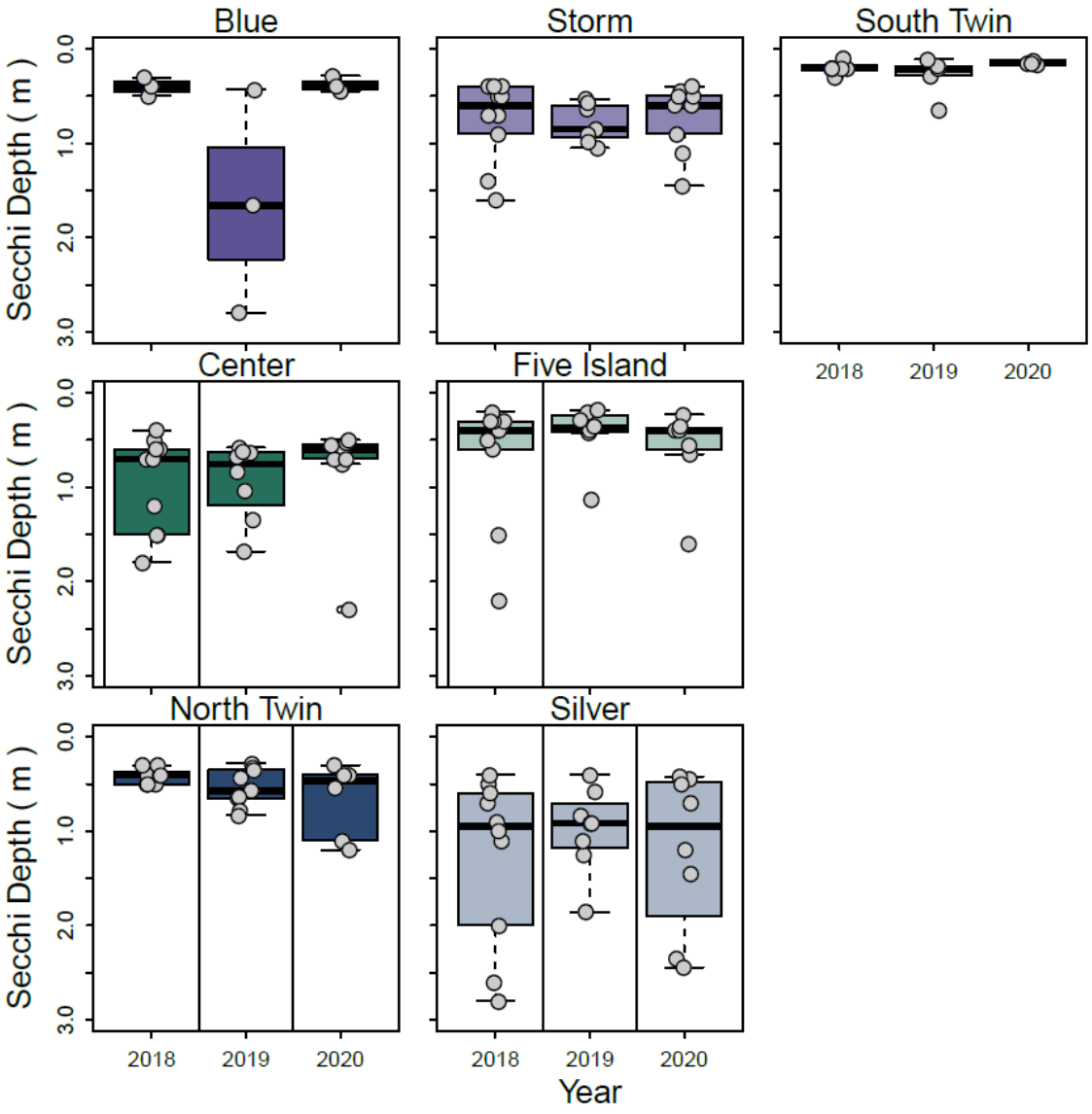

Figure S2. Secchi depth in meters (m) for each study lake derived from published data in Albright et al. (2022). Vertical lines denote when fish were harvested prior to the summer sampling season.

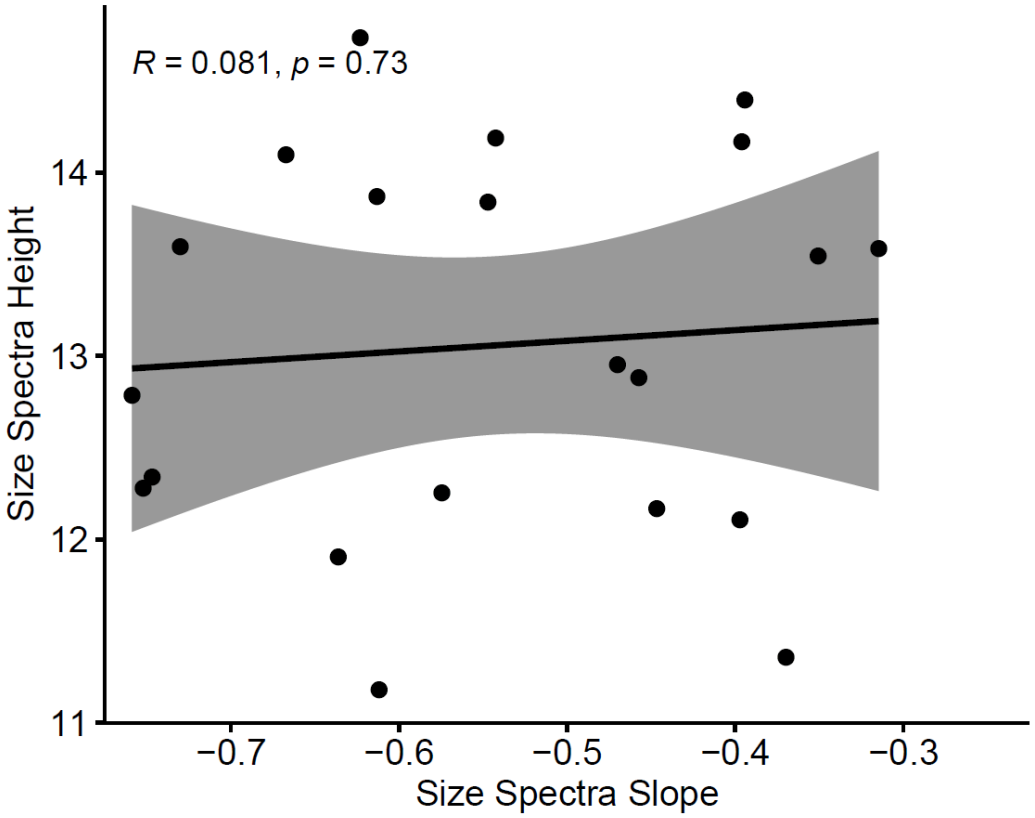

Figure S3. Height and slope independent measures.

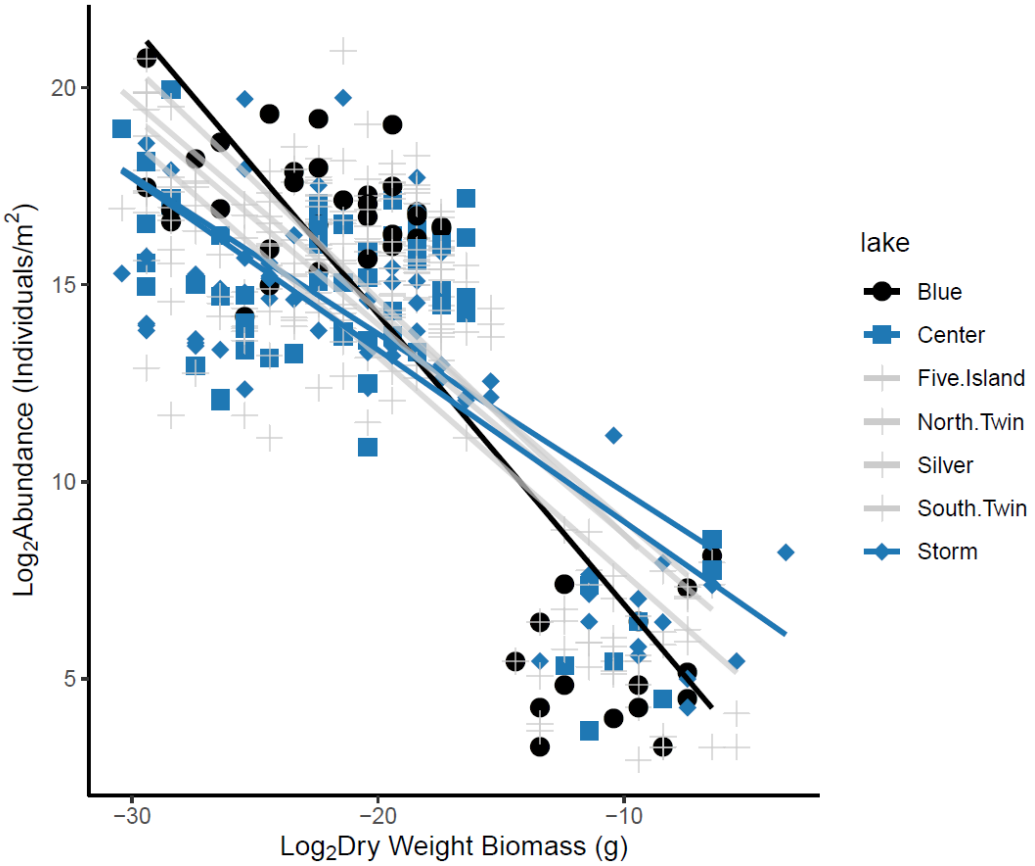

Figure S4. Difference in slope by lake visualizing the significant interaction between lake and the $\log_2$[middle of dry weight bin]. Center and Storm Lake slopes (blue) are significantly different from Blue lake (black). All other lakes did not have significant interactions (gray).

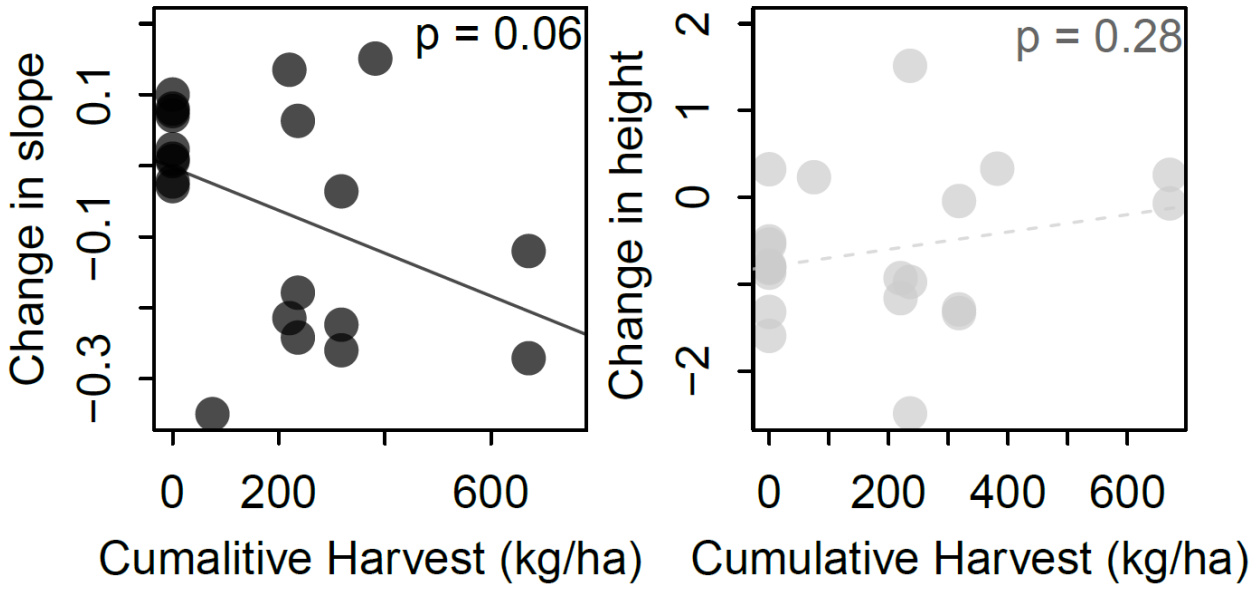

Figure S5. Change in slope (A) and height (B) for each lake and year in relation to the cumulative harvest of both common carp and bigmouth buffalo.

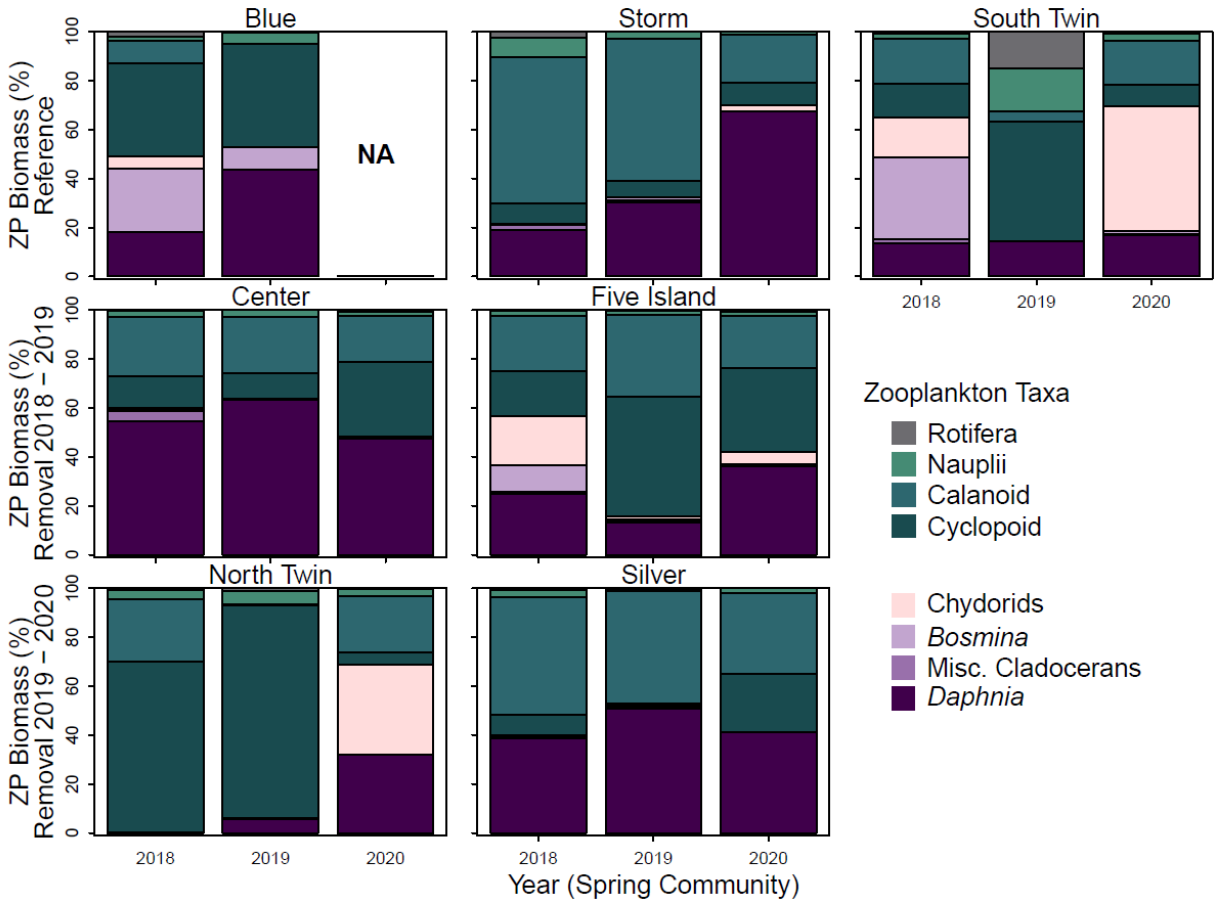

Figure S6. Zooplankton (ZP) biomass in micrograms per liter (µg L^{-1}) expressed as a percentage (%) of the total community biomass for all lakes and years for sampling dates between July and October 2018 - 2020. Samples were not collected prior to July in Blue Lake in 2020 due to COVID-19 pandemic sampling restrictions; thus, there are no data available for that lake year.

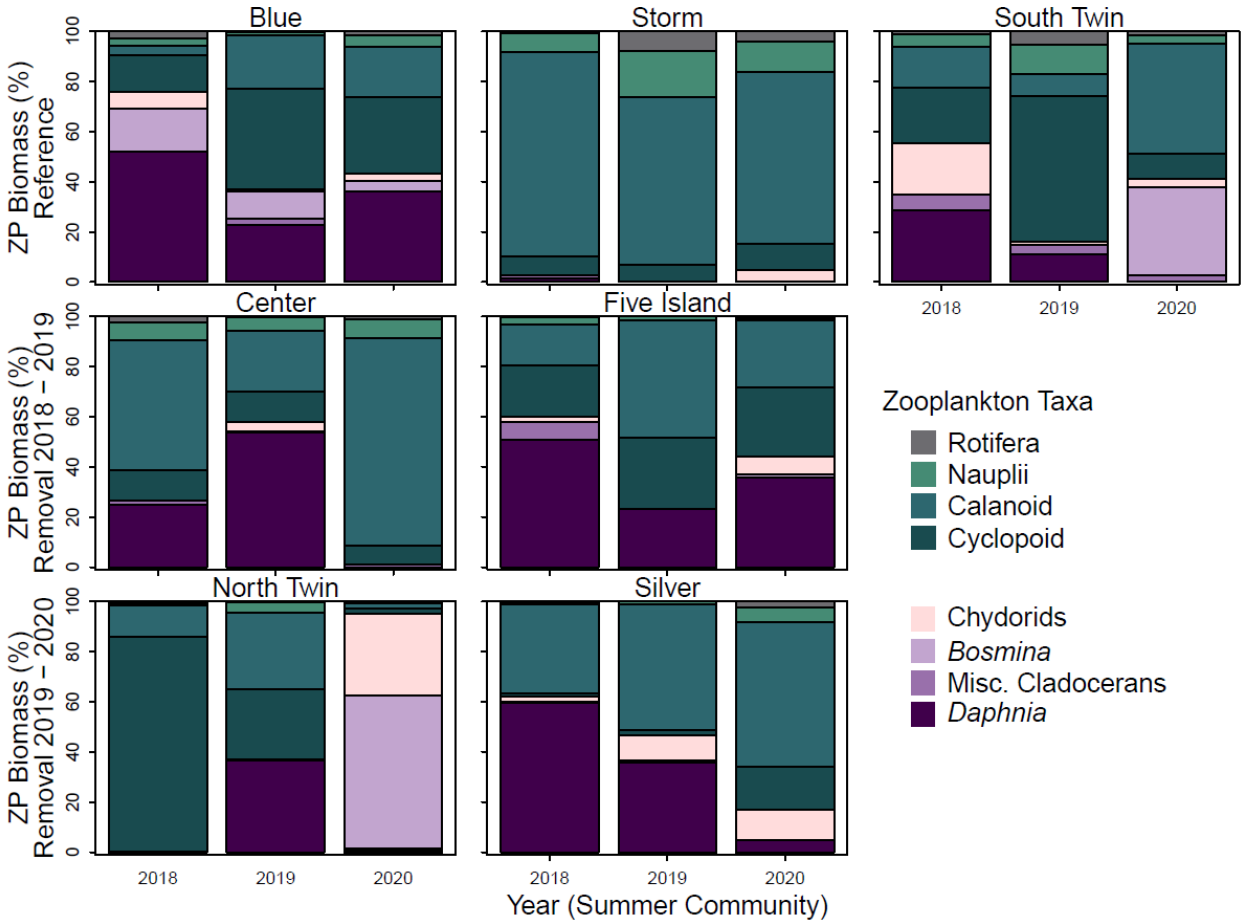

Figure S7. Zooplankton (ZP) biomass in micrograms per liter (µg L^{-1}) expressed as a percentage (%) of the total community biomass for all lakes and years for sampling dates between May and June.

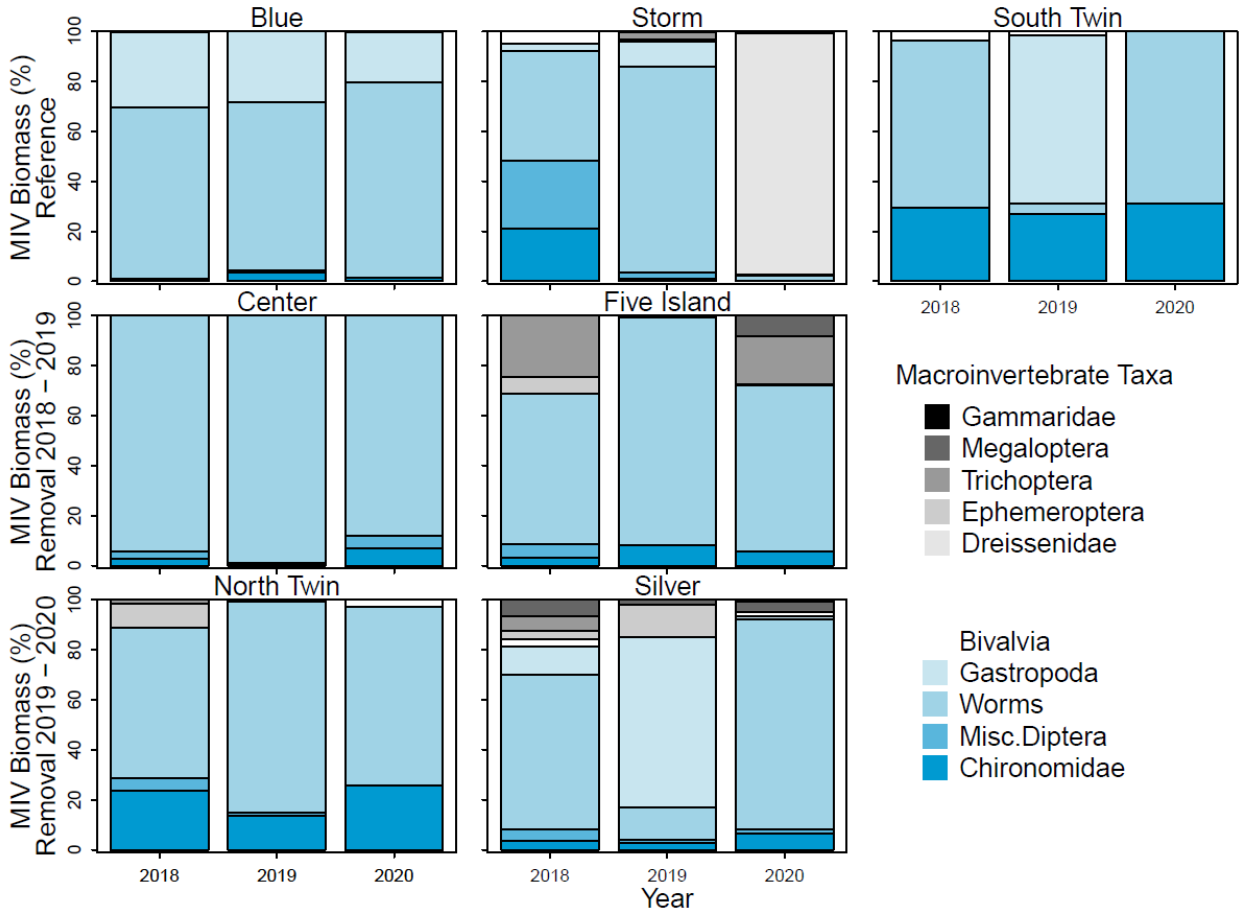

Figure S8. Macroinvertebrate (MIV) biomass in milligrams per square meter (mg m^{-2}) expressed as a percentage (%) of the total community biomass for all lakes and years.

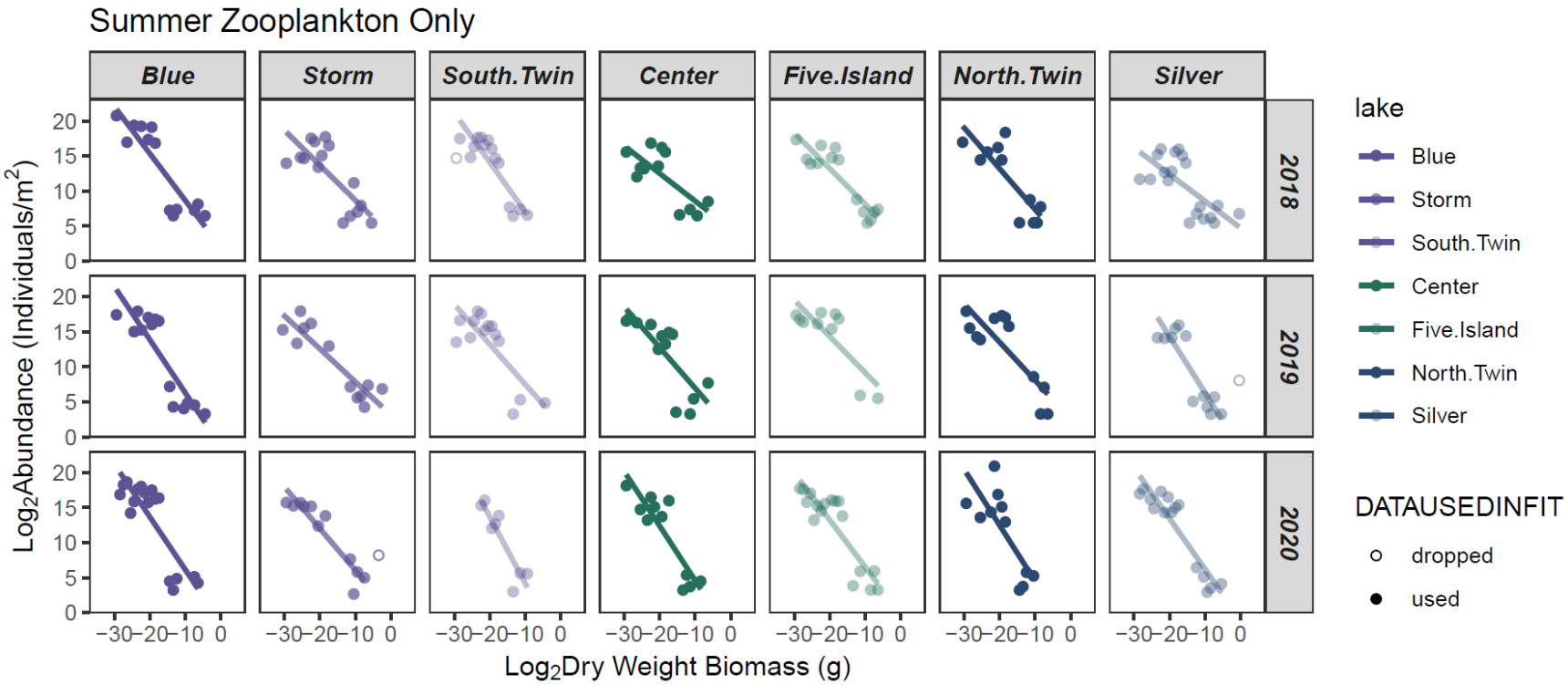

Figure S9. Abundance size spectra plots with slope with spring zooplankton data removed. Color denotes the pattern of incentivized harvest with purple indicating no harvest occurred, green that harvest occurred in 2018 and 2019, and blue that harvest occurred in 2019 and 2020. Open circles denote data that was dropped due to high leverage within the ordinary least squares regression analysis.

CHAPTER 3

BENTHIC-PELAGIC COUPLING IN AQUATIC FOOD WEBS AFFECTS THE RESISTANCE AND RESILIENCE OF EXPERIMENTAL POND ECOSYSTEMS TO NUTRIENT PULSE DISTURBANCES

In preparation for submission with coauthors R.A. Johnson, M.J. Weber, and G.M. Wilkinson to *Ecology*

Author Contributions: Butts designed the study; performed all field and laboratory work; cleaned, analyzed, and visualized the data; and wrote the manuscript. Johnson and Wilkinson contributed to study design, data analysis, and data collection. Weber contributed to study design and data collection; and Johnson, Weber, and Wilkinson provided writing feedback.

ABSTRACT

The frequency and intensity of ecosystem disturbances is increasing due to climate change. However, the structure of trophic interactions within food webs may mediate the resistance and resilience of ecosystems to disturbance events. In aquatic ecosystems, high connectivity between benthic and pelagic food chains (i.e., benthic-pelagic coupling) is theorized to generate more pathways for nutrients and energy to flow as well as strengthen top-down control. As such, we predicted that greater benthic-pelagic coupling would increase the resistance (longer response time) and resilience (shorter recovery time) of aquatic primary production to pulse disturbances and reduce the chance of a critical transition. To test this prediction, we simulated two storm-induced pulse disturbances by adding N and P (~3% and ~5% increase in ambient concentrations) to three experimental ponds with food webs containing low, intermediate, and high benthic-pelagic coupling. Another set of ponds with matching food web structures served as reference ecosystems. We evaluated the primary production response time

(resistance) and recovery time (resilience) following each nutrient pulse using a response detection algorithm and quantified the occurrence of a critical transition in algal biomass. The high coupling pond never exceeded the response threshold. Following our prediction, chlorophyll concentrations exceeded the response threshold after 23 and 18 days in the intermediate and low coupling ponds, respectively. There was also evidence of a critical transition in the low coupling pond following the first pulse. After the second nutrient pulse, chlorophyll exceeded the response threshold again in both low and intermediate ponds, but the response was much faster in the low coupling pond (8 days). Recovery time increased substantially after the second pulse. In the low coupling pond recovery following the second pulse increased from 8 to 22 days and did not occur following the second pulse in the intermediate pond. Together, these results support our prediction that greater benthic-pelagic coupling confers greater resistance and resilience to repeated pulses of nutrient loading, demonstrating that the degree of connectivity can mediate the response to disturbance.

INTRODUCTION

The frequency, scale, and intensity of ecosystem disturbances are increasing as accelerating climate change drives more frequent and intense temperature extremes and precipitation events (Seneviratne et al. 2021). Changes to disturbance regimes driven by climate change are also increasing the likelihood of abrupt changes, or rapid shifts in ecosystem state relative to typical rates of change within the ecosystem (Ratajczak et al. 2018, Turner et al. 2020). For example, extreme heat waves have been linked to mass bleaching events in coral reefs (Hughes et al. 2018) and extreme precipitation, along with agricultural land use, has been tied to increased eutrophication and higher abundances of toxin-producing phytoplankton in aquatic

ecosystems (Ho and Michalak 2020). Abrupt changes can also become critical transitions, a transition from one equilibrium state to another, which may prevent ecosystem recovery to the prior state and increased vulnerability to further disturbances (Scheffer and Carpenter 2003, Taranu et al. 2018). Understanding the mechanisms mediating effects of disturbance on ecosystem function is imperative for effective ecosystem management in the face of rapid change.

Pulse disturbances, sudden and temporally constrained disturbances that alter biomass or composition of ecological communities, are ubiquitous in aquatic ecosystems and expected to increase (Prein et al. 2017, Jentsch and White 2019). For example, large precipitation events, which are increasing in frequency and magnitude in some regions (Seneviratne et al. 2021), deliver pulses of nitrogen (N) and phosphorus (P) to surface waters (Joosse and Baker 2011). In many lakes, annual nutrient loading is disproportionately dominated by a few loading events during large storms (Carpenter et al. 2015, 2018). In agricultural watersheds, inputs of P from fertilizer and manure to the landscape exceed crop uptake by 50% in some areas, generating surplus P that is readily mobilized into aquatic ecosystems (Kelly et al. 2019, Sabo et al. 2021). Excess nutrients fuel eutrophication resulting in increasing turbidity, depleting dissolved oxygen, and favoring toxin-producing phytoplankton that adversely affect human health (Thornton et al. 2013, Carmichael and Boyer 2016, le Moal et al. 2019). However, not all lakes will respond to nutrient pulses in the same way as antecedent conditions, ecosystem properties, and watershed characteristics affect whether nutrient pulses linked to storm events will alter ecosystem function or trigger an abrupt change (Stockwell et al. 2020). Thus, there is a pressing need to better understand the mechanisms that mediate aquatic ecosystem responses to pulse nutrient disturbances.

The strength of interactions between species and overall food web architecture plays a critical role in determining how ecological communities will react to increasing and interacting disturbances (McCann et al. 1998, Kuiper et al. 2015, Polazzo et al. 2022). Food web structure can produce differences in the resistance (defined here as the response time and response magnitude to the nutrient pulse) and resilience (defined here as the rate at which the system recovered from the nutrient pulse) of aquatic ecosystems to nutrient additions (Cottingham and Schindler 2000). For example, during a whole-ecosystem nutrient pulse experiment in two small lakes in northern Wisconsin, increasing the number of trophic levels from two to three through the addition of a planktivore led to decreased ecosystem resistance to nutrient pulses (Cottingham and Schindler 2000). Other components of food web structure (e.g., connectivity, structural asymmetry, functional diversity) may also alter the ability of aquatic ecosystems to mitigate the effects of disturbances (Calizza et al. 2019, Kovalenko 2019, Wojcik et al. 2021). For example, the coupling of the algae-based food chain to the detritus/periphyton-based food chain by generalist consumers (Vadeboncoeur et al. 2002; Vander Zanden & Vadeboncoeur 2002; McCann et al. 2005) is a common food web architecture in lakes. Generalist consumers incorporate a diversity of prey items across different habitats increasing connectivity between benthic and pelagic food chains (hereafter benthic-pelagic coupling).

Benthic-pelagic coupling is theorized to improve ecosystem resilience to complex and interacting disturbances by increasing connectivity and modularity within food webs which provides stability in the face of changing resource availability (Thompson et al. 2012, McMeans et al. 2016). There is a mix of empirical and theoretical evidence that benthic-pelagic coupling can strengthen aquatic trophic cascades by providing resource subsidies and higher growth potential for top consumers in the food chain (Vadeboncoeur et al. 2005, Vander Zanden et al.

2005, Marklund et al. 2019). Furthermore, benthic-pelagic coupling may influence ecosystem stability, resilience, and nutrient cycling (Blanchard et al. 2011, Rooney and McCann 2012, Baustian et al. 2014). Such mechanisms may reduce the occurrence of abrupt changes or even critical transitions within aquatic ecosystems. While benthic-pelagic coupling in food webs is theorized to significantly influence ecosystem responses to disturbances, there is limited empirical evidence demonstrating how, and to what degree, benthic-pelagic coupling affects resistance and resilience to nutrient pulses.

We performed a set of whole-ecosystem manipulations to empirically evaluate how the degree of benthic-pelagic coupling affects ecosystem responses to pulse nutrient loading events using paired experimental ponds. Specifically, we asked (1) does the degree of benthic-pelagic coupling affect the response and recovery time of primary production to nutrient pulses? and (2) does the degree of benthic-pelagic coupling influence whether a critical transition occurs in response to a pulse nutrient loading event? We predicted that greater benthic-pelagic coupling would result in slower response times of primary production to nutrient pulses (i.e., greater resistance), faster return times (i.e., greater resilience), and a reduced chance of a critical transition occurring due to stronger top-down control and the presence of more pathways by which energy and nutrients could flow within the food web. To address these questions, we performed a series of paired ecosystem experiments in ponds with food web structures that varied in benthic-pelagic coupling subjecting one pond in each pair to two nutrient pulse disturbances.

METHODS

Study Site

The ecosystem experiment occurred in summer 2020 at the Iowa State Horticultural Research Station (42.110005, -93.580454) in a set of six experimental ponds. The ponds have a wetted surface area of roughly 400 m^2 and a mean depth of 0.8 m (maximum: 2 m) consistent with the functional definition of pond ecosystems (Richardson et al. 2022). The ponds' watersheds were limited to a few meters on each side and the bottom was sealed with bentonite clay to restrict groundwater flow. The only hydrologic input during the experiment was direct precipitation. In April 2020, the ponds were filled with water from the on-site irrigation reservoir seeding each pond with a similar, natural assemblage of phytoplankton and zooplankton. Communities of emergent longleaf pondweed (*Potamogeton nodosus*) and submerged leafy pondweed (*Potamogeton foliosus*) were naturally established in each pond.

Experimental Design

Across the six ponds, three fish assemblages were established to create food web structures with low, intermediate, and high connectivity between benthic and pelagic food chains (Figure 1). Each fish assemblage was randomly assigned to two ponds that were paired in the experiment with one receiving the pulse nutrient additions (see description below) and one serving as an unmanipulated reference. The low benthic-pelagic coupling ponds' assemblage consisted of largely planktivorous bluegill (*Lepomis macrochirus,* (Werner and Hall 1988), zooplankton, and phytoplankton in the pelagic pathway and largely zoobenthivorous yellow perch (*Perca flavescens*, (Tyson and Knight 2001), macroinvertebrates, periphyton, and detritus in the benthic pathway. The intermediate benthic-pelagic coupling ponds had the same

assemblage as the low coupling ponds with an added generalist consumer, largemouth bass which preys in both benthic and pelagic food chains (*Micropterus salmoides*, (Hodgson and Hodgson 2000). The assemblage in the high benthic-pelagic coupling ponds was the same as the intermediate coupling ponds with an additional generalist consumer, fathead minnows, to further increase the trophic connections between benthic and pelagic food chains (*Pimephales promelas*, Duffy 1998). These fishes represent common species in lakes throughout much of North America and were added at biomass densities consistent with natural waterbodies and other pond experiments (Carlander 1977, Carey and Wahl 2010). Fish biomass for each species was kept consistent across ponds. For example, the biomass of bluegill added to one pond was the same biomass added to all the other ponds. When a pond had an additional species, such as the intermediate and high coupling ponds, we kept the biomass of species consistent across ponds, but total fish biomass increased (i.e., an additive design; Carey and Wahl 2010, Collins et al. 2017). The total fish biomass for all ponds fell within the range of natural values (Carlander 1977).

All fish used to establish the food webs were collected via electrofishing from Brushy Creek Lake (42.39194, -93.98917) except for bluegill which were harvested from both Brushy Creek Lake and Five Island Lake (43.15806, -94.64667). Fathead minnows were purchased from Beemer Fisheries in Bedford, IA. Yellow perch were stocked in all ponds on day of year (DOY) 98 and 99 with additional perch added on DOY 127 to replace individuals that died from stress or natural mortality. Bluegill were added to all ponds on DOY 127 and 128 from Brushy Creek Lake and from Five Island Lake on DOY 133. On DOY 141, largemouth bass were added to both the intermediate and high benthic-pelagic coupling ponds, along with fathead minnows to the high benthic-pelagic coupling ponds.

We performed two discrete additions of nutrients (i.e., pulses) to three of the ponds on DOY 176 and DOY 211 (Figure 1). We designed the nutrient pulses to simulate the magnitude and stoichiometry of a storm-driven nutrient loading event in an agricultural watershed (Vanni et al. 2001, Lürling et al. 2018). The pond volume (~450 m^3) and ambient nutrient concentrations measured the week prior to the planned nutrient pulse additions were used to determine the mass of nitrogen (N) and phosphorus (P) to add (Table S1) such that the first and second pulses resulted in a 3% and 5% increase in P concentration, respectively. We added ammonium nitrate (NH_4NO_3) and sodium phosphate monobasic dihydrate ($NaH_2PO4•H_2O$) at a 24N:1P ratio. The nutrients were delivered to the ponds slowly, pouring the N and P mixture dissolved in pond water from a 4 L carboy over the side of a kayak while paddling around the pond for 30 minutes.

Data Collection

Daily data collection began on DOY 142, 34 days prior to the first addition of nutrients. To assess the response of primary production to the nutrient pulses among the different food web treatments, we measured chlorophyll-*a* concentration, a proxy for phytoplankton biomass, and ecosystem metabolism over the duration of the experiment (DOY 142 – 241). Chlorophyll-*a* was measured in situ daily using a Total Algae PC Sensor on a YSI Handheld sonde (Yellow Springs Instruments, Yellow Springs, Ohio, USA). The sensor was slowly lowered at a rate of 1 m per 15 s through the water column each day, continuously logging chlorophyll-*a* concentrations. The mean chlorophyll-*a* value from 0.1-0.3 m depth was used in the statistical analyses (see below). As phytoplankton were not the only primary producers in the ponds, we measured ecosystem metabolism to quantify the response of all primary production by phytoplankton, macrophytes, and periphyton. Ecosystem metabolism was estimated using the free-water oxygen method

(Staehr et al. 2012). Dissolved oxygen was recorded every 30 minutes using PME miniDOT loggers (Precision Measurement Engineering, Vista, California, USA) deployed at 0.25 m depth over the deepest point in each pond. An on-site weather station (Onset HOBO U30 USB) provided measurements of photosynthetic active radiation and wind speed (Winslow et al. 2016). We calculated rates of gross primary production (GPP), ecosystem respiration (R), and net ecosystem production (NEP) using a Kalman filter described within the LakeMetabolizer R package (Winslow et al. 2016). Raw DO data were cleaned prior to calculating metabolism to remove anomalous measurements. Briefly, all times when DO concentration decreased by more than 2.0 mg L^{-1} from the previous measurement were identified. These points, along with the subsequent five DO measurements, were removed (three hours total) and backfilled via linear interpolation. Of the 576 pond days of dissolved oxygen measurements, removal and interpolation was not necessary for 61% of pond days, only one measurement for 25% of pond days, two measurements for 12.2% of pond days, and three or more measurements per day for 2.8% of pond days. Metabolic rates calculated from free-water oxygen measurements can result in erroneous estimates (i.e., negative GPP, positive R), for example, when physical processes have a stronger effect on daily dissolved oxygen dynamics than biological processes (Rose et al. 2014, Winslow et al. 2016). For each pond, all days that contained an erroneous estimate of metabolism were removed prior to statistical analyses. This step removed between 12 – 19% of days for the two low-coupling ponds and the pulsed high-coupling pond and between 4 – 7% of days were removed for the remaining three ponds.

In addition to measuring chlorophyll and ecosystem metabolism daily, we also measured periphyton areal biomass and macrophyte biomass less frequently over the course of the experiment. For periphyton, a modified Hester-Dendy sampler (173.28 cm^2) was deployed for

two-week periods in each pond and areal chlorophyll was measured based on analysis of the biomass that grew on the artificial substrate during the deployment (see supplement for measurement details). We collected samples of macrophyte dry biomass in all ponds twice over the course of the experiment, one week prior to the two nutrient pulse additions (see supplement for measurement details). Water samples from 0.25 m depth were collected three times per week to measure concentrations of total and dissolved nutrients. For dissolved nutrients, samples were filtered in the field through Whatman glass fiber filters (0.45 μm), while samples for total nutrients were not filtered. All samples were kept on ice in a cooler before being transported back to the lab, preserved with 100 μL of concentrated sulfuric acid, and stored for later analysis (see supplement for details).

We also monitored other components of the food webs including zooplankton biomass, macroinvertebrate areal density, and fish gut content over the course of the experiment. Zooplankton were sampled twice per week via a 1 m vertical tow of a Wisconsin net (63 μm mesh). We preserved samples with 10% formalin in the field then later transferred them to 70% ethanol. Zooplankton crustaceans and rotifers were identified to genus, excluding copepods which were identified to order. Standard length-mass regressions were used to calculate biomass (see supplement for measurement details). Macroinvertebrates were sampled biweekly in the littoral region of each pond using a modified stovepipe sampler (0.3 m diameter, (Jackson et al. 2019). This sampling frequency is consistent with other pond studies that collected data on macroinvertebrates (Carey and Wahl 2010, 2011). Macroinvertebrates were preserved in 70% ethanol and identified in the lab using a stereomicroscope to family (mollusks and insects) or class (leeches and oligochaetes) (see supplement for measurement details). At the end of the experiment, the remaining fish were collected and subjected to gastric lavage to retrieve stomach

contents. Stomach content samples were preserved with 70% ethanol and organisms were viewed under a Leica MZ8 stereomicroscope and identified to the lowest possible taxonomic order.

Data Analysis

We used the recently developed response detection algorithm (Walter et al. 2022) to quantify the response and recovery of chlorophyll and ecosystem metabolism to nutrient pulses in each food web treatment. The algorithm calculates empirical cumulative distribution functions from a rolling window of the disturbed time-series (i.e., the ecosystem which received the nutrient pulse) and compares it to the entirety of the reference time-series (i.e., the ecosystem which did not receive a nutrient pulse). Briefly, the algorithm takes a high-frequency state variable and calculates an empirical cumulative distribution function within a specified moving window. This empirical cumulative distribution function is then compared to the empirical cumulative distribution function of the reference time series in its entirety to quantify the magnitude of difference between the disturbed and reference time series of the state variable. We elected to use the entire reference time-series rather than an adaptive window as there was no strong seasonality over the duration of our experiment for these variables, and it allows us to compare the response of the disturbed ecosystem to the total variability expected without any nutrient pulse disturbances. We chose a rolling window of seven days for the disturbed time-series to capture rapid changes in primary production following each nutrient pulse. We also performed sensitivity analyses using five- and ten-day rolling windows to evaluate the sensitivity of our conclusions to window length and found minimal differences using shorter or longer window length (see supplemental information; Table S4).

To determine response and recovery from a disturbance, the algorithm calculates the integral of the absolute difference between the disturbed rolling window and the reference time-series. The magnitude of difference between the disturbed moving window and reference time series is then calculated by comparing the reference sample mean and standard deviation creating a time-series of Z-scores. A response occurs when the time-series of Z-scores exceeds a user-defined disturbance threshold and recovers when the Z-scores fall below a user-defined recovery threshold. As recommended by Walter et al (2022), we chose a disturbance threshold of 2.0 representing a significant and rare event that signals a substantial departure from reference conditions, and a recovery threshold of 0.5 which represents a substantial return to reference conditions. Using this algorithm, we can calculate the response time of primary production to the nutrient pulses (here defined as resistance) defined as the number of days after the pulse until the z-score exceeds 2.0. In addition, we can calculate the return time from nutrient pulses (here defined as resilience) defined as the number of days after the z-scores return to below 0.5 after already exceeding the threshold of 2.0.

To identify if, and when, a critical transition occurred within a pond related to the nutrient pulse we used online dynamic linear modeling on the time series of chlorophyll-*a* concentration (Taranu et al. 2018, Wilkinson et al. 2018). The method requires a complete daily time series and therefore could not be applied to the metabolism estimates due to the removal of days with erroneous estimates. Briefly, this method calculates the eigenvalues of a time series by fitting autoregressive models (AR) with time-varying coefficients (c.f. Ives and Dakos, 2012). Evidence that a critical transition occurred is determined by the eigenvalues crossing above one from below. However, if eigenvalues do not cross above one from below, that suggests no critical transition occurred. We fit time-varying AR (p) models to time series of chlorophyll-*a* for each

pond with an optimal order of one or two (i.e., lag-1 or lag-2) determined by Akaike's Information Criteria (AIC_c) model selection (Hurvich and Tsai 1993). If the change in AICc was less than two, both models were considered for evidence of a critical transition (Burnham and Anderson 2004; Table S2). All analyses were performed in R version 4.2.1 (R Core Team 2022) using the *disturbhf* (Walter and Buelo 2022), *LakeMetabolizer* (Winslow et al. 2016), *lubridate* (Garrett and Wickham 2011), and *tidyverse* (Wickham et al. 2019) packages.

RESULTS

The different food web structures established within the experimental ponds successfully increased benthic-pelagic coupling based on the biomass and dynamics of benthic primary producers as well as zooplankton biomass and macroinvertebrate density (Figure 2). Over the course of the experiment, zooplankton biomass was generally lowest in the low coupling ponds (Figure 2A), greatest in the intermediate coupling ponds (Figure 2B), but only slightly greater within the high coupling ponds (Figure 2C). Similarly, macroinvertebrate density was lowest in the low coupling ponds and greatest in the high coupling ponds (Figure 2D – F). However, there was substantial variation in macroinvertebrate density between the pulsed and reference intermediate coupling ponds (Figure 2E). Zooplankton biomass and macroinvertebrate density remained elevated further into the experiment in the intermediate and high coupling ponds, whereas zooplankton and macroinvertebrates steadily decreased in the low coupling ponds (Figure S1A – F). Finally, there was greater variability in periphyton biomass in the intermediate and high coupling ponds in comparison to the low coupling ponds (Figure 2G-I). Periphyton areal biomass steadily increased in the pulsed low coupling pond and all reference ponds, however, the intermediate and high coupling ponds fluctuated between high and low areal

biomass over the course of the study period (Figure S1G – I). In the low coupling ponds, periphyton biomass increased as macroinvertebrate density decreased whereas in the intermediate and high coupling ponds periphyton-macroinvertebrate dynamics were lagged with high macroinvertebrate density preceding periphyton decrease, though to a lesser degree in the intermediate coupling ponds (Figure S1D – I). Fish diets roughly corresponded to our expectations of trophic interactions with bluegill preying on more zooplankton and yellow perch largely consuming macroinvertebrates and little to no zooplankton (Table S3). Largemouth bass preyed on a diversity of organisms, but mostly fish and macroinvertebrates (Table S3). Mean nutrient concentrations and macrophyte dry biomass were similar across all ponds though total phosphorus was slightly elevated in the reference ponds (Table 1). We did observe a clear increase in nutrient concentrations in the pulsed ponds following each nutrient pulse in comparison to their concentrations prior to nutrient addition (Figure S2).

In support of our prediction that benthic-pelagic coupling would affect the response of primary production to nutrient pulses, greater benthic-pelagic coupling resulted in reduced responses of primary production to benthic-pelagic coupling (Figure 3). Chlorophyll-*a* concentration increased following the first nutrient pulse and peaked at roughly the same time in both the low (DOY 198) and intermediate (DOY 194) coupling ponds (Figure 3A – B). In comparison, there was no apparent response in chlorophyll-*a* in the high benthic-pelagic coupling pulsed pond (Figure 3C). Following the second nutrient pulse, chlorophyll-*a* concentration increased in all three pulsed ponds with the low coupling pond peaking first on DOY 224, the intermediate coupling pond following on DOY 232, and finally the high coupling pond peaking on DOY 236. Gross primary production (GPP), which encompasses production from all primary producers was similar to the chlorophyll-*a* dynamics after both nutrient pulses

in the intermediate and high coupling ponds but did not follow chlorophyll-*a* dynamics in the low coupling pulsed pond (Figure 3D – F). Respiration (R) steadily increased for all pulsed ponds over the duration of the experiment and followed the reference pond dynamics closely (Figure 3G – I). Net ecosystem production (NEP) initially decreased then remained largely heterotrophic for all ponds following the first nutrient pulse (Figure 3J – L). There was an increase in NEP following the first nutrient pulse in the intermediate coupling pulsed pond akin to the dynamics observed in gross primary production and chlorophyll-*a* (Figure 3H). However, the reference intermediate coupling pond had similar dynamics. The low and intermediate coupling ponds became heterotrophic prior to the first nutrient pulse (between DOY 151 – 172) and remained heterotrophic for the rest of the summer until the end of the experiment (Figure 3J – K). Both the pulsed and reference high coupling ponds remained autotrophic further into the summer than the other two food web structures only becoming heterotrophic on DOY 192 (Figure 3L).

We found support for our prediction that the resistance (response time) and resilience (return time) of primary production to the nutrient pulses would be greatest in the high benthic-pelagic coupling pond (Figure 4). Following the first nutrient pulse, the z-scores of chlorophyll-a for the low and intermediate coupling ponds surpassed the threshold of 2, indicating a significant response, whereas there was no significant response detected in the high coupling ponds (Figure 4A – B). There was also a significant recovery (z-score of chlorophyll decreased below 0.5) prior to the second nutrient pulse in the low coupling pond, but there was not a significant recovery in the intermediate coupling pond until a few days after the second nutrient pulse. The response time of chlorophyll a in both the low and intermediate coupling ponds to the first nutrient pulse were similar, though the intermediate coupling pond had a longer return time to baseline

conditions (Table 2). Following the second nutrient pulse, chlorophyll-*a* concentration again significantly responded in the low and intermediate coupling ponds again, exceeding the z-score threshold of 2 (Figure 4A – C). However, the low coupling pond responded 15 days faster to the second nutrient pulse and took 16 days longer to recover whereas the intermediate coupling pond had a similar response time to the first nutrient pulse and did not recover before the experiment was terminated (although the z-score was trending towards recovery) (Table 2).

For GPP, there was only a significant response (z-score of GPP >2) in the intermediate coupling pond with a seven-day rolling window after both nutrient pulses (Figure 4D – F). GPP in the intermediate coupling pond responded 11 days after the first nutrient pulse and 21 days after the second nutrient pulse. Additionally, GPP in the intermediate coupling pond recovered (z-score of GPP<0.5) from the first and second pulses in eleven and five days, respectively (Table 2). There was a significant GPP response detected in the low coupling pond with a shorter rolling window (5-day) on DOY 185 with recovery on DOY 190 (Figure S3; Table S4). There was no significant response of R or NEP following either nutrient pulse in most of the ponds (Figure 4G – L) except for the intermediate coupling pond where the z-score of R exceeded the threshold 21 days after the second nutrient pulse, recovering 4 days later (Figure 4H). There was a significant response of R in the high coupling pond early in the time-series, but it was before the first nutrient pulse (Figure 4L). With a longer rolling window (10-day) there was a significant response of R in the pulsed high coupling pond 21 days after the second nutrient pulse with no recovery observed as the experiment ended shortly thereafter (Figure S4; Table S4).

We found some support for our prediction that greater benthic-pelagic coupling would reduce the chance of a critical transition occurring following a nutrient pulse. We used a lag-1 autocorrelation in the dynamic online linear model based on AICc for all experimental ponds

(Table S2). At lag-1, there was no clear evidence of a critical transition in either the pulsed or reference ponds for each food web treatment after either nutrient pulse (Figure 5A – F). The bootstrapped standard error crossed above one from below in some ponds indicating the potential for a critical transition, but there was no evidence that once occurred within the time series (Figure 5). We also considered the lag-2 autocorrelation for low coupling ponds and the high coupling reference pond as the ΔAICc showed the lag-2 models were not significantly different for those ponds (Table S2). At lag-2, the low coupling pulsed pond eigenvalues did move above one from below on DOY 192 and dropped below one on DOY 194 which was evidence of a critical transition (Figure S5A). The moment of critical transition for chlorophyll-*a* eigenvalues was about ten days prior to the peak in chlorophyll-*a* concentration observed in the time series data (Figure 3) and six days prior to the reported significant response from the response detection algorithm (Figure 4). In addition, the low coupling reference pond eigenvalues moved above one from below briefly weeks after the second nutrient pulse on DOY 231.

DISCUSSION

With this experiment, we established three food web structures that varied in their degree of benthic-pelagic coupling. While food web complexity, the number of trophic guilds, and overall fish biomass increased across the three food web structures, the different dynamics of zooplankton, periphyton, and macroinvertebrates, particularly between the intermediate and high coupling ponds, suggests we increased benthic-pelagic coupling between the three established food web structure. There was stronger top-down control on planktivores in the intermediate and high coupling ponds evidenced by higher zooplankton biomass and greater persistence of zooplankton biomass across the summer sampling season, especially within the high coupling

pond. In addition, macroinvertebrate and periphyton biomass dynamics were akin to standard predator-prey cycles (Blasius et al. 2020) in the high coupling pond, but only partially in the intermediate and low coupling ponds. This indicates a greater importance of the benthic food chain in the intermediate and high coupling ponds, with the greatest effect occurring in the high coupling ponds, based on the larger shifts in periphyton and macroinvertebrate biomass and consistently higher zooplankton biomass in both the reference and pulsed ponds. Thus, we demonstrated empirically that a greater degree of benthic-pelagic coupling within aquatic food webs led to reduced ecosystem response times (higher resistance) and lower benthic-pelagic coupling led to slower recovery (lower resilience) from nutrient pulses.

In support of our prediction, there was no response (and therefore, no recovery) of primary production in the high benthic-pelagic coupling pond to nutrient pulses, whereas there was a response in chlorophyll-*a* in the low and intermediate coupling ponds. This suggests that the added nutrients did not result in increased primary production (based on the ecosystem metabolism response) or increased phytoplankton biomass (based on the chlorophyll a response) in the high coupling pond. While there was a relatively fast recovery in chlorophyll-*a* from the first nutrient pulse in the low coupling pond, this is consistent with other nutrient pulse disturbance experiments where faster recovery was observed in food webs with higher zooplanktivory (Cottingham and Schindler 2000). Conversely, following the second nutrient pulse, we observed a faster response and slower recovery in the low coupling pond suggesting a potential decrease in resistance and resilience to the repeated nutrient pulse disturbances. There was a similar response time after each nutrient pulse within the intermediate coupling pond suggesting that there was no such change in resistance. Additionally, the intermediate coupling pond was on track for a faster recovery time in chlorophyll-*a* after the second nutrient pulse

compared to the first; however, the experiment was terminated before the threshold for recovery was reached.

Benthic-pelagic coupling can be a stabilizing force for species within food webs (Wolkovich et al. 2014, Mougi 2020) which is supported by the lower trophic level dynamics in this experiment. The differences in response and recovery times between the intermediate and high coupling ponds also support our prediction that differences in response were due to stronger top-down control and greater food web connectivity rather than simply a difference in the number of trophic levels (Carpenter et al. 2001, Ward and McCann 2017). In ponds with a greater degree of benthic-pelagic coupling, there was higher zooplankton biomass, macroinvertebrate density, and periphyton biomass consistent with other studies of benthic-pelagic coupling, likely due to stronger top-down control (Vadeboncoeur et al. 2005, Vander Zanden et al. 2005, Marklund et al. 2019). However, there may have been an additional refuge effect in the high coupling ponds where the presence of predators led to altered behavior and reduced feeding rates for bluegill, yellow perch, and fathead minnows (Zanette and Clinchy 2019). We only observed a steady decrease in zooplankton biomass and macroinvertebrate density in the low coupling ponds indicating that greater benthic-pelagic coupling facilitated more stable zooplankton biomass dynamics. Macroinvertebrate density in the pulsed intermediate coupling pond was consistently lower than the reference intermediate coupling pond throughout the experimental period (Figure S1E). This may explain the lower macroinvertebrate abundance in diet samples collected from fishes in the pulsed intermediate coupling pond at the end of the experiment. Although, within the intermediate and high coupling ponds, the cyclical recovery and decline of both macroinvertebrate density and periphyton areal biomass may suggest that fishes were switching to benthivory when macroinvertebrate density

was high allowing periphyton to recover and take up more nutrients. Prey availability can be influential on diet preference and consumption dynamics, particularly for largemouth bass (Sammons and Maceina 2006, Butts et al. 2020) which were present in both the intermediate and high coupling ponds

The dynamics of ecosystem metabolism supported our prediction that greater benthic-pelagic production would reduce the response of primary production to nutrient inputs, though the patterns were far noisier than our chlorophyll-*a* data. There was only a significant response (z-scores exceeded threshold of 2) in GPP following both nutrient pulses in the intermediate ponds which aligned with the peak in chlorophyll-*a* biomass observed following the first nutrient pulse. Using a smaller rolling window (5 days), GPP significantly responded in the low coupling pond following the first nutrient pulse coinciding with observed chlorophyll-*a* response at the same time. This follows the trophic dynamics we observed within the ponds, indicating phytoplankton production was stimulated under lower top-down control (Cottingham and Schindler 2000, Jeppesen et al. 2003). Periphyton was higher in the intermediate coupling ponds in comparison to the low coupling ponds. Thus, the GPP response for the intermediate coupling pond also likely included periphyton (Vadeboncoeur et al. 2001). It is not surprising there were no significant responses for net ecosystem production (NEP) given that it's a balance of GPP and respiration (R) (Ask et al. 2012); indeed, it had the most stable z-scores across ponds among all response variables. The complex nature of stratification dynamics, floating leaf macrophytes, and dissolved oxygen changes in the bottom waters of the ponds (Albright et al. 2022), made it difficult to estimate ecosystem metabolism in these ecosystems. Nevertheless, the GPP patterns do support the chlorophyll-*a* dynamics we observed.

There was some support for our prediction that the degree of benthic-pelagic coupling would reduce the chance of a critical transition. We found evidence of a critical transition only within the low coupling food web structure after the first nutrient pulse using a lag-2 autoregressive model (though with both optimal orders, the bootstrapped standard error moved above one from below) with no evidence of a critical transition in the paired reference pond. Evidence for a critical transition in only the pulsed low coupling pond, and in none of the reference ponds following either nutrient pulse, indicates that the response was due to the first nutrient pulse rather than stochastic environmental dynamics. There was additional evidence of a critical transition in the low-coupling reference pond following an extreme storm event (derecho), though given the minimal watershed for these ponds, the dynamics were not driven by external nutrient loading with the storm. A decrease in ecosystem resilience is often used as an early-warning sign of a critical transition (Scheffer et al. 2015, Ortiz et al. 2020). The faster response and slower recovery times in the low coupling pond following the second nutrient pulse suggests there was a decrease in ecosystem resilience to these nutrient pulses (van de Leemput et al. 2018).

Within the experimental ponds, there were several factors that produced uncertainty we were unable to control. In particular, there was enhanced zooplanktivory due to the unknown presence of remnant bigmouth buffalo *(Ictiobus cyprinellus*) in the pulsed low coupling pond (n=10) and reference high coupling pond (n=2) from an ecosystem experiment the previous year (Wilkinson et al. 2022). Bigmouth buffalo are endemic planktivores and may have caused the lower zooplankton biomass in the pulsed low coupling pond compared to the reference. It is also possible bigmouth buffalo contributed to the chlorophyll-*a* response in the low coupling pond as well as the evidence of a critical transition. However, bigmouth buffalo rely on zooplankton for

food, mainly copepods and large-bodied cladocerans; thus, it is unlikely that their presence affected the degree of benthic-pelagic coupling as they are not generalist consumers (Starostka and Applegate 1970, Adámek et al. 2003). All ponds, however, were subject to increased zooplanktivory from larval bluegill and largemouth bass spawned during the study period. This may explain the consistent drop in zooplankton biomass across all six ponds over the course of the experiment.

The experimental ponds were subjected to two unanticipated extreme weather events that may have influenced ecosystem dynamics in addition to our nutrient pulse additions. First, there was a five-day period of elevated surface water temperatures that occurred nine days after the first nutrient pulse on DOY 185 – 190 (Figure S6). The combination of nutrients and elevated temperatures may have helped stimulate phytoplankton production following the first nutrient pulse (Albright et al. 2022). This also led to the senescence of macrophytes in the deeper portions of the pond in the pulsed treatments, but the floating macrophytes which ringed the pond were unaffected. Elevated temperatures and macrophyte senescence driving alterations in stratification dynamics likely affected metabolism estimates (Cole et al. 2000, Hornbach et al. 2020), perhaps explaining why we did not observe stronger responses. The derecho on DOY 223 fully and violently mixed the water columns of all the ponds (Albright et al. 2022), but the duration of effects was short. Following the derecho, if any nutrient or organic matter were released by the alteration of stratification via mixing (Lehman 2014, Salmaso et al. 2018), that may have stimulated primary production, especially within the pulsed ponds. This process may have resulted in the small increase in phytoplankton, GPP, and R in the high coupling pond we observed, but the increase was not a significant response. Overall, the derecho did not have a stronger effect than the nutrient additions.

Benthic-pelagic coupling is increasingly recognized as an important component of food web structure within aquatic ecosystems (McMeans et al. 2016, Gutgesell et al. 2022, Borrelli and Relyea 2022). Here, we demonstrate empirically that, even in highly spatially constrained ecosystems, coupling between benthic and pelagic energy pathways produced increased resistance and resilience of the ecosystems to nutrient pulses. While other studies have demonstrated the importance of benthic-pelagic coupling, our study provides empirical and mechanistic evidence that greater benthic-pelagic coupling could be a key target for lake management programs to increase ecosystem resistance and resilience to increasingly frequent and severe disturbances. Preserving or enhancing benthic-pelagic coupling is vital for aquatic ecosystems, especially as coupling and energy flow can be adversely affected by increasing eutrophication (Wang et al. 2020). However, how benthic-pelagic coupling may interact with fishes that substantially affect nutrient cycling, both native (e.g., gizzard shad; Schaus et al. 1997) and non-native (e.g., common carp; (Weber and Brown 2011), should be explored further. Nonetheless, our research also provides further empirical support that biodiversity and the architecture of species interactions within a food web, is a key ecosystem property that makes ecosystems more resistant and resilient to environmental change and must be preserved.

ACKNOWLEDGEMENTS

We would like to thank Michael Tarnow, Elena Sandry, Quin Shingai, Ellen Albright, Adriana Le Compte, Emily Grausgruber, Psalm Amos, Brittany Howes, Katie Cope, Kylee Gehl, Rachel Fleck, Eric Moody, and James Thompson for assistance with sample collection and analysis, and Martin Simonson and the whole Weber Lab for collecting fish species for the experiment. Additionally, we thank Michael Tarnow, Sofia Ferrer, and Kayleigh Winston for

assisting with macroinvertebrate and zooplankton identification and enumeration. Finally, we thank Cal Buelo and Jonathan Walter for their assistance with data analysis. This research was supported by the Iowa Water Center's Graduate Student Supplemental Research Competition. Butts was additionally supported by the National Science Foundation Graduate Research Fellowship Program (DGE-1747503). Any opinions, findings, and conclusions or recommendations expressed in this material are those of the authors and do not necessarily reflect the views of the National Science Foundation.

DATA AVAILABILITY

The data for this study will be archived using the Environmental Data Initiative repository and given a unique digital object identifier. Metadata will follow the ecological metadata language and be published under a creative commons license. The data files and analysis scripts are available through GitHub (https://github.com/tjbutts/hort-benthic-pelagic) and will be archived on Zenodo following acceptance.

REFERENCES

Adámek, Z., I. Sukop, P. M. Rendón, and J. Kouřil. 2003. Food competition between 2+ tench (Tinca tinca L.), common carp (Cyprinus carpio L.) and bigmouth buffalo (Ictiobus cyprinellus Val.) in pond polyculture. Journal of Applied Ichthyology 19:165–169.

Albright, E. A., R. Ladwig, and G. M. Wilkinson. 2022. Macrophyte-hydrodynamic interactions mediate stratification and dissolved oxygen dynamics in ponds. *EarthArXiv.* https://doi.org/10.31223/X51M19.

Ask, J., J. Karlsson, and M. Jansson. 2012. Net ecosystem production in clear-water and brown-water lakes. Global Biogeochemical Cycles 26.

Baustian, M. M., G. J. a. Hansen, A. de Kluijver, K. Robinson, E. N. Henry, L. B. Knoll, K. C. Rose, and C. C. Carey. 2014. Linking the bottom to the top in aquatic ecosystems: mechanisms and stressors of benthic-pelagic coupling. Pages 25–47 Eco-DAS X Symposium Proceedings.

Blanchard, J. L., R. Law, M. D. Castle, and S. Jennings. 2011. Coupled energy pathways and the resilience of size-structured food webs. Theoretical Ecology 4:289–300.

Blasius, B., Rudolf, L., Welthoff, G., Gaedke, U. and Fussmann, G.F. 2020. Long-term cyclic persistence in an experimental predator-prey system. Nature 577: 226–230

Borrelli, J. J., and R. A. Relyea. 2022. A review of spatial structure of freshwater food webs: Issues and opportunities modeling within-lake meta-ecosystems. Limnology and Oceanography 67: 1746–1759.

Burnham, K. P., and D. R. Anderson. 2004. Multimodel inference: Understanding AIC and BIC in model selection. Sociological Methods and Research 33: 261 – 304.

Butts, T. J., J. Y. S. Hodgson, M. Guidone, and J. R. Hodgson. 2020. Episodic zooplanktivory by largemouth bass (Micropterus salmoides) on Daphnia: a 25-year natural history record from a small northern temperate lake. Journal of Freshwater Ecology 35:469–490.

Calizza, E., L. Rossi, G. Careddu, S. S. Caputi, and M. L. Costantini. 2019. Species richness and vulnerability to disturbance propagation in real food webs. Scientific Reports 9:19331.

Carey, M. P., and D. H. Wahl. 2010. Interactions of multiple predators with different foraging modes in an aquatic food web. Oecologia 162:443–452.

Carey, M. P., and D. H. Wahl. 2011. Fish diversity as a determinant of ecosystem properties across multiple trophic levels. Oikos 120:84–94.

Carlander, K. 1977. Biomass, Production, and Yields of Walleye (Stizostedion vitreum vitreum) and Yellow Perch (Perca flavescens) in North American Lakes. Journal of Fisheries Research Board of Canada 34:1602–1612.

Carmichael, W. W., and G. L. Boyer. 2016. Health impacts from cyanobacteria harmful algae blooms: Implications for the North American Great Lakes. 54: 194–212.

Carpenter, S. R., E. G. Booth, and C. J. Kucharik. 2018. Extreme precipitation and phosphorus loads from two agricultural watersheds. Limnology and Oceanography 63:1221–1233.

Carpenter, S. R., E. G. Booth, C. J. Kucharik, and R. C. Lathrop. 2015. Extreme daily loads: role in annual phosphorus input to a north temperate lake. Aquatic Sciences 77:71–79.

Carpenter, S. R., J. J. Cole, J. R. Hodgson, J. F. Kitchell, M. L. Pace, D. Bade, K. L. Cottingham, T. E. Essington, J. N. Houser, and D. E. Schindler. 2001. Trophic cascades, nutrients, and lake productivity: whole lake experiments. Ecological Monographs 71:163–186.

Cole, J. J., M. L. Pace, S. R. Carpenter, and J. F. Kitchell. 2000. Persistence of net heterotrophy in lakes during nutrient addition and food web manipulations. Limnology and Oceanography 45:1718–1730.

Collins, S. F., K. A. Nelson, C. S. DeBoom, and D. H. Wahl. 2017. The facilitation of the native bluegill sunfish by the invasive bighead carp. Freshwater Biology 62:1645–1654.

Cottingham, K., and D. Schindler. 2000. Effects of grazers community structure on phytoplankton response to nutrient pulses. Ecology 81:183–200.

Duffy, W. G. 1998. Population dynamics, production, and prey consumption of fathead minnows (Pimephales promelas) in prairie wetlands: a bioenergetics approach. Canadian Journal of Fisheries and Aquatic Sciences 54:15–27.

Gutgesell, M. K., K. S. McCann, G. Gellner, K. Cazelles, C. J. Greyson-Gaito, C. Bieg, M. M. Guzzo, C. P. K. Warne, C. A. Ward, R. F. O'connor, A. M. Scott, B. C. Graham, E. J.

Champagne, and B. C. McMeans. 2022. On the Dynamic Nature of Omnivory in a Changing World. BioScience 72: 416–430.

Ho, J. C., and A. M. Michalak. 2020. Exploring temperature and precipitation impacts on harmful algal blooms across continental U.S. lakes. Limnology and Oceanography 65:992–1009.

Hodgson, J. Y., and J. R. Hodgson. 2000. Exploring optimal foraging by largemouth bass (Micropterus salmoides) from three experimental lakes. Verhandlungen des Internationalen Verein Limnologie 27:1–6.

Hornbach, D. J., E. G. Schilling, and H. Kundel. 2020. Ecosystem metabolism in small ponds: The eects of floating-leaved macrophytes. Water (Switzerland) 12:1–25.

Hughes, T. P., J. T. Kerry, A. H. Baird, S. R. Connolly, A. Dietzel, C. M. Eakin, S. F. Heron, A. S. Hoey, M. O. Hoogenboom, G. Liu, M. J. McWilliam, R. J. Pears, M. S. Pratchett, W. J. Skirving, J. S. Stella, and G. Torda. 2018. Global warming transforms coral reef assemblages. Nature 556:492–496.

Hurvich, C. M., and C. -L Tsai. 1993. A Corrected Akaike Information Criterion for Vector Autoregressive Model Selection. Journal of Time Series Analysis 14:271–279.

Ives, A. R., and V. Dakos. 2012. Detecting dynamical changes in nonlinear time series using locally linear state-space models. Ecosphere 3: art58

Jackson, J., V. Resh, D. Batzer, R. Merritt, and K. Cummins. 2019. Sampling Aquatic Insects: Collection Devices, Statistical Considerations, and Rearing Procedures. Pages 17–42 *in* R. Merritt, K. Cummins, and M. Berg, editors. An Introduction to the Aquatic Insects of North America. Fifth edition. Kendall Hunt Publishing Company, Dubuque, IA.

Jentsch, A., and P. White. 2019. A theory of pulse dynamics and disturbance in ecology. Ecology 100.e02734.

Jeppesen, E., J. Jensen, C. Jensen, B. Faafeng, D. Hessen, M. Søndergaard, T. Lauridsen, P. Brettum, and K. Christoffersen. 2003. The Impact of Nutrient State and Lake Depth on Top-Down Control in the Pelagic Zone of Lakes: A Study of 466 Lakes from the Temperate Zone to the Arctic. Ecosystems 6:313–325.

Joosse, P. J., and D. B. Baker. 2011. Context for re-evaluating agricultural source phosphorus loadings to the great lakes. Canadian Journal of Soil Science 91:317–327.

Kelly, P. T., W. H. Renwick, L. Knoll, and M. J. Vanni. 2019. Stream Nitrogen and Phosphorus Loads Are Differentially Affected by Storm Events and the Difference May Be Exacerbated by Conservation Tillage. Environmental Science and Technology 53:5613–5621.

Kovalenko, K. E. 2019. Interactions among anthropogenic effects on aquatic food webs. Hydrobiologia 841:1–11.

Kuiper, J. J., C. Van Altena, P. C. De Ruiter, L. P. A. Van Gerven, J. H. Janse, and W. M. Mooij. 2015. Food-web stability signals critical transitions in temperate shallow lakes. Nature Communications 6:1–7.

van de Leemput, I. A., V. Dakos, M. Scheffer, and E. H. van Nes. 2018. Slow Recovery from Local Disturbances as an Indicator for Loss of Ecosystem Resilience. Ecosystems 21:141–152.

Lehman, J. T. 2014. Understanding the role of induced mixing for management of nuisance algal blooms in an urbanized reservoir. Lake and Reservoir Management 30:63–71.

Lürling, M., M. M. Mello, F. van Oosterhout, L. de S. Domis, and M. M. Marinho. 2018. Response of natural cyanobacteria and algae assemblages to a nutrient pulse and elevated temperature. Frontiers in Microbiology 9:1–14.

Marklund, M. H. K., R. Svanbäck, and P. Eklöv. 2019. Habitat coupling mediates trophic cascades in an aquatic community. Ecosphere 10.

McCann, K., A. Hastings, and G. Huxel. 1998. Weak trophic interactions and the balance of nature. Nature 395:794–798.

McCann, K. S., J. B. Rasmussen, and J. Umbanhowar. 2005. The dynamics of spatially coupled food webs. Ecology Letters 8:513–523.

McMeans, B. C., K. S. McCann, T. D. Tunney, A. T. Fisk, A. M. Muir, N. Lester, B. Shuter, and N. Rooney. 2016. The adaptive capacity of lake food webs: From individuals to ecosystems. Ecological Monographs 86:4–19.

le Moal, M., C. Gascuel-Odoux, A. Ménesguen, Y. Souchon, C. Étrillard, A. Levain, F. Moatar, A. Pannard, P. Souchu, A. Lefebvre, and G. Pinay. 2019. Eutrophication: A new wine in an old bottle? Science of the Total Environment 651:1–11.

Mougi, A. 2020. Coupling of green and brown food webs and ecosystem stability. Ecology and Evolution 10: 9192–9199.

Ortiz, D., J. Palmer, and G. Wilkinson. 2020. Detecting statistical early warning indicators of algal blooms in shallow eutrophic lakes. Ecosphere.

Polazzo, F., T. I. Marina, M. Crettaz-Minaglia, and A. Rico. 2022. Food web rewiring drives long-term compositional differences and late-disturbance interactions at the community level. Proceedings of the National Academy of Sciences 119: e2117364119.

Prein, A. F., C. Liu, K. Ikeda, S. B. Trier, R. M. Rasmussen, G. J. Holland, and M. P. Clark. 2017. Increased rainfall volume from future convective storms in the US. Nature Climate Change 7:880–884.

R Core Team. 2022. R: A language and environment for statistical computing. R Foundation for Statistical Computing, Vienna, Austria.

Ratajczak, Z., S. R. Carpenter, A. R. Ives, C. J. Kucharik, T. Ramiadantsoa, M. A. Stegner, J. W. Williams, J. Zhang, and M. G. Turner. 2018. Abrupt Change in Ecological Systems: Inference and Diagnosis. Trends in Ecology and Evolution 33: 513–526

Richardson, D. C., M. A. Holgerson, M. J. Farragher, K. K. Hoffman, K. B. S. King, M. B. Alfonso, M. R. Andersen, K. S. Cheruveil, K. A. Coleman, M. J. Farruggia, R. L. Fernandez, K. L. Hondula, G. A. López Moreira Mazacotte, K. Paul, B. L. Peierls, J. S. Rabaey, S. Sadro, M. L. Sánchez, R. L. Smyth, and J. N. Sweetman. 2022. A functional definition to distinguish ponds from lakes and wetlands. Scientific Reports 12.

Rooney, N., and K. S. McCann. 2012. Integrating food web diversity, structure and stability. Trends in Ecology and Evolution 27:40–46.

Rose, K. C., L. A. Winslow, J. S. Read, E. K. Read, C. T. Solomon, R. Adrian, and P. C. Hanson. 2014. Improving the precision of lake ecosystem metabolism estimates by identifying predictors of model uncertainty. Limnology and Oceanography: Methods 12:303–312.

Sabo, R. D., C. M. Clark, D. A. Gibbs, G. S. Metson, M. J. Todd, S. D. LeDuc, D. Greiner, M. M. Fry, R. Polinsky, Q. Yang, H. Tian, and J. E. Compton. 2021. Phosphorus Inventory for

the Conterminous United States (2002–2012). Journal of Geophysical Research: Biogeosciences 126.

Salmaso, N., A. Boscaini, C. Capelli, and L. Cerasino. 2018. Ongoing ecological shifts in a large lake are driven by climate change and eutrophication: evidences from a three-decade study in Lake Garda. Hydrobiologia 824:177–195.

Sammons, S. M., and M. J. Maceina. 2006. Changes in diet and food consumption of largemouth bass following large-scale hydrilla reduction in Lake Seminole, Georgia. Hydrobiologia 560:109–120.

Schaus, M. H., M. J. Vanni, M. T. Wissing, M. T. Brmigan, J. E. Garvey, and R. A. Stein. 1997. Nitrogen and Phosphorus Excretion by Detritivorous Gizzard Shad in a Reservoir Ecosystem. Limnology and Oceanography:1386–1397.

Scheffer, M., and Carpenter. 2003. Catastrophic regime shifts in ecosystems: linking theory to observation. Trends in Ecology and Evolution 18:648–656.

Scheffer, M., S. R. Carpenter, V. Dakos, and E. H. van Nes. 2015. Generic Indicators of Ecological Resilience: Inferring the Chance of a Critical Transition. Annual Review of Ecology, Evolution, and Systematics 46:145–167.

Seneviratne, S., X. Zhang, M. Adnan, W. Badi, C. Dereczynski, A. Di Luca, S. Ghosh, I. Iskandar, J. Kossin, S. Lewis, F. Otto, I. Pinto, M. Satoh, S. M. Vicente-Serrano, M. Wehner, and B. Zhou. 2021. Weather and Climate Extreme Events in a Changing Climate. Pages 1513–1766 *in* V. Masson-Delmotte, P. Zhai, A. Pirani, S. L. Connors, C. Péan, S. Berger, N. Caud, Y. Chen, L. Goldfarb, M. I. Gomis, M. Huang, K. Leitzell, E. Lonnoy, J. B. R. Matthews, T. K. Maycock, T. Waterfield, ,O. Yelekçi, R. Yu, and B. Zhou, editors. Climate Change 2021: The Physical Science Basis. Contribution of Working Group I to the Sixth Assessment Report of the Intergovernmental Panel on Climate Change. Cambridge University Press, Cambridge, United Kingdom and New York, NY, USA.

Starostka, V. J., and R. L. Applegate. 1970. Food Selectivity of Bigmouth Buffalo , Ictiobus cyprinellus , in Lake Poinsett , South Dakota. Transactions of the American Fisheries Society 99:571–576.

Stockwell, J. D., J. P. Doubek, R. Adrian, O. Anneville, C. C. Carey, L. Carvalho, L. N. de Senerpont Domis, G. Dur, M. A. Frassl, H.-P. Grossart, B. W. Ibelings, M. J. Lajeunesse, A. M. Lewandowska, M. E. Llames, S.-I. S. Matsuzaki, E. R. Nodine, P. Nõges, V. P. Patil, F. Pomati, K. Rinke, L. G. Rudstam, J. A. Rusak, N. Salmaso, C. T. Seltmann, D. Straile, S. J. Thackeray, W. Thiery, P. Urrutia-Cordero, P. Venail, P. Verburg, R. I. Woolway, T. Zohary, M. R. Andersen, R. Bhattacharya, J. Hejzlar, N. Janatian, A. T. N. K. Kpodonu, T. J. Williamson, and H. L. Wilson. 2020. Storm impacts on phytoplankton community dynamics in lakes. Global Change Biology:1–27.

Taranu, Z. E., S. R. Carpenter, V. Frossard, J. P. Jenny, Z. Thomas, J. C. Vermaire, and M. E. Perga. 2018. Can we detect ecosystem critical transitions and signals of changing resilience from paleo-ecological records? Ecosphere 9: e02438.

Thompson, R. M., U. Brose, J. A. Dunne, R. O. Hall, S. Hladyz, R. L. Kitching, N. D. Martinez, H. Rantala, T. N. Romanuk, D. B. Stouffer, and J. M. Tylianakis. 2012. Food webs: Reconciling the structure and function of biodiversity. Trends in Ecology and Evolution 27:689–697.

Thornton, J. A., W. R. Harding, M. Dent, R. C. Hart, H. Lin, C. L. Rast, W. Rast, S. O. Ryding, and T. M. Slawski. 2013. Eutrophication as a "wicked" problem. Lakes and Reservoirs: Research and Management 18:298–316.

Turner, M. G., W. J. Calder, G. S. Cumming, T. P. Hughes, A. Jentsch, S. L. LaDeau, T. M. Lenton, B. N. Shuman, M. R. Turetsky, Z. Ratajczak, J. W. Williams, A. P. Williams, and S. R. Carpenter. 2020. Climate change, ecosystems and abrupt change: Science priorities. Philosophical Transactions of the Royal Society B: Biological Sciences 375.

Tyson, J. T., and R. L. Knight. 2001. Response of Yellow Perch to Changes in the Benthic Invertebrate Community of Western Lake Erie. Transactions of the American Fisheries Society 130: 766–782.

Vadeboncoeur, Y., D. Lodge, and S. Carpenter. 2001. WHOLE-LAKE FERTILIZATION EFFECTS ON DISTRIBUTION OF PRIMARY PRODUCTION BETWEEN BENTHIC AND PELAGIC HABITATS. Ecology 82:1065–1077.

Vadeboncoeur, Y., K. S. McCann, M. J. Vander Zanden, and J. B. Rasmussen. 2005. Effects of multi-chain omnivory on the strength of trophic control in lakes. Ecosystems 8:682–693.

Vadeboncoeur, Y., M. J. Vander Zanden, and D. M. Lodge. 2002. Putting the Lake Back Together : Reintegrating Benthic Pathways into Lake Food Web Models BioScience 44: 44–52.

Vanni, M. J., W. H. Renwick, J. L. Headworth, J. D. Auch, and M. H. Schaus. 2001. Dissolved and particulate nutrient flux from three adjacent agricultural watersheds: A five-year study. Biogeochemistry 54:85–114.

Walter, J. A., C. D. Buelo, A. F. Besterman, S. J. Tassone, J. W. Atkins, and M. L. Pace. 2022. An algorithm for detecting and quantifying disturbance and recovery in high-frequency time series. Limnology and Oceanography: Methods 20:338–349.

Walter, J., and C. Buelo. 2022. jonathan-walter/disturbhf: lno-methods paper version (v1.0.0). Zenodo. 10.5281/zenodo.6472554

Wang, S. C., X. Liu, Y. Liu, and H. Wang. 2020. Benthic-pelagic coupling in lake energetic food webs. Ecological Modelling 417:108928.

Ward, C. L., and K. S. McCann. 2017. A mechanistic theory for aquatic food chain length. Nature communications 8:2028.

Weber, M. J., and M. L. Brown. 2011. Relationships among invasive common carp, native fishes and physicochemical characteristics in upper Midwest (USA) lakes. Ecology of Freshwater Fish 20:270–278.

Werner, E. E., and D. J. Hall. 1988. Ontogenetic habitat shifts in bluegill: the foraging rate-predation risk trade-off. Ecology 69:1352–1366.

Wilkinson, G., T. Butts, E. Sandry, M. Simonson, and M. Weber. 2022. Experimental evaluation of the effects of bigmouth buffalo (Ictiobus cyprinellus) density on shallow lake ecosystems. Earth Arxiv.

Wilkinson, G. M., S. R. Carpenter, J. J. Cole, M. L. Pace, R. D. Batt, C. D. Buelo, and J. T. Kurtzweil. 2018. Early warning signals precede cyanobacterial blooms in multiple whole-lake experiments. Ecological Monographs 88:188–203.

Winslow, L. A., J. A. Zwart, R. D. Batt, H. A. Dugan, R. I. Woolway, J. R. Corman, P. C. Hanson, and J. S. Read. 2016. LakeMetabolizer: an R package for estimating lake

metabolism from free-water oxygen using diverse statistical models. Inland Waters 6:622–636.

Wojcik, L. A., R. Ceulemans, and U. Gaedke. 2021. Functional diversity buffers the effects of a pulse perturbation on the dynamics of tritrophic food webs. Ecology and Evolution 11:15639–15663.

Wolkovich, E., S. Allesina, K. Cottingham, K. Moore, S. Sandin, and C. de Mazancourt. 2014. Linking the green and brown worlds : the prevalence and effect of multichannel feeding in food webs. Ecology 95:3376–3386.

Vander Zanden, M. J., T. E. Essington, and Y. Vadeboncoeur. 2005. Is pelagic top-down control in lakes augmented by benthic energy pathways? Canadian Journal of Fisheries and Aquatic Sciences 62:1422–1431.

vander Zanden, M. J., and Y. Vadeboncoeur. 2002. Fishes as integrators of benthic and pelagic food webs in lakes. Ecology 83:2152–2161.

Zanette, L. Y., and M. Clinchy. 2019. Ecology of fear. Current Biology 29: 309–313

TABLES

Table 1. Mean (s.d.) of water quality metrics (n=46 – 47) and macrophyte dry biomass (n = 2) along with the added fish biomass for each food web (n.p. = not present). Pulsed refers to ponds that received the two nutrient additions and reference are ponds that did not.

	Low Coupling		**Intermediate**		**High Coupling**	
Variable	***Pulsed***	***Reference***	***Pulsed***	***Reference***	***Pulsed***	***Reference***
Total P (µg L^{-1})	39 (11)	47 (22)	70 (47)	51 (36)	35 (12)	46 (12)
Total N (mg L^{-1})	0.39 (0.15)	0.41 (0.15)	0.41 (0.2)	0.42 (0.18)	0.39 (0.16)	0.36 (0.15)
Soluble P (µg L^{-1})	0.16 (0.32)	2.1 (2.2)	0.86 (1.4)	3.5 (3.8)	0.19 (0.31)	5.5 (6.5)
Nitrate – N (mg L^{-1})	0.13 (0.07)	0.12 (0.07)	0.14 (0.08)	0.14 (0.08)	0.14 (0.07)	0.13 (0.08)
Ammonium – N (mg L^{-1})	0.03 (0.03)	0.04 (0.04)	0.04 (0.04)	0.03 (0.04)	0.02 (0.03)	0.02 (0.03)
Macrophytes (g m^{-2})	76 (3.4)	80 (15)	79 (55)	190 (96)	100 (40)	100 (12)
Bluegill (kg ha^{-1})	21.0	20.4	20.5	20.5	20.3	20.5
Yellow Perch (kg ha^{-1})	19.8	19.8	19.9	19	19.4	19.7
Largemouth Bass (kg ha^{-1})	n.p.	n.p.	23.9	25.7	22.9	30.4
Fathead Minnow (kg ha^{-1})	n.p.	n.p.	n.p.	n.p.	9	9

Table 2. Response and recovery times of experimental ponds based on a response threshold of 2.0 and recovery threshold of 0.5. If a response did not occur, it was listed as not detected (n.d.), and therefore a recovery could not be recorded. The days to response is the difference between the day when a response was triggered and the addition of a nutrient pulse. The days to recover is the difference between the day a response was detected and the day the pond recovered.

		Chlorophyll-*a*		Gross Primary Production		Respiration	
	Nutrient Pulse	***Days to Respond***	***Days to Recover***	***Days to Respond***	***Days to Recover***	***Days to Respond***	***Days to Recover***
Low Coupling	Pulse 1	23	6	n.d.	--	n.d.	--
	Pulse 2	8	22	n.d.	--	n.d.	--
Intermediate Coupling	Pulse 1	18	24	11	11	n.d.	--
	Pulse 2	20	n.d.	21	5	21	4
High Coupling	Pulse 1	n.d.	--	n.d.	--	n.d.	--
	Pulse 2	n.d.	--	n.d.	--	n.d.	--

FIGURES

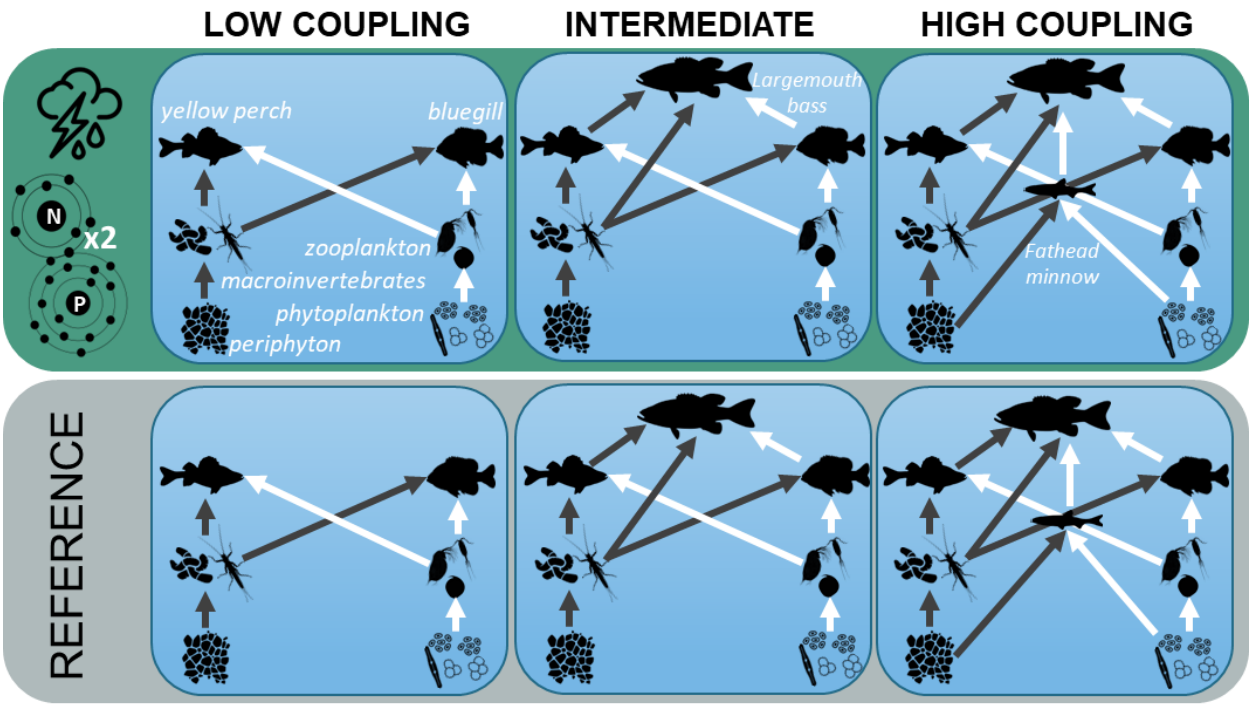

Figure 1. Conceptual diagram of the experimental design of the six pond ecosystems. Dark arrows indicate benthic food web pathways and light arrows indicate pelagic food web pathways. Text labels denote common names of organisms. This diagram does not represent the actual layout of the reference and pulsed ponds which were randomized.

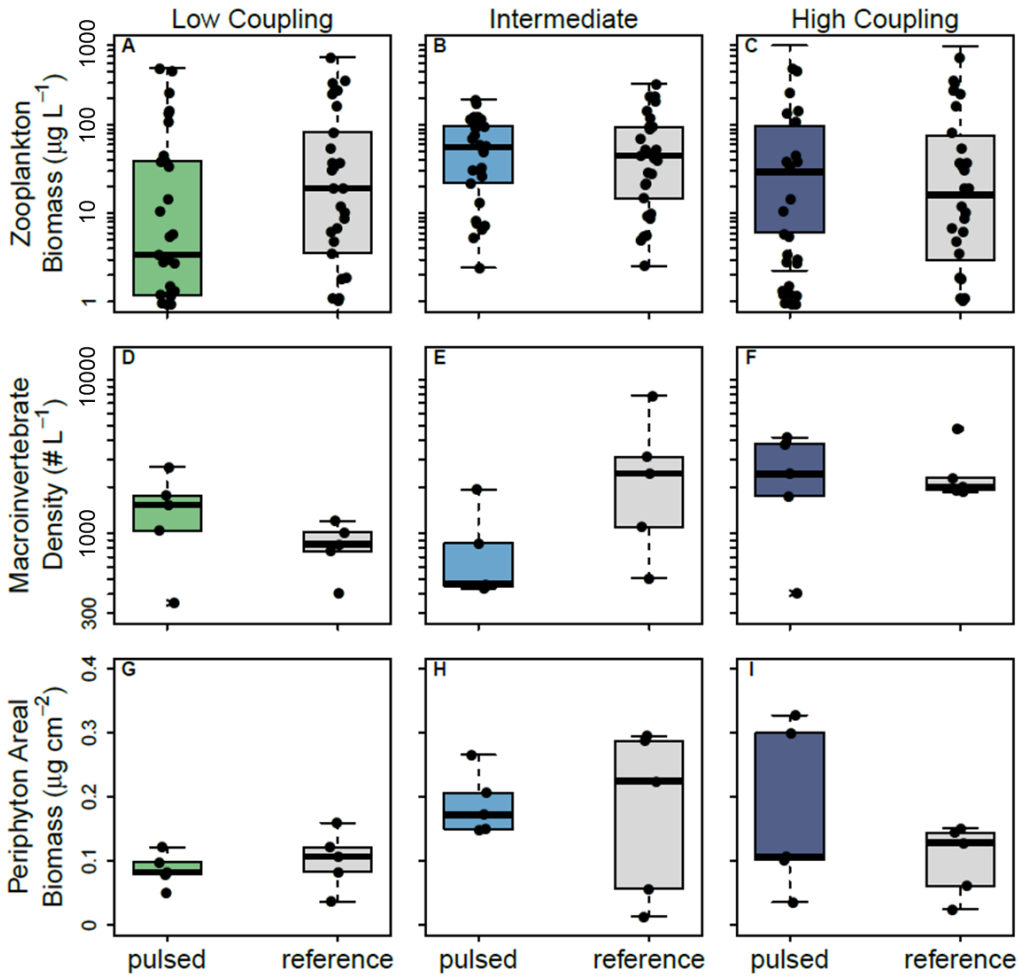

Figure 2. Food web context for experimental ponds over the course of the experiment for zooplankton biomass (A – C), macroinvertebrate density (D – F), and periphyton areal biomass (G – I).

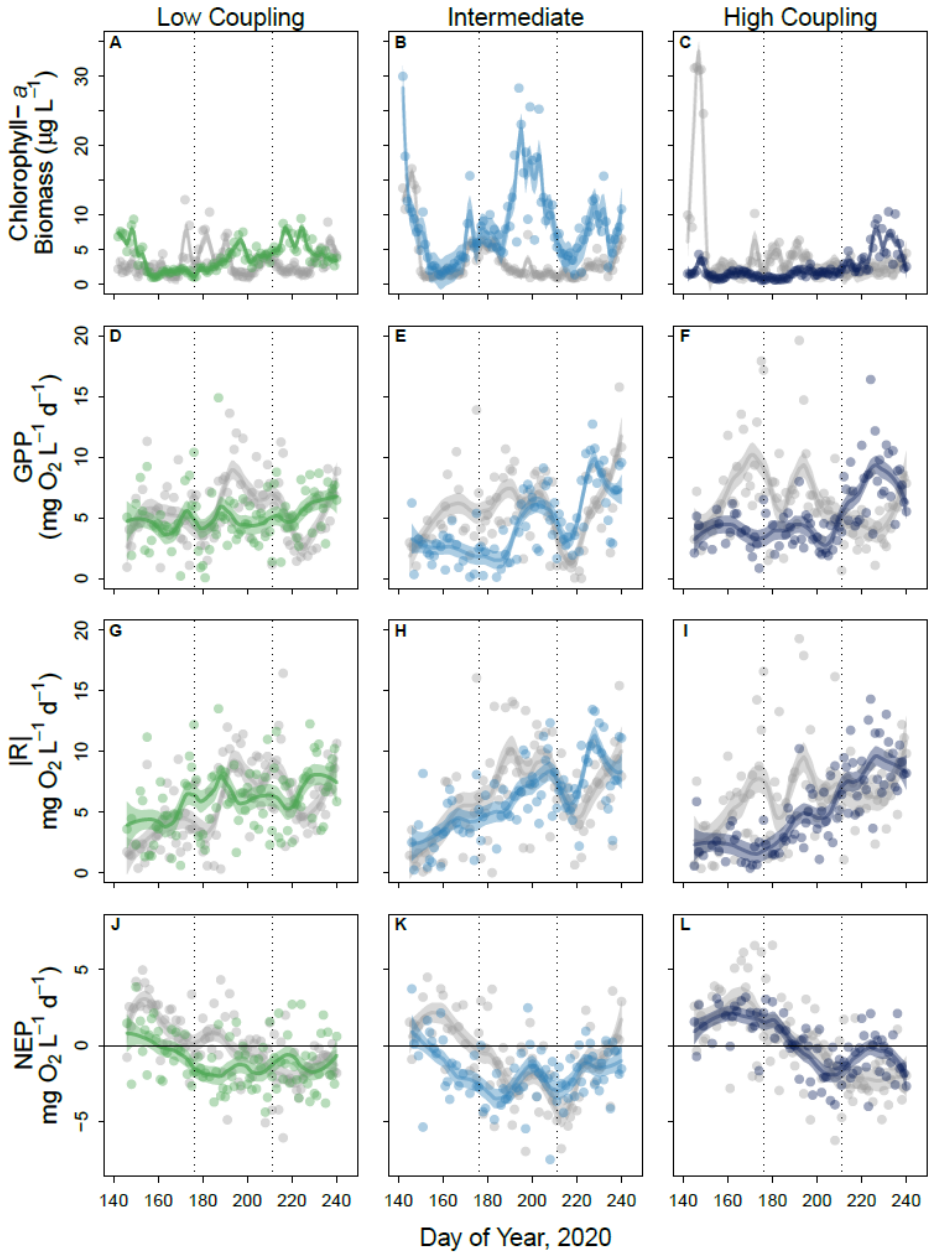

Figure 3. Dynamics of chlorophyll-*a* concentration, gross primary production (GPP), respiration (absolute value, |R|), and net ecosystem production (NEP). Data were fitted with LOESS regression analysis (10% span) for visualization purposes, standard error is defined by the shaded region. The dark colored line indicates the disturbed time series, and the dark gray line indicates the reference time series. In all figures, the dashed vertical line denotes the nutrient pulses on day of year 176 and 211 and the horizontal line at zero (panels J-L) shows whether the ecosystem was autotrophic (NEP > 0) or heterotrophic (NEP < 0).

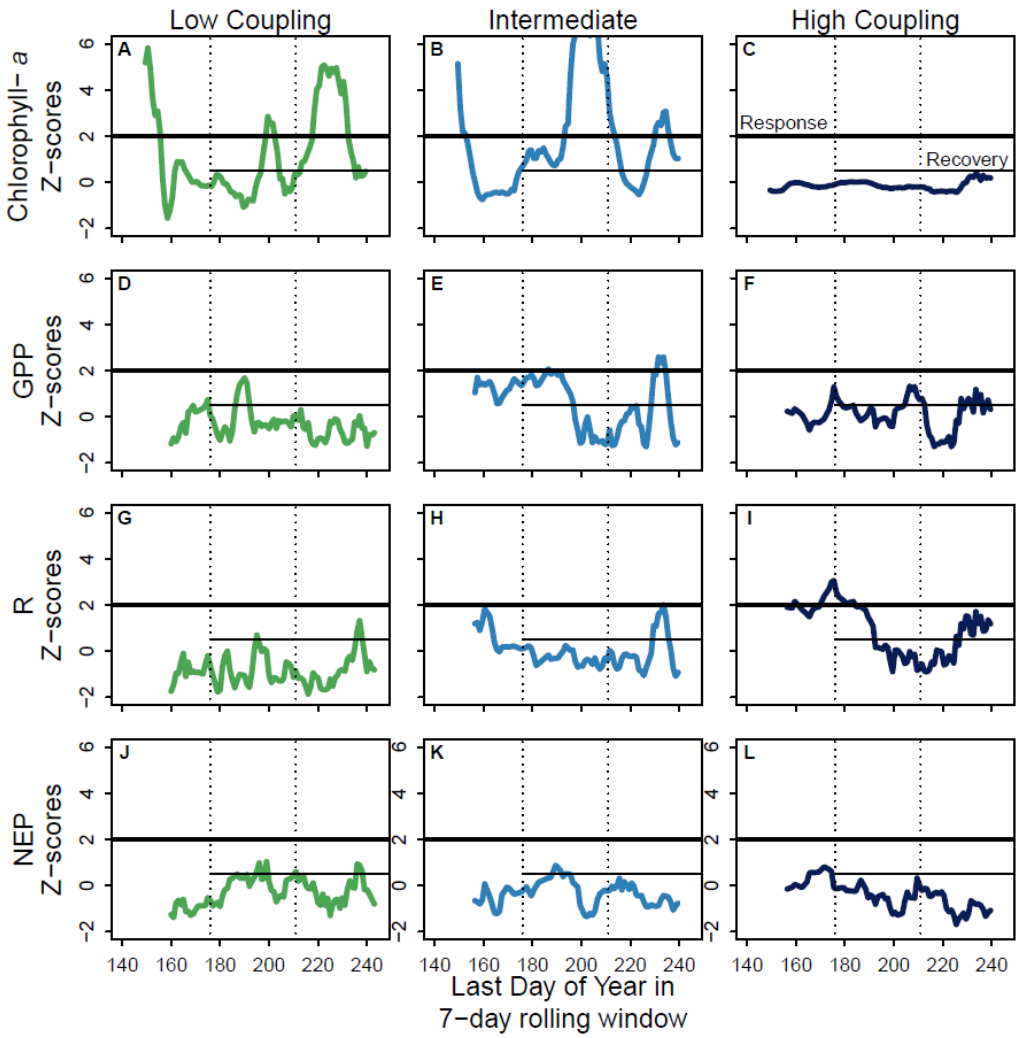

Figure 4. Time series of modified Z-scores of chlorophyll-*a* concentrations (A – C), gross primary production (D – F), respiration (G – I), and net ecosystem production (J – L) generated by the response detection algorithm (Walter et al. 2022). In all figures, the thick horizontal line denotes the response threshold, and the thin horizontal line denotes the recovery threshold. The recovery threshold cannot be documented until a disturbance has occurred. The dashed vertical lines indicate when the nutrient pulses were delivered to each pond.

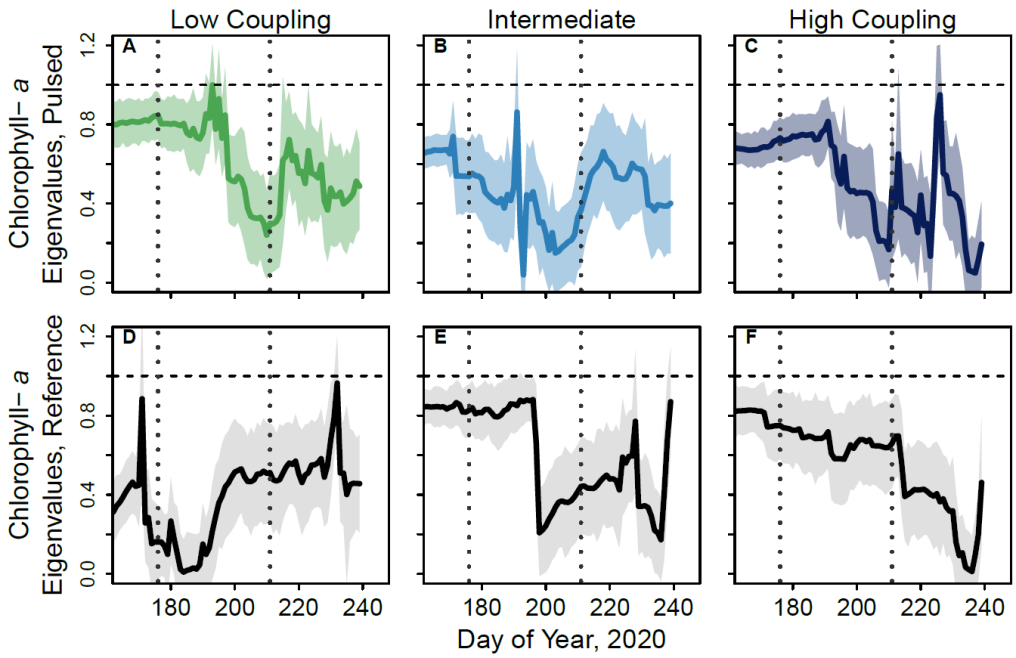

Figure 5. The eigenvalues (dark lines) and their bootstrapped standard error (shaded polygons) of chlorophyll-*a* time series from ponds that received nutrient pulses (A-C) and reference ponds (D-F) at optimal order 1. In all figures, the dashed vertical line denotes the nutrient pulses and the horizontal dashed line at 1 is the threshold by which eigenvalues must cross above from below to be considered a critical transition.

SUPPLEMENTAL INFORMATION FOR CHAPTER 3

SUPPLEMENTAL METHODS

Periphyton

Periphyton was brushed, scraped, and rinsed off the substrate (0.017 m^2) with deionized water and diluted to a known volume in amber bottles before analysis (Jacoby et al. 1991, Carey and Wahl 2011). Samples from each pond were homogenized to loosen algal 'clumps' and filtered onto Whatman glass fiber filters (0.45 µm). Areal chlorophyll-a (µg/m^2) was measured via acetone extraction using sonication (Bidigare et al. 2005) and analyzed using fluorometry (EPA Method 445.0) on a Turner Designs Trilogy Fluorometer (Arar and Collins 1997, Childress et al. 1999, Turner Designs 2001).

Nutrients

Phosphorus was measured via the phosphomolybdenum blue method (EPA method 365.1 v2) and nitrogen was measured via second-derivative ultraviolet spectroscopy (Crumpton et al. 1992, Childress et al. 1999) using an HP 8435 Spectrophotometer. Total phosphorus and nitrogen samples underwent a persulfate digestion before analysis to transform all P- or N- containing compounds into dissolved forms.

Macrophytes

To assess macrophyte biomass, we established a transect parallel to the natural shoreline of the pond and biomass samples were collected at six points along the transect with a two-sided rake (0.4 m^2; Mikulyuk et al., 2011). Macrophyte stems and leaves were then dried for 48 hours at 60 ºC and weighed to quantify dry-weight biomass.

Zooplankton

Zooplankton were identified using a Leica MZ8 stereomicroscope connected to Motic Images software in a 1 mL subsample. If less than 60 organisms were identified within the 1 mL subsample, another subsample was counted. Up to 25 individuals per taxon were measured per sample to calculate dry mass per liter using standard length-mass regressions (Dumont et al. 1975; McCauley 1984).

Macroinvertebrates

We added 0.1% Rose Bengal Dye to preserved macroinvertebrate samples in order to assist with later sorting. In the lab, macroinvertebrates were further sieved on a 500-µm pan sieve and individuals were removed and identified to the lowest possible order or family. A stereomicroscope was used to identify mollusks and insects to family. Leeches and oligochaetes were identified to class. This level of taxonomic resolution is sufficient to reflect community patterns (Bowman and Bailey 1997). Sorted individuals were then used to calculate taxon richness and density (number of individuals/m^2).

Dissolved Oxygen Data Cleaning

Dissolved oxygen (DO) concentration was measured every 30 minutes in the surface waters of each pond over the course of the 96-day experiment. Prior to calculating daily rates of ecosystem metabolism, DO data were inspected and cleaned to account for times when a change in DO concentration was likely a result of physical processes (e.g., vertical mixing) rather than biological production or respiration. We used a conservative threshold of a change of 2.0 mg DO L^{-1} to identify these times. All times when DO concentration decreased by 2.0 mg L^{-1} or more

from the previous measurement (i.e., a 2.0 mg L^{-1} drop in 30 minutes) were flagged and removed along with the subsequent five measurements (three hours total). These three-hour periods were then backfilled via linear interpolation. The majority of days did not require any cleaning and backfilling of DO data. Out of 576 total days (96 per pond), 345 days did not have any flagged DO measurements, 144 days had one flagged measurement, 71 days had two flagged measurements, and only 16 days had three or more flagged measurements.

As described in the manuscript text, calculating daily rates of metabolism using the free-oxygen method can result in erroneous estimates (i.e., negative GPP, positive R), and any days for which calculations returned an erroneous estimate were removed prior to further analyses. This resulted in the removal of 62 days due to erroneous metabolism estimates (range 4 – 18 days across all ponds), 40 of which were from days that did not have any flagged and cleaned DO measurements.

SUPPLEMENTAL REFERENCES

Bowman, M. F., & Bailey, R. C. (1997). Does taxonomic resolution affect the multivariate description of the structure of freshwater benthic macroinvertebrate communities? *Canadian Journal of Fisheries and Aquatic Sciences*, *54*(8), 1802–1807. https://doi.org/10.1139/f97-085

Burnham, K. P., & Anderson, D. R. (2004). Multimodel inference: Understanding AIC and BIC in model selection. In *Sociological Methods and Research* (Vol. 33, Issue 2, pp. 261–304). https://doi.org/10.1177/0049124104268644

Dumont, H. J., van de Velde, I., & Dumont, S. (1975). The dry weight estimate of biomass in a selection of Cladocera, Copepoda and Rotifera from the plankton, periphyton and benthos of continental waters. *Oecologia*, *19*(1), 75–97. https://doi.org/10.1007/BF00377592

McCauley, E. (1984). The estimation of the abundance and biomass of zooplankton in samples. In J. Downing & F. Rigler (Eds.), *A manual on methods for the assessment of secondary productivity in fresh waters* (pp. 228–265). Blackwell Publishing Ltd.

Mikulyuk, A., Sharma, S., van Egeren, S., Erdmann, E., Nault, M. E., & Hauxwell, J. (2011). The relative role of environmental, spatial, and land-use patterns in explaining aquatic macrophyte community composition. *Canadian Journal of Fisheries and Aquatic Sciences*, *68*(10), 1778–1789. https://doi.org/10.1139/f2011-095

SUPPLEMENTAL TABLES

Table S1. Mass, in grams, of nitrogen and phosphorus added to the experimental research ponds for each nutrient pulse along with the percent increase in ambient phosphorus concentrations.

	NH_4NO_3	$NaH_2PO_4(H_2O)_2$	Ambient increase
Nutrient Pulse 1	21.36	3.33	3 %
Nutrient Pulse 2	45.01	7.02	5 %

Table S2. Akaike Information Criterion corrected for small sample size (AICc) of online dynamic linear autoregressive models of chlorophyll-*a* concentration for each experimental pond at optimal order (p) of 1 or 2 . Bold indicates a model was significantly different than the other optimal order (ΔAICc > 2; Burnham & Anderson, 2004).

	p = 1	p = 2	ΔAICc
Low Coupling – pulsed	318.06	319.64	1.58
Low Coupling – reference	357.32	357.29	0.03
Intermediate – pulsed	**530.03**	559.52	29.49
Intermediate – reference	**319.05**	325.18	6.13
High Coupling – pulsed	**239.41**	267.05	27.64
High Coupling – reference	382.26	383.24	0.98

Table S3. The number of individuals identified in the stomach contents of fish at the end of the experiment collected via gastric lavage grouped by taxonomic identity. Macrophytes included plant pieces and stems, miscellaneous eggs were mostly frog eggs but some fish eggs as well, and frog refers to adults. If individuals of a certain taxa were not identified, they were marked as not detected (n.d.).

		Bluegill	***Yellow Perch***	***Largemouth Bass***
Low Coupling	Zooplankton	32	6	--
	Macroinvertebrate	115	45	--
	Misc. Eggs	3	n.d.	--
	Macrophytes	16	8	--
	Larval fish	n.d.	11	--
	Frog	n.d.	n.d.	--
Intermediate	Zooplankton	11	n.d.	n.d.
	Macroinvertebrate	55	25	22
	Misc. Eggs	10	n.d.	n.d.
	Macrophytes	16	1	1
	Larval fish	n.d.	7	4
	Frog	n.d.	n.d.	n.d.
High Coupling	Zooplankton	11	2	n.d.
	Macroinvertebrate	72	35	6
	Misc. Eggs	1	--	n.d.
	Macrophytes	15	2	1
	Minnow	n.d.	2	1
	Larval fish	n.d.	n.d.	n.d.
	Frog	n.d.	n.d.	1

Table S4. Response detection algorithm results for chlorophyll-*a*, gross primary production, respiration, and net ecosystem production with three rolling window lengths: five days, seven days, and ten days. The days to respond quantifies the number of days following the first or second nutrient pulse that it took Z-scores to move above the response threshold (Z = 2.0). Days to recover quantifies the number of days, once the Z-scores passed the response threshold, to move below the recovery threshold (Z = 0.5).

			Chlorophyll-*a*		Gross Primary Production		Respiration	
	Window	***Nutrient Pulse***	***Days to Respond***	***Days to Recover***	***Days to Respond***	***Days to Recover***	***Days to Respond***	***Days to Recover***
Low Coupling	7 days	Pulse 1	23	6	n.d.	--	n.d.	--
	7 days	Pulse 2	8	22	n.d.	--	n.d.	--
Intermediate Coupling	7 days	Pulse 1	18	24	11	11	n.d.	--
	7 days	Pulse 2	20	n.d.	21	5	21	4
High Coupling	7 days	Pulse 1	n.d.	--	n.d.	--	n.d.	--
	7 days	Pulse 2	n.d.	--	n.d.	--	n.d.	--
Low Coupling	5 days	Pulse 1	24	4	9	5	n.d.	--
	5 days	Pulse 2	7	15	n.d.	--	n.d.	--
Intermediate Coupling	5 days	Pulse 1	18	25	18	22	n.d.	--
	5 days	Pulse 2	19	9	19	9	21	4
High Coupling	5 days	Pulse 1	n.d.	--	n.d.	--	n.d.	--
	5 days	Pulse 2	n.d.	--	n.d.	--	n.d.	--
Low Coupling	10 days	Pulse 1	25	6	n.d.	--	n.d.	--
	10 days	Pulse 2	7	20	n.d.	--	n.d.	--
Intermediate Coupling	10 days	Pulse 1	5	38	4	17	n.d.	--
	10 days	Pulse 2	19	n.d.	22	4	n.d.	--
High Coupling	10 days	Pulse 1	n.d.	--	n.d.	--	n.d.	--
	10 days	Pulse 2	n.d.	--	n.d.	--	21	--

SUPPLEMENTAL FIGURES

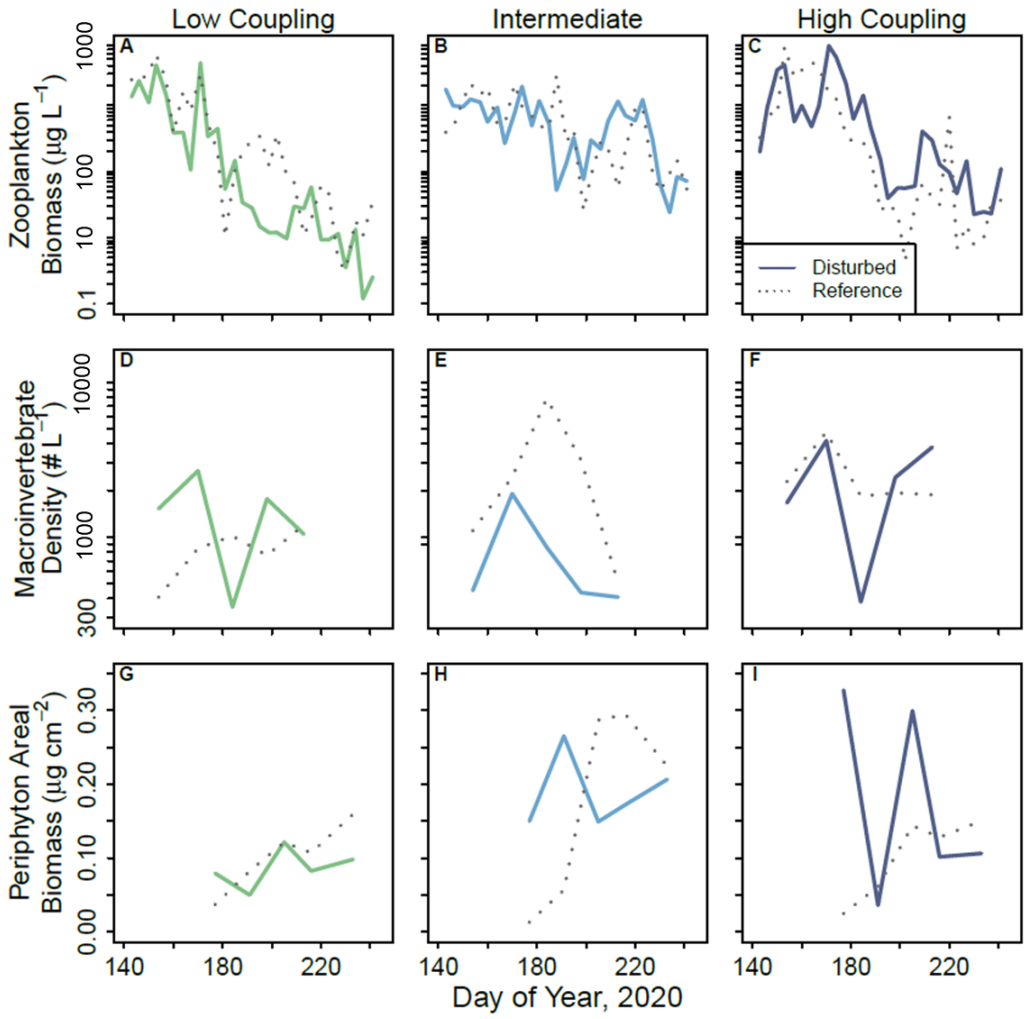

Figure S1. Time series of zooplankton biomass (top row, *A* - *C*), macroinvertebrate density (middle row, *D* - *F*), and periphyton areal biomass (bottom row, *G* - *I*). The dark colored line indicates the disturbed time series, and the gray line indicates the reference time series.

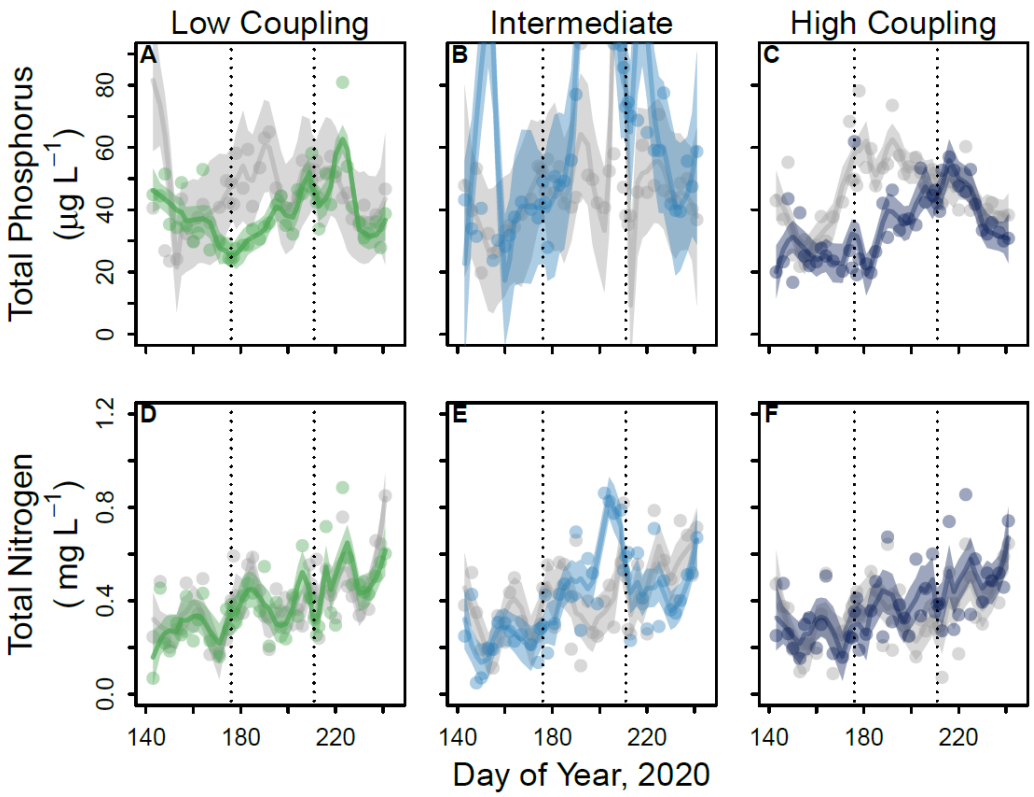

Figure S2. Time series of total nitrogen (mg L^{-1}) and phosphorus (µg L^{-1}). Data were fitted with LOESS regression analysis (20% span) for visualization purposes, error is defined by the shaded region. The dark colored line indicates the disturbed time series, and the gray line indicates the reference time series. In all figures, the dashed vertical line denotes the nutrient pulses on day of year 176 and 211.

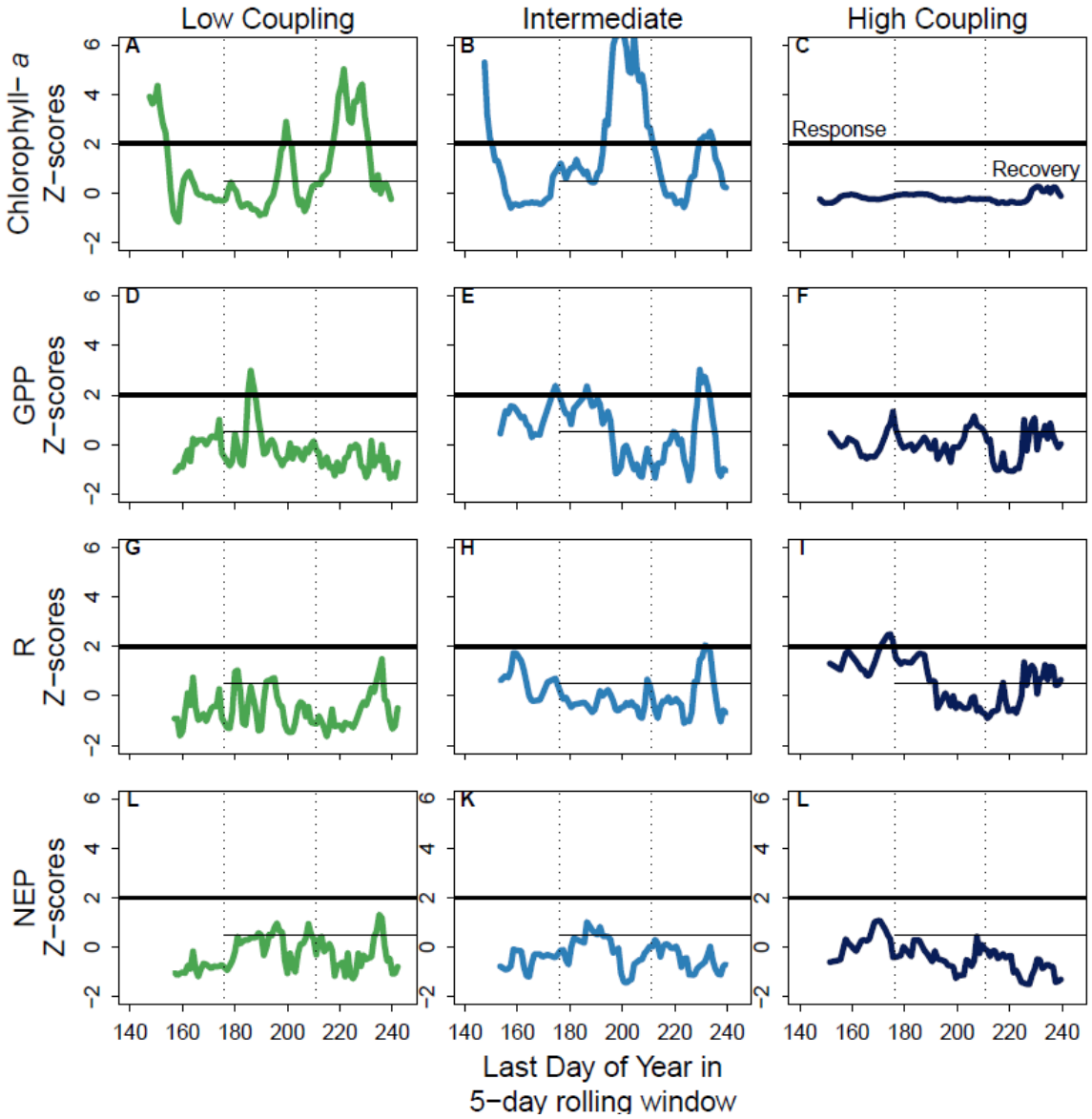

Figure S3. Time series of modified Z-scores of chlorophyll-*a* concentrations (A – C) and gross primary production (D – F) generated by the response detection algorithm (Walter et al. 2022) with a 5-day window. In all figures the thick horizontal line denotes the response threshold, and the thin horizontal line denotes the recovery threshold. The recovery threshold can't be documented until a disturbance has occurred. The dashed vertical lines indicate when the nutrient pulses were delivered to each pond on day of year 176 and 211.

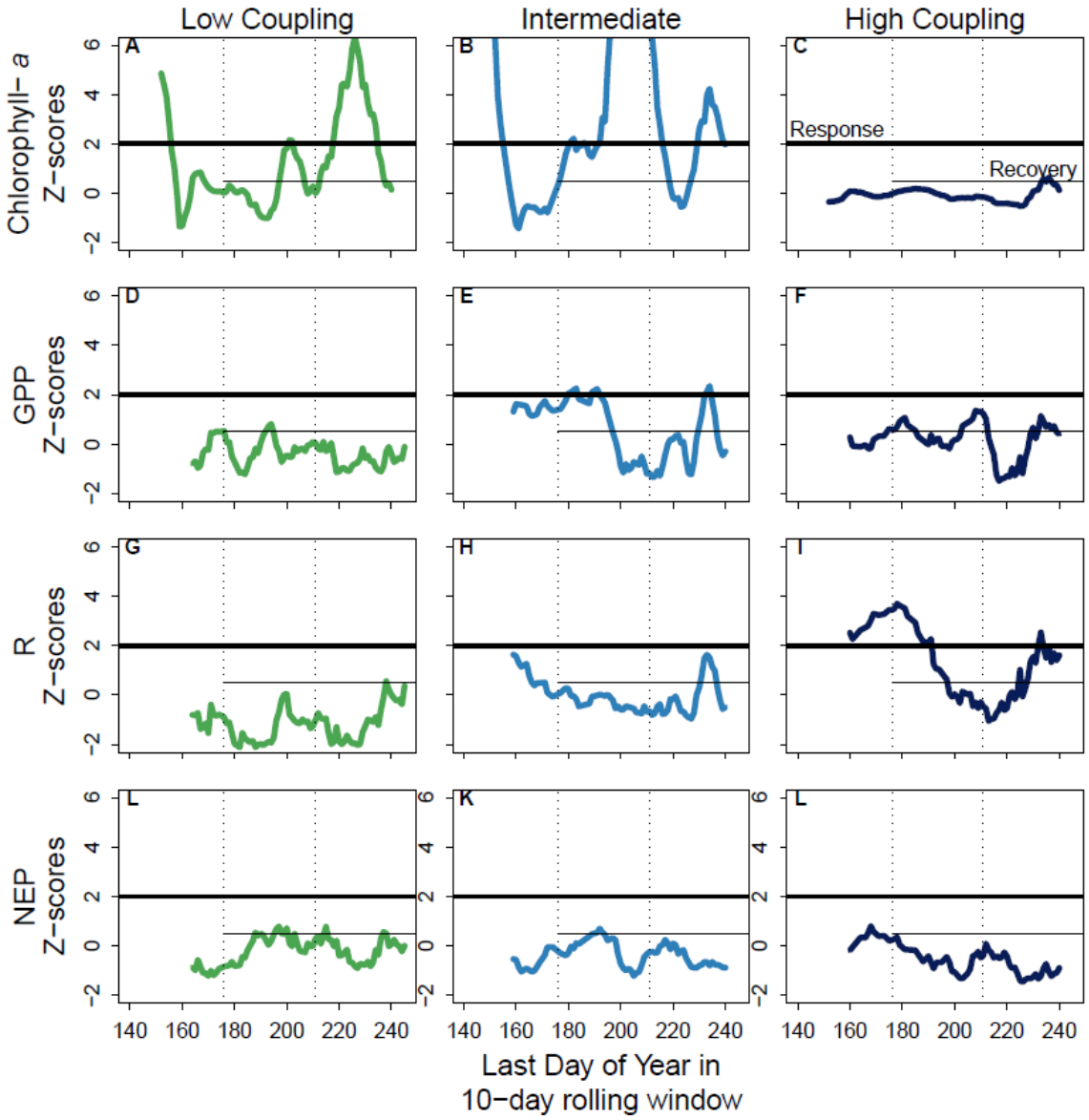

Figure S4. Time series of modified Z-scores of chlorophyll-*a* concentrations (A – C) and gross primary production (D – F) generated by the response detection algorithm (Walter et al. 2022) with a 10-day window. In all figures the thick horizontal line denotes the response threshold, and the thin horizontal line denotes the recovery threshold. The recovery threshold can't be documented until a disturbance has occurred. The dashed vertical lines indicate when the nutrient pulses were delivered to each pond on day of year 176 and 211.

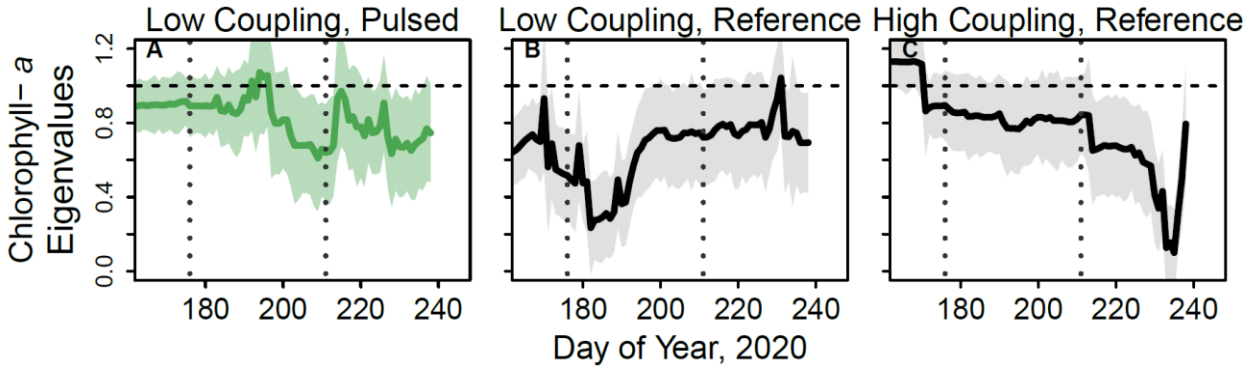

Figure S5. The eigenvalues (dark lines) and their bootstrapped standard error (shaded polygons) of chlorophyll-*a* time series at optimal order 2 which was not significantly different than the optimal order 1 plots. In all figures, the dashed vertical line denotes the nutrient pulses on day of year 176 and 211. The horizontal dashed line at 1 is the threshold by which eigenvalues must cross above from below to be considered a critical transition.

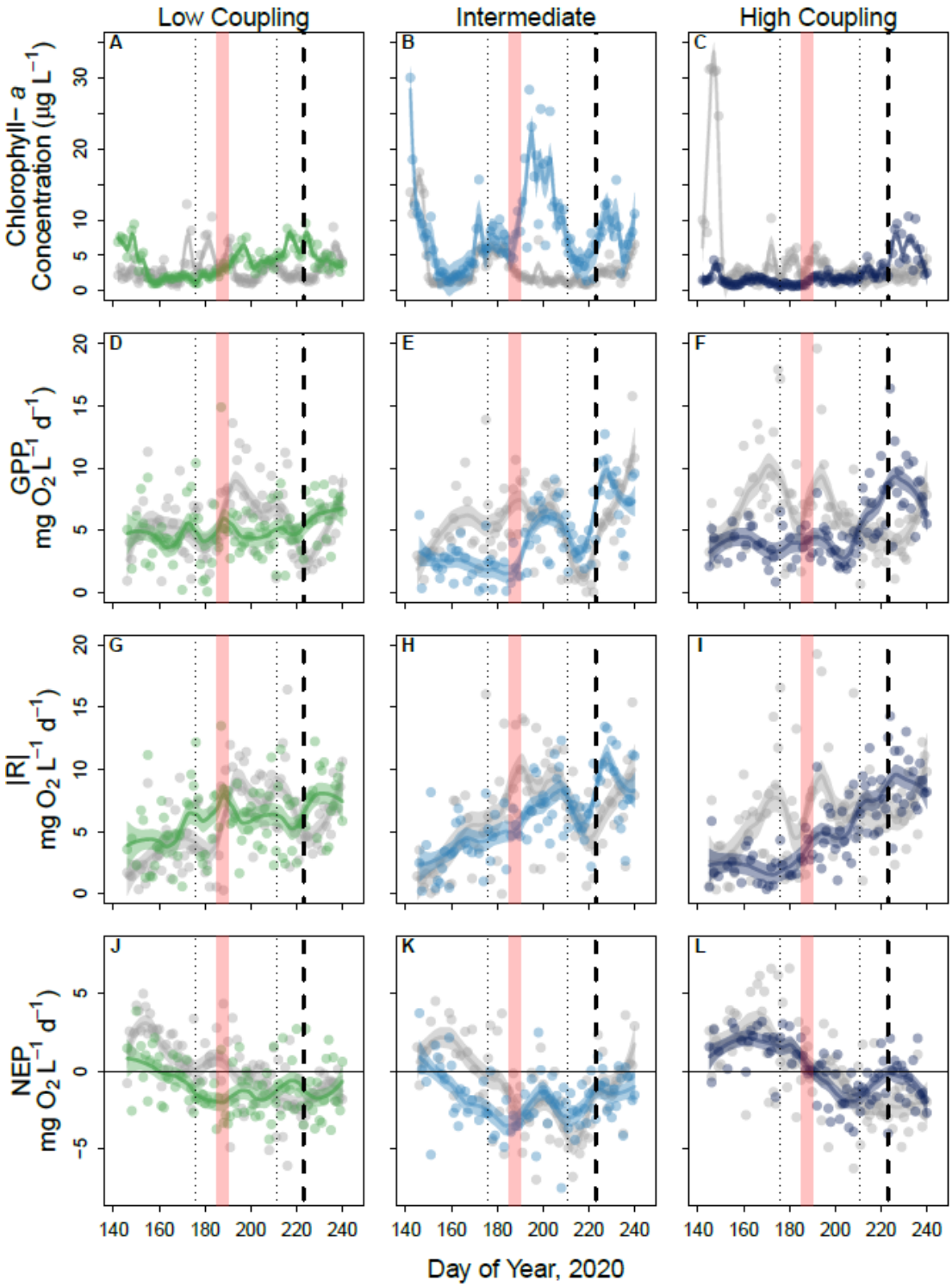

Figure S6. Dynamics of chlorophyll-*a*, gross primary production (GPP), respiration (absolute value, |R|), and net ecosystem production (NEP). Data were fitted with LOESS regression analysis for visualization purposes, error is defined by the shaded region. The dark colored line

indicates the disturbed time series, and the gray line indicates the reference time series. In all figures, the dashed vertical line denotes the nutrient pulses on day of year 176 and 211 and the horizontal line at zero (J – L) shows whether the ecosystem was autotrophic (NEP > 0) or heterotrophic (NEP < 0). The five-day period of elevated surface water temperature is a red polygon, and the thick dashed vertical line indicates when the 2020 Iowa derecho occurred on DOY 223.

CHAPTER 4

CHANGES IN ENERGY FLOW AND FOOD WEB STABILITY IN A NORTH TEMPERATE LAKE PRIOR TO AND FOLLOWING INVASION OF SPINY WATER FLEA (*BYTHOTREPHES LONGIMANUS)*

In preparation for submission with coauthors B. Martin, J. Mrnak, G. Sass, M. J. Vander Zanden, C. Warden, G. M. Wilkinson.

Author contributions: Butts designed the study; performed all laboratory work; cleaned, analyzed, and visualized the data; and wrote the manuscript. Martin, Mrnak, Sass, Vander Zanden, and Warden contributed to study design and data analysis. Wilkinson contributed to study design, data analysis, and provided feedback on writing.

ABSTRACT

Food web structure is highly dynamic with major consequences for ecosystem function and services. Species invasions can 'rewire' food webs, altering the flow of energy through the network, and food web stability. However, our understanding of how species invasion affects the distribution and magnitude of energy flux, in addition to food web stability dynamics, is limited. Thus, it is unclear how long and how intensely species invasion alters energy flux and food web stability. We used a 19-year, multi-trophic dataset of pelagic food web dynamics in Trout Lake, WI, USA with three distinct periods: (1) dominance by the zooplanktivore, cisco (*Coregonus artedi*); (2) increase in apex predators, lake trout (*Salvelinus namaycush*) and walleye (*Sander vitreus*); and (3) establishment of a mid-trophic level invader, spiny water flea (*Bythotrephes longimanus*). We employed a bioenergetics approach to quantify the dynamics and magnitude of

energy flux between species in the food web, in addition to quantifying food web stability through derivation of a Jacobian matrix using energy flux as a proxy for interaction strength. Energy flux dynamics were relatively steady across the first two periods with consistent distribution of energy flux within the food web. The introduction of *Bythotrephes* resulted in an overall decrease in total energy flux, in addition to affecting the flux of energy among lower and higher trophic levels. Food web stability was steady from 2001 – 2014, before sharply decreasing once *Bythotrephes* appeared in 2015. The following year, food web stability swiftly returned to pre-invasion levels, indicating that the Trout Lake food web was able to absorb the shock of species invasion. This analysis provided evidence that mid-trophic level invaders decrease total ecosystem energy flux, and thus overall ecosystem function, and shifted the magnitude of flux between lower and higher trophic levels. Despite the substantial decline in food web stability immediately following invasion, the change was transient, indicating that the network was able to recover quickly. Improving our understanding of how food web dynamics change over time is crucial to better predict how ecosystems may be affected by species invasion, or other disturbances, in the future.

INTRODUCTION

Food webs are a tangled web of species interactions, yet the patterning of those interactions (i.e., food web structure) can have a profound influence on population dynamics, ecosystem functions, and ecosystem services (Pimm, Lawton & Cohen, 1991; Barnes *et al.*, 2018; Moore *et al.*, 2018). This is due to the substantial influence of food web structure on the flow of energy through ecosystems (Lindeman, 1942; Odum, 1968; Barnes *et al.*, 2018). However, food web structure is not static, rather, it is highly dynamic with changes occurring

over a span of weeks (Sommer *et al.*, 2012; Boit & Gaedke, 2014) to decades (Olivier *et al.*, 2019). Changes in food web structure through time can result in the 'rewiring' of trophic links where species interactions may be generated, dissolved, or altered affecting the magnitude and pathways of energy flow within an ecosystem (Bartley *et al.*, 2019; Olivier *et al.*, 2019; Kortsch *et al.*, 2021). A major threat facing ecosystems are species invasions which are predicted to expand as globalization increases and global change opens new avenues for species invasion (Rahel & Olden, 2008; Hulme, 2017). Biological invasions can substantially affect food web structure and ecosystem functions, and in turn, ecosystem services like tourism, recreation, and recreational fisheries (Pejchar & Mooney, 2009; David *et al.*, 2017; Flood *et al.*, 2020).

Biological invasions in lakes directly alter food web structure through direct predation of native species, increasing exploitative and interference competition, shifting species niche breadth, lowering the trophic level of consumers, and increasing interaction strengths by reinforcing existing trophic pathways (Vander Zanden, Casselman & Rasmussen, 1999; Bobeldyk & Lamberti, 2008; Crowder & Snyder, 2010; Galiana *et al.*, 2014; Tran *et al.*, 2015). Biological invasion can be an even stronger driver of energy flow in food webs than eutrophication or the addition or removal of planktivores (Wang *et al.*, 2021). The effects of invasive species at higher trophic levels (Simon & Townsend, 2003; Bradley *et al.*, 2019) along with primary consumers and producers (Strayer, 2009; Wahl *et al.*, 2011; Karatayev, Burlakova & Padilla, 2015) are well known. However, for mid-trophic level invaders, our understanding of the potential multi-directional (e.g., top-down, bottom-up, horizontal) effects on food web structure, stability, and ecosystem function through time is less predictable though potentially substantial (Kimbro *et al.*, 2009; Ellis *et al.*, 2011). Opportunities to document changes in network stability and energy flux among species from before invasion, immediately following,

and longer-term effects are rare, but can greatly improve our understanding of the ecosystem-scale effects of biological invasion (Barnes *et al.*, 2018; Flood *et al.*, 2020).

Quantifying the distribution of energy flux within food webs, or the transfer of energy through trophic interactions, can aid in understanding how whole food webs respond to mid-trophic level invaders. For example, changes in total energy flux or flux among trophic levels can quantify food web properties that are difficult to assess such as top-down versus bottom-up forcing (Barnes *et al.*, 2020), or be used to quantify food web responses to perturbations (Schwarz *et al.*, 2017). In addition, energy flux can be used as a proxy for overall ecosystem function as it comprises the sum of several individual trophic functions (Wagg *et al.,* 2014; Barnes *et al.,* 2018). Furthermore, the strength and distribution of energy flux between species in a food web are strongly related to local food web stability (de Ruiter, Neutel & Moore, 1995; McCann, Hastings & Huxel, 1998; Neutel *et al.*, 2007; Moore & de Ruiter, 2012). Food web stability is a theoretical concept, defined as the ability of a food web to return to a stable equilibrium following a perturbation (May, 1972; McCann, 2000; Neutel & Thorne, 2014). Understanding how much and how long food web stability is altered by biological invasions can provide key insights into how vulnerable a food web may be to other disturbances following invasion. It remains unclear, however, how strongly a mid-trophic level invader would affect the distribution of energy flux within a food web and, ultimately, food web stability over time. Furthermore, it is uncertain what the consequences of lost stability are for real ecosystems, nor is it clear how long stability and energy flux may be changed in response to a species invasion. This is largely due to a paucity of long-term food web data and lack of clarity assessing the effects of invaders within ecosystems (Jeschke *et al.*, 2014). Improving the mechanistic basis of

food web structure response to biological invasion is crucial to effectively manage ecosystems confronting local to global change.

We estimated changes in energy flux and food web stability prior to, during, and following the invasion of spiny water flea (*Bythotrephes longimanus*) over 19 years (2001 – 2019) in Trout Lake, Wisconsin (USA) using multi-trophic, temporally resolved species biomass data collected by the North Temperate Lakes – Long Term Ecological Research (NTL – LTER) program. Specifically, we expand on previous work in the pelagic food web of Trout Lake, WI which documented two major changes in food web structure (Martin, Walsh & Vander Zanden, 2022). In 2007, a native apex predator, lake trout (*Salvelinus namaycush*), became more abundant following decades of dominance by zooplanktivorous cisco (*Coregonus artedi*). Then, in 2014, spiny water flea (*Bythotrephes longimanus*) appeared in the lake, a mid-trophic level invader that affects multiple trophic levels by feeding on zooplankton (Straile & Hälbich, 2000; Yan *et al.*, 2011; Brown, Branstrator & Shannon, 2012), competing with other mid-trophic level consumers (e.g., *Leptodora, Chaoborus, Mysis*), and becoming a prey item for planktivorous fishes large enough to overcome its barbed caudal spine (Compton & Kerfoot, 2004; Foster & Sprules, 2010; Martin, Mrnak & Vander Zanden, 2023).

Our objectives were to (1) quantify the dynamics and distribution of biomass and energy flux within the Trout Lake pelagic food web across 19 years, (2) quantify how the invasion of spiny water flea affected the flux of energy between trophic levels over time, and (3) quantify the dynamics of food web stability following documented changes in food web structure. We expected that the increase in lake trout abundance would shift the dominant energy flux pathways from zooplanktivory to piscivory, and the invasion of spiny water flea would substantially change the distribution and magnitude of energy flux within the food web by

altering interaction strength and species biomass. In addition, we anticipated that following the introduction of spiny water flea, food web stability would be lower in comparison to previous years due to higher energy flux from zooplankton to spiny water flea, increasing the number of strong interactions within the food web, thus decreasing food web stability (McCann, 2000; Zhao *et al.*, 2019).

METHODS

Study system

Trout Lake is an oligotrophic, north-temperate, large (1564 ha drainage, 35.7 m max depth), lake located in Vilas County, Wisconsin, USA. Trout Lake has been a part of the Northern Temperate Lakes – Long Term Ecological Research (NTL-LTER) program since 1981 which has generated a long-term ecological record that has documented several significant shifts within the pelagic (spiny water flea, *Bythotrephes longimanus* invasion) (Martin *et al.*, 2022) and littoral (rusty crayfish, *Faxonius rusticus*) (Wilson *et al.*, 2004) food web. Long-term studies of fish populations from hydroacoustic surveys and gill netting have documented that zooplanktivorous cisco (*Coregonus artedi*) numerically dominates the pelagic food web of Trout Lake (Ahrenstorff *et al.*, 2013). The relative abundance of cisco predators, lake trout (*Salvelinus namaycush)* and walleye (*Sander vitreus*) have increased in the pelagic zone of Trout Lake since 2007 (Magnuson, Carpenter & Stanley, 2023b), with lake trout having a significant influence on cisco population dynamics (Parks & Rypel, 2018)**.** Cisco can also be an important prey item for larger walleye, comprising up to 20 % of the pelagic component of walleye diet (Kaufman, Morgan & Gunn, 2009; Herwig, Zimmer & Staples, 2022). In addition to fishes, long-term data on the mesozooplankton and rotifer community and biomass, predatory pelagic macroinvertebrates (i.e., *Chaoborus, Mysis, Leptodora*) and the invasive *Bythotrephes* have been

collected annually. Here, we focus on the major interactions within the pelagic food web of Trout Lake including lake trout, walleye, cisco, pelagic macroinvertebrates, and zooplankton over 19 years (2001 – 2019).

Food web data collection and processing

We quantified biomass density (g ha^{-1}) for each major component of the Trout Lake pelagic food web in late-July to early-August from 2001-2019 using data from the NTL-LTER program. Sampling design and methodological details are available in greater detail through the NTL-LTER program (Magnuson, Carpenter & Stanley, 2023a), but we describe specific methods in brief here.

Pelagic fish abundance was estimated using NTL-LTER standardized methods (Lawson *et al.*, 2015; Mrnak *et al.*, 2021) consisting of hydroacoustic and vertical gillnet surveys between late-July and early-August (Magnuson *et al.*, 2023b). Data include both fish density (fish ha^{-1} ± standard error) and species composition, though species at lower abundances may be absent from the hydroacoustic output yet still be present within the system (e.g., lake trout, walleye). To calibrate species composition estimates, standard hydroacoustic processing recommends three individuals per species must be collected on a vertical gillnet to assign density estimates to species within hydroacoustic models (Parker-Stetter *et al.*, 2009; DuFour *et al.*, 2021; Mrnak *et al.*, 2021), which can lead to species known to be in the lake not appearing in each year's estimates. Greater detail on the standard NTL-LTER calibration of species-specific density estimates can be found in Mrnak *et al.* (2021). The average size of each fish species, each year, was quantified by applying a dorsal aspect equation converting species' average target strength in decibels to fish total length in millimeters (Love, 1971; Lawson *et al.*, 2015; Parks & Rypel,

2018). Trout Lake-specific length-weight regressions were then calculated for each target fish species (i.e., lake trout, cisco, walleye) from length and weight data collected via vertical gill nets at multiple depths, fyke nets, seining, and electrofishing since 1981 (Supplementary Table S1;Magnuson, Carpenter & Stanley, 2022a). Annual species average length derived from the hydroacoustic surveys was then applied to the Trout Lake-specific length-weight regression to get an average weight (g) per fish species per year. The average weight was then applied to each species' density estimate (fish ha^{-1}) to calculate fish species' biomass density (g ha^{-1}). Lake whitefish (*Coregonus clupeaformis*) were also reported in the hydroacoustic surveys for Trout Lake (Magnuson *et al.*, 2023b); however, whitefish are ecologically benthivores (Rennie, Gary Sprules & Johnson, 2009), and thus did not have a substantial effect on the pelagic food web of Trout Lake considered here. To account for pelagic-littoral walleye feeding behavior (Vander Zanden & Vadeboncoeur, 2002) we reduced walleye biomass to 20% of their observed biomass density. We chose 20% as cisco accounted for roughly 20% of walleye diet in another north temperate lake in Minnesota with a similar food web determined via stable isotope analyses (Herwig *et al.*, 2022).

Pelagic macroinvertebrates, including *Bythotrephes* (2014), were collected via annual nighttime tows (1 mm mesh, 1 mm diameter) between late-July to early-August to calculate density (pelagic macroinvertebrates $m^{-2} \pm$ standard error) (Magnuson, Carpenter & Stanley, 2022b). The pelagic macroinvertebrate community consisted of *Chaoborus, Leptodora, Mysis,* and following 2014, *Bythotrephes.* Data were converted to pelagic macroinvertebrates ha^{-1} to match the density estimates for other species. Nighttime tows occurred at five sampling stations throughout Trout Lake, though we restricted depths to three sampling stations ranging between 20 – 32 m. Night sampling was performed to provide the best estimate of macroinvertebrates that

perform diel vertical migration (Nero & Davies, 1982; Voss & Mumm, 1999; Doubek, Goldfarb & Stockwell, 2020). Density was averaged among sampling stations, and the standard error was propagated between depths. *Bythotrephes* appeared in Trout Lake in 2014; however, the pelagic macroinvertebrate samples were collected prior to *Bythotrephes* invasion thus they only appear in the time series beginning in 2015. Biomass density was estimated using length measurements to the nearest 0.1 mm using a Leica MZ8 stereomicroscope and applied to taxa-specific length-mass regressions and density estimates to calculate biomass density (g ha^{-1}) for each taxon (Dumont, Van de Velde & Dumont, 1975; Dumont & Balvay, 1979; Sell, 1982; Branstrator, 2005) (supplemental information).

Zooplankton were sampled fortnightly during the ice-free season at Trout Lake's maximum depth (35.7 m) (Magnuson, Carpenter & Stanley, 2022c), though we only used samples taken between July and August to match the sampling time of pelagic macroinvertebrates and fish biomass. Zooplankton were sampled via a single tow 1-m above the bottom using a Wisconsin net (80 μm) in addition to a 2-m long Schindler trap (53 µm) sampled at multiple depths. Data were hypsometrically pooled over the entire water column and counted for copepods, cladocerans, and rotifers which were summed over sex and stage to attain a lake wide density estimate (zooplankton L^{-1}). Multiple samples within a given year were averaged (± standard error) to obtain a single estimate of zooplankton biomass per year based on density estimates and length-mass regressions from the literature and NTL-LTER lakes (Kratz, Montz & Frost, 2022). Finally, we converted zooplankton biomass to cubic meters and multiplied the value by the depth of the water column (35. 7 m) to get a biomass density estimate akin to our estimates for fish and pelagic macroinvertebrates biomass (g ha^{-1}). We grouped zooplankton species into three groups for later analyses: Cladocera, Copepoda, and Rotifera.

Food Web Interaction Matrices

We generated two interaction matrices to specify trophic links between species in the Trout Lake pelagic food web (Figure 1). First, we created a binary interaction matrix (Figure 1, Table S2) that stated whether two species are likely to interact within a food web with the assumption that predators will feed the most on prey that is the most readily available in terms of biomass density (Gauzens *et al.*, 2019). A binary interaction matrix may under- or over-estimate the energetic flux between taxa as species prey preference is influential in determining food web dynamics (Post, Conners & Goldberg, 2000). Thus, we also created a preference matrix (Figure 1, Table S3) where interactions were weighted by estimated contributions to a predators diet. Preferences were based on stable isotope studies and diet data from similar north-temperate lakes in addition to recommendations from managers and fisheries scientists working in Trout Lake. Greater detail on the decisions made for trophic links and prey preferences are provided in the supplement.

Energy Flux and Food Web Stability

To assess the distribution and magnitude of energy flux over time we used a bioenergetics approach to quantify the flux of energy between species (Barnes *et al.*, 2018; Gauzens *et al.*, 2019; Jochum *et al.*, 2021). In addition to biomass density, average body mass, and trophic interactions, it is also necessary to quantify metabolic demand, losses to predators via consumption, and assimilation efficiency (Moore & de Ruiter, 2012). To do so, we used the R package, *fluxweb*, that relies on the metabolic theory of ecology to quantify energy flux between species (Brown, 2004; Gauzens *et al.*, 2019). Calculation of energy flux, and calculation of inputs for metabolic losses (Brown, 2004), assimilation efficiencies (Lang *et al.*, 2017), and average body mass per year are available in the supplementary information (Supplementary

Information). Briefly, the model quantifies energy flux from the top-down where a species loss to predation and metabolism are balanced by the energy gained from its prey which are then multiplied by a prey's assimilation efficiency (Lang *et al.*, 2017; Jochum *et al.*, 2021). Thus, energy flux is quantified by calculating the sum of ingoing fluxes for each species to account for all losses, either by consumption or physiological loss, then individual fluxes for pair-wise predatory-prey interactions are calculated based on predator preferences and resource availability (Gauzens *et al.,* 2019). For Trout Lake, lake trout and walleye are the apex predators and zooplankton were the lowest trophic level considered. Average body mass and areal biomass density estimates of phytoplankton are not available for Trout Lake, however, given the model takes a top-down approach, this does not distort the energy flux estimates within the food web. Thus, we calculated energy flux for five major energy fluxes in the Trout Lake pelagic food web: (1) cisco → lake trout/walleye flux, (2) pelagic macroinvertebrates → lake trout/cisco flux, (3) zooplankton → cisco/pelagic macroinvertebrates flux, (4) zooplankton → cisco/pelagic macroinvertebrates/*Bythotrephes* flux, and (5) *Bythotrephes* → cisco flux which has been recently reported as a potentially significant interaction (Martin *et al.*, 2023).

To quantify the dynamics of food web stability over time we again used a bioenergetics approach using the R package, *fluxweb*, to calculate food web stability under a steady state assumption following the framework presented in Moore & De Ruiter (2012). Briefly, the model takes the estimates of energy flux from each food web and generates Jacobian matrices (J_{ij}) where J_{ij} relates the effect that species *j* has on species *i*. The model also requires growth rates for the lowest trophic level considered in the food web, in this instance, zooplankton. Growth rates were estimated using a standard allometric equation (Brown, 2004) based on species' body mass as recommended by Gauzens *et al.* (2019). The model then considers a food web stable only

when the real parts of eigenvalues from the Jacobian matrix are all negative (Neutel, Heesterbeek & de Ruiter, 2002; Neutel *et al.*, 2007). In this case, the stability metric (*s*) is the absolute value of the real part of the largest eigenvalue with a smaller value of *s* indicating that a food web is more stable, and negative values representing the food web is within a stable state (Moore & de Ruiter, 2012). Stability, here, is an inference of the likelihood of food web interactions to persist over time and in the face of external and internal perturbations. It is important to note, however, that this definition of stability simply implies that a food web with a low value of *s* is more stable than higher values of *s* (Neutel *et al.*, 2002; Sauve *et al.*, 2016), and decreased stability infers there is a higher chance that the food web is more vulnerable to change over time. Detailed equations and a description of how model estimates were selected or calculated to estimate food web stability are discussed in the supplement (Supplementary Information).

We assessed temporal dynamics in comparison to the framework presented by Martin et al., (2022) where Trout Lake had three periods of distinct food web structures. First, from 2001 – 2006 the food web was dominated by cisco biomass, then, in 2007, lake trout and walleye increased in relative abundance within the pelagic food web, and finally, *Bythotrephes* appeared in 2014. We also performed sensitivity analyses as described in Gauzens et al. (2019) to assess whether uncertainty in the parameter estimates (e.g., assimilation efficiency, metabolic losses, species' prey preferences) led to large deviations in the estimation of energy flux and food web stability. Parameter values were increased in steps of 0.01 from 0 to 0.12 for 50 replicates each to quantify the mean standard deviation of an estimate's departure from its original value (e.g., coefficient of variation, *cv*). If a parameter's *cv* increases swiftly as the parameter moves further away from its original value, then the energy flux estimate is significantly affected by the input parameters and may not be robust to measurement uncertainty. Whereas, if a parameter's *cv*

increases slowly, or not at all, then the estimates of energy flux or food web stability are robust. All analyses were conducting using the statistical software R (R Core Team, 2022) using the *tidyverse* (Wickham *et al.*, 2019)*, lubridate* (Grolemund & Wickham, 2011)*,* and *fluxweb* (Gauzens *et al.*, 2019) packages.

RESULTS

Trout Lake pelagic food web biomass dynamics

The dynamics and distribution of species biomass varied between the three periods (2001 – 2006; 2007 – 2014, after an increase in lake trout abundance from 2015 – 2019, following *Bythotrephes* invasion) in Trout Lake. From 2001 – 2006, cisco biomass (kilograms per hectare, kg ha^{-1}) was relatively steady (81.98 ± 18.71, mean ± standard deviation (s.d.)), with a peak in 2004 (Figure 2A). *Mysis* biomass (milligrams per square meters, mg m^{-2}) dominated the pelagic macroinvertebrate community across all three food web periods, whereas *Chaoborus* and *Leptodora* biomass (mg m^{-2}) diverged in 2005 and 2006 (Figure 2B). The zooplankton community followed a cyclical pattern increasing then decreasing year-to-year, roughly opposite of the cisco biomass dynamics (Figure 2). Zooplankton community biomass (mg m^{-2}) was dominated by Copepoda and Cladocera, with Rotifera biomass an order of magnitude lower but following similar annual dynamics (Figure 2C).

From 2007 – 2014, lake trout and walleye were detected by hydroacoustic surveys for the first time, altering fish community dynamics with lake trout dominating initially before gradually decreasing across the period (Figure 1A). The pelagic-adjusted estimate of walleye biomass (kg ha^{-1}) was lower than cisco and lake trout biomass (kg ha^{-1}) throughout the period were relatively steady (2.70 ± 1.54, mean ± s.d.). The only exception was 2011 when both apex predators increased (walleye by 152% and lake trout by 30%), co-occurring with a 72 % decrease in cisco

biomass. *Mysis, Chaoborus,* and *Leptodora* biomass remained relatively steady from 2007 – 2012 (Figure 2B). However, *Chaoborus* decreased by 92% from 2012 - 2014 concurrent with a 169% increase in *Leptodora* biomass over the same period. Like 2001 – 2006, zooplankton biomass dynamics were largely steady with major changes corresponding to cisco biomass dynamics. For example, a 66 ± 3% (mean ± s.d.) decrease in total zooplankton biomass was concurrent with a 201% increase in cisco biomass in 2012 from the previous year. In addition, zooplankton community biomass corresponded to the increase of *Leptodora* biomass in 2013 and 2014 (Figure 2C). Cladocera biomass decreased by 74% in 2014 and Rotifera biomass increased by 647% in 2013 and remained elevated. Meanwhile, Copepoda biomass remained relatively steady.

From 2015 – 2019, when *Bythotrophes* established within the lake, there was a slight decrease in cisco biomass (32%) and a substantial decrease in the pelagic-adjusted estimate of walleye biomass from 2013 to 2015 (87%). Although walleye biomass did return to previously estimated biomass densities (2007 – 2014) in 2017 and 2018, cisco continued to gradually decline. Lake trout also continued to gradually decline and were only detected by hydroacoustic surveys every other year starting in 2015 (Figure 1A). *Bythotrephes* biomass gradually increased following 2015, peaking in 2017 (14 ± 2 mg m^{-2}, estimate ± standard error), then gradually decreasing until the end of the record. *Bythotrephes* introduction also coincided with an overall drop in *Chaoborus* and *Leptodora* biomass from 2015 – 2019 in comparison to previous periods. We observed the greatest decrease in *Leptodora* biomass which dropped by 100% in 2015. Both *Chaoborus* and *Leptodora* increased following 2014, though both species' biomass remained lower in comparison to previous periods. Zooplankton biomass did not vary as much as other trophic levels. Rotifera remained elevated, continuing the trend that began in 2013, and

Copepoda biomass remained relatively steady. Cladocera biomass dynamics continued their decreasing trend began in 2013 and remained lower than Copepoda biomass before once again closely following Copepoda biomass dynamics (Figure 2C)

Distribution and dynamics of energy flux

Total energy flux ranged between 26,090,066 – 147,721,122 **(**binary interaction matrix) or 25,969,561– 141,745,640 kilojoules per hectare per day (preference interaction matrix) across the three periods (Figure 3). Across the first two periods (2001 – 2014), total energy flux followed a relatively consistent pattern: decreasing for two – three years before increasing again. Within these cycles, total energy flux peaked in 2001, 2004, 2007, 2010, 2014, and 2016, with the highest total energy flux estimated in 2004. Apart from 2004, total energy flux dynamics remained relatively steady across all three periods. However, the two estimates of energy flux in 2018 and 2019 were the lowest recorded for the entire time-series following the peak in *Bythotrephes* biomass reported above. Energy flux estimates derived from the binary interaction matrix were similar to estimates derived from the preference interaction matrix; however, the binary interaction matrix tended to produce slightly higher estimates of total energy flux.

The distribution of energy fluxes within the Trout Lake food web substantially varied along with their dynamics across the three periods (Figure 4). Qualitative dynamics of energy flux were largely consistent between estimates derived from either the binary interaction matrix (Figure 4A) or preference interaction matrix (Figure 4B). However, for the estimates derived from the preference interaction matrix, the flux from pelagic macroinvertebrates → lake trout/cisco was 93 ± 1% (mean ± s.d.) lower than the binary matrix estimates. Regardless of interaction matrix, the largest energy flux was, by far, the flux from zooplankton → cisco/pelagic macroinvertebrates which remained relatively invariant over the first two time periods (2001 –

2015). This trend continued for the third food web period with the flux from zooplankton → cisco/pelagic macroinvertebrates/*Bythotrephes* remaining the highest flux, although the flux gradually decreased from 2016 – 2019. The flux from cisco → lake trout/walleye was relatively steady, however, following *Bythotrephes* introduction the flux decreased by 33% (binary matrix) or 32% (preference matrix), and remained lower than previous periods**.** As noted above, the flux from pelagic macroinvertebrates → lake trout/cisco was lower for estimates derived from the preference interaction matrix, but the temporal dynamics were consistent. The flux was cyclical from 2001 – 2007, increasing over three years, then decreasing over three years. Beginning in the second food web period, the flux from pelagic macroinvertebrates → lake trout/cisco increased slightly and remained relatively invariant before gradually decreasing following the introduction of *Bythotrephes* in the third food web period (2015 – 2019). The flux from *Bythotrephes* → cisco was also lower for estimates derived from the preference matrix, though estimates derived from both interaction matrices showed the flux gradually increase, peaking in 2017, and decreasing thereafter.

Food web stability dynamics

The inferred stability metric, *s*, showed the Trout Lake food web was in an unstable state across all three food web periods, though *s* varied little year-to-year for the first two periods. Stability sharply decreased (higher *s* indicating lower stability) when *Bythotrephes* appeared in 2015 during the third food web period (Figure 5). In 2015, *s* increased by 7757% using the binary interaction matrix (Figure 5A) and by 1970% using the preference interaction matrix (Figure 5B). Temporal dynamics in *s* varied depending on the choice of interaction matrix. The temporal dynamics of *s* were steadier using the preference interaction matrix with subtle

increases and decreases year-to-year, in contrast to estimates using the binary interaction matrix. Using the binary interaction matrix, the stability metric, *s*, increased over three years, dropped, then increased again over three years in the first food web period from 2001 – 2006. Temporal dynamics of *s* were then largely steady using either interaction matrix with *s* decreasing (i.e., higher stability) in 2014 by 89% (binary) or 63% (preference) the year before *Bythotrephes* appeared and stability decreased sharply. Following 2015, *s* gradually increased (i.e., lower stability) from 2016 – 2019 using the binary interaction matrix but remained consistent over the same period using the preference interaction matrix.

All sensitivity analyses demonstrated our model estimates, and the qualitative temporal dynamics, were robust to variation in input parameters. Increasing variability in our model inputs for energy flux produced minimal departures from our original estimates ($cv < 5\%$) (Figure S1 – S4). Similarly, our estimates of metabolic loss and assimilation efficiency used to estimate stability were similarly robust to variation (Supplementary Information). However, increasing the variability for our input of growth rate generated greater departures from our original estimates, but only for some years, and only when using the binary interaction matrix (Supplementary Information; Figure S5 – 6).

DISCUSSION

We sought to analyze how energy flux and food web stability were altered over three periods in a long-term record following known changes in the fish community and the invasion by a mid-trophic level consumer, spiny water flea (*Bythotrephes longimanus*). The three periods followed a previously defined framework (Martin *et al.*, 2022): dominance by cisco from 2001 – 2006, increased abundance of apex fish predators from 2007 – 2014, and the aftermath of

Bythotrephes invasion from 2015 – 2019. While the increased abundance of top fish predators, lake trout (*Salvelinus namaycush*) and walleye (*Sander vitreus*), slightly altered certain pathways of energy flux within the food web, the invasion by *Bythotrephes* affected all energy fluxes within the pelagic food web and substantially decreased food web stability, regardless of which interaction matrix was used. However, we found that food web stability swiftly returned to pre-invasion levels within a year, though total energy flux remained suppressed following the peak in *Bythotrephes* biomass suggesting reduced ecosystem function (Wagg *et al.,* 2014; Barnes *et al.,* 2018).

Energy flux dynamics

Assessing the distribution and dynamics of energy flux within food webs facilitates a greater understanding of how ecosystem function may be altered by major disturbances like species invasion (Odum, 1968; Barnes *et al.*, 2018; Jochum *et al.*, 2021). Changes in energy flux may reflect changes in ecosystem multifunctionality, the support of multiple trophic functions by the food web (Wagg *et al.,* 2014; Barnes *et al.,* 2018). Prior to the *Bythotrephes* invasion, energy flux within Trout Lake was dominated by cisco-zooplankton dynamics (Parks & Rypel, 2018), with the largest energy flux from zooplankton into the planktivores cisco and pelagic macroinvertebrates. The dominance of cisco zooplanktivory is illustrated by the spike in cisco biomass in 2004 corresponding to both the highest estimated total energy flux among years and energy flux into cisco over 19 years. Cisco control over zooplankton community composition and biomass is well-documented in lakes (Rudstam, Lathrop & Carpenter, 1993; Vivian & Frazer, 2021). Though lower in relative biomass, pelagic macroinvertebrates also exert top-down control on zooplankton, particularly *Chaoborus* and *Leptodora* (Moore, Yan & Pawson, 1994; Mcnaught, Kiesling & Ghadouani, 2004). In 2012, there was a substantial drop in *Chaoborus*

biomass corresponding with an increase in *Leptodora* biomass, likely due to a reduction in competitive interactions (Campbell & Knoechel, 1990). This shift likely drove the large increase in Rotifera biomass which are less preferred diet items for zooplankton predators (Browman, Kruse & John O'brien, 1989; Ahrenstorff *et al.*, 2013). Even so, energy flux dynamics remained relatively steady during this period among trophic levels. While mysids can be significant pelagic planktivores in some (Ellis *et al.*, 2011) but not all lakes (Griffin, O'Malley & Stockwell, 2020), there was no evidence of a strong influence of *Mysis* on zooplankton in Trout Lake.

The increase of lake trout and walleye in the pelagic food web beginning in 2007 resulted in top-down control on cisco biomass (Parks & Rypel, 2018), steadying the energy flux from zooplankton and pelagic macroinvertebrates → cisco, and from cisco → lake trout compared to the first period. This shift coincided with a period of greater water clarity and lower algal biomass (Martin *et al.*, 2022), similar to other trophic cascades (Carpenter, Kitchell & Hodgson, 1985; Carpenter *et al.*, 2001; Pace *et al.*, 1999). The increase in lake trout abundance was potentially related to stocking events which increased a few years prior to 2007 (Martin *et al.*, 2022). The greater abundance of walleye in the pelagic zone during this period may have been influenced by changes in littoral habitat and littoral prey availability due to the peak in rusty crayfish (*Faxonius rusticus*) abundance, a littoral invasive species also present in the lake (Wilson *et al.*, 2004; Willis & Magnuson, 2006; Roth *et al.*, 2007). While walleye were most likely preying on cisco in the pelagic (Herwig *et al.*, 2022), it is unlikely they drove cisco dynamics given the presence of lake trout (Parks & Rypel, 2018). However, in 2011, walleye biomass substantially increased in comparison to the previous year along with a slight increase in trout biomass, corresponding to a substantial drop in cisco biomass. (Bronte *et al.*, 1998; Nicolle *et al.*, 2011). Our estimates of fish biomass were based on the average size of a species derived

from target strength data which may have masked important differences in diet and predation pressure driven by ontogenetic changes in fish species (Galarowicz, Adams & Wahl, 2006; Zimmerman *et al.*, 2009). Further, fish diets are not static and can vary seasonally (Liao, Pierce & Larscheid, 2002), and our focus on general preferences may over- or underestimate the weight of prey preference for fishes. However, we still observed clear shifts in prey biomass dynamics in response to fish biomass dynamics suggesting we were able to capture general predator-prey interactions within the food web (Perkins *et al.*, 2022). In addition, our sensitivity analyses indicated our estimates were robust to variation in our inputs for prey preference across all years.

With the introduction of *Bythotrephes* in Trout Lake, there were substantial changes in the distribution and magnitude of energy flux of the whole food web from 2015-2019. The two lowest years of total energy flux estimates occurred in the two years following peak *Bythotrephes* biomass suggesting overall ecosystem function was lowered (Barnes *et al.,* 2018; Manning *et al.,* 2018). *Leptodora* biomass substantially dropped following the invasion, consistent with other records of *Bythotrephes* invasions (Branstrator, 1995, 2005; Weisz & Yan, 2011). There was also lower overall *Chaoborus* and *Mysis* biomass during the third food web period, which is consistent with previous *Bythotrephes* invasion (Foster & Sprules, 2010). The presence of pelagic macroinvertebrates and cisco can cause a behavioral response in *Bythotrephes* restricting their habitat to the epilimnion and reducing their ability to target preferred prey items such as *Daphnia* (Young & Yan, 2008; Jokela, Arnott & Beisner, 2011). This may explain why *Chaoborus* biomass increased following *Bythotrephes* invasion as their diet breadth is less narrow than *Bythotrephes* (Boudreau & Yan, 2003; Strecker *et al.*, 2006), and they may have taken advantage of the greater availability of Rotifera biomass (Pastorok, 1980; Moore *et al.*,

1994). Despite this, *Chaoborus* biomass was still reduced in comparison to the previous two food web periods (2001 – 2014).

Bythotrephes invasion also potentially influenced fish biomass dynamics within Trout Lake through competitive interactions with cisco (Walsh, Lathrop & Vander Zanden, 2017). While the initial increase in cisco biomass in 2016 was likely related to the decline in lake trout and walleye biomass (Parks & Rypel, 2018; Herwig *et al.*, 2022), cisco biomass declined for the remainder of the third period (Walsh *et al.*, 2017) which drove the decline in energy flux from zooplankton → cisco, and in turn, total energy flux. The flux from cisco to lake trout and walleye also decreased, particularly in 2018, though both lake trout and walleye were sporadically detected by hydroacoustic surveys and had been on a declining trend since they first appeared in 2007. While all energy fluxes among trophic levels shifted in their temporal dynamics following the introduction of *Bythotrephes,* the major changes in biomass dynamics lasted only until 2017 when *Bythotrephes* began to decline which may be attributable to cisco predation (Martin *et al.*, 2022, 2023). Recent work in Trout Lake demonstrated that in the early invasion period *Bythotrephes* biomass production outpaced cisco consumption, but that flipped in 2017 such that cisco consumption was greater than *Bythotrephes* biomass production indicating cisco were controlling *Bythotrephes* populations (Martin *et al.*, 2023). This finding is also supported by the biomass dynamics of pelagic macroinvertebrates and zooplankton which either began to return to pre-invasion levels or completely recovered as in the case of Cladocera. While *Bythotrephes* had a substantial effect on energy flux dynamics as *Bythotrephes* biomass increased, as *Bythotrephes* influenced species biomass and interaction strength both above and below the middle trophic levels (Flood *et al.*, 2020), there was no clear evidence of substantial or permanent shifts in food web structure. Our analysis provided a broad overview of the Trout Lake food web based on

average species biomass per year and inferred interactions. Future investigations would be improved by using refined estimates of fish size and age structure (Galarowicz *et al.*, 2006; Zimmerman *et al.*, 2009), empirical estimates of predator-prey interactions based on interaction probability and system-specific diet data (Poisot, Stouffer & Gravel, 2015; Pomeranz *et al.*, 2018), and estimates of metabolic loss and assimilation efficiency derived from species- and system-specific measurements (Gauzens *et al.*, 2019).

Food web stability dynamics

The inferred stability metric, *s*, indicated that the Trout Lake food web was in an unstable state across all three periods. This implies the food web was less likely to persist through time and recover slowly from perturbations (Morin & Lawler, 1995; Neutel *et al.*, 2002). However, the system may be stabilized by processes that we did not measure here. Indeed, stability analyses using Jacobian matrices, however, often find real food webs to be unstable (Moore & de Ruiter, 2012). This is due to ecosystem properties not well captured in steady state analyses of network stability which can drive the persistence of 'unstable' food webs (McCann, 2000). For example, incorporating the oscillation of interactions through time (McCann *et al.*, 1998; McCann, 2000; Neutel *et al.*, 2002), allometric scaling (Quévreux & Brose, 2019), and adaptive foraging (Kondoh, 2003) improve estimates of food web stability. Though Trout Lake was within an unstable state, we still a sharp decline in stability once *Bythotrephes* invaded, suggesting the invasion of a mid-trophic level consumer can affect food web stability. Food web stability was mostly invariant to whether only cisco were dominant within the food web (2001 – 2006) or when lake trout and walleye became more abundant (2007 – 2014) suggesting changes in native

predator-prey population cycles did not affect food web stability (Vandermeer, 2006; Kadoya, Gellner & McCann, 2018).

When *Bythotrephes* appeared in 2015, there was an extreme decrease in food web stability (i.e., higher *s*) which was likely driven by decreases in zooplankton and zooplankton predator (e.g., cisco, pelagic macroinvertebrate) biomass in 2015, and the introduction of an additional strong interaction within the food web. Invasive species can have profound effects on energy flow within food webs through competitive exclusion and strengthening consumer-resource interactions through predation on novel prey (Vander Zanden *et al.*, 1999; McCann, 2000), both of which decrease network stability (McCann, 2000; Wootton & Stouffer, 2015; Gellner & McCann, 2016). The substantial decrease in food web stability concurrent with *Bythotrephes* introduction, and decreasing trend in energy flux, suggest these dynamics likely drove the decreased food web stability of Trout Lake in 2015. However, food web stability swiftly returned to pre-invasion levels, potentially indicating that the Trout Lake food web was able to rapidly 'absorb' the shock of *Bythotrephes* interactions within the network.

Food web stability dynamics may be a useful indicator of the effects of species invasion on food webs, particularly for mid-trophic level invaders which have less consistent ecosystem effects compared to higher trophic level invaders (Flood *et al.*, 2020; Bradley *et al.*, 2023). Food web stability returned to pre-invasion levels within one year, suggesting investigating food web stability dynamics may be beneficial even with only a few years of data. In Trout Lake, the swift return to pre-invasion food web stability, before the observed recovery of species negatively affected by *Bythotrephes,* was likely driven by cisco regulation of *Bythotrephes* biomass (Martin *et al.*, 2023). Successful *Bythotrephes* biomass control by native consumers has been documented in other ecosystems as well (Branstrator, 2005; Keeler *et al.*, 2015), though long-

term effects are unclear. Boom-bust dynamics in invasive species are common (Strayer *et al.*, 2019; Szydlowski *et al.*, 2023), and inferring long-term trajectories is difficult (Strayer *et al.*, 2017). The *Bythotrephes* invasion is relatively recent in Trout Lake (<10 years; Strayer et al., 2017), thus whether food web stability will remain relatively steady, remains uncertain.

Conclusions

Flux-based approaches are a powerful tool to assess subtle changes in food web structure over time and provide a way to understand the effects of invasive species in that focuses on ecosystem function (David *et al.*, 2017; Flood *et al.*, 2020). The long-term, multi-trophic food web record of Trout Lake provided a rare opportunity to assess the dynamics of energy flux and food web stability over 19 years. Here, we demonstrate how changes in food web structure related to changes in ecosystem function using a flux-based approach (Gauzens *et al.*, 2019; Jochum *et al.*, 2021). Further, we showed that mid-trophic level consumers can decrease the overall magnitude of energy flux within aquatic food webs and alter energy flux dynamics in both higher and lower trophic levels, while also being influenced by native consumers (i.e., cisco). In addition, we provide an ecological context to long-term changes in food web stability, showing that stability following an invasion may decrease substantially and then quickly rebound as the network absorbs the shock of a species invasion. To our knowledge this is one of the first analyses to assess food web stability through time pre- and post-species invasion using a long-term food web record. While it remains uncertain what the longer-term effects of *Bythotrephes* invasion will be in Trout Lake, continued use of energy flux-based approaches will be useful for understanding and potentially predicting the changing trajectory of ecosystem structure and function in the face of continuing global change.

ACKNOWLEDGEMENTS

We would like to thank the scientists of the North Temperate Lakes – Long-Term Ecological Research (NTL-LTER) program for the collection and availability of the data, along with the University of Wisconsin-Madison Zoological Museum for access to preserved samples. The walleye silhouette in Fig. 1 was illustrated by the NOAA Great Lakes Environmental Research Laboratory with silhouette by Timothy Bartley (CC BY-SA 3.0). This work was funded by the National Science Foundation (DEB-2025982) and the National Science Foundation Graduate Research Fellowship Program (DGE-1747503). Any opinions, findings and conclusions or recommendations expressed in this material are those of the authors and do not necessarily reflect the views of the National Science Foundation.

REFERENCES

Ahrenstorff T.D., Hrabik T.R., Jacobson P.C. & Pereira D.L. (2013). Food resource effects on diel movements and body size of cisco in north-temperate lakes. *Oecologia* **173**, 1309–1320. https://doi.org/10.1007/s00442-013-2719-3

Barnes A.D., Jochum M., Lefcheck J.S., Eisenhauer N., Scherber C., O'Connor M.I., *et al.* (2018). Energy Flux: The Link between Multitrophic Biodiversity and Ecosystem Functioning. *Trends in Ecology and Evolution* **33**, 186–197. https://doi.org/10.1016/j.tree.2017.12.007

Barnes A.D., Scherber C., Brose U., Borer E.T., Ebeling A., Gauzens B., *et al.* (2020). *Biodiversity enhances the multitrophic control of arthropod herbivory*.

Bartley T.J., McCann K.S., Bieg C., Cazelles K., Granados M., Guzzo M.M., *et al.* (2019). Food web rewiring in a changing world. *Nature Ecology and Evolution* **3**, 345–354. https://doi.org/10.1038/s41559-018-0772-3

Bobeldyk A.M. & Lamberti G.A. (2008). A Decade after Invasion : Evaluating the Continuing Effects of Rusty Crayfish on a Michigan River. *Journal of Great Lakes Research* **34**, 265–275. https://doi.org/10.3394/0380-1330(2008)34

Boit A. & Gaedke U. (2014). Benchmarking successional progress in a quantitative food web. *PLoS ONE* **9**. https://doi.org/10.1371/journal.pone.0090404

Boudreau S.A. & Yan N.D. (2003). The differing crustacean zooplankton communities of Canadian Shield lakes with and without the nonindigenous zooplanktivore Bythotrephes longimanus. *Canadian Journal of Fisheries and Aquatic Sciences* **60**, 1307–1313. https://doi.org/10.1139/f03-111

Bradley B.A., Laginhas B.B., Whitlock R., Allen J.M., Bates A.E., Bernatchez G., *et al.* (2019). Disentangling the abundance-impact relationship for invasive species. https://doi.org/10.5281/zenodo.2605254

Bradley B.A., Laginhas B.B., Whitlock R., Allen J.M., Bates A.E., Bernatchez G., *et al.* (2023). Disentangling the abundance-impact relationship for invasive species. *Proceedings of the National Academy of Sciences* **116**, 9919–9924. https://doi.org/10.5281/zenodo.2605254

Branstrator D. (1995). Ecological interactions between Bythotrephes cederstroemi and Leptodora kindtii and the Implications for Species Replacement in Lake Michigan. *Journal of Great Lakes Research* **21**, 670–679

Branstrator D.K. (2005). Contrasting life histories of the predatory cladocerans Leptodora kindtii and Bythotrephes longimanus. *Journal of Plankton Research* **27**, 569–585. https://doi.org/10.1093/plankt/fbi033

Browman H.I., Kruse S. & John O'brien W. (1989). *Foraging behavior of the predaceous cladoceran, Leptodora kindti, and escape responses of their prey*.

Brown J.H. (2004). Toward a Metabolic Theory of Ecology. *Ecology* **85**, 1771–1789. https://doi.org/10.1890/03-9000

Brown M.E., Branstrator D.K. & Shannon L.J. (2012). Population regulation of the spiny water flea (Bythotrephes longimanus) in a reservoir: Implications for invasion. *Limnology and Oceanography* **57**, 251–271. https://doi.org/10.4319/lo.2012.57.1.0251

Campbell C.E. & Knoechel R. (1990). Distribution patterns of vertebrate and invertebrate planktivores in Newfoundland lakes with evidence of predator-prey and competitive interactions. *Canadian Journal of Zoology* **68**, 1559–1567

Carpenter S.R., Cole J.J., Hodgson J.R., Kitchell J.F., Pace M.L., Bade D., *et al.* (2001). Trophic cascades, nutrients, and lake productivity: whole lake experiments. *Ecological Monographs* **71**, 163–186

Carpenter S.R., Kitchell J.F. & Hodgson J.R. (1985). Cascading Trophic Interactions and Lake Productivity. *BioScience* **35**, 634–639. https://doi.org/10.2307/1309989

Compton J.A. & Kerfoot W.C. (2004). Colonizing inland lakes: Consequences of YOY fish ingesting the spiny cladoceran (Bythotrephes cederstroemi). In: *Journal of Great Lakes Research*. pp. 315–326. International Association of Great Lakes Research.

Crowder D.W. & Snyder W.E. (2010). Eating their way to the top? Mechanisms underlying the success of invasive insect generalist predators. *Biological Invasions* **12**, 2857–2876. https://doi.org/10.1007/s10530-010-9733-8

David P., Thébault E., Anneville O., Duyck P.-F., Chapuis E. & Loeuille N. (2017). Impacts of Invasive Species on Food Webs : A Review of Empirical Data. *Advances in Ecological Research* **56**, 1–60. https://doi.org/10.1016/bs.aecr.2016.10.001

Doubek J.P., Goldfarb S.K. & Stockwell J.D. (2020). Should we be sampling zooplankton at night? *Limnology And Oceanography Letters* **5**, 313–321

DuFour M.R., Qian S.S., Mayer C.M. & Vandergoot C.S. (2021). Embracing uncertainty to reduce bias in hydroacoustic species apportionment. *Fisheries Research* **233**. https://doi.org/10.1016/j.fishres.2020.105750

Dumont H.J. & Balvay G. (1979). The dry weight estimate of chaoborus flavicans (Meigen) as a function of length and instars. *Hydrobiologia* **64**, 139–145. https://doi.org/10.1007/BF00023189

Dumont H.J., van de Velde I. & Dumont S. (1975). The dry weight estimate of biomass in a selection of Cladocera, Copepoda and Rotifera from the plankton, periphyton and benthos of continental waters. *Oecologia* **19**, 75–97. https://doi.org/10.1007/BF00377592

Ellis B.K., Stanford J.A., Goodman D., Stafford C.P., Gustafson D.L., Beauchamp D.A., *et al.* (2011). Long-term effects of a trophic cascade in a large lake ecosystem. *Proceedings of the National Academy of Sciences of the United States of America* **108**, 1070–1075. https://doi.org/10.1073/pnas.1013006108

Flood P.J., Duran A., Barton M., Mercado-Molina A.E. & Trexler J.C. (2020). Invasion impacts on functions and services of aquatic ecosystems. *Hydrobiologia* **847**, 1571–1586. https://doi.org/10.1007/s10750-020-04211-3

Foster S.E. & Sprules W.G. (2010). Effects of Bythotrephes on the trophic position of native macroinvertebrates. *Canadian Journal of Fisheries and Aquatic Sciences* **67**, 58–69. https://doi.org/10.1139/F09-164

Galarowicz T.L., Adams J.A. & Wahl D.H. (2006). The influence of prey availability on ontogenetic diet shifts of a juvenile piscivore. *Canadian Journal of Fisheries and Aquatic Sciences* **63**, 1722–1733. https://doi.org/10.1139/F06-073

Galiana N., Lurgi M., Montoya J.M. & Bernat C.L. (2014). Invasions cause biodiversity loss and community simplification in vertebrate food webs. *Oikos* **123**, 721–728. https://doi.org/10.1111/j.1600-0706.2013.00859.x

Gauzens B., Barnes A., Giling D.P., Hines J., Jochum M., Lefcheck J.S., *et al.* (2019). fluxweb: An R package to easily estimate energy fluxes in food webs. *Methods in Ecology and Evolution* **10**, 270–279. https://doi.org/10.1111/2041-210X.13109

Gellner G. & McCann K.S. (2016). Consistent role of weak and strong interactions in high- and low-diversity trophic food webs. *Nature Communications* **7**, 1–7. https://doi.org/10.1038/ncomms11180

Griffin J.E., O'Malley B.P. & Stockwell J.D. (2020). The freshwater mysid Mysis diluviana (Audzijonyte & Väinölä, 2005) (Mysida: Mysidae) consumes detritus in the presence of Daphnia (Cladocera: Daphniidae). *Journal of Crustacean Biology* **40**, 520–525. https://doi.org/10.1093/jcbiol/ruaa053

Grolemund G. & Wickham H. (2011). Dates and Times Made Easy with lubridate. *Journal of Statistical Software* **40**, 1–25

Herwig B.R., Zimmer K.D. & Staples D.F. (2022). Using stable isotope data to quantify niche overlap and diets of muskellunge, northern pike and walleye in a deep Minnesota lake. *Ecology of Freshwater Fish* **31**, 60–71. https://doi.org/10.1111/eff.12608

Hulme P.E. (2017). Climate change and biological invasions: evidence, expectations, and response options. *Biological Reviews* **92**, 1297–1313. https://doi.org/10.1111/brv.12282

Jeschke J.M., Bacher S., Blackburn T.M., Dick J.T.A., Essl F., Evans T., *et al.* (2014). Defining the impact of non-native species. *Conservation Biology* **28**, 1188–1194. https://doi.org/10.1111/cobi.12299

Jochum M., Barnes A.D., Brose U., Gauzens B., Sünnemann M., Amyntas A., *et al.* (2021). For flux's sake: General considerations for energy-flux calculations in ecological communities. *Ecology and Evolution* **11**, 12948–12969. https://doi.org/10.1002/ece3.8060

Jokela A., Arnott S.E. & Beisner B.E. (2011). Patterns of Bythotrephes longimanus distribution relative to native macroinvertebrates and zooplankton prey. *Biological Invasions* **13**, 2573–2594. https://doi.org/10.1007/s10530-011-0072-1

Kadoya T., Gellner G. & McCann K.S. (2018). Potential oscillators and keystone modules in food webs. *Ecology Letters* **21**, 1330–1340

Karatayev A.Y., Burlakova L.E. & Padilla D.K. (2015). Zebra versus quagga mussels: a review of their spread, population dynamics, and ecosystem impacts. *Hydrobiologia* **746**, 97–112

Kaufman S.D., Morgan G.E. & Gunn J.M. (2009). The Role of Ciscoes as Prey in the Trophy Growth Potential of Walleyes. *North American Journal of Fisheries Management* **29**, 468–477. https://doi.org/10.1577/m07-117.1

Keeler K.M., Bunnell D.B., Diana J.S., Adams J. V., Mychek-Londer J.G., Warner D.M., *et al.* (2015). Evaluating the importance of abiotic and biotic drivers on Bythotrephes biomass in Lakes Superior and Michigan. *Journal of Great Lakes Research* **41**, 150–160. https://doi.org/10.1016/j.jglr.2015.07.010

Kimbro D.L., Grosholz E.D., Baukus A.J., Nesbitt N.J., Travis N.M., Attoe S., *et al.* (2009). Invasive species cause large-scale loss of native California oyster habitat by disrupting trophic cascades. *Oecologia* **160**, 563–575. https://doi.org/10.1007/s00442-009-1322-0

Kondoh M. (2003). Foraging Adaptation and the Relationship Between Food-Web Complexity and Stability. *Science* **299**, 1388–1391

Kortsch S., Frelat R., Pecuchet L., Olivier P., Putnis I., Bonsdorff E., *et al.* (2021). Disentangling temporal food web dynamics facilitates understanding of ecosystem functioning. *Journal of Animal Ecology*, 633. https://doi.org/10.1111/1365-2656.13447

Kratz T., Montz P. & Frost T. (2022). North Temperate Lakes LTER Zooplankton conversion formulas length to biomass ver 2.

Lang B., Ehnes R.B., Brose U. & Rall B.C. (2017). Temperature and consumer type dependencies of energy flows in natural communities. *Oikos* **126**, 1717–1725. https://doi.org/10.1111/oik.04419

Lawson Z.J., Vander Zanden M.J., Smith C.A., Heald E., Hrabik T.R. & Carpenter S.R. (2015). Experimental mixing of a north-temperate lake: Testing the thermal limits of a cold-water invasive fish. *Canadian Journal of Fisheries and Aquatic Sciences* **72**, 926–937. https://doi.org/10.1139/cjfas-2014-0346

Liao H., Pierce C.L. & Larscheid, J.G. (2002). Diet dynamics of the adult piscivorous fish community in Spirit Lake, Iowa, USA 1995–1997. *Ecology of Freshwater Fish* **11,** 178–189

Lindeman R.L. (1942). The Trophic-Dynamic Aspect of Ecology. *Ecology* **23**, 399–417

Love R. (1971). Measurements of Fish Target Strength: A Review. *Fishery Bulletin* **63**, 703–715

Magnuson J., Carpenter S. & Stanley E. (2023a). North Temperate Lakes: US Long-Term Ecological Research Network

Magnuson J.J., Carpenter S.R. & Stanley E.H. (2022a). North Temperate Lakes LTER: Fish Lengths and Weights 1981 - current ver 34. *Environmental Data Initiative.* https://doi.org/10.6073/pasta/968299a53784f9649eb67f421cc33340.

Magnuson J.J., Carpenter S.R. & Stanley E.H. (2022b). North Temperate Lakes LTER: Pelagic Macroinvertebrate Summary 1983 - current ver 34. *Environmental Data Initiative.* https://doi.org/10.6073/pasta/ac6386b0583a2a6838c4f8bf5350d054.

Magnuson J.S., Carpenter S. & Stanley E. (2023b). North Temperate Lakes LTER: Pelagic Prey - Sonar Data 2001 - current ver 33. *Environmental Data Initiative.* https://doi.org/10.6073/pasta/5eacf039425717bc9bc766962489e184.

Magnuson J.S., Carpenter S. & Stanley E. (2022c). North Temperate Lakes LTER: Zooplankton - Trout Lake Area 1982 - current ver 37. *Environmental Data Initiative.* https://doi.org/10.6073/pasta/aba16e9867e8f7b41b08dae0e92d6a98.

Manning P., van der Plas, F., Soliveres, S., Allan, E., Maestre, F.T., Mace, G., Whittingham, M.J. & Fischer, M. (2018). Redefining ecosystem multifunctionality. *Nature Ecology & Evolution* **2,** 427–436.

Martin B.E., Mrnak J.T. & Vander Zanden M.J. (2023). Evaluating the potential role of predation by native fish regulating the abundance of invasive spiny water flea. *Journal of Freshwater Ecology* **38**. https://doi.org/10.1080/02705060.2023.2187470

Martin B.E., Walsh J.R. & Vander Zanden M.J. (2022). Rise of a native apex predator and an invasive zooplankton cause successive ecological regime shifts in a North Temperate Lake. *Limnology and Oceanography* **67**, S163–S172. https://doi.org/10.1002/lno.12049

May R.M. (1972). Will a Large Complex System be Stable? *Nature* **238**, 413–414

McCann K., Hastings A. & Huxel G. (1998). Weak trophic interactions and the balance of nature. *Nature* **395**, 794–798. https://doi.org/10.1038/27427

McCann K.S. (2000). The diversity–stability debate. *Nature* **405**, 228–233

Mcnaught A.S., Kiesling R.L. & Ghadouani A. (2004). *Changes to zooplankton community structure following colonization of a small lake by Leptodora kindti*.

Moore J., De Ruiter P., McCann K. & Wolters V. eds (2018). *Adaptive Food Webs: Stability and Transitions of Real and Model Ecosystems*. Cambridge University Press, Cambridge.

Moore J.C. & de Ruiter P.C. (2012). *Energetic Food Webs: An Analysis of Real and Model Ecosystems*. Oxford University Press , Oxford, UK .

Moore M. V, Yan N.D. & Pawson T. (1994). Omnivory of the larval phantom midge (Chaoborus spp.) and its potential significance for freshwater planktonic food webs. *Canadian Journal of Zoology* **72**, 2055–2065

Morin P.J. & Lawler S.P. (1995). Food Web Architecture and Population Dynamics: Theory and Empirical Evidence. *Annual Review of Ecology and Systematics* **26**, 505–529

Mrnak J.T., Sikora L.W., Jake Vander Zanden M., Hrabik T.R. & Sass G.G. (2021). Hydroacoustic Surveys Underestimate Yellow Perch Population Abundance: The Importance of Considering Habitat Use. *North American Journal of Fisheries Management* **41**, 1079–1087. https://doi.org/10.1002/nafm.10605

Nero R.W. & Davies I.J. (1982). Comparison of Two Sampling Methods for Estimating the Abundance and Distribution of Mysis relicta. *Canadian Journal of Fisheries and Aquatic Sciences* **39**, 349–355

Neutel A., Heesterbeek J.A.P. & de Ruiter P. (2002). Stability in Real Food Webs: Weak Links in Long Loops. *Science* **296**, 1120–1124. https://doi.org/10.1126/science.1068326

Neutel A.M., Heesterbeek J.A.P., Van De Koppel J., Hoenderboom G., Vos A., Kaldeway C., *et al.* (2007). Reconciling complexity with stability in naturally assembling food webs. *Nature* **449**, 599–602. https://doi.org/10.1038/nature06154

Neutel A.-M. & Thorne M.A.S. (2014). Interaction strengths in balanced carbon cycles and the absence of a relation between ecosystem complexity and stability. *Ecology Letters* **17**, 651–661. https://doi.org/10.1111/ele.12266

Odum E.P. (1968). Energy Flow in Ecosystems: A Historical Review. *American Zoologist* **8**, 11–18

Olivier P., Frelat R., Bonsdorff E., Kortsch S., Kröncke I., Möllmann C., *et al.* (2019). Exploring the temporal variability of a food web using long-term biomonitoring data. *Ecography* **42**, 2107–2121. https://doi.org/10.1111/ecog.04461

Pace M.L., Cole J.J., Carpenter S.R. & Kitchell J.F. (1999). Trophic cascades revealed in diverse ecosystems. *Trends in Ecology and Evolution* **14**, 483–488. https://doi.org/10.1016/S0169-5347(99)01723-1

Parker-Stetter S.L., Rudstam G., Sullivan P.J. & Warner D.M. (2009). *Standard operating procedures for fisheries acoustic surveys in the Great Lakes*. Ann Arbor, MI.

Parks T.P. & Rypel A.L. (2018). Predator–prey dynamics mediate long-term production trends of cisco (Coregonus artedi) in a northern Wisconsin lake. *Canadian Journal of Fisheries and Aquatic Sciences* **75**, 1969–1976. https://doi.org/10.1139/cjfas-2017-0302

Pastorok R.A. (1980). The effects of predator hunger and food abundance on prey selection by Chaoborus larvae. *Limnology and Oceanography* **25**, 910–921. https://doi.org/10.4319/lo.1980.25.5.0910

Pejchar L. & Mooney H.A. (2009). Invasive species, ecosystem services and human well-being. *Trends in Ecology and Evolution* **24**, 497–504

Perkins D.M., Hatton I.A., Gauzens B., Barnes A.D., Ott D., Rosenbaum B., *et al.* (2022). Consistent predator-prey biomass scaling in complex food webs. *Nature Communications* **13**. https://doi.org/10.1038/s41467-022-32578-5

Pimm S., Lawton J. & Cohen J. (1991). Food web patterns and their consequences. *Nature* **350**, 669–674

Poisot T., Stouffer D.B. & Gravel D. (2015). Beyond species: Why ecological interaction networks vary through space and time. *Oikos* **124**, 243–251. https://doi.org/10.1111/oik.01719

Pomeranz J.P.F., Thompson R.M., Poisot T. & Harding J.S. (2018). Inferring predator-prey interactions in food webs. *Methods in Ecology and Evolution* **1**, 1–34

Post D.M., Conners M.E. & Goldberg D.S. (2000). Prey preference by a top predator and the stability of linked food chains. *Ecology* **81**, 8–14. https://doi.org/10.1890/0012-9658(2000)081[0008:PPBATP]2.0.CO;2

Quévreux P. & Brose U. (2019). Metabolic adjustment enhances food web stability. *Oikos* **128**, 54–63. https://doi.org/10.1111/oik.05422

R Core Team (2022). R: A language and environment for statistical computing

Rahel F.J. & Olden J.D. (2008). Assessing the effects of climate change on aquatic invasive species. *Conservation Biology* **22**, 521–533

Rennie M.D., Gary Sprules W. & Johnson T.B. (2009). Factors affecting the growth and condition of lake whitefish (Coregonus clupeaformis). *Canadian Journal of Fisheries and Aquatic Sciences* **66**, 2096–2108. https://doi.org/10.1139/F09-139

Roth B.M., Tetzlaff J.C., Alexander M.L. & Kitchell J.F. (2007). Reciprocal relationships between exotic rusty crayfish, macrophytes, and Lepomis species in northern Wisconsin lakes. *Ecosystems* **10**, 74–85. https://doi.org/10.1007/s10021-006-9004-9

Rudstam L.G., Lathrop R.C. & Carpenter S.R. (1993). The rise and fall of a dominant planktivore: direct and indirect effects on zooplankton. *Ecology* **74**, 303–319. https://doi.org/10.2307/1939294

de Ruiter P.C., Neutel A. & Moore J.C. (1995). Energetics, Patterns of Interaction Strengths, and Stability in Real Ecosystems. *Science* **269**, 1257–1260

Sauve A.M.C., Thébault E., Pocock M.J.O. & Fontaine C. (2016). How plants connect pollination and herbivory networks and their contribution to community stability. *Ecology* **97**, 908–917. https://doi.org/10.1890/15-0132.1

Schwarz B., Barnes A.D., Thakur M.P., Brose U., Ciobanu M., Reich P.B., *et al.* (2017). Warming alters energetic structure and function but not resilience of soil food webs. *Nature Climate Change* **7**, 895–900. https://doi.org/10.1038/s41558-017-0002-z

Sell D.W. (1982). Size-frequency estimates of secondary production by Mysis relicta in Lakes Michigan and Huron. *Hydrobiologia* **93**, 69–78. https://doi.org/10.1007/BF00008100

Simon K.S. & Townsend C.R. (2003). Impacts of freshwater invaders at different levels of ecological organisation, with emphasis on salmonids and ecosystem consequences. *Freshwater Biology* **48**, 982–994. https://doi.org/10.1046/j.1365-2427.2003.01069.x

Sommer U., Adrian R., De Senerpont Domis L., Elser J.J., Gaedke U., Ibelings B., *et al.* (2012). Beyond the Plankton Ecology Group (PEG) Model: Mechanisms Driving Plankton Succession. *Annual Review of Ecology, Evolution, and Systematics* **43**, 429–448. https://doi.org/10.1146/annurev-ecolsys-110411-160251

Straile D. & Hälbich A. (2000). Life history and multiple antipredator defenses of an invertebrate pelagic predator, Bythotrephes longimanus. *Ecology* **81**, 150–163. https://doi.org/10.1890/0012-9658(2000)081[0150:lhamad]2.0.co;2

Strayer D. (2009). Twenty years of zebra mussels : lessons from the mollusk that made headlines. *Frontiers in Ecology and the Environment* **7**, 135–141. https://doi.org/10.1890/080020

Strayer D.L., Adamovich B. V., Adrian R., Aldridge D.C., Balogh C., Burlakova L.E., *et al.* (2019). Long-term population dynamics of dreissenid mussels (Dreissena polymorpha and D. rostriformis): a cross-system analysis. *Ecosphere* **10**. https://doi.org/10.1002/ecs2.2701

Strayer D.L., D'Antonio C.M., Essl F., Fowler M.S., Geist J., Hilt S., *et al.* (2017). Boom-bust dynamics in biological invasions: towards an improved application of the concept. *Ecology Letters* **20**, 1337–1350

Strecker A.L., Arnott S.E., Yan N.D. & Girard R. (2006). Variation in the response of crustacean zooplankton species richness and composition to the invasive predator Bythotrephes longimanus. *Canadian Journal of Fisheries and Aquatic Sciences* **63**, 2126–2136. https://doi.org/10.1139/F06-105

Szydlowski D.K., Elgin A.K., Lodge D.M., Tiemann J.S. & Larson E.R. (2023). Long-term macrophyte and snail community responses to population declines of invasive rusty crayfish (Faxonius rusticus) . *Ecological Applications* **33**, e2818. https://doi.org/10.1002/eap.2818

Tanentzap A.J., Morabito G., Volta P., Rogora M., Yan N.D. & Manca M. (2020). Climate warming restructures an aquatic food web over 28 years. *Global Change Biology* **26**, 6852–6866. https://doi.org/10.1111/gcb.15347

Tran T.N.Q., Jackson M.C., Sheath D., Verreycken H. & Britton J.R. (2015). Patterns of trophic niche divergence between invasive and native fishes in wild communities are predictable from mesocosm studies. *Journal of Animal Ecology* **84**, 1071–1080. https://doi.org/10.1111/1365-2656.12360

Vandermeer J. (2006). Oscillating Populations and Biodiversity Maintenance. *BioScience* **56**, 967–975

Vivian M.K. & Frazer D. (2021). Zooplankton Community Response to the Introduction of Cisco in Tiber Reservoir, Montana. *North American Journal of Fisheries Management* **41**, 1838–1849. https://doi.org/10.1002/nafm.10699

Voss S. & Mumm H. (1999). Where to stay by night and day: Size-specific and seasonal differences in horizontal and vertical distribution of Chaoborus flavicans larvae. *Freshwater Biology* **42**, 201–213. https://doi.org/10.1046/j.1365-2427.1999.444444.x

Wagg C., Bender S.F., Widmer, F. & van der Heijden M.G.A. (2014). Soil biodiversity and soil community composition determine ecosystem multifunctionality. *Proceedings of the National Academy of Sciences* **111**, 5266–70. https://doi.org/10.1073/pnas.1320054111

Wahl D.H., Wolfe M.D., Santucci V.J. & Freedman J.A. (2011). Invasive carp and prey community composition disrupt trophic cascades in eutrophic ponds. *Hydrobiologia* **678**, 49–63. https://doi.org/10.1007/s10750-011-0820-3

Walsh J.R., Lathrop R.C. & Vander Zanden M.J. (2017). Invasive invertebrate predator, Bythotrephes longimanus, reverses trophic cascade in a north-temperate lake. *Limnology and Oceanography* **62**, 2498–2509. https://doi.org/10.1002/lno.10582

Wang S.C., Liu X., Liu Y. & Wang H. (2021). Disentangling effects of multiple stressors on matter flow in a lake food web. *Ecology and Evolution*, 9652–9664. https://doi.org/10.1002/ece3.7789

Weisz E.J. & Yan N.D. (2011). Shifting invertebrate zooplanktivores: Watershed-level replacement of the native Leptodora by the non-indigenous Bythotrephes in Canadian Shield lakes. *Biological Invasions* **13**, 115–123. https://doi.org/10.1007/s10530-010-9794-8

Wickham H., Averick M., Bryan J., Chang W., McGowan L., François R., *et al.* (2019). Welcome to the Tidyverse. *Journal of Open Source Software* **4**, 1686. https://doi.org/10.21105/joss.01686

Willis T. V. & Magnuson J.J. (2006). Response of fish communities in five north temperate lakes to exotic species and climate. *Limnology and Oceanography* **51**, 2808–2820. https://doi.org/10.4319/lo.2006.51.6.2808

Wilson K.A., Magnuson J.J., Lodge D.M., Hill A.M., Kratz T.K., Perry W.L., *et al.* (2004). A long-term rusty crayfish (Orconectes rusticus) invasion: Dispersal patterns and community change in a north temperate lake. *Canadian Journal of Fisheries and Aquatic Sciences* **61**, 2255–2266. https://doi.org/10.1139/F04-170

Wootton K. & Stouffer D. (2015). Many weak interactions and few strong ; food-web feasibility depends on the combination of the strength of species ' interactions and their correct arrangement. *Theoretical Ecology* **9**, 185–195. https://doi.org/10.1007/s12080-015-0279-3

Yan N.D., Leung B., Lewis M.A. & Peacor S.D. (2011). The spread, establishment and impacts of the spiny water flea, Bythotrephes longimanus, in temperate North America: A synopsis of the special issue. *Biological Invasions* **13**, 2423–2432. https://doi.org/10.1007/s10530-011-0069-9

Young J.D. & Yan N.D. (2008). Modification of the diel vertical migration of Bythotrephes longimanus by the cold-water planktivore, Coregonus artedi. *Freshwater Biology* **53**, 981–995. https://doi.org/10.1111/j.1365-2427.2008.01954.x

Vander Zanden M.J., Casselman J.M. & Rasmussen J.B. (1999). Stable isotope evidence for the food web consequences of species invasions in lakes. *Nature* **401**, 464–467

Vander Zanden M.J. & Vadeboncoeur Y. (2002). Fishes as integrators of benthic and pelagic food webs in lakes. *Ecology* **83**, 2152–2161. https://doi.org/10.1890/0012-9658(2002)083[2152:FAIOBA]2.0.CO;2

Zhao Q., Van den Brink P.J., Carpentier C., Wang Y.X.G., Rodríguez-Sánchez P., Xu C., *et al.* (2019). Horizontal and vertical diversity jointly shape food web stability against small and large perturbations. *Ecology Letters* **22**, 1152–1162. https://doi.org/10.1111/ele.13282

Zimmerman M.S., Schmidt S.N., Krueger C.C., Zanden M.J. Vander & Eshenroder R.L. (2009). Ontogenetic niche shifts and resource partitioning of lake trout morphotypes. *Canadian Journal of Fisheries and Aquatic Sciences* **66**, 1007–1018. https://doi.org/10.1139/F09-060

FIGURES

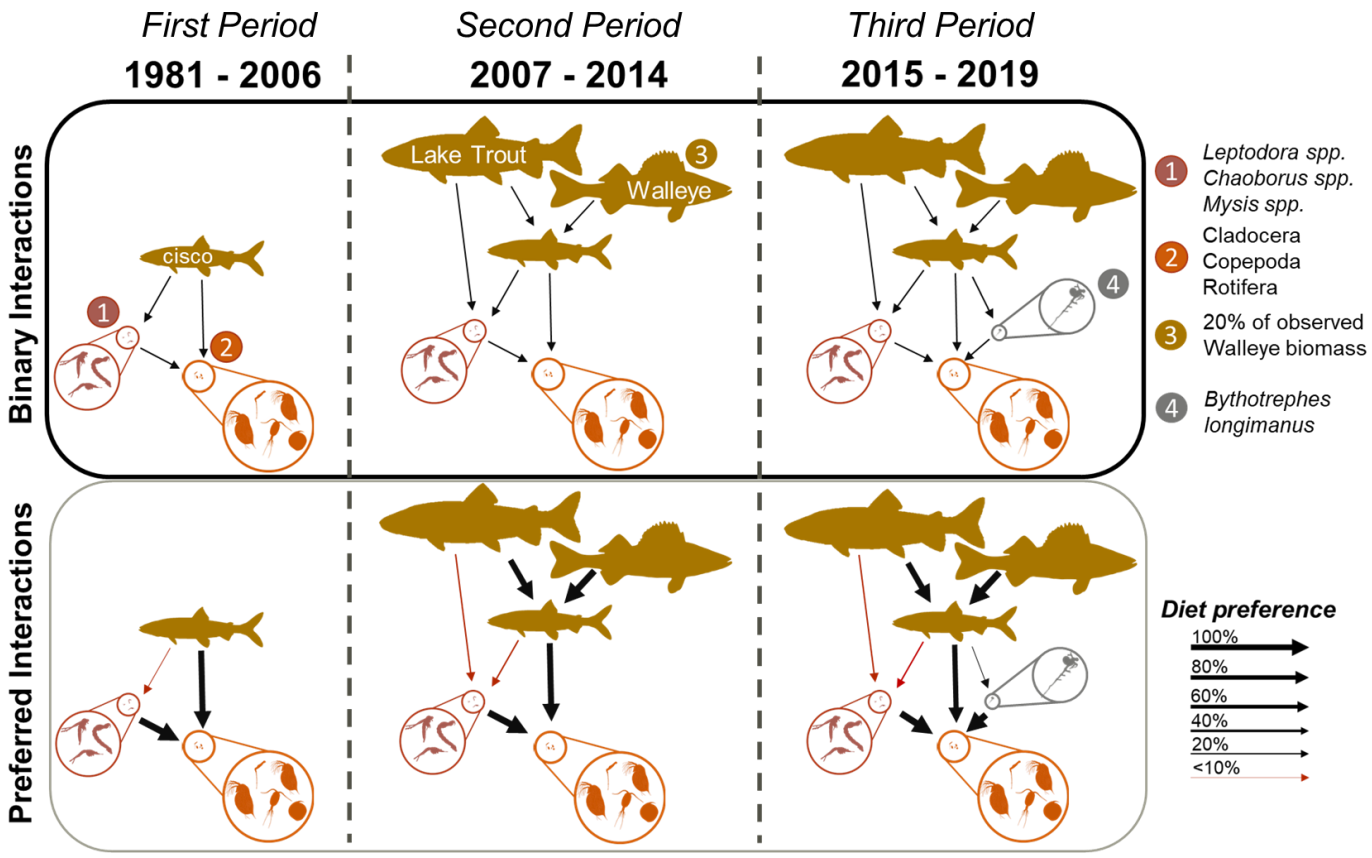

Figure 1. Conceptual of Trout Lake pelagic food web with species interactions described as binary (top) or preferred (bottom). Binary interactions describe only whether a predator does, or does not, feed on a prey item whereas preferred interactions quantify the preference of a predator to feed on one prey species versus another. Specific diet preference values are detailed in the supplement. Dashed lines denote three different periods within the Trout Lake food web following the framework of Martin *et al.,* 2022. Before the first dashed line denotes cisco dominance, between the dashed line denotes an increase in lake trout and walleye biomass in the food web, and following the second dashed line denotes the invasion of spiny water flea.

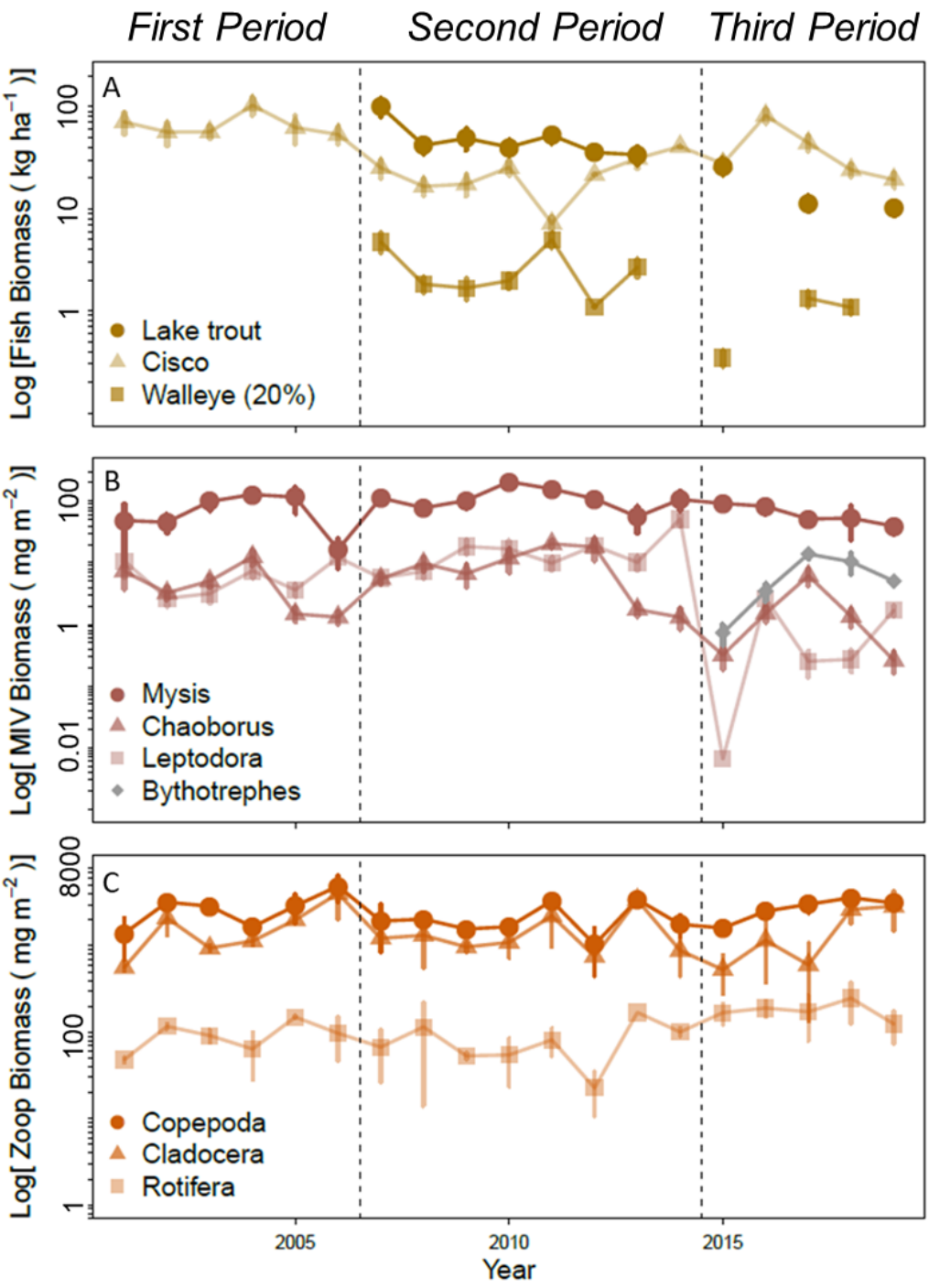

Figure 2. Time-series of species log-transformed biomass within the Trout Lake food web representing (A) fish species' biomass in kilograms per hectare (ha^{-1}), (B) pelagic macroinvertebrates (MIV) biomass in milligrams per square meter (m^{-2}), and (C) zooplankton group biomass in milligrams per square meter (m^{-2}). Note differences in y-axis and units between

each grouping of species. Dashed lines denote three different periods within the Trout Lake food web following the framework of Martin *et al.,* 2022. Before the first dashed line denotes cisco dominance, between the dashed line denotes an increase in lake trout and walleye biomass in the food web, and following the second dashed line denotes the invasion of spiny water flea.

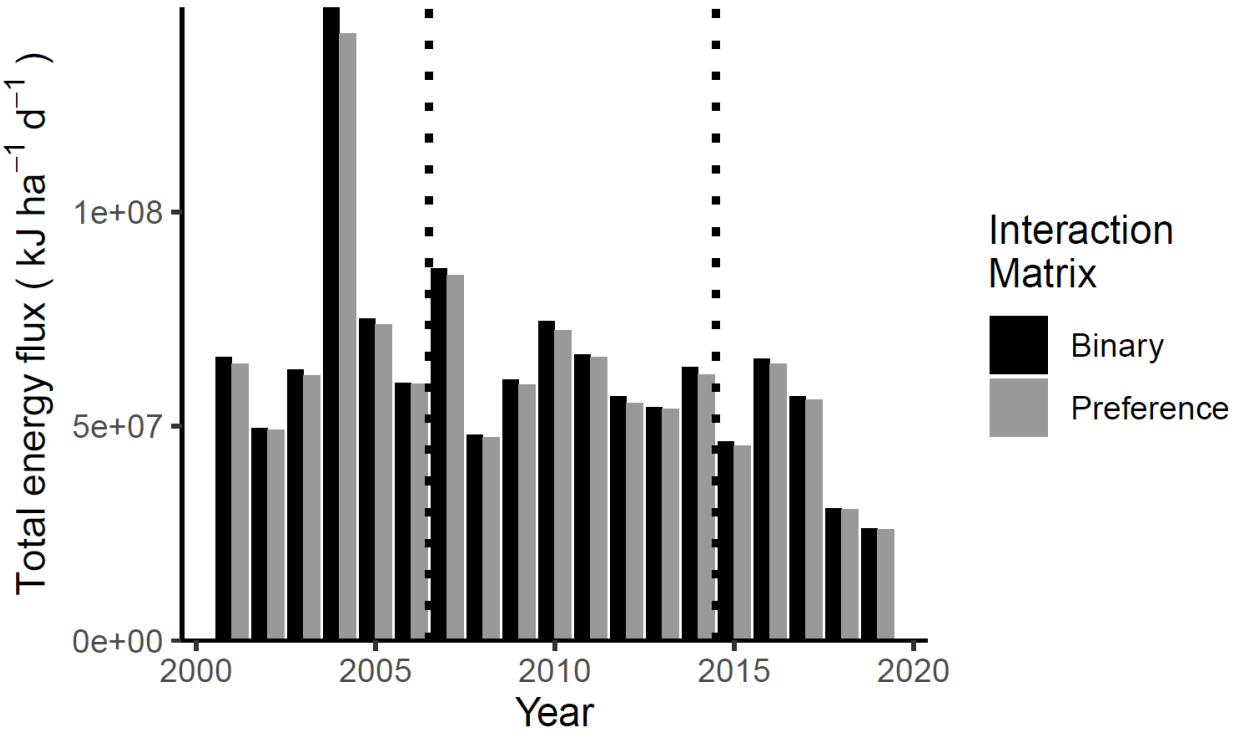

Figure 3. Total energy flux in kilojoules per hectare per day (kJ ha^{-1} d^{-1}). Dashed lines denote three different periods within the Trout Lake food web following the framework of Martin *et al.,* 2022. Before the first dashed line denotes cisco dominance, between the dashed line denotes an increase in lake trout and walleye biomass in the food web, and following the second dashed line denotes the invasion of spiny water flea.

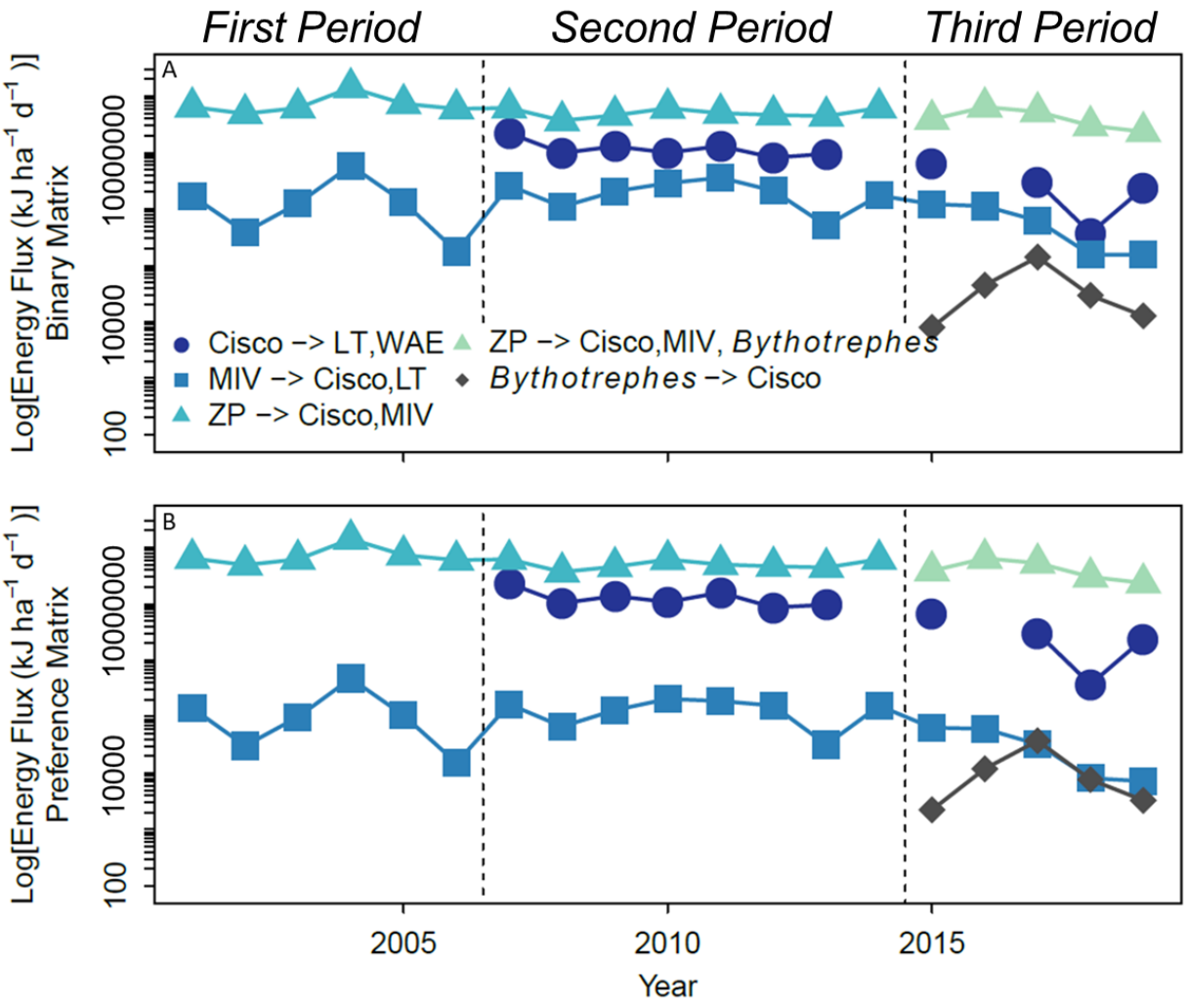

Figure 4. Energy flux for five trophic pathways in Trout Lake using the (A) binary interaction matrix and (B) preference interaction matrix in kilojoules per hectare per day (kJ ha^{-1} d^{-1}). LT are lake trout, WAE is walleye, MIV is pelagic macroinvertebrates, and ZP is zooplankton. Dashed lines denote three different periods within the Trout Lake food web following the framework of Martin *et al.,* 2022. Before the first dashed line denotes cisco dominance, between the dashed line denotes an increase in lake trout and walleye biomass in the food web, and following the second dashed line denotes the invasion of spiny water flea.

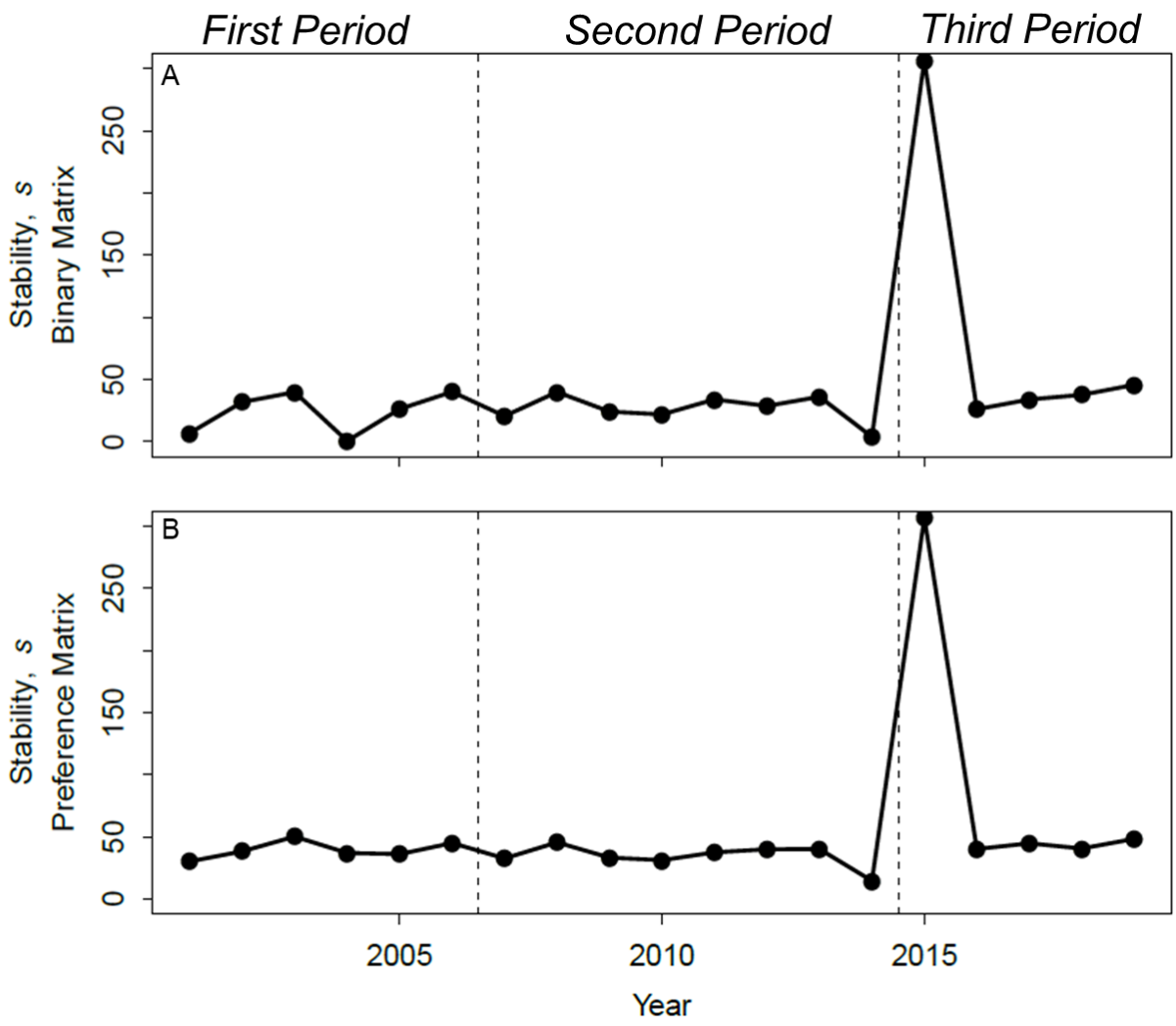

Figure 5. Estimated stability metric, *s*, for the Trout Lake food web using the (A) binary interaction matrix and (B) preference interaction matrix. Lower values of *s* represent food webs that are more stable compared to higher values of *s,* with negative values indicating a food web is within a stable state. Before the first dashed line denotes cisco dominance, between the dashed line denotes an increase in lake trout and walleye biomass in the food web, and following the second dashed line denotes the invasion of spiny water flea.

SUPPLEMENTARY INFORMATION FOR CHAPTER 4

SUPPLEMENTAL METHODS

Fish length-weight regressions

Fish lengths and weights were from data collected via the North Temperate Lakes – Long-Term Ecological Research program. Greater detail about collection methods is described in Magnuson, Carpenter & Stanley (2022). Briefly, sampling was conducted at six littoral sites with seine and fyke nets, electrofishing over four littoral transects, and vertically hung gill nets to obtain two pelagic samplers per lake from the deepest point from 1981 - 2020. Species were identified, measured to length in millimeters (mm), and a subset were weighed to grams (g). To calculate Trout Lake specific length-mass regressions for the main pelagic fish species in Trout Lake, we used simple linear regression to quantify the relationship between length (mm) and weight (g). Lake trout (*Salvelinus namaycush*), walleye (*Sander vitreus*), and cisco (*Coregonus artedi*) length-mass regressions were developed (Table S1).

Pelagic macroinvertebrate length measurements

To calculate the mass (g) of *Chaoborus spp., Leptodora kindtii, Mysis spp.,* and *Bythotrephes longimanus* we measured each taxa according to specifications described in species-specific length-mass regressions from the literature. *Chaoborus, Leptodora,* and *Mysis* were measured from the anterior part of their head capsule to the posterior part of their last abdominal segment. *Bythotrephes* were measured over their core body length ending at the base of the caudal spine as described in Branstrator (2005). The number of taxa measured per species was determined by the number of individuals required to reduce the coefficient of variation in length to less than 20% per year (McCauley, 1984). The number of individuals required to represent average length per year were 20 for *Chaoborus,* 25 for *Leptodora,* 25 for *Bythotrephes*, and 10 for *Mysis*. Individual *Chaoborus* mass was estimated based on dry mass estimates of

Chaoborus flavicans (Dumont & Balvay, 1979), which have been reported in northern Wisconsin lakes previously (Dodson *et al.*, 2009). Individual *Mysis* mass was estimated based on dry mass estimates of *Mysis relicta* (Sell, 1982), which are present in Trout Lake (Juday & Birge, 1927). *Leptodora kindtii* and *Bythotrephes longimanus* dry mass was estimated from species-specific length-mass regressions (Dumont, Van de Velde & Dumont, 1975; Branstrator, 2005). Individual length measurements were applied to length-mass regressions, and we took the average of the mass estimate to attain the average dry mass of an individual within a given year. If too few individuals were present, or samples were missing for a given year, we included length estimates from the two years before and after to calculate the average dry mass.

Binary and preference interaction matrices

Values for interactions between species were determined from the literature as noted in the footnotes of the interaction matrices (Pastorok, 1980; Bowers & Vanderploeg, 1982; Browman, Kruse & O'Brien, 1989; Vander Zanden & Rasmussen, 1996; Vander Zanden, Cabana & Rasmussen, 1997; Hovius, Beisner & McCann, 2006; Herwig, Zimmer & Staples, 2022; Martin, Mrnak & Vander Zanden, 2023; Table S2 – S3).Within the *fluxweb* model, preferences determine how predators quantify their foraging choices following equation (1):

$$W_{ij} = \frac{w_{ij} B_i}{\sum_k w_{kj} B_k} \quad (1)$$

where W_{ij} represents preference, B_i sets the biomass of species i and w is the preference value determined in the matrix (i.e., the value of the i^{th} line and j^{th} column is non-zero if a predator j feeds on prey i (Gauzens *et al.*, 2019). Here, when using the binary interaction matrix, energy flux from prey to predators is determined only by the relative availability of prey (determined by

biomass), whereas when using the preference interaction matrix, energy flux is determined via both the relative availability of prey and weighted by preference.

Energy Flux and food web stability estimation

To calculate metabolic losses per food web node, mass-specific metabolic rates (i.e., per unit biomass) were derived from body mass metabolic relationships using allometric equations (Brown, 2004) provided in Gauzens *et al.* (2019). Species metabolic rates to define energetic losses related to physiology were calculated with equation (2):

$$X_i = x_0 M_i^b \quad (2)$$

Where X_i represents a parameter related to the physiology of species i, x_0 and b are constants associated with X_i and M_i is body mass (g). Parameter values were determined by metabolic type from Brown et al. (2004) and listed in Gauzen *et al.* (2019); 17.17 for invertebrates and 18.18 for fish. Assimilation efficiencies were defined as the proportion of eaten biomass used for biomass production plus metabolism (Lang *et al.*, 2017); for the Trout Lake food web, all prey were considered animal prey with an assimilation efficiency of 0.906 (Gauzens *et al.*, 2019). A biomass per taxon was input as grams per hectare (see methods), energy flux was calculated as joules per hectare per second. We then transformed fluxes into kilojoules per hectare per day by multiplying the energy flux value by 86.4 (3).

$$\frac{Joules}{hectare * second} * \frac{1\ kilojoule}{1000\ Joules} * \frac{86400\ seconds}{1\ day} = \frac{Kilojoules}{hectare * day} \quad (3)$$

Greater details that describe the application and calculation of energy flux are provided in Gauzens *et al.* (2019).

Network stability was estimated by interpreting biomass fluxes as link weights to assess the patterning of interaction strength within the food web (Neutel, Heesterbeek & de Ruiter, 2002; Gauzens *et al.*, 2019). The *stability.value* function can then quantify food web stability

through derivation of a Jacobian matrix, with greater details provided in Gauzens *et al.* (2019). The *stability.value* function requires the same information as the function that quantifies energy flux, however instead of a matrix of interactions it requires a matrix of energy flux estimates in addition to estimated growth rates of the lowest trophic level considered in the food web. Growth rates were calculated by applying equation (4) to average body mass estimates for Cladocera, Copepoda, and Rotifera as suggested in Gauzens *et al.* (2019).

$$growth\ rate = 0.71 * bodymass^{-0.25} \quad (4)$$

Sensitivity analyses

The *fluxweb* R package (Gauzens *et al.*, 2019) includes a *sensitivity* function to estimate the uncertainty (i.e., lack of precision) within parameter estimation in order to assess whether reduced precision leads to large errors in the estimation of energy flux and food web stability. Greater detail on sensitivity analyses is provided in Gauzens *et al.* (2019). Briefly, the *sensitivity* function applies a random variation to a selected input parameter (e.g., metabolic losses, assimilation efficiencies, prey preferences, etc.). This returns a matrix containing the average coefficient of variation (*cv*):

$$cv = \frac{F''[i,j] - F[i,j]}{F[i,j]} \quad (5)$$

where *F[i, j]* is the flux from species *i* to species *j* when no variation is applied to parameters and *F"[i, j]* is the equivalent with random variation applied.

We considered the sensitivity of input parameters for our estimation of energy flux for the binary interaction matrix (Figure S1) and preference interaction matrix (Figure S2). For all years, parameter estimates for metabolic losses, assimilation efficiency, and prey preference (only for the preference interaction matrix) indicated our results were robust to parameter uncertainty. In addition, we manually manipulated biomass inputs to assess whether uncertainty in our biomass

estimates changed energy flux qualitatively. We doubled fish biomass and halved zooplankton and pelagic macroinvertebrate biomass (Figure S3), then input the reverse (Figure S4). Both figures demonstrate the qualitative patterns in energy flux are robust for the Trout Lake food web. For the sensitivity analysis of food web stability, we took a similar approach. Food web stability estimation required an additional parameter, growth rate of the species within the lowest trophic level considered. For the binary interaction matrix, uncertainty in the estimate for growth rate led to relatively high *cv*'s in 2001 and 2014 and produced large errors in 2004 (Figure S5). However, for the preference interaction matrix, the *cv* stayed below the identity line for all years indicating uncertainty in the estimate for growth rate did not produce large errors in our estimate of food web stability (*cv* < 20%). Thus, given that the qualitative dynamics of food web stability were roughly similar when quantified with either the binary or preference interaction matrix, it is likely our estimate of food web stability is robust. However, interpretation should be weighted more strongly towards estimates produced by the preference interaction matrix which were the most robust to uncertainty for all years.

SUPPLEMENTAL REFERENCES

Bowers J.A. & Vanderploeg H.A. (1982). In situ predatory behavior of Mysis relicta in Lake Michigan*. *Hydrobiologia* **93**, 121–131

Branstrator D.K. (2005). Contrasting life histories of the predatory cladocerans Leptodora kindtii and Bythotrephes longimanus. *Journal of Plankton Research* **27**, 569–585. https://doi.org/10.1093/plankt/fbi033

Browman H.I., Kruse S. & O'Brien W.J. (1989). Foraging behavior of the predaceous cladoceran, Leptodora kindti, and escape responses of their prey. *Journal of Plankton Research* **11**, 1075–1088

Brown J.H. (2004). Toward a Metabolic Theory of Ecology. *Ecology* **85**, 1771–1789. https://doi.org/10.1890/03-9000

Dodson S.I., Newman A.L., Will-Wolf S., Alexander M.L., Woodford M.P. & Van Egeren S. (2009). The relationship between zooplankton community structure and lake characteristics

in temperate lakes (Northern Wisconsin, USA). *Journal of Plankton Research* **31**, 93–100. https://doi.org/10.1093/plankt/fbn095

Dumont H.J. & Balvay G. (1979). The dry weight estimate of chaoborus flavicans (Meigen) as a function of length and instars. *Hydrobiologia* **64**, 139–145. https://doi.org/10.1007/BF00023189

Dumont H.J., Van de Velde I. & Dumont S. (1975). The dry weight estimate of biomass in a selection of Cladocera, Copepoda and Rotifera from the plankton, periphyton and benthos of continental waters. *Oecologia* **19**, 75–97. https://doi.org/10.1007/BF00377592

Gauzens B., Barnes A., Giling D.P., Hines J., Jochum M., Lefcheck J.S., *et al.* (2019). fluxweb: An R package to easily estimate energy fluxes in food webs. *Methods in Ecology and Evolution* **10**, 270–279. https://doi.org/10.1111/2041-210X.13109

Herwig B.R., Zimmer K.D. & Staples D.F. (2022). Using stable isotope data to quantify niche overlap and diets of muskellunge, northern pike and walleye in a deep Minnesota lake. *Ecology of Freshwater Fish* **31**, 60–71. https://doi.org/10.1111/eff.12608

Hovius J.T., Beisner B.E. & McCann K.S. (2006). Epilimnetic rotifer community responses to Bythotrephes longimanus invasion in Canadian Shield lakes. *Limnology and Oceanography* **51**, 1004–1012. https://doi.org/10.4319/lo.2006.51.2.1004

Juday C. & Birge E.A. (1927). Pontoporeia and Mysis in Wisconsin Lakes. *Ecology* **8**, 445–452

Lang B., Ehnes R.B., Brose U. & Rall B.C. (2017). Temperature and consumer type dependencies of energy flows in natural communities. *Oikos* **126**, 1717–1725. https://doi.org/10.1111/oik.04419

Magnuson J.J., Carpenter S.R. & Stanley E.H. (2022). North Temperate Lakes LTER: Fish Lengths and Weights 1981 - current ver 34. https://doi.org/10.6073/pasta/968299a53784f9649eb67f421cc33340

Martin B.E., Mrnak J.T. & Vander Zanden M.J. (2023). Evaluating the potential role of predation by native fish regulating the abundance of invasive spiny water flea. *Journal of Freshwater Ecology* **38**. https://doi.org/10.1080/02705060.2023.2187470

McCauley E. (1984). The estimation of the abundance and biomass of zooplankton in samples. In: *A manual on methods for the assessment of secondary productivity in fresh waters*. (Eds J. Downing & F. Rigler), pp. 228–265. Blackwell Publishing Ltd, Oxford (UK).

Neutel A., Heesterbeek J.A.P. & de Ruiter P. (2002). Stability in Real Food Webs: Weak Links in Long Loops. *Science* **296**, 1120–1124. https://doi.org/10.1126/science.1068326

Pastorok R.A. (1980). The effects of predator hunger and food abundance on prey selection by Chaoborus larvae. *Limnology and Oceanography* **25**, 910–921. https://doi.org/10.4319/lo.1980.25.5.0910

Sell D.W. (1982). Size-frequency estimates of secondary production by Mysis relicta in Lakes Michigan and Huron. *Hydrobiologia* **93**, 69–78. https://doi.org/10.1007/BF00008100

Vander Zanden M.J., Cabana G. & Rasmussen J.B. (1997). Comparing trophic position of freshwater fish calculated using stable nitrogen isotope ratios d15N and literature dietary data. *Canadian Journal of Fisheries and Aquatic Sciences* **54**, 1142–1158

Vander Zanden M.J. & Rasmussen J.B. (1996). A trophic position model of pelagic food webs: Impact on contaminant bioaccumulation in lake trout. *Ecological Monographs* **66**, 451–477. https://doi.org/10.2307/2963490

SUPPLEMENTAL TABLES

Table S1. Trout Lake specific length-mass regressions ($Log_{10}(W) = a*Log_{10}(L) + b$, where W is weight (g), L is total body length (mm), and *a* and *b* are constants) for lake trout (*Salvelinus namaycush*), walleye (*Sander vitreus*), and cisco (*Coregonus artedi*) using simple linear regression. *n* = the number of individuals used to develop each equation, SE is standard error, and Adj.R^2 is the adjusted coefficient of determination.

Species	n	*a* ± 1 SE	*b* ± 1 SE	Adj.R^2	Length range (mm)
Lake trout	200	3.097 ± 0.068	-5.382 ± 0.187	0.91	353 – 882
Walleye	1232	3.085 ± 0.007	-5.293 ± 0.018	0.99	50 – 730
Cisco	14029	3.120 ± 0.003	-5.389 ± 0.006	0.99	62 – 530

Table S2. Trout Lake binary predator-prey interaction matrix. Predators are column names and prey are row names. A value of 1 denotes a predator-prey interaction exists, and a value of zero denotes it does not.

	Cisco[a,b]	Lake trout[a]	Walleye[c,d]	*Bythotrephes*[e]	*Chaoborus*[f]	*Leptodora*[g]	*Mysis*[h]	Cladocera	Copepoda	Rotifera
Year range: 2001 – 2014										
Cisco	0	1	1	--	0	0	0	0	0	0
Lake Trout	0	0	0	--	0	0	0	0	0	0
Walleye	0	0	0	--	0	0	0	0	0	0
Bythotrephes	--	--	--	--	--	--	--	--	--	--
Chaoborus	1	1	0	--	0	0	0	0	0	0
Leptodora	1	1	0	--	0	0	0	0	0	0
Mysis	1	1	0	--	0	0	0	0	0	0
Cladocera	1	0	0	--	1	1	1	0	0	0
Copepoda	1	0	0	--	1	0	1	0	0	0
Rotifera	1	0	0	--	0	1	1	0	0	0
Year range: 2015 – 2019										
Cisco	0	1	1	0	0	0	0	0	0	0
Lake Trout	0	0	0	0	0	0	0	0	0	0
Walleye	0	0	0	0	0	0	0	0	0	0
Bythotrephes	1	0	0	0	0	0	0	0	0	0
Chaoborus	1	1	0	0	0	0	0	0	0	0
Leptodora	1	1	0	0	0	0	0	0	0	0
Mysis	1	1	0	0	0	0	0	0	0	0
Cladocera	1	0	0	1	1	1	1	0	0	0
Copepoda	1	0	0	1	1	0	1	0	0	0
Rotifera	1	0	0	0	0	1	1	0	0	0

[a]Vander Zanden & Rasmussen, 1996
[b]Martin, Mrnak & Vander Zanden, 2023
[c]Vander Zanden, Cabana & Rasmussen, 1997
[d]Herwig, Zimmer & Staples, 2022
[e]Hovius, Beisner & McCann, 2006
[f]Pastorok, 1980
[g]Browman, Kruse & O'Brien, 1989
[h]Bowers & Vanderploeg, 1982

Table S3. Trout Lake preference predator-prey interaction matrix. Predators are column names and prey are row names. Values represent percentages of predator diet with higher percentages reflecting greater weight to prey choice for predators.

	Cisco[a,b]	Lake trout[a]	Walleye[c,d]	*Bythotrephes*[e]	*Chaoborus*[f]	*Leptodora*[g]	*Mysis*[h]	Cladocera	Copepoda	Rotifera
Year range: 2001 – 2014										
Cisco	0	0.9	1	--	0	0	0	0	0	0
Lake Trout	0	0	0	--	0	0	0	0	0	0
Walleye	0	0	0	--	0	0	0	0	0	0
Bythotrephes	--	--	--	--	--	--	--	--	--	--
Chaoborus	0.03	0.06	0	--	0	0	0	0	0	0
Leptodora	0.04	0.01	0	--	0	0	0	0	0	0
Mysis	0.03	0.03	0	--	0	0	0	0	0	0
Cladocera	0.4	0	0	--	0.5	0.5	0.4	0	0	0
Copepoda	0.4	0	0	--	0.5	0	0.3	0	0	0
Rotifera	0.1	0	0	--	0	0.5	0.3	0	0	0
Year range: 2015 – 2019										
Cisco	0	0.9	1	0	0	0	0	0	0	0
Lake Trout	0	0	0	0	0	0	0	0	0	0
Walleye	0	0	0	0	0	0	0	0	0	0
Bythotrephes	0.1	0	0	0	0	0	0	0	0	0
Chaoborus	0.02	0.06	0	0	0	0	0	0	0	0
Leptodora	0.03	0.01	0	0	0	0	0	0	0	0
Mysis	0.02	0.03	0	0	0	0	0	0	0	0
Cladocera	0.4	0	0	0.5	0.5	0.5	0.4	0	0	0
Copepoda	0.4	0	0	0.5	0.5	0	0.3	0	0	0
Rotifera	0.03	0	0	0	0	0.5	0.3	0	0	0

[a]Vander Zanden & Rasmussen, 1996
[b]Martin, Mrnak & Vander Zanden, 2023
[c]Vander Zanden, Cabana & Rasmussen, 1997
[d]Herwig, Zimmer & Staples, 2022
[e]Hovius, Beisner & McCann, 2006
[f]Pastorok, 1980
[g]Browman, Kruse & O'Brien, 1989
[h]Bowers & Vanderploeg, 1982

SUPPLEMENTAL FIGURES

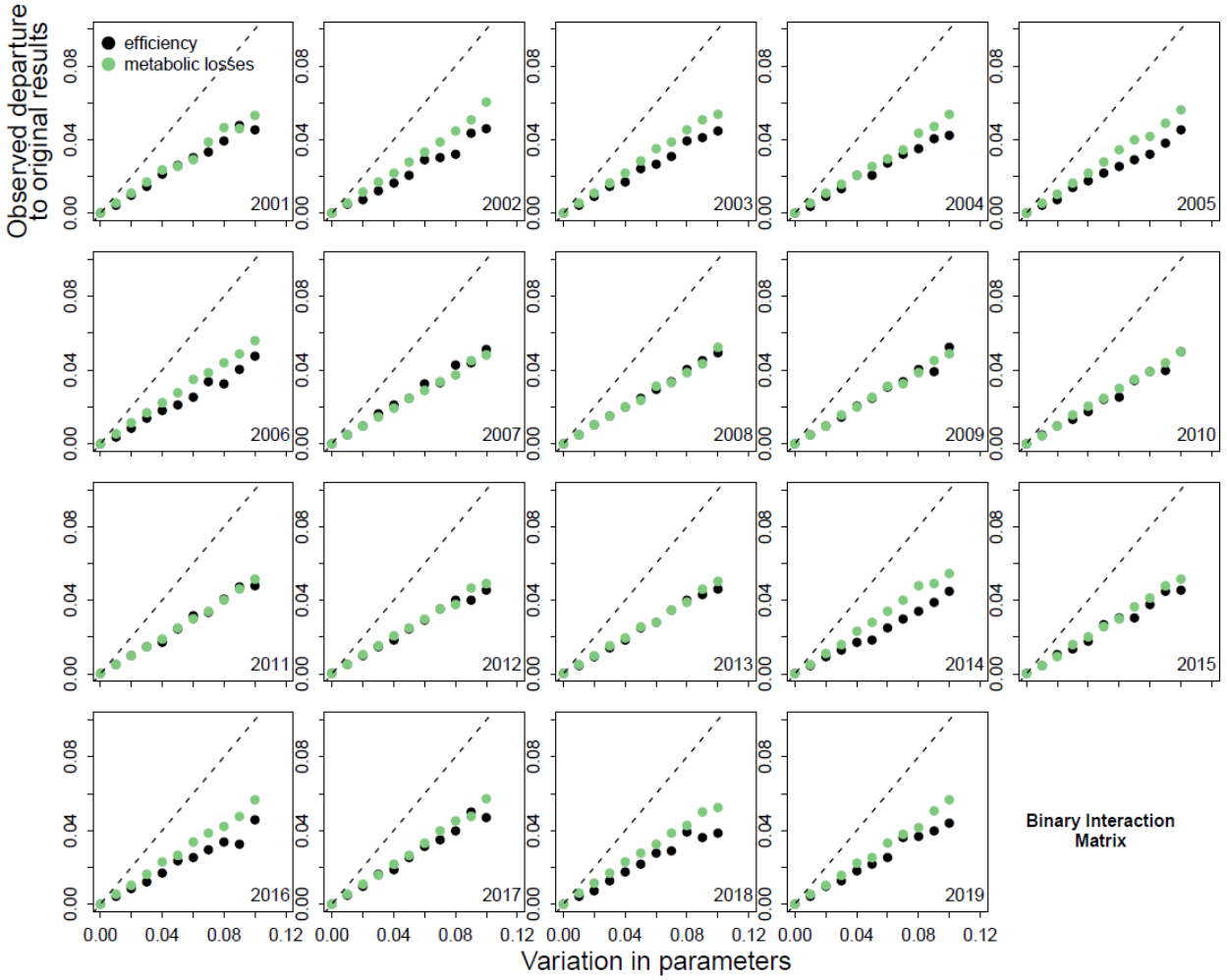

Figure S1. Sensitivity analysis of the input parameters (i.e., efficiency, metabolic losses) used to estimate energy flux from the *fluxing* function in *fluxweb* based on the binary interaction matrix ***(Gauzens et al. 2019).*** The y-axis represents the mean standard deviation of the departure of energy flux to the original value and the x-axis represents the simulated uncertainty applied to the parameter estimate. The dashed line represents the identity. Years where the estimates moved substantially above the identity line as variation in the parameter increased indicate uncertainty in the parameters would have a substantial effect on the estimation of energy flux.

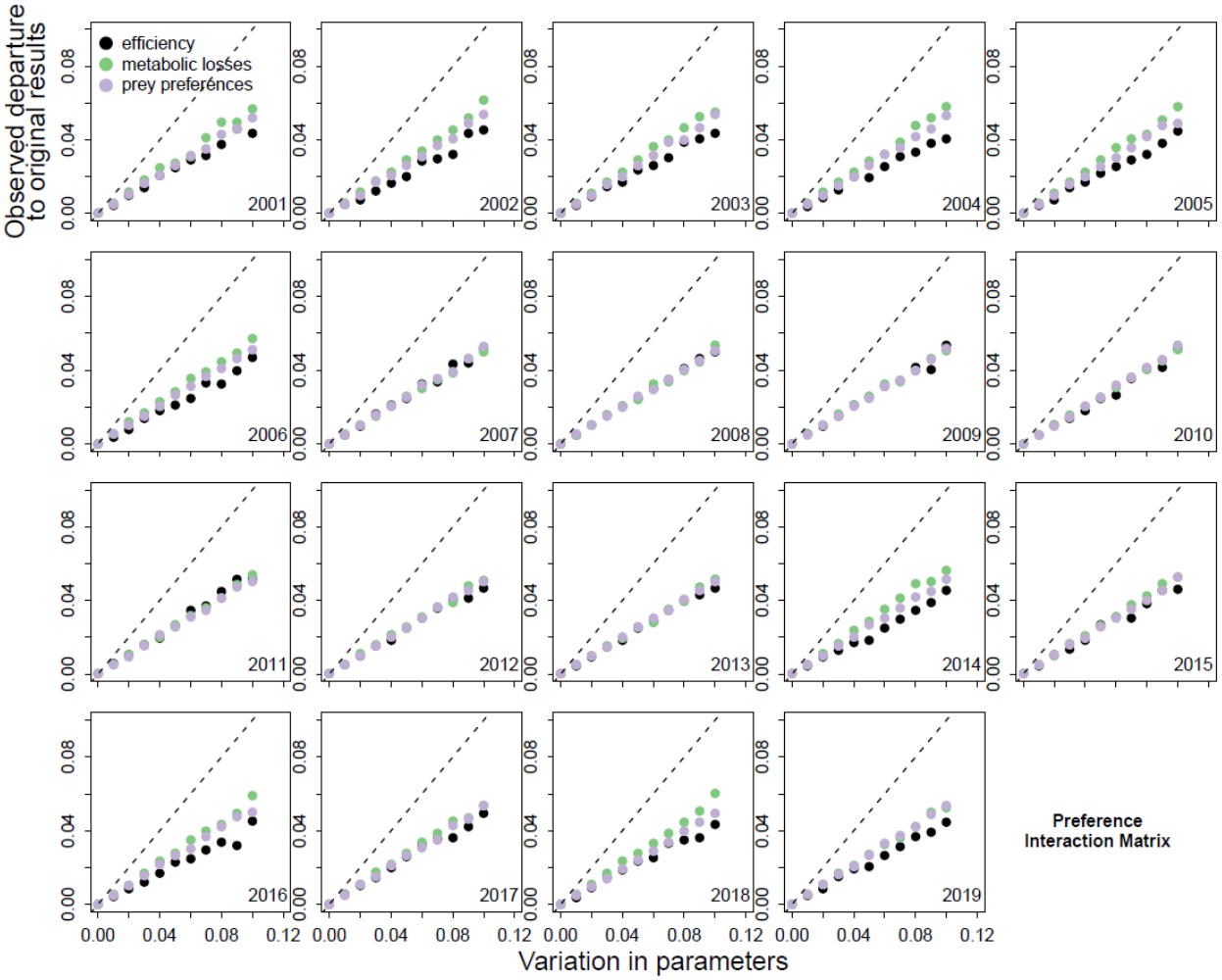

Figure S2. Sensitivity analysis of the input parameters (i.e., efficiency, metabolic losses, and prey preferences) used to estimate energy flux from the *fluxing* function in *fluxweb* based on the preference interaction matrix ***(Gauzens et al. 2019).*** The y-axis represents the mean standard deviation of the departure of energy flux to the original value and the x-axis represents the simulated uncertainty applied to the parameter estimate. The dashed line represents the identity. Years where the estimates moved substantially above the identity line as variation in the parameter increased indicate uncertainty in the parameters would have a substantial effect on the estimation of energy flux.

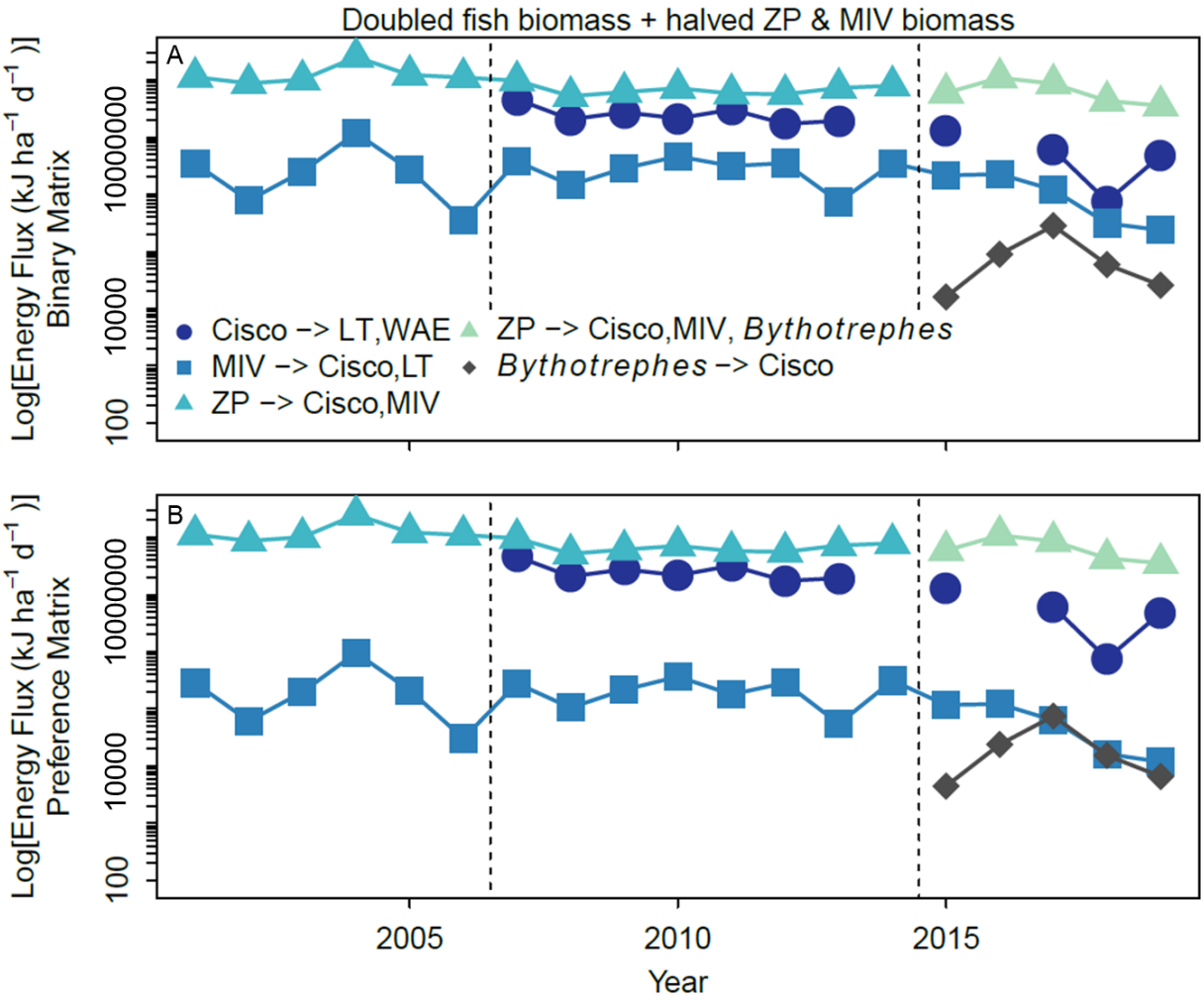

Figure S3. Energy flux for five trophic pathways in Trout Lake using the (A) binary interaction matrix and (B) preference interaction in kilojoules per hectare per day (kJ ha^{-1} d^{-1}), with biomass input manipulated to assess sensitivity. Fish species biomass were doubled, and zooplankton and pelagic macroinvertebrate biomass were halved before estimating energy flux. LT are lake trout, WAE is walleye, MIV is pelagic macroinvertebrates, and ZP is zooplankton. Dashed lines denote three different periods within the Trout Lake food web following the framework of Martin *et al.,* 2022. Before the first dashed line denotes cisco dominance, between the dashed line denotes an increase in lake trout and walleye biomass in the food web, and following the second dashed line denotes the invasion of spiny water flea.

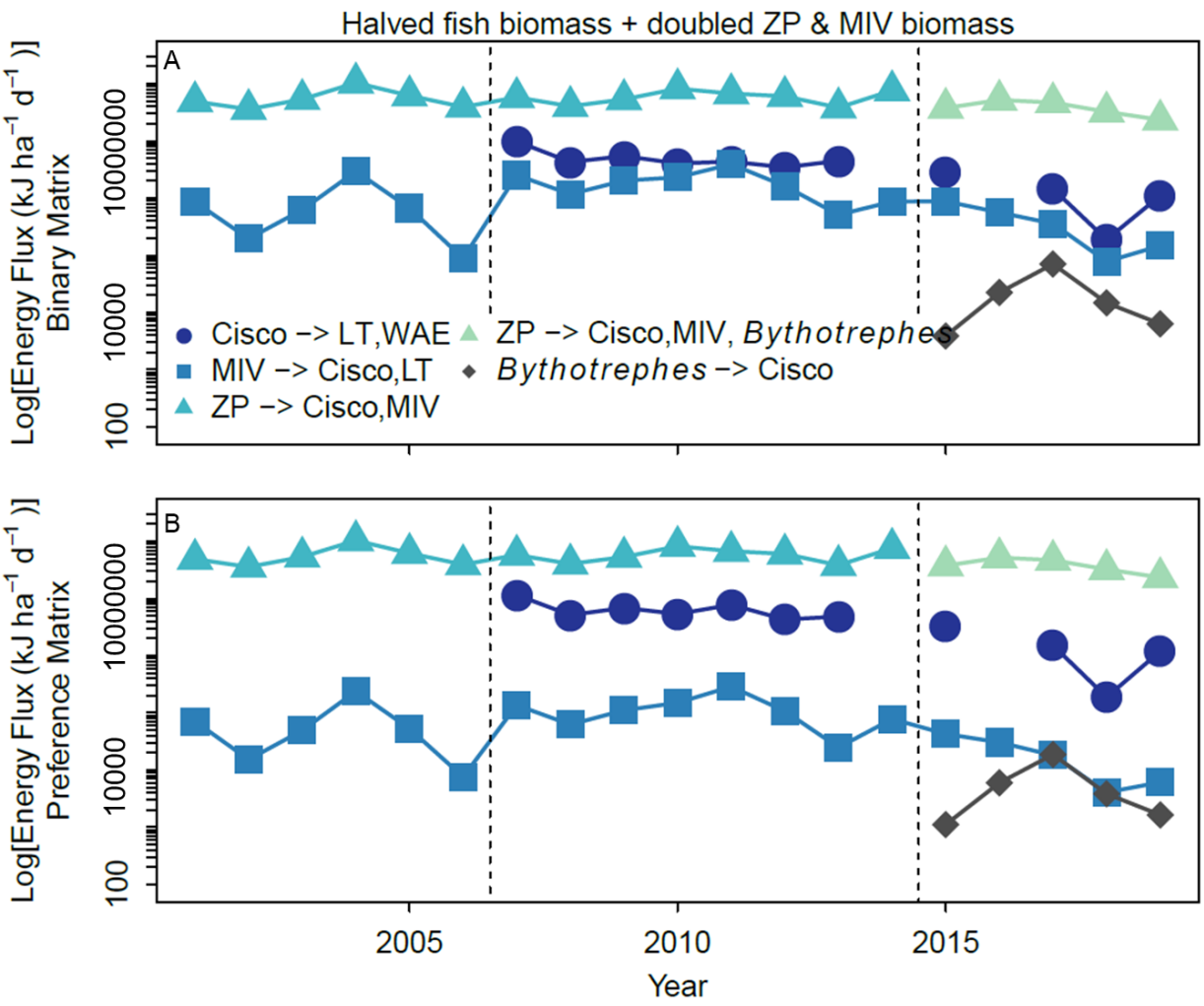

Figure S4. Energy flux for five trophic pathways in Trout Lake using the (A) binary interaction matrix and (B) preference interaction in kilojoules per hectare per day (kJ ha^{-1} d^{-1}), with biomass input manipulated to assess sensitivity. Fish species biomass were halved, and zooplankton and pelagic macroinvertebrate biomass were doubled before estimating energy flux. LT are lake trout, WAE is walleye, MIV is pelagic macroinvertebrates, and ZP is zooplankton. Dashed lines denote three different periods within the Trout Lake food web following the framework of Martin *et al.,* 2022. Before the first dashed line denotes cisco dominance, between the dashed line denotes an increase in lake trout and walleye biomass in the food web, and following the second dashed line denotes the invasion of spiny water flea.

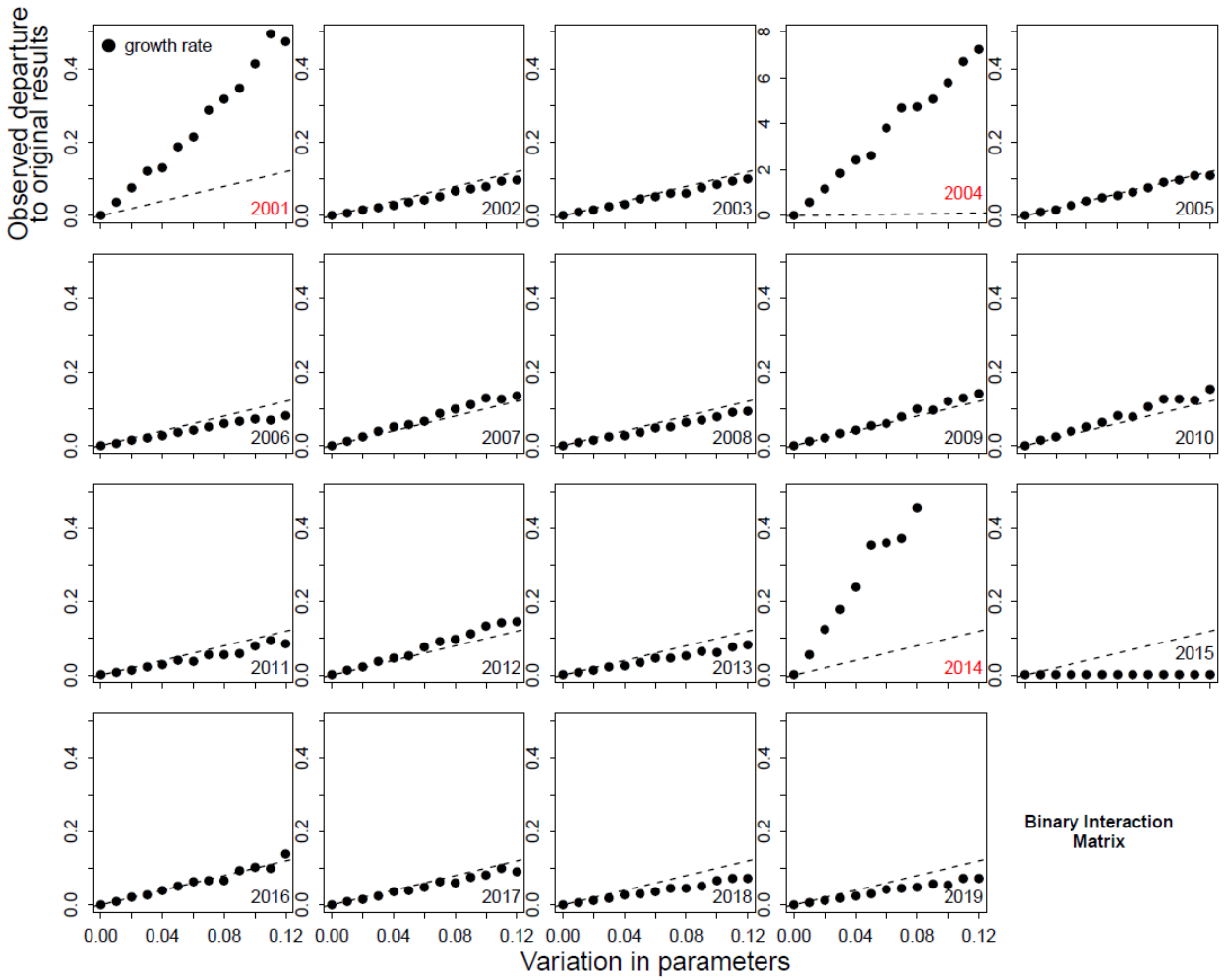

Figure S5. Sensitivity analysis of the input parameter, growth rate, used to estimate the inferred stability metric, *s*, from the *stability.value* function in *fluxweb* using the binary interaction matrix ***(Gauzens et al. 2019).*** The y-axis represents the mean standard deviation of the departure of *s* to the original value and the x-axis represents the simulated uncertainty applied to the parameter estimate. The dashed line represents the identity. Red labels represent years where the estimate for *s* moved substantially above the identity line as variation in the parameter increased, indicating uncertainty in the parameters would have a substantial effect on the estimation of stability. Not the different y-axis scale for our model estimates in 2004 which was expanded to show all data points.

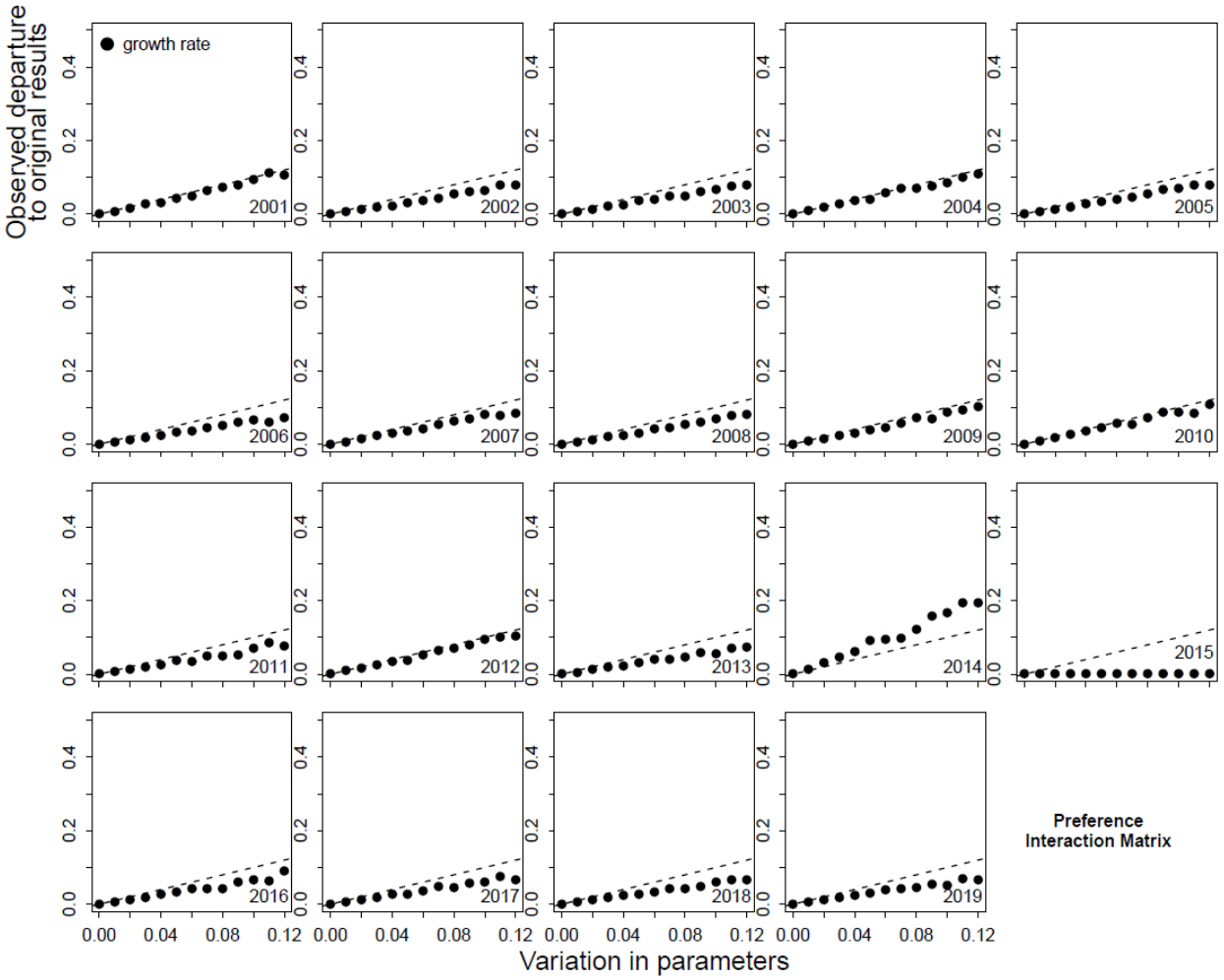

Figure S6. Sensitivity analysis of the input parameter, growth rate, used to estimate the inferred stability metric, *s*, from the *stability.value* function in *fluxweb* using the preference interaction matrix ***(Gauzens et al. 2019).*** The y-axis represents the mean standard deviation of the departure of *s* to the original value and the x-axis represents the simulated uncertainty applied to the parameter estimate. The dashed line represents the identity. Years where the estimate for *s* moved substantially above the identity line as variation in the parameter increased indicate uncertainty in the parameters would have a substantial effect on the estimation of stability.

CONCLUSIONS

Understanding changes in ecosystem function and dynamics in response to increasingly frequent and intense disturbances is a pressing management need. In this dissertation, I strengthen our understanding of the connections between food web structure and ecosystem response to press and pulse disturbances, management interventions, and species invasion. In chapter 1 and 2, I used lower food web dynamics to improve our understanding of ecosystem function in disturbed ecosystems and assess changes to food web structure following a management intervention. In chapter 1, I quantified the seasonal dynamics of zooplankton, phytoplankton, and nutrient concentrations across the summer growing season in a hypereutrophic reservoir. I showed that zooplankton community composition had a relatively substantial influence on early summer phosphorus availability and extended our understanding of the temporal dynamics of zooplankton and phytoplankton within hypereutrophic ecosystems. I also demonstrated that zooplankton grazing plays a potentially significant role in affecting phytoplankton community size structure, even in a community dominated by cyanobacteria. Despite the extreme nutrient concentrations within hypereutrophic reservoirs, zooplankton still contributed substantially to phosphorus availability and phytoplankton size structure, though only within a short window in early summer. In chapter 2, I showed that inconsistent responses of zooplankton and benthic macroinvertebrate size spectra to incentivized harvest provided evidence that the incentivized harvest of common carp (*Cyprinus carpio*) and bigmouth buffalo (*Ictiobus cyprinellus*) did not significantly alter food web structure. The analysis expanded our understanding of size spectra analyses within shallow, nutrient-rich lakes which were previously not well characterized and provided insights into why a management intervention was

unsuccessful across multiple shallow lakes. Using size spectra as a tool to assess food web structure changes may be more feasible than more data intensive food web modeling approaches.

In chapter 3 and 4, I used investigations of whole food webs to understand how food web structure mediates ecosystem responses to disturbances, and how food web structure and ecosystem function can vary through time. In chapter 3, I used ecosystem experiments to produce empirical evidence that a greater degree of coupling between benthic and pelagic energy pathways within food webs increased ecosystem resistance and resilience to a simulated storm-driven pulse nutrient additions. As such, I provide evidence that preserving or enhancing benthic-pelagic coupling within food webs may be a powerful management target to reduce the vulnerability of aquatic ecosystems to increasingly frequent and intense precipitation events. In chapter 4, I used a bioenergetics method to quantify the distribution and magnitude of energy flux, in addition to food web stability, within a pelagic food web over 19 years. I demonstrated how changes in food web structure over time corresponded to shifts in total energy flux and the distribution of energy flux between species. I also show that the introduction of a mid-trophic level macroinvertebrate invader decreased total energy flux and, using food web stability dynamics, provide evidence that the Trout Lake food web as able to absorb the shock of species invasion without sustained changes in energy flux This analysis improved our understanding of the long-term dynamics of food web structure and ecosystem function, particularly in response to mid-trophic level invaders.

Overall, in this dissertation I used food web theory combined with ecosystem experiments, observational studies, and long-term data to attain greater understanding of the dynamics of ecosystem function and responses to disturbances and management interventions through time.